Fortschritt-Berichte VDI

VDI

Reihe 3

Verfahrenstechnik

Dipl.-Ing. Elizabeth Heischkamp,
Mülheim a. d. Ruhr

Nr. 953

Scrubbing System Design for CO_2 Capture in Coal-Fired Power Plants

Scrubbing System Design for CO_2 Capture in Coal-Fired Power Plants

Von der Fakultät für Ingenieurwissenschaften, Abteilung Maschinenbau und Verfahrenstechnik

der

Universität Duisburg-Essen

zur Erlangung des akademischen Grades

einer

Doktorin der Ingenieurwissenschaften

Dr.-Ing.

genehmigte Dissertation

von

Elizabeth Heischkamp
aus
Tampico, Mexiko

Gutachter:	Univ.-Prof. Dr.-Ing. habil. Klaus Görner Univ.-Prof. Dr. techn. Günter Scheffknecht
Tag der mündlichen Prüfung:	20.02.2017

Fortschritt-Berichte VDI

Reihe 3

Verfahrenstechnik

Dipl.-Ing. Elizabeth Heischkamp,
Mülheim a. d. Ruhr

Nr. 953

Scrubbing System Design for CO_2 Capture in Coal-Fired Power Plants

LUAT Lehrstuhl für Umweltverfahrens-technik und Anlagentechnik

Heischkamp, Elizabeth
Scrubbing System Design for CO_2 Capture in Coal-Fired Power Plants
Fortschr.-Ber. VDI Reihe 3 Nr. 953. Düsseldorf: VDI Verlag 2017.
194 Seiten, 72 Bilder, 23 Tabellen.
ISBN 978-3-18-395303-5, ISSN 0178-9503,
€ 71,00/VDI-Mitgliederpreis € 63,90.

Keywords: CO_2 capture – chemical absorption – post-combustion – CCS – simulation – absorber intercooling

Within the last decades a continuous tightening of environmental regulations has been observed in several countries around the world. These include restriction of anthropogenic CO_2 emissions, since they are considered responsible for intensifying global warming. Coal-fired power plants represent a good possibility for capturing CO_2 before it is emitted in the atmosphere, thereby contributing to combat global warming. This work focuses on reducing the CO_2 emissions of such a power plant by 90 %. For this purpose a hard coal power plant is retrofitted with a chemical absorption using different solutions of piperazine promoted potassium carbonate. The resulting power plant's efficiency losses have been accounted for. A comparison of different scenarios such as the variation of operating parameters offer an insight in detecting suitable operating conditions that will allow to minimize efficiency penalties. Simulation details are provided along with a technical and an economic analysis.

Bibliographische Information der Deutschen Bibliothek
Die Deutsche Bibliothek verzeichnet diese Publikation in der Deutschen Nationalbibliographie; detaillierte bibliographische Daten sind im Internet unter http://dnb.ddb.de abrufbar.

Bibliographic information published by the Deutsche Bibliothek
(German National Library)
The Deutsche Bibliothek lists this publication in the Deutsche Nationalbibliographie (German National Bibliography); detailed bibliographic data is available via Internet at http://dnb.ddb.de.

Von der Fakultät für Ingenieurwissenschaften,
Abteilung Maschinenbau und Verfahrenstechnik
der Universität Duisburg-Essen
genehmigte Dissertation
Gutachter:
Prof. Dr.-Ing. habil. Klaus Görner
Prof. Dr. techn. Günter Scheffknecht
Datum der mündlichen Prüfung:
20.02.2017

Als Manuskript gedruckt. Printed in Germany.
ISSN 0178-9503
ISBN 978-3-18-395303-5

Acknowledgements

This work was developed while I was a member of the research staff at the Chair for Environmental Process Engineering and Plant Design (LUAT from the name in German) in the Faculty of Engineering, Department of Mechanical and Process Engineering at the University of Duisburg-Essen.

At this point, I would like to express my gratitude to many people who have supported me directly or indirectly in the completion of this dissertation. Special thanks go to my doctoral supervisor Prof. Dr.-Ing. habil. K. Görner, who encouraged me to do research in the field of advanced power plants and carbon capture technologies and who always supported me in pursuing my goals and interests. His unwavering support, patience, as well as the trust he granted me, have been a crucial contribution for this work's completion. I would like to thank Prof. Dr. techn. G. Scheffknecht for taking over the task of second referee and for his interest in my work. Prof. Dr. rer. nat. B. Atakan and Prof. Dr.-Ing. D. Bathen, thank you for your participation in the examination committee.

I would also like to thank current and former LUAT employees and students, who helped me in the creation of this work. I especially would like to thank my adviser Dr.-Ing. G. Oeljeklaus, to whom I am most grateful. His continuous contributions have had a great impact in my development as a researcher and as a person. Doing research with him was a real pleasure. Dr. rer. nat. P. Behr, thank you for having read my drafts so many times and for being able to explain chemical phenomena so easily. For all those real "Big Bang Theory" moments I would like to thank Dr.-Ing. H. Yilmaz, Dr.-Ing. Ö. Korkmaz, Dr.-Ing. T. Klasen, M. Sc. S. Perumalsamy, M. Sc. A. Al-Zuhairi, Dr.-Ing. S. Multhaupt, Dr.-Ing. T. Vogel, M. Sc. L. Woetki and Dipl.-Ing. M. Varlik.

I am deeply grateful to my Mexican family: my parents, Roberto and Esther, and my sister, Ingrid, for their ongoing support of any kind and their immensurable source of motivation. This also applies to my German family, including my husband Peter and my kids Natascha and Ben. Thank you so much for supporting me, even if it often meant that you had to be left out for a while. Finally, I would like to express my gratitude to my sister Lilia. Words can hardly describe how thankful I am to her. Indeed, she went beyond the duties of a big sister by reading all of my drafts and discussing them with me countless times to assist me in the editing of

this work in what must have felt like forever. Thank you Lilia, I will be eternally grateful.

Mülheim an der Ruhr, 2017

Elizabeth Heischkamp

Index

Acronyms and abbreviations

AHPC	Activated Hot Potassium Carbonate
aMDEA	Activated Methyl Diethanolamine
AMP	2-Amino-2-Methyl-1-Propanol
ASU	Air Separation Unit
CaL	Calcium Looping
CAP	Chilled Ammonia Process
CAPEX	Capital EXpenditure
CLC	Chemical Looping Combustion
DCC	Direct Contact Cooler
DEA	Diethanolamine
DIPA	Diisopropanolamine
EPC	Engineering, Procurement, and Construction costs
ESA	Electric Swing Adsorption
EUA	European Emission Allowance
FG	Flue Gas
FGD	Flue Gas Desulphurisation
GDPC	Generalized Pressure Drop Correlation
GTCC	Gas Turbine Combined Cycle
GWP	Global Warming Potential
HETP	Height Equivalent to a Theoretical Plate
HP	High Pressure
HPC	Hot Potassium Carbonate
IEA	International Energy Agency
IEA GHG	IEA Greenhouse Gas R&D Programme
IGCC	Integrated Gasification Combined Cycle
IMTP	Intalox Metal Tower Packing
IP	Intermediate Pressure
IPCC	Intergovernmental Panel on Climate Change
IPFO	Interface-Pseudo-First-Order
L/G ratio	Liquid to Gas ratio
LCOE	Levelised Cost of Electricity
LHV	Lower Heating Value
LNG	Liquefied Natural Gas
LP	Low Pressure
MAPA	Methyl Amino Propylamine

MDEA	Methyl diethanolamine (also known as N-methyl diethanolamine)
MEA	Monoethanolamine
NRTL	Non-Random Two-Liquid
OPEX	OPerational EXpenditure
PIP	Piperidine
PSA	Pressure Swing Absorption or Adsorption (as the case may be)
PYR	Pyrrolidine
PZ	Piperazine
RPP NRW	Reference Power Plant NRW
TA-Luft	Technische Anleitung zur Reinhaltung der Luft – Technical Instructions on Air Quality Control
TEA	Triethanolamine
TSA	Temperature Swing Adsorption
UOM	Unit Operation Model
VLE	Vapour-Liquid Equilibrium
WoI	Working Investment
ZEP	Zero Emissions Platform
ZEP PP	Zero Emissions Platform reference Power Plant

Nomenclature

A	[m^2]	Heat transfer area
a	[-]	Annuity factor
A_T	[m^2]	Column cross-sectional area
b	[mol/kg] also [m]	Molality
c	[mol/L] also [M]	Molarity
CaI_{fixed}	[M€]	Fixed capital investment
$CAPEX$	[€/MW]	Capital expenditure
C_{av,CO_2}	[€/t_{CO_2}]	CO_2 avoidance cost
C_{fuel}	[€/MWh]	Levelised fuel cost
$Column_i$	[M€]	Price of selected reference column
$Compressor$	[M€]	CO_2 compressor investment
CP	[(m/s)$(m^{-1})^{0.5}(m^2/s)^{0.5}$]	Capacity factor (packed towers)
C_s	[m/s]	C-factor based on tower superficial cross-sectional area
d	[m]	Column diameter
DC_{total}	[M€]	Total direct cost
E	[kJ/kmol]	Activation energy
e_b	[t_{CO_2}/MWh]	Specific CO_2 emission factor for hard coal
$e_{CO_2,CC}$	[t_{CO_2}/MWh]	Specific CO_2 emissions of RPP NRW with carbon capture
$e_{CO_2,ref}$	[t_{CO_2}/MWh]	Specific CO_2 emissions of RPP NRW
F	[m/s$(kg/m^3)^{0.5}$]	F-factor for gas loading
F_{LG}	[-/-]	Flow parameter
F_p	[m^{-1}]	Packing factor
F_p	[m^{-1}]	Packing factor
G	[kg/(s·m^2)]	Gas phase mass velocity
h	[h]	Operating hours
h	[m]	Packing height

H_u	[kJ/kg]	Lower heating value
i	[mol/L]	species *i* concentration
IC_{total}	[M€]	Total indirect cost
$ISBL$	[M€]	Inside the battery limits
k	[mol/(l·s)]	Pre-exponential factor (independent of temperature)
k	[W/m^{2}K]	Heat transfer coefficient
k_a	[-]	Activity-based rate constant
k_c	[-]	Concentration-based rate constant
L	[kg/(s·m^2)]	Liquid mass velocity
L/G	[l/m^3]	Liquid to gas ratio
$LCOE_{CC}$	[€/MWh]	Cost of electricity with carbon capture
$LCOE_i$	[€/MWh]	Levelised cost of electricity
$LCOE_{ref}$	[€/MWh]	RPP NRW's levelised cost of electricity
$\dot{m}_{CO_2}$	[kg/s]	CO_2 mass flow rate
$\dot{m}_{fuel}$	[kg/s]	Fuel mass flow rate
n	[-]	Temperature exponent
N_i	[kmol/(m^{2}s)]	species *i* molar flux
$OPEX$	[€]	Operational expenditure
$OSBL$	[M€]	Outside the battery limits
P	[W]	Power
$P_{compression}$	[kW]	Electric demand by compression
p_{des}	[bar]	Desorber pressure (gauge)
$P_{expansion}$	[kW]	Electric demand by expansion
P_i	[MW]	Power plant net output
p_{ref}	[bar]	Reference pressure
$\dot{Q}$	[W]	Heat duty, heat transfer capacity (heat exchanger)
r	[mol/(l·s)]	Reaction's rate
r	[-]	Interest rate

R_{CC}	[%]	CO_2 capture rate (0% < R < 100%)
R_{CO_2}	[kJ/kg·K]	CO_2 gas constant
$Solvent$	[M€]	Solvent cost
$Startup$	[M€]	Start-up cost
T	[K]	Reference temperature (298.15K)
T	[-]	Plant life
T_{amb}	[bar]	Ambient temperature
u_s	[m/s]	Superficial gas velocity
$\dot{V}_G$	[m^3/s]	Gas rate
V_{new}	[m^3]	New column's packing volume
V_{ref}	[m^3]	Reference column's packing volume (MEA Case I)
w_{comp}	[kJ/kg]	Specific compressor work
x_i	[-]	species *i* fraction of reactant
x_i	[-]	reactant species *i* mole fraction
x_i	[kmol/kmol]	species *i* liquid phase mole fraction
y_i	[kmol/kmol]	species *i* gas phase mole fraction

Greek symbols

α	[$mol_{acid\ gas}/mol_{alkalinity}$]	Loading
α_i	[-]	species *i* reaction order
α_{lean}	[$mol_{CO_2}/mol_{alkalinity}$]	Lean loading
α_{rich}	[$mol_{CO_2}/mol_{alkalinity}$]	Rich loading
δ	[m]	film thickness
ρ_G	[kg/m^3]	Gas density
ρ_L	[kg/m^3]	Liquid density
$\Delta\theta$	[K]	Temperature difference
$\Delta\eta$	[% points]	Efficiency losses due to CCS
γ	[-]	activity coefficient

η	[-]	Efficiency
η_i	[-]	Power plant net efficiency
η_{is}	[-]	Isentropic efficiency
η_{ref}	[%]	RPP NRW's net efficiency
ν	[m^2/s]	Kinematic viscosity of liquid

Subscripts	
el	electric
flood	at flood
i	RPP NRW or carbon capture (CC)
PZ	Piperazine

Superscripts	
B	bulk
gross	gross value
G	gas
i	species i
I	interface
L	liquid
net	net value
ref	reference

1 Introduction

1.1 Research motivation

Within the last decades humanity has witnessed the growing effect of climate change. The so called *greenhouse effect* is held responsible for this phenomenon, which has been caused by increasing CO_2 emissions. There are both natural and anthropogenic sources of CO_2. The first ones come from volcanic gases as well as from human and animal respiration process. Anthropogenic ones are produced from fossil fuel combustion used for energy generation in the industrial, transport and domestic sectors [1]. Anthropogenic emissions of CO_2 have led to a serious environmental problem. There are in fact other gases like Methane (CH_4) or nitrous oxide (N_2O), whose global warming potential (GWP) of 21 and 310 respectively is higher than that of CO_2 with a GWP of 1 [2]. However, given the amount of emitted CO_2 compared to those gases, it has become imperative to reduce anthropogenic emissions of CO_2 [3].

A special IPCC[1] report [1] lists five technological options to abate anthropogenic CO_2 emissions:

- *Reduction of energy consumption,* for example by increasing efficiency of energy conversion and/or utilisation.
- *Substitution of fuels for less carbon intensive ones,* i.e. switching from coal to natural gas.
- *Increase use of renewable energy sources or to nuclear power[2],* which produce less or no net CO_2 at all.
- *Natural storage of CO_2* by enhancing biological capacity in forests and soils.
- *Chemical or physical capture and storage of CO_2*.

The implementation of such alternatives has already been taking place since the past decades. However, options like switching to use less carbon intensive fuels implicate a growing dependency on foreign resources for countries like Germany, where little or no natural gas is to be found. Considering the available resources of natural gas worldwide and comparing them with coal, both lignite and bituminous, it makes sense not to abandon coal. This fossil fuel accounts for about 43.8 % of the electricity generation in Germany [4]. Moreover, according to the International

[1] IPCC – *Intergovernmental Panel on Climate Change.*
[2] Not a feasible option in Germany due to political reasons since the nuclear disaster in Fukushima in 2011.

Energy Agency (IEA) in the World Energy Outlook 2012 [5], between 2010 and 2035 demand for electricity expands annually between 1.7 % and 2.6 % depending on the contemplated scenario. Consequently, generating capacity increases by almost three quarters, from 5,429 GW in 2011 to 9,340 GW by 2035. As stated in the World Energy Outlook 2012 coal remains globally the backbone fuel for electricity generation and, in absolute terms, its use for this purpose continues to raise, albeit its share of total generation falls from 41 % in 2011 to 33 % in 2035 [5].

Since dismissing coal as an energy source is not likely to be a viable option, the capture, transport and storage of CO_2 seem to be an alternative to containing global warming, while at the same time being able to meet the worldwide growing energy demand. Technology for CO_2 capture from flue gases is in fact commercially available and currently in use within the oil (for enhanced oil recovery – EOR), chemical and food industries, but not in the scale required for a 500 MW_{el} power plant, where approximately 8,000 t/d of CO_2 would make out for about 90 % of its total emissions. The biggest commercial plants are designed to capture 1,000, 800 and 300 t/d of CO_2 in the oil, chemical and food industries respectively [6]. Although a scale-up might be an initial obstacle for implementation of this technology, the actual major drawback for post-combustion capture of CO_2 from coal-fired power plants is the high energy demand required for regeneration of solvents used within CO_2 scrubbing plants. The power plant itself would provide this energy, which implies that the power plant's net electric work would be reduced as well as its efficiency. Given that the electricity demand remains constant, more fossil fuels would have to be consumed, in order to be able to supply the same amount of electricity; which also means, that more CO_2 emissions would be generated. In order to counteract this tendency, a way must be found to efficiently produce electricity with coal and reduce CO_2 emissions at the same time.

1.2 Analysis procedure

This work focuses on reducing CO_2 emissions of an advanced coal-fired power plant and the main objective is to keep related efficiency losses as low as possible. To this end different configurations of the scrubbing process are analysed and their impact on a coal-fired power plant determined, for which previous integration is necessary. Moreover, an economic study of the best detected technical solutions pretends to give an insight on their feasibility.

The analysis begins with a flue gas preconditioning step. Aqueous solutions of alkanolamines have been used for reactive absorption since the 1930s [7]. In gen-

eral, solvents can suffer from thermal and/or chemical degradation. This can be observed at high temperatures, as well as at high acid gas concentrations. Chemical degradation also occurs when the used solvent does not only react with the desired gas, but also with impurities like SOx or NOx that are present within a flue gas. By-products of these reactions are heat stable salts that lower the absorption capacity of the solvent. If a coal-fired power plant was to be retrofitted with a CO_2 scrubbing process, an intermediate flue gas conditioning step would have to be implemented between the conventional flue gas desulphurisation (FGD) and CO_2 scrubber, to prevent solvent degradation. This step includes cooling, treating and blowing of the flue gas previous to reaching the CO_2 scrubbing process, which implicates additional energy penalties and costs. This extra flue gas conditioning step has been accounted for in this work. In addition, a study on different operating parameters of an SO_2-absorber has been conducted. The commercial software Aspen Plus® V7.1 has been used for modelling this work's section.

In recent years, research has been focused on the pursuit of new solvents that require less energy for their regeneration, which would represent a possible solution to avoid power plants' efficiency losses [6], [8], [9]. While such solvents are certainly important, they alone do not account for the whole energy penalties of a power plant. The scrubbing process configuration might be almost as important as the solvents in use. A proper integration of the scrubbing process with the power plant also plays a key role in avoiding efficiency penalties. As Figure 1.1 shows, successful post combustion capture process design and optimisation require considering the following areas: *solvent selection, scrubbing process performance and integration with the power plant* [10]. These factors affect each other, making it indispensable to keep all three in mind when altering one of them.

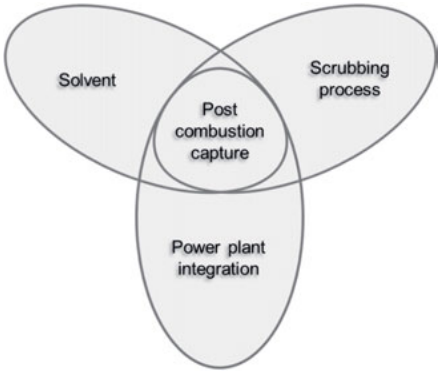

Figure 1.1: Areas involved in post combustion capture process design and optimisation [10]

Scrubbing process representation requires a fairly good prediction of the chemical phenomena that occur in such a system. To this end the simulation software Aspen Plus® versions 2006.5 and 7.1 has been used. With this tool it is possible to make several parameter variations of the main components in the absorption process: *absorber, heat exchanger and desorber*. In addition, different solvents have been contemplated: *aqueous solutions of monoethanolamine (MEA) and different blends of piperazine activated potassium carbonate*. The parameter variations intend to quantify and compare energy duties, which help identify possible energy savings in the overall system power cycle – capture plant.

The results delivered from the scrubbing process operating conditions variation can then be used for a first integrating approach with a coal-fired power plant. In this case the most promising blend of piperazine activated potassium carbonate was used, as well as two MEA cases based on literature data. The location of the steam tapping for regeneration of solvent depends on steam parameters required in the stripper column, which are dependent of its operating conditions.

The outcomes of parameter variations conducted in several simulations of the scrubbing process, power plant and flue gas conditioning can finally be accounted for in a last integration step, where all the determined parameters that present the lowest energy consumption effect are implemented. In addition, results are contemplated in a techno-economic analysis that makes it possible to compare different scenarios and show the lowest price that CO_2 emission allowances have to have, in order to make coal-fired power plants with carbon capture a feasible alternative to combat climate change.

1.3 Electricity generation with coal

In the power generation sector there are not only several ways to produce electricity, but also different ways to capture CO_2 from emitted flue gases. The method that will be considered throughout this whole work is power generation with an advanced coal-fired power plant, for which post-combustion capture of CO_2 will be implemented.

1.3.1 Coal-fired power plants – State of the art technology

There are two main types of coal that can be used in this sort of power plants: brown and hard coal. They differ from each other in their composition. Hard coal exhibits a lower content of water and ash than brown coal and hence, its lower

heating value is higher, which has a positive impact in overall plant efficiency. The working principle for both types of coal remains the same. Coal is combusted in a boiler. Produced heat is used to evaporate water at supercritical pressure (>250 bar). Steam drives a turbine, which is connected to a generator.

Performance or efficiency of a power plant can be expressed in terms of the output to required input energy as

$$\eta = \frac{output}{required\ input} \tag{1.1}$$

Electrical efficiency is frequently used to compare quality of power plants. The output is the saleable energy, while the input is the product of the lower heating value with the required mass flow rate of coal. The net output of a power plant indicates available electric energy of a power plant, after the station's supply has been deducted.

$$\eta_{el} = \frac{P_{el,net}}{\dot{m}_{fuel} \cdot H_u} = \frac{P_{el,\,gross} - P_{el,\,auxiliary}}{\dot{m}_{fuel} \cdot H_u} \tag{1.2}$$

Worldwide there are significant differences in average efficiency rating for coal-fired power plants. Global average accounts for an efficiency of 30 %. German hard coal average is 38 % [11]. Modern power plants reach an efficiency of 46 % [12] and the world record is 47 % [13]. An important factor to consider is the influence of environmental conditions, which strongly depends on the geographical location of a power plant.

1.3.1.1 Reference Power Plant

Technology used in state of the art power plants in Germany corresponds to that of the Reference Power Plant NRW (RPP NRW). This is the power plant used as a basis for this work. Main technical parameters can be found in Table 1.1.

A thermodynamic model of RPP NRW is shown in Figure 1.2. The water/steam cycle consists of a steam generator, a turbine set that includes a high, an intermediate and two low pressure turbines, two feedwater pumps and –including the feedwater tank– a total of eight feedwater preheaters, out of which the first five operate at low pressure and the last three at high.

Table 1.1: Generic technical parameters of RPP NRW [11]

Parameters		RKW NRW
Lower heating value (black coal)	GJ/t	25
Net electricity output	MW_{el}	555.6
HP Turbine steam inlet	bar	285
HP Turbine inlet temperature	°C	600
IP Turbine inlet steam reheat temperature	°C	620
Net full load plant efficiency	% LHV[3]	45.9
Plant load factor	h/year	7500
Plant life	Years	40
CO_2 Emissions from calculated fuel carbon content	kg/MWh	750

The water/steam cycle works as follows: after the feedwater has been preheated, it enters the steam generator, where it will be evaporated and superheated to 600°C at 285 bar. Steam then enters a single-flow high pressure (HP) turbine. Before the steam has been completely expanded, the turbine is tapped twice. Resulting steam flow rates are used in the second and third feedwater preheaters.

Remaining steam is led to the boiler and is reheated to 620°C at a pressure of 60 bar, before it reaches a double flow intermediate pressure (IP) turbine. During the expansion, this unit is tapped three times. These steam flow rates are used for the first (HP) feedwater preheater, feedwater tank, and fourth low pressure (LP) pre heater. The residual steam is then split previous to entering two LP turbines. In this last step, steam is expanded to a condenser pressure of 45 mbar, but not without having tapped the turbines once more in order to use partial flows in the first three (LP) feedwater preheaters. As soon as water has been collected from the condenser, it is led with pumps through the feedwater preheaters, to complete the cycle.

In addition to the water/steam cycle, Figure 1.2 also displays the air/flue gas path. This path begins with air and coal preconditioning, which consists in preheating ambient air to a temperature of 350°C and delivering it to the furnace with a fan. Parallel to ambient air, coal is also preheated to the same temperature. Once both, air and coal, have been delivered to the furnace, combustion takes place. RPP NRW's operating conditions assume combustion at an air ratio of 1.15. Within the furnace, air and coal form a mixture that consists of hot flue gas and ash at a temperature of approximate 380°C.Flue gas is then led to a denitrification unit (DENOX), followed by an air heater. This unit's task is to cool it down to a temper-

[3] Low heating value.

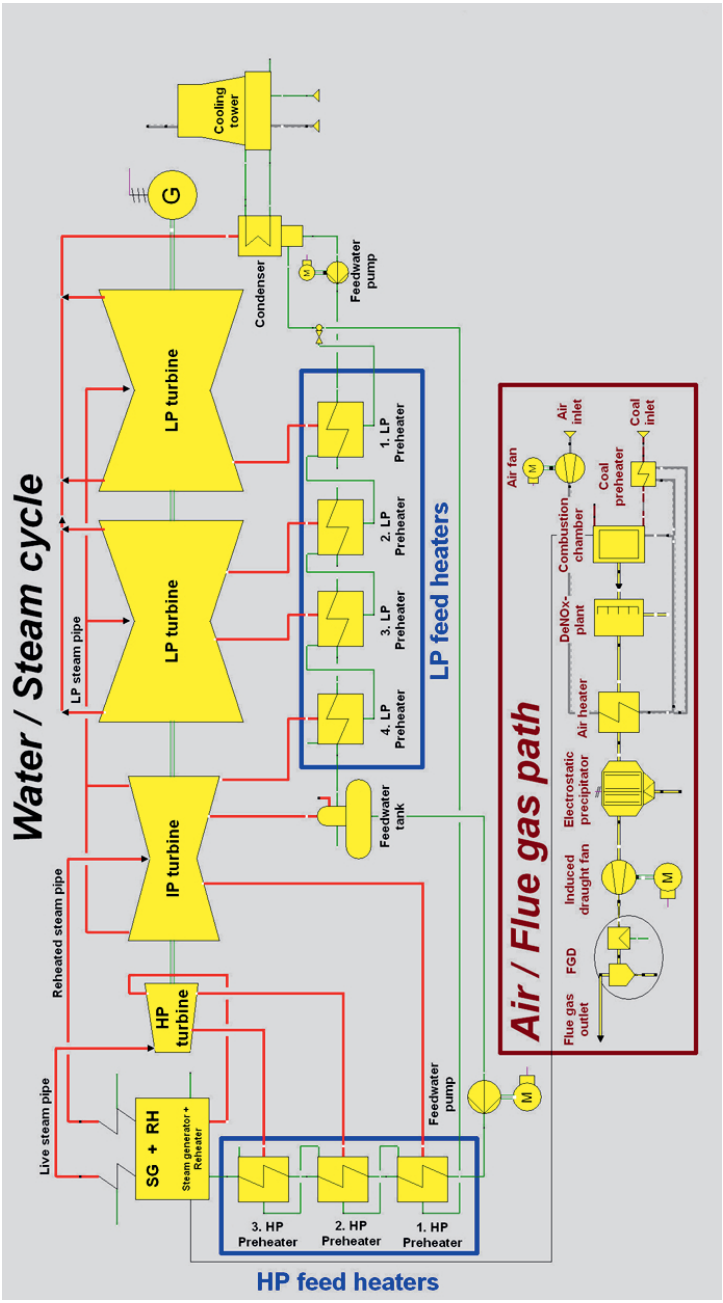

Figure 1.2: Process flowsheet of RPP NRW in EBSILON®Professional [14]

ature of around 115°C and preheat ambient air to the required temperature of 350°C. Once the flue gas has passed through the air heater, it reaches the electrostatic precipitator for dust removal. An induced draught fan is then required for flue gas prior to entering a desulphurisation unit (FGD). After this last step, flue gas can finally be emitted through a cooling tower to the atmosphere at a temperature of about 50°C.

To be able to choose an adequate technology for capturing CO_2 from flue gas of a coal-fired power plant, several characteristics have to be considered, which will be discussed in shortly.

1.3.2 CO_2 reduction alternatives in coal-fired power plants

CO_2 capture in conventional power plants is often classified in three categories: *Pre-combustion, oxy-fuel* and *post-combustion capture*. They differ from each other in location, where the actual capture occurs. Strictly speaking CO_2 capture of an oxy-fuel process takes place after combustion and thus it might be considered as a special case of post-combustion capture, although some might argue that the actual gas separation takes place before combustion and hence an oxy-fuel process should belong to pre-combustion capture.

To determine where capture should take place, conditions of CO_2-laden gas stream have to be considered, and they are dependent on the kind of power plant technology used. Figure 1.3 and Figure 1.4 show different types of fossil fuel power plants and technology options according to Rubin [15] that affect selection of a CO_2 capture system. For example, some of the factors that affect the content of CO_2 in the resulting flue gas are:

1. *Type of fuel*. Due to its composition, coal exhibits higher specific CO_2 emissions than natural gas does.
2. *Type of oxidant*. It makes a significant difference if air or oxygen is used for combustion. In an air environment the content of CO_2 is much lower (3-5 Vol.-% for natural gas and approx. 15 Vol.-% for coal) than in an oxygen environment (80 Vol.-% and higher).
3. *Kind of technology used in power plant*. The specific emissions with the single cycle technology are –due to the lower overall efficiencies– higher than with the combined cycle one.

As a result of the different operation conditions, there are three main CO_2 capture categories whose characteristics are described by Herzog [16] as follows:

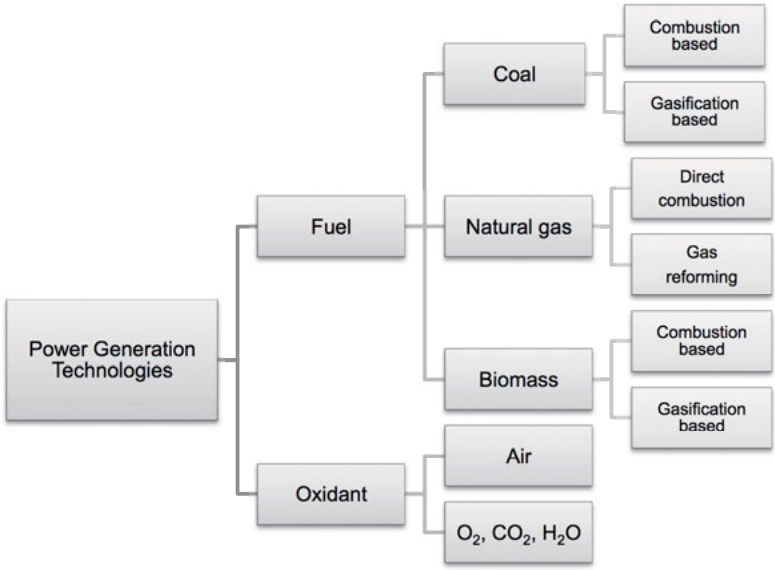

Figure 1.3 Technology Options for Fossil-Fuel based Power Generation [15]

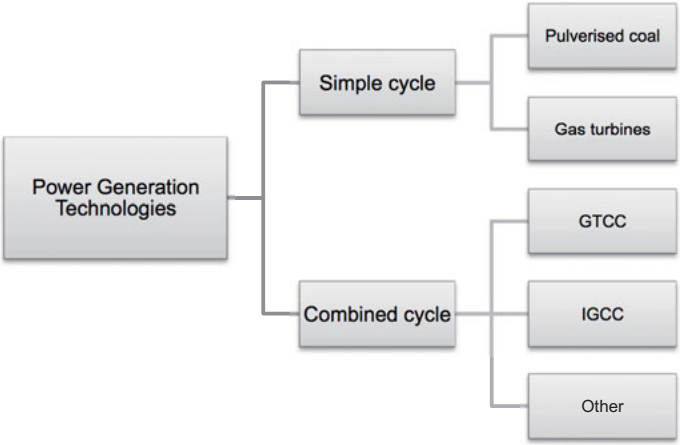

Figure 1.4 Further Technology Options for Fossil-Fuel based Power Generation [15]

1.3.2.1 Pre-Combustion Capture

As the name suggests, capture takes place before combustion which is only feasible by using gasifier technology. This option offers some advantages. To begin with, CO_2 has not yet been mixed and thereby diluted by combustion air. In addition, the CO_2 rich stream stands at high pressure. This enables the use of more efficient capture techniques, like pressure swing absorption (PSA) in physical solvents like methanol or polyethylene glycol. Commercial names of these separation methods are Rectisol and Selexol [16]. Due to the high pressure of the CO_2 main stream, Pre-combustion capture can be applied in Integrated Gasification Combined Cycle (IGCC) power plants. This process begins with coal gasification to produce a synthesis gas that consists of CO and H_2O. In a water-gas shift-reaction CO and H_2O react to CO_2 and H_2 respectively. CO_2 can then be captured and H_2 can be used in a turbine to produce electricity. Since hydrogen is a gas with a high LHV (approx. 120 MJ/kg) , the H_2 stream can also be bled off for separate use [16].

1.3.2.2 Oxy-Fuel Combustion

Conventional coal-fired power plants have a CO_2 content of approximate 15 Vol.-% and gas-fired power plants 3-5 Vol.-%. These values consider air as oxidant. Combustion in a rich or pure oxygen environment increases CO_2 content of the flue gas to approximate 80 Vol.-% and higher, which facilitates capture. That is exactly the principle behind this kind of technology [17]. Oxygen is selected from the rest of air components in an air separation unit (ASU), so that combustion takes place in pure or enriched oxygen ambient. The resulting flue gas contains almost only CO_2 and H_2O. As a result of combusting fuel in pure oxygen, flame temperature is extremely high. To counteract this, a part of the flue gas has to be recycled into the combustion chamber [18]. Albeit CO_2 is free from water after the main flue gas stream has run through a condenser, the effluent still shows minor impurities such as SO_2, NO_x and non-condensables like oxygen and nitrogen, so that a clean-up is required before CO_2 can be compressed and transported for its storage [17].

In order for oxy-combustion capture to be competitive with post-combustion capture, it is necessary to have more operating experience with this technology. That is why Vattenfall started the operation of a 30 MW_{th} oxy-combustion pilot plant in September 2008 at Schwarze Pumpe, Germany [17]. The main outcome of the first's years test phase is the verification of oxy-fuel combustion as a feasible pro-

cess at industrial scale. The produced CO_2 showed a high level of purity and a capture rate greater than 90 %. Operation results indicate that implementation of this kind of technology is safe and efficient and hence suitable for a demonstration project[4] [19].

Due to the high amount of energy required by the ASU, which can account for up to 15 % of a power plant's electric output, this unit is considered as the biggest hitch for this technology [16]. There are, though, alternative oxy-fuel technologies that operate without ASU. One of such processes is the one known as *chemical looping combustion* (CLC), which basically consists of a solid material used as oxygen-carrier circulating between two fluidised bed reactors. In one reactor the solid material assimilates oxygen from air, while in the second reactor the oxygen is released in an air free environment to react with fuel, thus producing a flue gas with high CO_2 content [20, 17].

1.3.2.3 Post-Combustion Capture

Actual CO_2 separation in this process takes place after the fuel has been combusted in excess air. In conventional coal-fired power plants, flue gas usually undergoes treating processes like denitrification and desulphurisation which have to comply with limits set in air pollution control policies that vary from region to region. Capture of CO_2 would take place after these processes.

The capture process is commonly based on a chemical absorption. Basically a solvent is used to chemically bind the CO_2 in the flue gas. The solvent is then regenerated by applying heat to it, which breaks the bond, thereby releasing the CO_2, which can then be prepared for its compression and later transportation.

Due to the fact that the combustion process stays untouched by the CO_2 scrubbing process, an existent power plant can be retrofitted to capture CO_2. This however implies that certain conditions have to be available like enough space within the power plant's yard in order to consider a retrofit as a viable option for coal-fired power plants in the future. In addition, it would be necessary to implement changes within the power cycle for the bleed of the turbines, as well as a tightened air pollution control limits to prevent solvent degradation, which implies an improvement of the current equipment or, again, enough space available.

[4] As reported by Schroeter in [19], Vattenfall announced the end of this project's operation by July 2014 due to lack of a legal regulatory framework. However, obtained results will still be used in the Canadian Boundary Dam carbon capture project, which represents one of the biggest CCS demonstration projects worldwide.

1.3.3 CO_2 capture technologies

There are commercially available technologies (see Figure 1.5). However their industrial applications were designed for a much smaller scale. Capture processes can be classified in absorption, adsorption, carbonate looping, cryogenics, membranes and microbial/algal systems [15].

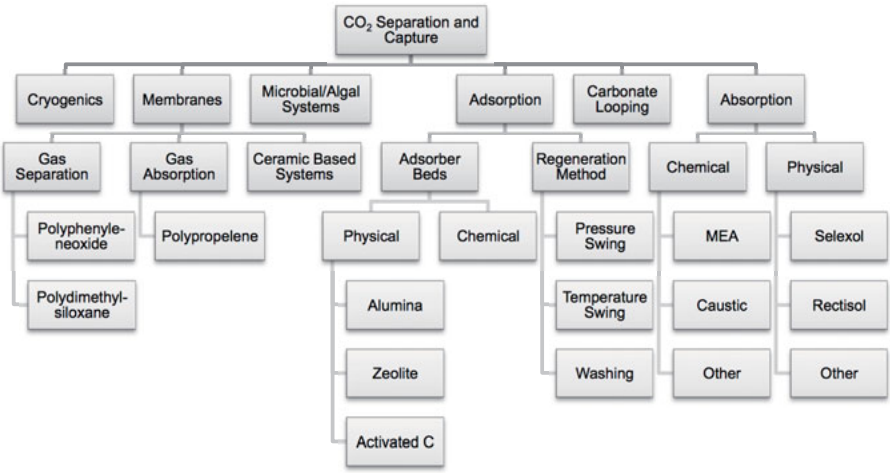

Figure 1.5 : Technology Options for CO_2 Separation and Capture [14]

1.3.3.1 Adsorption

According to [21] “Adsorption involves, in general, the accumulation (or depletion) of solute molecules at an interface (including gas-liquid interfaces, as in foam fractionation, and liquid-liquid interfaces, as in detergency).” They also mention gas-solid and liquid-solid interfaces. The first ones are the ones considered for the separation of CO_2 from a main flue gas stream. Adsorption accuracy depends on different factors such as temperature, partial pressure of the desired gas and adsorbent pore size [18]. There are two types of adsorption: physical and chemical. There are however adsorbent surfaces that can experience both of them, but since chemical adsorption tends to decrease the capacity of the adsorbent, then the physical type should be pursued. Some adsorbent examples are: aluminas, silicates and aluminosilicates, carbons and organic polymers [21].

The adsorption process consists of two main steps: adsorption and regeneration. In the first one a gas has to flow through a bed of solids, so that the desired gas is selected. Once solids have been fully loaded, they have to be regenerated. In or-

der to do this, the entering gas is directed to a second bed full of clean solids. The method applied for regeneration of the adsorbent gives the name to process, i.e. PSA stands for pressure swing adsorption, TSA for temperature swing adsorption and ESA for electric swing adsorption [18].

Gupta et al. [18] state that the problem for deploying adsorption for CO_2 capture of power plants' flue gases lies within the low CO_2 selectivity of adsorbents.

1.3.3.2 Cryogenics

This sort of technology is commercially available for CO_2 purification of streams with a high concentration of this gas (> 50 %). Hence, pre and oxy-fuel combustion are good candidates for this kind of capture method. In theory, this process can also be applied for flue gases with a low content of CO_2, such as the ones from coal or natural gas combustion, but given the high amount of energy required for refrigeration, it is not considered as a viable option [18]. Tuinier, et al. [22] consider the possibility to avoid the expensive refrigeration by exploiting the cold duty available at liquefied natural gas (LNG) regasification sites. Some of the advantages of cryogenic separation are: no chemical absorbents are needed; process can be operated at atmospheric pressure and it enables the direct production of liquid CO_2, which is required for transport and storage purposes [18, 22].

1.3.3.3 Membranes

They are a film barrier that acts like a filter, allowing permeation of a selected component from the gas contacting a membrane. Unlike common filters, they are capable of reaching separation up to a molecular level, thus able to compete with other processes such as Distillation and Adsorption [23]. According to Gupta et al. [18], there are two types of membranes that are considered for CO_2 capture: gas separation and gas absorption membranes. The driving force for separation in the first ones is the difference in partial pressures between both sides of the membrane. The second ones use gas on one side of the membrane and a liquid on the other side. The liquid absorbs the CO_2. Membrane gas absorption processes can also be referred to as membrane contactors, which combine the advantages of membrane technology with those of absorption technology [24].

A third kind of membranes is ceramic based and still remains at an early stage of development. These are fabricated from mixed protonic and electronic conductors and ceramic-metal (cermet) composites and are of interest for advanced coal-based power and fuel production technologies. It is expected, that by using this kind of membranes to separate hydrogen from a shifted syngas a higher concen-

trated CO_2 steam at higher pressures will be produced, which facilitates its capture [25].

A general trade-off relationship between permeability and selectivity has been observed, which basically states that the permeability and selectivity of a membrane are indirectly proportional to each other [26, 27, 28]. In other words, a problem with membranes is that unless several membrane stages are used, only a bulk separation of CO_2 will be reached. Hence, not only does the complexity to obtain high CO_2 purity increase, but also energy demand, as well as costs of such systems [29, 18].

1.3.3.4 Microbial/Algal Systems

The main idea behind this alternative consists in enhancing the growth of algae in artificial ponds by feeding them with captured CO_2 from flue gas. The harvest can then be used as food, feed, or fuel. Rather than considering algae as a sequestration method, it should be regarded as a neutralizing one, since CO_2 will reappear by combustion of produced biomass as a fuel, thereby releasing CO_2 from the flue gas once again into the atmosphere. The same thing will happen when using it as food or feed, CO_2 will be released upon respiration and digestion. To feed ruminating animals with algae might be a questionable procedure, considering that they produce Methane, whose GWP is twenty-one times that of CO_2 [16, 30].

1.3.3.5 Carbonate Looping

This is a rather recent alternative for post combustion capture of CO_2. This process operates with solids circulating between two fluidised reactors. In theory different types of materials can be used for this process, but due to its widespread availability natural limestone ($CaCO_3$) seems to be increasingly accepted, so that carbonate looping can also be referred to as *calcium looping* (CaL). This method is based on the reversible reaction between calcium carbonate and calcium oxide. Basically, flue gas is treated in a first reactor, where calcium oxide and CO_2 react to calcium carbonate at a temperature between 600°C and 650°C. In a second reactor the reverse reaction takes place in an oxygen rich environment provided by an ASU. This reaction is endothermic and thus occurs at a temperature above 850°C. As a result a flue gas with a low content of CO_2 leaves the first reactor, while a CO_2 rich gas leaves the second reactor [31]. Although this process requires an ASU, Hawthorne, et al. [32] reported an energy penalty of 6.3 % on the overall electric efficiency of a retrofitted coal-fired power plant with an original effi-

ciency of 45.6 % (LHV). This penalty does not only include the energy demand of the ASU, but also includes the energy requirement for CO_2 conditioning needed for transport purposes. In addition, though the sorbent suffers deactivation after a few cycles, and hence a constant make-up stream is indispensable, the waste product from the first reactor consists mainly of calcium oxide, which is used as feedstock for cement production.

1.3.3.6 Absorption

It is defined as assimilation and dissolving of a gas or vapour in a liquid [33]. Absorption can be classified into physical or physisorption and chemical or chemisorption. The solvent loading is a function of the partial pressure of the absorbed gas within the absorption unit [18].

In physical absorption the solvent loading behaves according to Henry's law, meaning an almost linear dependence on the gas partial pressure that is favoured by low temperatures. Given that no chemical bonding occurs in physical absorption, regeneration of the solvent used can be easily carried out by reducing the pressure, which also turns out to be cost effective [7].

In chemical absorption one or more components of a gas stream are assimilated in the solvent used. The absorbed components are first physically dissolved in the liquid and subsequently take part in one or more chemical reactions, which is why a high physical solubility is not necessary in chemical absorption [7]. The solvent loading –unlike physical absorption– does not behave according to Henry's law, but shows a rather non-linear dependence on partial pressure and is higher at low partial pressures [18]. The solvent is regenerated by applying heat to it, which is cost intensive, but given the continuous tightening of environmental emission specifications, chemical absorption has gained interest in the range of gas cleaning/purification within the last years, due to its high selective capacity, even at low partial pressures of the desired components [7, 33].

1.3.4 Alternative options for CO_2 emission reduction

Despite the fact that greenhouse gas emissions' rate should slow down, it has increased. According to data presented by Canadell, et al. [34], global carbon emissions due to human activities between 2000 and 2006 amounted to 9.1 Gt/a, from which 1.5 Gt/a correspond to land use change and the rest to fossil fuels. Apparently this is the highest rate since continuous monitoring was introduced back in 1959 and represents a significant increase compared to growth rates of past dec-

ades. While CO_2 capture technologies can be used to mitigate anthropogenic sources of CO_2, they are only appropriate for concentrated point sources such as power stations. CCS-Technologies, as well as the management of fossil fuel will not suffice to stabilise greenhouse gas concentrations at a minimum level of 430 parts per million carbon dioxide equivalent (CO_2e), as suggested by the IPCC.

A study by the *United Nations Environment Programme* (UNEP) emphasizes carbon management in living systems as a further feasible possibility to prevent serious climate change within the next decades [35]. This study states that managing ecosystems for carbon would not only contribute to reducing carbon emissions, but also help to actively remove carbon dioxide from the atmosphere at large.

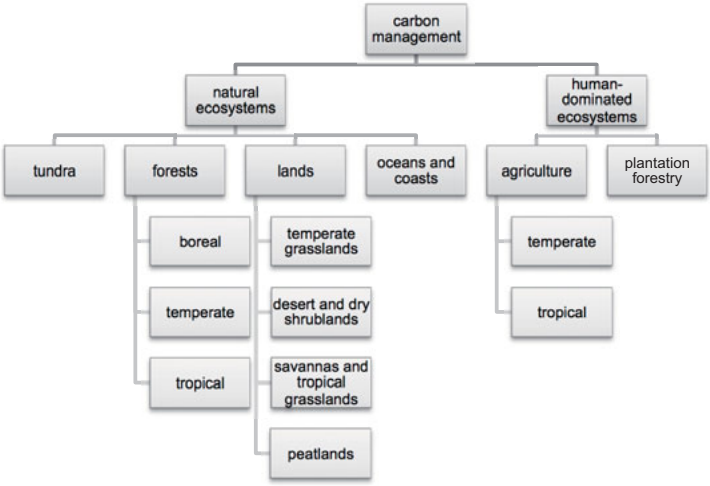

Figure 1.6: Carbon management in natural and human-dominated ecosystems with data from Trumper, et al. [35]

Figure 1.6 depicts different ecosystems susceptible to carbon management. While some of these are at present beyond direct control or technological intervention such as tundra or oceans[5], there are still many areas where both appropriate policies and direct interventions could have a major impact, such as: tropical forests, peatlands and agriculture. For example, by reducing deforestation rates by 50 % by 2050 and by keeping rates constant, it would be possible to avoid an emission of 50 Gt C, as indicated by Trumper, et al. [35]. This corresponds to 12 % of the

[5] Although large-scale experiments are being conducted to enhance CO_2 capture rate by photosynthesis, only limited human influence can be expected on the physical and purely chemical role of the ocean in the carbon cycle [35].

emission reduction required to keep atmospheric concentrations below the value suggested by the IPCC as previously mentioned.

Yet current land use practices will lead to significant increases in greenhouse gas concentrations. Indeed the UNEP study identifies agricultural systems as offering many opportunities for both carbon sequestration and emission reduction. Through this measure it could be possible to replenish highly depleted soil carbon stocks by adopting suitable techniques, which include conservation tillage and integrated nutrient management with compost and manure. In this respect the developing world has actually the greatest potential for increasing carbon storage in agricultural systems where apparently, according to Trumper, et al. [35], “lack of knowledge and access to appropriate technologies are major barriers to change.”

Overcoming barriers that help implement an effective ecosystem carbon management includes the commitment to capacity-building on a very extensive scale, along with carefully applied incentive-led systems. These include encouraging i.e. deforestation for the purpose of planting biofuels on marginal lands, since the value of forests as carbon stores overweighs any possible benefits to be obtained from biofuel harvests. However, by rising to these challenges, it is believed that Earth’s living ecosystems can have a tremendous effect to successfully create a climate change [35].

2 Downstream scrubbing of flue gases

Given its properties and over 60 years of experience in industrial applications, chemical absorption is considered a feasible option to capture CO_2 from coal-fired power plants.

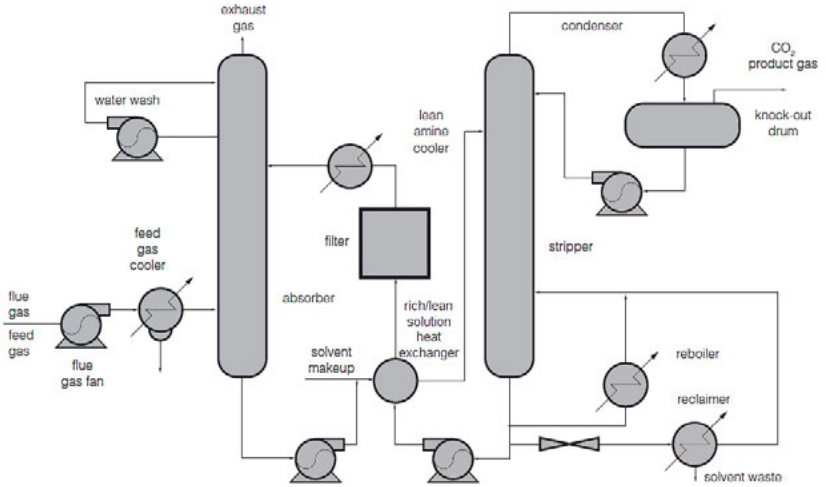

Figure 2.1: Process flow diagram for CO_2 capture from flue gas by chemical absorption [36, 1]

In chemical absorption, carbon dioxide reacts with a solvent. The standard regenerative absorber-desorber configuration is shown in Figure 2.1. This process begins with the flue gas been lead to an absorber column, where it is introduced at the bottom and a temperature of approximately 40°C. The flue gas is contacted countercurrently with a solvent, introduced at the top of the scrubber, or absorber column. To prevent species and aerosols carry-over, a wash section (not depicted in Figure 2.1) is included at the top of the absorber column. Afterwards, the clean flue gas can be emitted to the atmosphere while the solvent is recycled back into the column.

The solvent introduced at the top of the scrubber is called *lean solvent*, since it contains a little amount of CO_2 chemically bounded. In the same way, the solvent at the bottom of the column is called *rich solvent*. This last one is collected at the bottom of the absorber and then pumped through a heat exchanger to the stripper column.

For solvent regeneration, the reactions that took place in the absorber need to be reversed. This is achieved by heating the rich solvent, in the so called stripper column, where the solvent enters near the top. The applied heat is used for three purposes. First of all, though the liquid entering this unit has previously been warmed up in the heat exchanger, it has not yet reached the operating temperature required in this column and thus part of the applied heat is used for this purpose. Another part of the delivered heat is used to boil up a portion of the solution, in order to generate steam that acts as a transport medium for CO_2. The third and remaining part of the applied heat is used for solvent regeneration purposes. As regeneration occurs, CO_2 is released and ascends to the column's top, while lean solution accumulates at the bottom. Gas leaving the stripper column does not only consist of CO_2, but it is rather a mixture of steam, CO_2, and rests of reagent. By cooling this stream down, it condensates and can be sent back to the scrubbing cycle, whereas the CO_2 can be sent to a compressor previous to its transport. Lean solvent leaves the stripper column at the bottom, is pumped through the heat exchanger and, since its temperature still is not low enough to enter the absorber, it has to be further cooled down before being able to finally close the cycle.

2.1 Solvents in chemical absorption

Alkanolamine solvents are widely used in sour gas sweetening. The kind of amine used depends on each process specifics [37]. The most frequently encountered amine used for capture of CO_2 from flue gases is monoethanolamine [36]. Figure 2.2 shows other alternatives to alkanolamines that can be used for the same purpose. Strictly speaking, solvents are either organic or inorganic; however, there is a third category shown in Figure 2.2: *blends*. The use of amine blends is indeed not new and rather widespread, but in the last years new blends consisting of both an organic and inorganic solvent have emerged. This will be further discussed in the following sections.

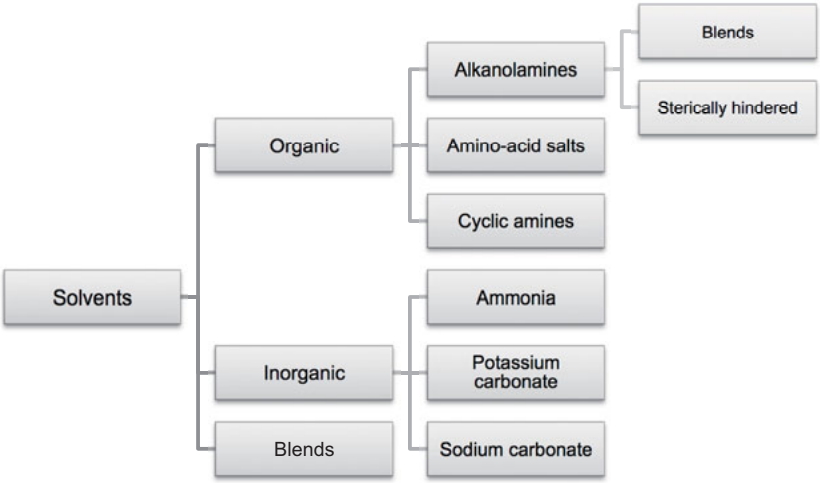

Figure 2.2: Solvents for chemical absorption of CO_2

2.1.1 Organic solvents

These can be categorized in the following main groups: alkanolamines, amino-acid salts and cyclic amines.

2.1.1.1 Alkanolamines

They are amines that feature at least one hydroxyl group besides an amino group. Alkanolamines are derivatives of ammonia, which can be achieved by substituting hydrogen atoms for alkanol, alkyl and/or aryl groups [7]. Depending on the number of substituents at the nitrogen atom, amines can be classified as: *primary*, like MEA, *secondary*, like DEA and DIPA, and *tertiary*, like MDEA and TEA. According to [38] primary and secondary amines react in the same order of magnitude, whereas tertiary ones react at least two to three orders of magnitude less.

CO_2 capture by chemical absorption is based on a reversible reaction of a weak alkanolamine base with CO_2 to produce a water-soluble salt. The reaction's direction of equilibrium is temperature dependant and can be simplified as follows [36]:

$$CO_2 + 2RNH_2 \leftrightarrow RNHCOO^- + RNH_3^+ \tag{2.1}$$

In primary and secondary amines, it is possible to substitute hydrogen atoms by other compounds with an available nitrogen atom. According to reaction (2.1) the

capacity of primary and secondary amines can reach approximately 0.5 mol CO_2 per mol amine within the rich solution. The product of this reaction is species $RNHCOO^-$, which is a carbamate ion. The capacity of formation of this ion is an important property for absorption of CO_2, given that this reaction occurs fast and hence high absorption rates can be reached [7]. However, carbamate formation means that CO_2 underlies a stable chemical bond with the solvent, which will require a substantial amount of energy for its regeneration [39].

Since tertiary amines lack a hydrogen atom attached to nitrogen, they are not capable of forming carbamates and react instead to bicarbonate ions (see equation (2.2)) [36]. As a result, lower absorption rates are attained. Yet, tertiary amines possess a higher capacity than primary and secondary ones. Besides, the resulting chemical bond is not as stable as a carbamate ion and therefore less energy is required to break it for means of solvent regeneration [39].

$$CO_2 + R_3N \overset{H_2O}{\longleftrightarrow} HCO_3^- + R_3NH^+ \tag{2.2}$$

$$CO_2 + OH^- \leftrightarrow HCO_3^- \tag{2.3}$$

Among commercial alkanolamines MEA has a relatively high reaction rate. In addition, it has a low solvent cost, a low molecular weight and hence high absorbing capacity on a mass basis, as well as reasonable thermal stability and thermal degradation rate. The reason for trying to find new amines for chemical absorption lies in the disadvantages of MEA. These include: high energy requirement for regeneration due to formation of stable carbamate and of undesired degradation products by reacting with COS or oxygen-bearing gases; vaporisation losses due to high vapour pressure; and more corrosive effects than many other alkanolamines, making the use of corrosion inhibitors unavoidable when used in higher concentration [36].

Blends

As an alternative to finding new amines, there is also the possibility of mixing existing ones, the so called blends. The idea is to try to maximise their advantages and restrict disadvantages, in other words, to reach high reaction rates of primary and secondary amines with higher CO_2 absorption capacity, lower corrosion rate and lower energy requirement for regeneration of tertiary amines [7].

Blends can be found in industrial praxis, like aqueous solutions of MEA/MDEA or DEA/MDEA. The aMDEA Process from BASF is also a good example, in which

the advantages of secondary and tertiary amines have been successfully combined [7].

Sterically hindered amines

In this kind of amines a bulky alkyl group is attached on the amino group and, as a result of that reactivity is different from alkanolamines [18]. According to Feron [40], the reaction of CO_2 with these amines produces bicarbonate and a protonated amine, so that absorption capacity approaches 1 mole per each mole of CO_2, which is double as much as MEA with respect to carbamate formation. This contributes to reduce solvent circulation rate, which is one of the most important factors in the economics of gas treating with chemical solvents, so that high capital costs can be spared [41]. Moreover, thermal energy requirements for solvent regeneration are expected to be lower than the MEA process. Feron [40] claims that by avoiding carbamate formation the binding energy is reduced by $10\ kJ/mol_{CO_2}$.

Although some energy savings might have been detected by using sterically hindered amines, da Silva and Svendsen [42] conclude that steric hindrance is only one of several effects contributing to relative carbamate stability. They reached this conclusion after having studied carbamate stability of a series of amines - including sterically hindered ones- using ab initio methods and free-energy perturbations. In their study, they caution on the use of the term “sterically hindered”, since it conveys an “overly simple physical interpretation of carbamate stability”. According to da Silva and Svendsen [42] steric hindrance does have a notable effect on carbamate stability, but nevertheless there are other effects such as intramolecular hydrogen bonding and variations in solvation energy that can as well dominate and hence, it would not seem that carbamate stability can be explained in terms of a single molecular property. In a later study, da Silva and Svendsen [43] also state that solvent stabilisation, electron donation and withdrawal through bonds, as well as sterical effects are factors that determine the strength of amines as bases and stability of the carbamate species. In addition, the authors point out that literature on CO_2 absorption has perhaps been focusing too much on sterical effects to explain variations in reactivity.

KS-1 and 2-Amino-Methyl-1-Propanol (AMP) are examples of sterically hindered amines. KS-1 is a proprietary (commercially available) amine developed by Kansai Electric Power Company (KEPCO) and Mitsubishi Heavy Industries (MHI). A technical report by the IEA Greenhouse Gas R&D Programme, compared the energy consumption of CO_2 capture processes with MEA and KS-1, for a coal-fired and a natural gas combined cycle (NGCC) plant respectively. It was concluded that adding post-combustion capture and compression would decrease efficiency of a coal-

fired power plant by 8-9 percentage points, and 6-8 percentage points of a NGCC plant. The study states that by using MHI's KS-1 hindered amine solvent the energy penalty is 1-2 percentage points lower than the resulting one using MEA. However, after considering both capital and operating costs the overall capture costs for both cases are similar. The authors also indicate that there is a significant uncertainty regarding the assumptions taken to quantify the capital costs of capture using either MEA or KS-1 [6].

2.1.1.2 Amino-acid salts

Analogue to amines, amino-acid salts can be classified in three categories: *primary*, *secondary* and *tertiary*. Besides an amino group, amino-acids feature a carboxyl group. The fact that amino-acids possess both an alkaline and an acid group enables an almost complete ionic state in aqueous solutions, so that the resulting vapour pressure of amino-acid solutions is practically insignificant and thus, makeup losses due to vaporisation can be neglected [39].

According to Brouwer, J.P., et al. [44] amino-acid salt solutions have been considered an alternative to amine based solutions for chemical absorption of CO_2 for the following reasons:

- Fast reaction kinetics
- High achievable cyclic loading[6]
- Good stability towards oxygen
- Favourable binding energy

These properties make them suitable for application of membrane technology in gas absorption units, or more specifically membrane contactors, thus resulting in compact equipment design and consequently lower investment costs [44].

A study conducted by the University of Stuttgart [39] analysed different amino-acid salts as a possible alternative to alkanolamines and compared them with a 30 % MEA solution. According to the study KAla[7], Sarcosine (also known as N-methylglicine) and Lysine require thermal duties for regeneration of the solvent that are similar to a 30 % MEA solution. This contradicts the results observed by Brouwer, et al., [44], which indicate a thermal energy reduction from 4.2 GJ/t CO_2 for MEA to 2.3 GJ/t CO_2 for an amino-acid salt. Though it must be noted that the

[6] The cyclic loading is defined as *the difference between the rich and lean loadings of the used solvent*. It refers to the CO_2 content in the solvent before and after entering the absorber column. This will be further discussed in the section 3.1.1.

[7] KAla is an abbreviation of Kaliumalaninat (from the name in German), which is an equimolar solution of alanine that has been neutralized with potassium hydroxide (KOH). The evaporation of this solution produces potassium alaninate (Kaliumalaninat).

main reason for low energy demand reported by Brouwer, et al. [44] has to do with a special process that was implemented for the purpose of energy reduction: the so called DECAB[8] process.

Several amino-acids produce precipitates when absorbing CO_2, thus allowing the driving force to be maintained at increased loading, so that lower energy consumption can be expected [36]. As with amines, precipitates may be regenerated by increasing the temperature. Once CO_2 has been driven off, the precipitated salt redissolves. Brouwer, et al. [44] explain that amino-acid salts can reach lean loadings of 0.05 mol/mol, resulting in a cyclic loading of 0.35 mol/mol, which is considerably higher than MEA, with typical values of 0.2-0.25 mol/mol. In theory, MEA can also reach the same lean loading values as amino-acid salts, though the energy demand for regeneration would exceed any feasible limit and hence values of at least 0.25 mol/mol are used instead. Complete regeneration of amino-acid salts requires a temperature profile within the stripper column that ranges from 80-120°C, so that heat integration within this column is necessary, which is exactly what the DECAB process does. A thermal energy demand of 2.3 GJ/t CO_2 for amino-acids against 4.2 GJ/t CO_2 for MEA has been reported for a 500 MW pulverised coal-fired power station [44].

There is substantial information that varies with regard to the MEA case that was used as reference between the study conducted by IFK - University of Stuttgart [39] and that of Brouwer, et al. [44]. The base case of the first one considered an energy demand for regeneration of approximate 3.9 GJ/t CO_2, while Brouwer, et al. [44] report an energy demand of 4.2 GJ/t CO_2. In addition, lean loadings reported by the University of Stuttgart were not as low, as the ones reported by Brouwer, et al. [44]. It is possible that by implementing a better heat integration lower lean loadings can be reached and hence, results of the University of Stuttgart resemble the ones reported by Brouwer, et al. [44].

2.1.1.3 Cyclic amines

Due to their fast absorption rates and higher absorption capacities, these amines are regarded as good potential absorbents for CO_2 [45]. Rayer, A., et al. [46] compared cyclic amine piperazine with polyamine N-(2-aminoethyl)-1,3-propane diamine and concluded that piperazine is more suitable for CO_2 capture due to its lower molecular weight, as well as higher absorption rates.

[8] Patented absorption process based on precipitating amino-acids. A description can be found at [44] and [115].

In another study, Maun, A. [47] compared a wide range of amines: *alkanolamines, aliphatic* and *cyclic amines*. He measured the corresponding mass transfer rates and calculated the reaction rate between the absorbed CO_2 with the amines. In general, cyclic amines showed the highest absorption and reaction rates. Based on temperature dependent measurements he determined that studied amines have similar activation energies ranging from 28-39 kJ/mol. These values agree with data from literature such as [48, 49, 50]. A few examples of cyclic amines are listed in Table 2.1. Bischnoi and Rochelle [50] studied the absorption of CO_2 into aqueous piperazine (PZ) and analysed the reaction kinetics, mass transfer and solubility. The conclusion was that the system has two reaction zones and that these depend on solvent loading. At low loadings, the dominant reaction products are piperazine carbamate and protonated piperazine, whereas at high loadings, the dominant reaction product is protonated piperazine carbamate. García-Abuín, et al. [51] analysed the kinetics of CO_2 chemical absorption into cyclic amine solutions. Their research focused on piperidine (PIP) and pyrrolidine (PYR). Based on experimental data and theory, it was determined that these cyclic amines activation energy is higher than MEA, but a higher electronic density was also provided, which favours chemical absorption and hence, higher reaction rates can be achieved.

Singh, et al. [45], Singh, P. [52], Rayer, et al. [46] and Maun, A. [47] studied different kinds of amines, including cyclic amines. Considering their results piperazine often showed a better overall performance than the rest of analysed amines.

Table 2.1: Examples of various cyclic amines [38]

Cyclic amine	Molecular weight [g/mol]	Molecular structure
Piperazine	86,14	
Morpholine	87,12	
Piperidine	85,15	
Pyrrolidine	71,12	
Benzylamine	107,15	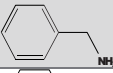
Cyclohexylamine	99,17	
Imidazole	68,08	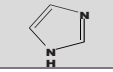

2.1.2 Inorganic solvents

These include aqueous ammonia, potassium and sodium carbonate. From the nonorganic based chemical solvents the biggest market share belongs to potassium carbonate [18]. The use of inorganic solvents presents an opportunity to reduce heat input required for solvent regeneration, which is why they have been given more attention.

2.1.2.1 Ammonia

Aqueous ammonia solutions have been proposed as an alternative to alkanolamines for the chemical absorption of CO_2. Some of the advantages of these solutions have been listed by Rowland, et al. [53]. To begin with, aqueous ammonia has been shown to be able to reach higher CO_2 loadings compared to alkanolamines, like MEA. This is a consequence of the CO_2-NH_3-H_2O system favouring bicarbonate over carbamate formation. Moreover, apparently aqueous ammonia requires less energy than MEA for its regeneration. This is because reaction's enthalpy for CO_2 absorption is smaller and because CO_2 partial pressure at elevated temperatures is higher for aqueous ammonia than it is for MEA. To go on with the advantages, aqueous ammonia offers some resistance to oxidative degradation, which is a major issue when treating flue gases from coal-fired power plants, since excess air is used for combustion. Furthermore, in presence of sulphur and nitrogen oxides in the gas stream, aqueous ammonia produces salts that have commercial value as fertilisers.

As it could be expected, the use of aqueous ammonia also has its drawbacks. As Rowland, et al. [53] state, a major one is its high vapour pressure. A consequence of this is its high volatility, which ends up in ammonia losses (slip). Zhuang, et al. [54] have experimentally confirmed, that ammonia's slip level is so high to either be released in the atmosphere or be kept in the CO_2 stream. In an attempt to address this problem, absorption's temperature has been varied, so that two different CO_2 capture processes have emerged. The first one absorbs CO_2 at low temperature (2-10°C) and is better known as chilled ammonia process (CAP). By reducing temperature it is possible to limit ammonia slip considerably. Unfortunately absorption reaction kinetics is also affected, so that CO_2 capture rate decreases. CAP allows precipitation of a number of ammonium carbonate compounds in the absorber. The second process captures CO_2 avoiding precipitation and is mainly developed by Powerspan [55].

Darde, et al. [56] and Jilvero, et al. [57] have analysed the effect of ammonia concentration in CAP. Darde, et al. [56] state that the absorption rate of a 10 wt%

ammonia solution at 304 K is comparable with a 30 wt% MEA solution at 314 K. Yet at low temperature, the absorption rate with ammonia solutions was found to be significantly lower than with MEA solutions at 314 K, and thus more contact area is needed than with amine solutions. This means that packing volume would increase and hence bigger equipment would be required. In order to counteract this issue Rowland, et al. [53] have investigated the possible use of three different promoters: alkanolamine, amino-acid and an inorganic base.

Jilvero, et al. [57] analysed the integration of CAP for CO_2 capture in a coal-fired power plant with 47 % net electric efficiency. They determined the ammonia concentration to be a critical parameter causing the specific reboiler duty to vary from 2200 to 2800 kJ/kg CO_2. This corresponds to 8-11 efficiency points, which is higher than previously expected. This trend has also been observed by Versteeg and Rubin [58] who compared high and low ammonia concentrations with an amine-based system. They found out that the power plant efficiency penalty was 2 percentage points lower than amine-based systems for high ammonia concentrations, whereas low ammonia ones showed a much higher efficiency penalty that are related to high flow rates and cooling duties. Versteeg and Rubin [58] suggest improved thermodynamic models, more detailed simulation of single equipment pieces and rate-based instead of equilibrium modelling for future ammonia-based CO_2 capture performance and cost models.

Jilvero, et al. [57] have also emphasized the need for improved Vapour-Liquid Equilibrium (VLE) data for modelling. Some authors like Ahn, et al. [59] have already started assessing this problem and their presented results seem promising.

2.1.2.2 Sodium carbonate

As Knuutila, et al. [60] explain, sodium carbonate solutions were used in dry ice plants at the beginning of the 20th century to capture CO_2 from flue gas. However, since alkanolamines offered both, a faster CO_2 absorption, as well as higher removal efficiencies, the use of sodium carbonate solutions decreased considerably once alkanolamines were introduced to the market.

Given the priority to minimize capture process' energy requirements, sodium carbonate solutions have regained attention. A few more advantages make of these solutions a feasible alternative to alkanolamines. Not only are sodium carbonate solutions non-hazardous, non-volatile and show a low corrosion rate, but they are also non-fouling and do not degrade. Moreover, compared to MEA sodium carbonate solutions have a "much lower" heat of reaction [60].

In spite of the listed advantages of sodium carbonate solutions there does not seem to be many literature references that regard them for CO_2 capture, but rather for SO_2 removal from flue gases (FGD). Knuutila, et al. [60] have recognized this and have been working on a rigorous thermodynamic model capable of describing the partial pressure of CO_2 and the liquid phase speciation as function of loading. With the resulting model it might be possible to combine SO_2 and CO_2 removal from flue gases, which would indeed make sodium carbonate solutions an interesting option to capture processes with alkanolamines [36].

2.1.2.3 Potassium carbonate

Potassium carbonate solutions also offer the possibility to operate CO_2 capture processes with relatively low heat input for solvent regeneration, and thus are considered as a good alternative for the post-combustion capture of CO_2.

The process with potassium carbonate is known as hot potassium carbonate (HPC) or simply “Hot Pot”. This process is commonly used in several ammonia, hydrogen, ethylene oxide and natural gas plants [61]. The CO_2 capture process with potassium carbonate can be used in different configurations, which are generally accompanied by slight changes in the solvent and catalytic additives in the process [18]. Due to the additives that work as activators or inhibitors these systems are known as activated hot potassium carbonate (AHPC) systems. According to Chapel, et al. [61] the most widely licensed of these are the Benfield and Catacarb processes.

The Benfield process was introduced over 30 years ago and uses an aqueous potassium carbonate solution to remove CO_2, H_2S and other acid gas components. The acid gas pressure is the main driving force of this process. Typical acid gas feed compositions range from 5 % to more than 35 % by volume [62].

The main drawbacks of potassium carbonate solutions are that absorption/desorption rates are slow and hence, required equipment is large. In an effort to counteract this, Eickmeyer and Associates developed a series of catalysts and corrosion inhibitors that gave way to the Catacarb process, which is an improvement of the original hot potassium carbonate (HPC) process [63].

According to Chapel, et al. [61] the Benfield and Catacarb processes are commercially offered for applications at a minimum CO_2 partial pressure of 2.1 to 3.45 barg[9]. They also report that the Benfield process was once proposed for capture of

[9] barg indicates gauge pressure. In order to obtain the absolute pressure the ambience one has to be added.

CO_2 from flue gases, but results of a study conducted by Grover, et al. [64] showed that the optimum operating pressure for the process would be 7 barg. Since flue gases of a coal-fired power plant are at atmospheric pressure, the use of HPC processes is not feasible for post-combustion capture of CO_2. Nonetheless, it might be possible to modify an existing process or –as in the case of the Catacarb process– develop new additives for potassium carbonate solutions to be able to capture CO_2 from flue gases at atmospheric pressure. The use of blends out of potassium carbonate and amines present such an opportunity, which will be shortly discussed in the next section.

2.1.3 Blends

Similar to amines there are also blends for inorganic solvents, or rather blends out of organic and inorganic components. As with amines the idea here also consists in maximizing advantages of one component and restricting disadvantages of the other. Inorganic components offer a low heat of reaction, whereas organic ones are capable of reacting fast with CO_2. By creating a suitable blend it would be possible to reduce energy requirements for solvent regeneration at acceptable CO_2 capture rates and hence, reasonable equipment size. Furthermore, a common problem with amines is that although they have a high selectivity for CO_2, they still react with other flue gas components. This leads to solvent's chemical degradation and/or corrosion. By reducing the organic fraction of the blend it would be possible to restrict losses due to chemical degradation that are usually replaced in a so called make up stream, while avoidance/restriction of corrosion would allow the use of other kinds of steel rather than only using stainless steel, which would contribute to reduce investment costs.

The idea of using blends is not new. A few examples for industrial applications of amines blends were given in section 2.1.1. A review of the available literature shows though, that the application of organic/inorganic blends for post-combustion capture of CO_2 from flue gases to be a rather new approach. Cullinane and Rochelle [65, 66] have examined aqueous blends of potassium carbonate and cyclic amine piperazine. According to Cullinane since piperazine is a diamine, its combination with potassium carbonate results in a higher capacity than MEA. Due to the presence of two amine groups, as well as the large amount of carbonate/bicarbonate, it was possible to increase the rate of absorption in a range between 1.5 to three times faster than with 30 wt% MEA solution.

Indeed, others have conducted a similar work. Knuutila, et al. [67] extended their original work with sodium carbonate to potassium carbonate and presented their

kinetics based on measurements with a string of discs apparatus. Instead of piperazine they used MEA and methyl amino propylamine (MAPA) as promoters and compared the results with literature data and the model of Weisenberger and Schumpe. They also concluded on much higher absorption rates of promoted solutions compared to pure ones.

This trend has also been observed in experiments conducted at the University of Duisburg-Essen. Figure 2.3 depicts experimental data of the CO_2 capture rate as a function of the flue gas volume rate for aqueous solutions of potassium carbonate, piperazine promoted potassium carbonate and monoethanolamine, represented with light blue, dark blue and magenta curves respectively. A high capture rate at the beginning of the absorption is an indicator of fast kinetics. A comparison between monoethanolamine and potassium carbonate shows that MEA clearly reacts faster with CO_2 than carbonates. This behaviour can be changed by adding Piperazine to the carbonates, which is represented with a dark blue line, thereby reaching an even higher CO_2 capture rate than MEA. Given the evident advantage of piperazine promoted potassium carbonate over pure potassium carbonate it was decided to conduct this study with different blends of potassium carbonate with piperazine, which will be introduced in the next section.

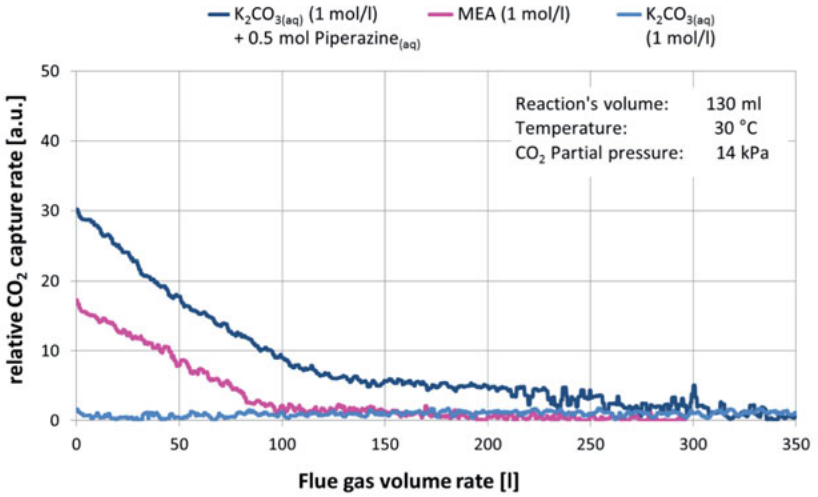

Figure 2.3: Comparison of CO_2 capture rates in aqueous solutions of MEA, potassium carbonate and piperazine promoted potassium carbonate

3 Modelling of CO_2 capture systems

Green, et al. [21] state that the widely used equilibrium-stage models for distillation have proved to be quite adequate for binary and close-boiling, and ideal and near-ideal multicomponent vapour-liquid mixtures. However, they also state that deficiencies of these models with respect to general multicomponent mixtures –like absorption of CO_2 from flue gases– have also been recognized.

Kucka [7] and Kennig, et al. [68, 37] share a similar opinion. Kucka [7] explains that often enough reactive absorption processes are simulated by using strongly simplified models, such as the equilibrium-stage model, which is hardly capable of describing the complex processes that take place in reality and, thus could lead to wrong dimensioning. Meanwhile, Kenig, et al. [68, 37] state that the description of reactive absorption based on chemical equilibrium is insufficient, since it depends on a combination of several kinetic controlled phenomena.

With respect to modelling of distillation and absorption processes, a new approach has become available in recent years: the *nonequilibrium* or *rate-based models*. These approaches supposedly treat classical separation processes as the mass-transfer rate governed processes that they really are [21].

The simulation programme Aspen Plus allows for rate-based modelling and hence was implemented in versions 2006.5, 7.1 and 7.2 for description of CO_2 capture systems in this work. The following sections will provide information that was required for the implementation in Aspen Plus.

3.1 Definitions and data on chemical media

For an accurate modelling of CO_2 capture systems it is essential to count with adequate data on chemical media. The corresponding specifications for this part implemented in Aspen Plus will follow in shortly after a few necessary definitions have been introduced.

3.1.1 CO_2 loading

The concentration of CO_2 in a solution is described by loading, α, which is defined as the ratio of CO_2 moles to moles of total alkalinity[10] of the solvent [69] as shown

[10] Number of active nitrogen groups.

in equation (3.1). The maximum value of loading is affected by several parameters, e.g. concentration of solvent in liquid, content of desired gas in the main gas stream, column geometry, among others. In theory the minimum value could be zero. However, the lower the loading the more energy has to be applied for solvent's regeneration and hence loading, as a rule, is higher than zero.

$$\alpha = \frac{moles_{CO_2}}{\sum moles_{alkalinity}} \tag{3.1}$$

CO_2 loading in an aqueous MEA solution can be expressed as:

$$\alpha = \frac{moles_{CO_2}}{moles_{MEA}} \tag{3.2}$$

If the solvent is a blend, like in the case of piperazine and potassium carbonate, they both have to be considered for loading's calculation. In addition, piperazine has two alkalinity groups per molecule and thus its loading is as follows:

$$\alpha = \frac{moles_{CO_2}}{moles_{K_2CO_3} + 2 \cdot moles_{PZ}} \tag{3.3}$$

Depending on the position at which loading is measured/calculated, it can be referred to as *lean* or *rich*. The first one usually denotes loading at the absorber's top or at the stripper column's bottom, while the second one refers to the one at the absorber's bottom, or rather at the stripper column's top.

The definition of cyclic loading or loading difference can be seen in equation (3.4). It determines the amount of solvent that is required within the absorber column and thereby affects the amount of solvent within the scrubbing cycle. In other words, the amount of solvent required to capture a certain amount of CO_2 increases proportional to the value of lean loading.

$$\Delta\alpha = \alpha_{rich} - \alpha_{lean} \tag{3.4}$$

Molality, *b*, of a solution is defined as the amount of substance of solute divided by mass in kg of the solvent, not mass of the solution (see equation 3.5). Although

the suggested SI unit is mol/kg, the molality of a solution is often referred to simply as "*m*", i.e. 5 mol/kg represents a 5 molal[11] solution or 5 *m* solution.

$$b = \frac{n_{solute}}{m_{solvent}} \tag{3.5}$$

Molality is not to be confused with molarity, *c*, which represents the molar concentration and is defined as the amount of a solute, *n*, divided by the volume of the solution, as shown in equation 3.6. The corresponding SI unit is mol per liter (M).

$$c = \frac{n_{solute}}{V_{solution}} \tag{3.6}$$

3.1.2 Monoethanolamine

Chemical media data for MEA was provided in October 2009 by Dr. Gary Rochelle's research team from the University of Texas at Austin. This data is the result of extensive experiments and has been implemented in computer models, whose development will be described in this section.

Freguia, et al. [70] improved a VLE model created by Austgen, et al. [71]. In both cases thermodynamics were described with the Electrolyte Non-Random Two-Liquid (NRTL) framework, but Freguia, et al. regressed some interaction parameters to match the solubility data of Jou, et al. [72] since they were considered more accurate than the ones used by Austgen. In addition, Austgen's VLE model was for acid-alkanolamine-water systems, whereas Freguia's model was designed exclusively for MEA. Moreover, Freguia analysed the process for CO_2 removal from flue gases with a rate based model in Aspen Plus that consisted of an absorber, a stripper and a heat exchanger. For this purpose he used RateFrac[12] to model both columns. According to Freguia, et al. [70] the rate model used in the absorber was made consistent with the Electrolyte-NRTL thermodynamic model and with the interface-pseudo-first-order (IPFO) approximate model for mass transfer, through a Fortran kinetic subroutine for RateFrac. Due to higher operating temperature, the stripper was modelled using the equilibrium approach.

Dugas [73] was interested in an accurate comparison of CO_2 capture performance of new solvents to MEA, for which it was required to run a baseline MEA cam-

[11] This notation is considered obsolete by both the National Institute of Standards and Technology and the German Institute for Standardisation (DIN from the name in German). This last one even advises against the use of this notation. The related norm (DIN 32625) was withdrawn in 2006.
[12] Predecessor of RateSep in Aspen Plus.

paign. He used the Fortran kinetic subroutine developed by Freguia, et al. [70] to do some modelling of pilot plant runs in Aspen Plus. The same VLE model was later used by Dugas, et al. [74] to develop an Aspen Plus RateSep absorber model that successfully matched the results of the CASTOR project pilot plant "Campaign 2". That work was based on a 7 *m* aqueous solution of MEA and flue gas with 11-13 wt% CO_2. This can be considered as a valuable contribution, since available data in literature is commonly based in lab conditions, rather than real ones. Indeed, Dugas [75] identified a lack of literature data for MEA kinetics that can be directly applied to industrial CO_2 capture systems. A problem is that industrial systems are likely to operate at absorber temperatures that range from 40 to 70°C, while most of literature data has been collected at near ambient conditions. Furthermore, some of the higher temperature data reviewed by Dugas is likely to be erroneous due to experimental or calculation inaccuracies. A list of the reviewed data can be found in [75].

Another issue with literature data listed by Dugas [75] is that industrial CO_2 capture systems operate at high amine concentrations with CO_2 loaded solutions, whereas most of the information collected using unloaded solutions and only limited data has been acquired at significant MEA concentrations.

Having realised the previous issues, Dugas [75] conducted a series of lab experiments using a wetted wall column to determine CO_2 equilibrium partial pressure and liquid film mass transfer coefficient (k_g') in 7 (30 wt% equivalent), 9, 11 and 13 *m* MEA and 2, 5, 8 and 12 *m* PZ solutions. Dugas also performed diaphragm diffusion cell experiments with CO_2 loaded MEA and PZ solutions that helped characterise diffusion behaviour.

For Modelling of RateSep in Aspen Plus, Dugas created a modified VLE model following the same sequential approach that Hilliard [76] employed. According to Dugas parameters such as nuclear magnetic resonance, heat capacity, amine partial pressure, and CO_2 partial pressure from Hilliard were included in the MEA data regression. Dugas mentions that MEA partial pressure data has received special attention since it leads to MEA activity coefficients, which are important factors to rate behaviour. For this reason, CO_2 partial pressure data from Jou, et al. [72] as well as Rochelle, et al. [77] was also included in the regression. The resulting MEA VLE model considers data ranging from 3.5 to 13 *m* MEA with temperatures from 25 to 120°C. The regression also included data with CO_2 loadings in a range from 0.25 to 0.6 mol_{CO_2}/mol_{MEA}.

Dugas [75] finally reported a good match of experimental results with available literature data.

This work's calculations are based on the model developed by Dugas [75] for a 7 *m*, which corresponds to a 30 wt% or 5 M aqueous MEA solution. This is what can be considered as the current industrial standard for chemical absorption of CO_2, and hence represents a good basis for comparison with other solvents.

Following the same methodology as Plaza [78], kinetics were represented using the next set of reactions:

$$2MEA + CO_2 \leftrightarrow MEA^+ + MEACOO^- \tag{3.7}$$

$$MEA + CO_2 + H_2O \leftrightarrow MEA^+ + HCO_3^- \tag{3.8}$$

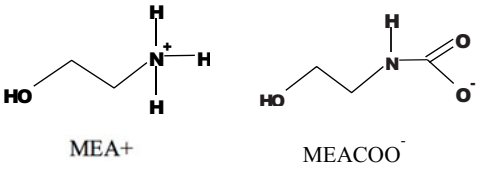

Figure 3.1: Molecular structures of some species from reactions (3.7) and (3.8)

Plaza's approach is based on results presented by Hilliard [76], who showed that the concentration levels of H^+, OH^- and CO_3^{-2} are so low, that they can be neglected and thus the model was simplified by either eliminating or combining the reactions involving these components.

3.1.3 Piperazine promoted potassium carbonate

The data on chemical media was obtained from references based on the work of Dr. Gary Rochelle's research team from the University of Texas, at Austin. As with MEA, this data is also the result of extensive experiments and has been implemented in computer models.

Cullinane [79] conducted a series of lab experiments to measure thermodynamics and kinetics of potassium carbonate, piperazine and carbon dioxide using a wetted wall column, until he was able to develop a rigorous thermodynamic model in FORTRAN using the electrolyte NRTL theory. This model was capable of predicting vapour-liquid-equilibrium and speciation for the H_2O-K_2CO_3-PZ-CO_2 system. He also developed a rigorous kinetic model that determined rate constants and

diffusion coefficients based on experimental data [29, 80]. Hilliard [81] continued Cullinane's work and created an Aspen Plus VLE model with thermodynamic data from Cullinane. This data was then used by Chen [29] to predict equilibrium and speciation, along with rate constants developed by Cullinane to predict kinetics, making it possible to develop a rate-based model using Aspen Plus' RateSep™.

The reactions that were considered for the rate-based simulations with carbonates according to the work of Cullinane [79] are:

$$PZ + CO_2 + \begin{cases} OH^- \overset{k_{PZ-OH^-}}{\longleftrightarrow} PZCOO^- + H_2O \\ H_2O \overset{k_{PZ-H_2O}}{\longleftrightarrow} PZCOO^- + H_3O \\ PZ \overset{k_{PZ-PZ}}{\longleftrightarrow} PZCOO^- + PZH^+ \\ CO_3^{2-} \overset{k_{PZ-CO_3^{2-}}}{\longleftrightarrow} PZCOO^- + HCO_3^- \\ PZCOO^- \overset{k_{PZ-PZCOO^-}}{\longleftrightarrow} PZCOO^- + H^+PZCOO^- \end{cases}$$

$$PZCOO^- + CO_2 + \begin{cases} H_2O \overset{k_{PZCOO^--H_2O}}{\longleftrightarrow} PZ(COO^-)_2 + H_3O \\ PZ \overset{k_{PZCOO^--PZ}}{\longleftrightarrow} PZ(COO^-)_2 + PZH^+ \\ CO_3^{2-} \overset{k_{PZCOO^--CO_3^{2-}}}{\longleftrightarrow} PZ(COO^-)_2 + HCO_3^- \\ PZCOO^- \overset{k_{PZCOO^--PZCOO^-}}{\longleftrightarrow} PZ(COO^-)_2 + H^+PZCOO^- \end{cases}$$

PZ reactions for absorber's kinetic modeling [79]

$$CO_2 + OH^- \overset{k_{OH^-}}{\longleftrightarrow} HCO_3^-$$
$$PZ + CO_2 + H_2O \overset{k_{PZ}}{\longleftrightarrow} PZH^+ + HCO_3^-$$
$$PZCOO^- + CO_2 + H_2O \overset{k_{PZCOO^-}}{\longleftrightarrow} H^+PZCOO^- + HCO_3^-$$

Bicarbonate reactions for absorber's kinetic modelling [79]

Chen [29] noted some discrepancies when he first started using the rate-based model to design an absorber. He identified an unexpected temperature profile, which was an indicator that the heat of absorption was not being properly predicted by Aspen Plus. Plaza [80] explains that the heat of absorption calculated by Aspen Plus derives from an enthalpy balance using heats of formation, heat capacities, as well as heats of vaporisation of the various species. And hence, in order to correct discrepancies Chen had to adjust the heats of formation of the pi-

perazine species (PZH^+, $PZCOO^-$, $PZ(COO^-)_2$ and H^+PZCOO^-) to provide the same heat of absorption as the one predicted from equilibrium constants used in the chemistry model. In addition, Chen also regressed entropy reference values for the four piperazine species to calculate heat capacities, since they were not originally included in the Hilliard model.

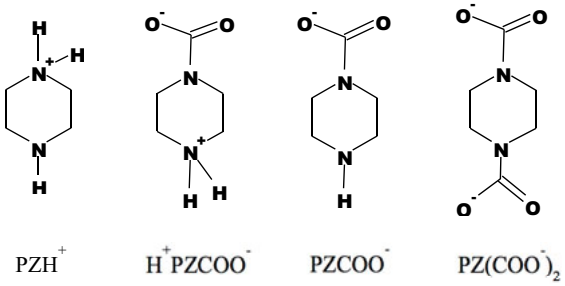

Figure 3.2: Molecular structures of some piperazine species

Another change used by Chen [29] was to give the H^+PZCOO^- ion a charge value of 0.0001 instead of 0. This was done since Aspen Plus does not consider the existence of net-neutrally charged zwitterions which were included by Hilliard in the VLE model. By giving the H^+PZCOO^- ion a net charge of 0, it was supposed to be treated as a molecule, but instead several issues aroused, including the slanted predictions of heats of absorption. However, Chen explains that by giving a negligible net charge the H^+PZCOO^- zwitterion could be effectively be treated as a "molecular solute".

To be consistent with the model's units of equilibrium and rate constants, Chen took advantage of the new version of RateSep^{TM} [13] that allows the user to enter activities in terms of mole gamma using the power law expression (see equation (3.9)). Since equilibrium constants were already activity based, it seemed reasonable to implement the same basis to rate constants from Cullinane, which were originally concentration based.

[13] First available with Aspen Plus V2006. In the following versions of Aspen Plus it was only referred to as *rate-based*.

$$r = k\left(\frac{T}{T_o}\right)^n exp^{\left(\frac{-E}{R}\left(\frac{1}{T}-\frac{1}{T_o}\right)\right)}\prod(x_i\gamma_i)^{\alpha_i} \tag{3.9}$$

Where,

r	[mol/(l·s)]	Reaction's rate
k	[mol/(l·s)]	Pre-exponential factor (independent of temperature)
n	[-]	Temperature exponent
E	[kJ/kmol]	Activation energy
T	[K]	Reference temperature (298.15K)
x_i	[-]	species *i* fraction of reactant
γ_i	[-]	species *i* activity coefficient
α_i	[-]	species *i* reaction order

For conversion from concentration to activity based units Chen [29] implemented the following algebraic manipulation:

$$k_a = \frac{k_c[PZ][CO_2][i]}{(x_{PZ}\gamma_{PZ})\left(x_{CO_2}\gamma_{CO_2}\right)(x_i\gamma_i)(total\ mol/L)} \tag{3.10}$$

Where,

k_a	[-]	Activity-based rate constant
k_c	[-]	Concentration-based rate constant
i	[mol/L]	species *i* concentration
x_i	[-]	reactant species *i* mole fraction
γ_i	[-]	reactant species *i* activity coefficient

Chen [29] also assumed the total molar concentration per liter of solvent to be constant across the column, for which a representative total molar concentration was selected. This term is last in the denominator of equation (3.10).

Plaza, et al. [80] report about selection of a representative ionic strength at 50°C and 0.5 loading (mol CO_2/total alkalinity), which was also assumed to be constant over different temperature and loading ranges. This was due to the fact that a correction for ionic strength cannot be directly implemented in Aspen Plus, which was originally considered in kinetics developed by Cullinane.

Forward and reverse activity-based rate parameters for piperazine, piperazine carbamate, and bicarbonate reactions, as input into Aspen Plus RateSep^{TM}, can be found in [29] for systems with:

- 5 *m* K^+/2.5 *m* PZ
- 6.4 *m* K^+/1.6 *m* PZ

Plaza et al. [80] then applied the same methodology as Chen to a system with:

- 4.5 *m* K^+/4.5 *m* PZ

The corresponding forward and reverse activity-based rate parameters can be found in [80].

The three listed systems have been considered in this work. To facilitate both information and graphic description of results, it was decided to substitute the nomenclature presented in literature for the one in Table 3.1.

Table 3.1: Nomenclature and molality of analysed blends [mol/kg$_{Water}$]

Nomenclature	Potassium Carbonate (K^+)	Piperazine (PZ)
K1	4,5	4,5
K2	5,0	2,5
K3	6,4	1,6

To maintain the same basis from literature, the blends' molality is listed in Table 3.1. Dugas [75] explained that a molality basis is commonly preferred, since it neither changes with the addition of new components, nor it needs new density measurements and hence it turns out to be especially suitable for experimental analyses.

3.2 System boundary and implementation

It has been previously mentioned that modelling of CO_2 capture systems was undertaken with the simulation program Aspen Plus, and that this software was selected, since it allows for rate-based calculations. These calculations are necessary for an accurate modelling of complex systems such as CO_2 capture systems with chemical absorption, which are highly non-ideal.

The rate-based capability however, does not make the modelling of a complete capture system any easier. The complexity of a computer model affects both the computing time and capacity required to conduct calculations, i.e. the more complex the model, the longer it will take to reach a solution. A simple but effective

approach to counteract this issue consists in splitting the whole system into different parts, thus simplifying the system. In this way, some computer models might be easier to converge. This principle can be applied to entire systems, as well as single components. This idea has also been applied for modelling of capture systems in this work, so the flow diagram in Figure 2.1 has been simplified to the one shown in Figure 3.3. The resulting diagram is also extremely difficult to solve if modelled all at once. For this reason the first modelling step consists in creating a rate-based absorber model for each blend. Then the capture model can be enhanced with further equipment components, until the cycle in Figure 3.3 is solved and ultimately will lead to the solution of the whole system shown in Figure 2.1.

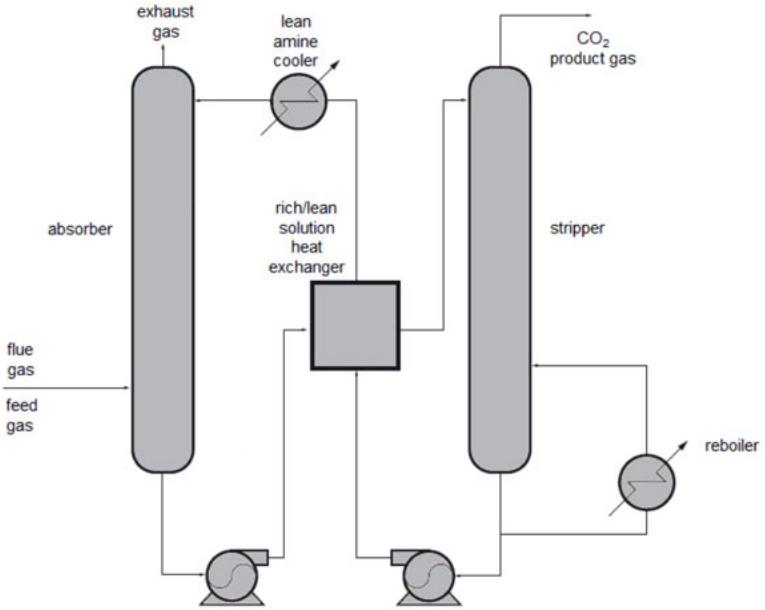

Figure 3.3: Simplified process flow diagram for modelling of CO_2 capture from flue gas by chemical absorption in Aspen Plus

3.2.1 Boundary conditions

Considering a CO_2 scrubbing process as an extension of a coal-fired power plant, the ideal process would present the following characteristics:

- Little or no flue gas conditioning requirement
- Low blower's electrical energy demand

- Negligible pressure drop within columns
- Small absorber and desorber column geometries
- Low liquid/gas (L/G) ratios
- Minor solvent losses due to carry-over
- Solvent with high CO_2 absorption capacity
- Low energy demand for solvent regeneration
- Negligible solvent degradation (chemical and thermal)
- Extensive heat recovery

Most of these characteristics though are dependant from intrinsic interactions, i.e. negligible pressure drop within columns can derivate from using a solvent with high CO_2 absorption capacity, which would lead to a low L/G ratio, to smaller column geometries and probably even to a lower blower's electrical demand. However, by using a solvent with high absorption capacity it might be necessary to supply a higher amount of energy for regeneration purposes in comparison with the required energy for a solvent with a lower absorption capacity. Whether this might apply or not is subject to further study that should include the integration of the scrubbing process in the power plant.

A glance at the literature reveals that often enough the focus of a study relies in analysing the impact of single components on energy demand of the capture process, thereby omitting the impact on the rest of the cycle ancillaries and the implications that this may have on the overall scrubbing cycle and the coal-fired power station. Therefore different parameter variations have been conducted and evaluated. The corresponding boundary conditions for modelling will be briefly presented in the following paragraphs. Unless mentioned otherwise, specifications remain constant for all models.

Flue Gas Composition

The components of the flue gas were taken according to the power plant previously introduced in section 1.3.1.1, which corresponds to the Reference Power Plant NRW (RPP NRW) and which data can be found in [11]. Conducted simulations assumed a mass flow rate of 550 kg/s and the following mass fraction composition after conventional flue gas cleaning: 6.98 % H_2O, 20.96 % CO_2, 68.27 % N_2, 3.78 % O_2 and 0.01 % SO_2.

Solvents

The lean solvent enters the absorber column with a temperature of 40°C at all times.

Absorber

The calculations are based on a research project by Behr, et al. [38], which can be seen as a continuation of a former project on post-combustion capture of CO_2 (see [82]).

One of the concerns expressed in a meeting of the ef-Ruhr project had to do with minimising pressure losses within the absorber column, for which a maximal pressure loss of 100 mbar was assumed as a maximum tolerance. This might seem as a high initial value, though considering estimated absorber diameters required for the capture of 90 % CO_2 of a coal-fired power station like RPP NRW of approximate 18 m, 100 mbar seemed to be a good starting point for absorber design.

In the more recent project by Behr, et al. [38] it was decided to reduce the previous tolerance to at least 70 mbar, although a lowest pressure loss value was not set, so as to quantify the potential of pressure loss reduction within this column.

Since packing columns are characterised by small pressure losses, high flow rates, as well as a good selectivity [83], they present a good choice for both absorber and stripper columns. In addition, it is essential to choose a packing that allows for diameters of approximate 18 m. Such an option is given by the Mellapak structured packing 250X from Sulzer for both absorber and stripper column. This manufacturer also offers a Y series for this kind of packing, but considering that the X series is characterised by lower pressure losses and higher working capacity [83] it was chosen over the Y series. The necessary properties data is stored in the Aspen Plus database.

The main task of the absorber consists in capturing 90 % CO_2 of the flue gas. To achieve this, the solvent flow rate was varied depending on the used concentration. An initial packing height of 30 m was assumed only for the cases with piperazine promoted potassium carbonate.

Sattler [33] states that the best selectivity of the column is reached when it is operated close to the flooding point, so that an operation at 80 % of this limit was set for all cases. In order to account for all the mentioned variations and at the same time, avoid flooding the column, it is necessary to adjust the column diameter according to the respective solvent flow rate.

Ideally, by setting an operation of the column at 80 % capacity the whole packing would be covered with a liquid layer uniformly. In reality only a few sections of the packing operate at this level due to the actual distribution of the solvent along the packing's surface. This is a known problem and the subject of continuous re-

search, i.e. [84]. However, although the original distribution properties have been improved along the years, the perfect packing is yet to be engineered. In other words, the limit of 80 % actually means that Aspen Plus implements a *maximum fractional capacity*[14] of 80 % at a precise location of the contemplated column, but the average value within a column is lower and might amount approximated 70 %. This can be explained by contemplating the reported values for the packing sections that range between 60 and 80 %. Increasing the *maximum fractional capacity* in order to reach a higher average operation capacity of a column is not an advisable option, since the operation with alkanolamines under these conditions could lead to operation problems such as foaming.

3.2.1.1 Flue gas conditioning

Flue gases from coal-fired power plants have to fulfil environmental regulations previous to their emission in the atmosphere. Part of those regulations concerns sulphur oxides SOx (SO_2 and SO_3) emission.

In Germany the “Law on Protection for Environmental Harms due to Air Pollution, Noise, etc.” is responsible for setting air pollutants emission limits. Albeit this law includes 39 ordinances, not all of them are in effect, since some of these have been abrogated over the years. The corresponding SOx emission limits for the base case power plant introduced in section 1.3.1.1 can be found in the Thirteenth Ordinance on the Implementation of the Federal Immission Control Act (Ordinance on Large Combustion Plants and Gas Turbine Plants – 13. BImSchV[15]). According to it, emission limits for SOx are 200 $mg_{SO_2}/m^3_{flue\ gas}$ or 85 % SO_2 reduction. The tighter specification is the one that will be implemented. These values are nonetheless considered too high for the use of alkanolamines within a scrubbing process, where the suggested impurities concentration should not exceed 10 ppmv [85, 36, 6] or even 10 $mg_{SO_2}/m^3_{flue\ gas}$ [86], if solvent degradation is not to become an issue. This implies a yet new flue gas conditioning step previous to reaching the actual CO_2 scrubbing process.

A simplified scheme of flue gas preconditioning is depicted in Figure 3.4. It basically consists of three steps: cooling, scrubbing and charging. The flue gas from a conventional flue gas desulphurisation - FGD plant is cooled down with water from approximately 48°C to 35°C. Flue gas cooling contributes to reduce solvent losses due to carry over. The flue gas then enters a SO_2 scrubber, where it countercur-

[14] Term used by Aspen Plus to specify the maximum proximity to flooding point.
[15] This ordinance complies with the Directive 2001/80/EC of the European Parliament and of the Council of 23 October 2001 on the limitation of emissions of certain pollutants into the air from large combustion plants [117].

rently contacts a slight sodium hydroxide solution to keep the new suggested limit of 10 $mg_{SO_2}/m^3_{flue\ gas}$.

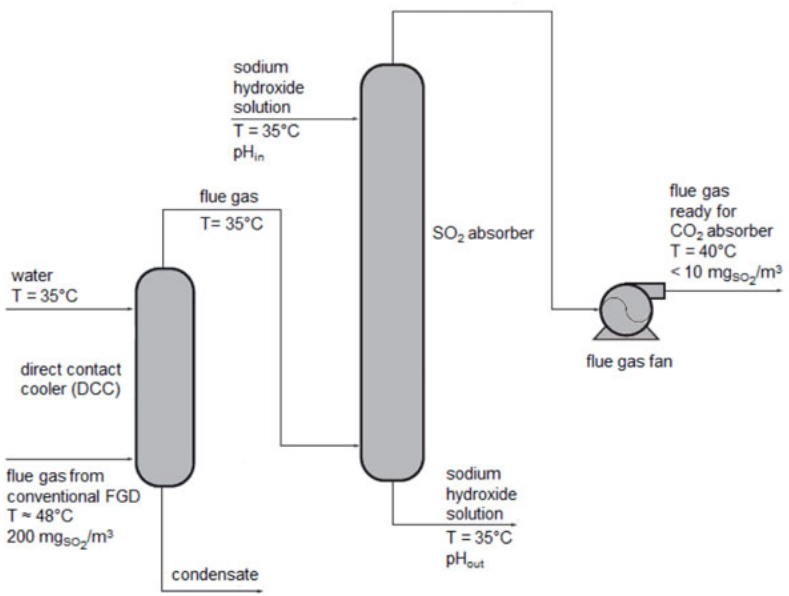

Figure 3.4: Flue gas conditioning sequence

The conditioning's last step consists in slightly compressing the flue gas in a blower. This is done to compensate pressure losses that take place between flue gas conditioning and CO_2 absorber. The SO_2 and CO_2 scrubbers entail equipment that lead to pressure losses; these include liquid collectors and distributors, support grids, bed limiters, etc. [21, 87, 88, 89]. The CO_2 absorber is operated at atmospheric pressure. Without charging the flue gas it would not be possible to emit the stack. The pressure difference provided by the blower has hence to be high enough to overcome atmospheric pressure.

Due to compression the flue gas temperature increases, but since it has been previously cooled, the absorber inlet temperature will not exceed 40°C, which is the assumed design parameter for all conducted calculations.

The specifications used for cooler and blower are presented in Figure 3.4.

Most of the variations conducted with respect to flue gas conditioning concern the SO_2 scrubber. These can be summarised in three main categories: L/G ratio, solutions pH value at SO_2 absorber's inlet and kind of packing. The respective values can be found in the following table.

Table 3.2: Variables for SO_2 scrubber's analysis

Variable	Value
L/G ratio	1.5 2.0 3.0 4.0
pH_{in}	6.0 6.3 6.5 6.8 7.0 7.2
Packing	IMTP 40 IMTP 50 Mellapack 250X

SO_2 scrubber's design was conducted assuming a packing height of 2.5 m for all cases and variable diameter depending on the respective L/G ratio. This is just an approximation and not the actual height required for guaranteying a concentration lower than 10 $mg_{SO_2}/m^3_{flue\ gas}$, which will be determined later as part of results analysis.

Under real operating conditions it is possible that flue gases exhibit a SO_2 concentration lower than the one specified by the 13. BImSchV. This can be attributed to coal composition, which is not constant. The SO_2 flue gas concentration used in simulations was assumed to be 200 $mg_{SO_2}/m^3_{flue\ gas}$ in all cases.

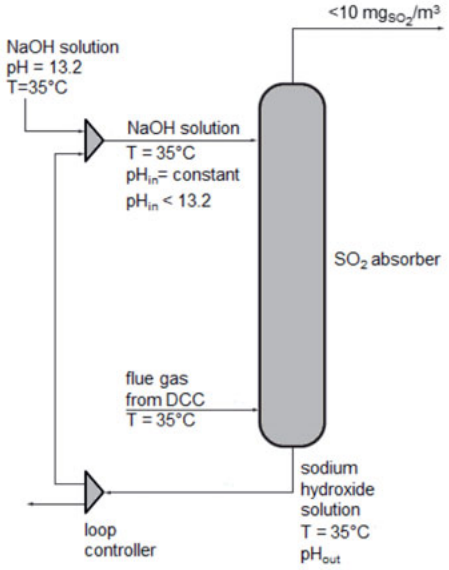

Figure 3.5: Specifications for SO_2 scrubber modelling

As stated previously special importance is given to keeping pressure losses as low as possible and hence three kinds of packing were considered in simulations. As with CO_2 absorber a capacity of 80 % was assumed for all cases.

Figure 3.5 depicts a more detailed diagram of the SO_2 scrubber. As previously stated a sodium hydroxide solution enters the absorber at the top. The solution's pH value decreases as SO_2 is absorbed. Since the solution should be used in a loop it is

therefore necessary to adjust the pH value to match the original one used at absorber's inlet. The scrubbing solution should fulfil two goals: absorb SO_2 and avoid CO_2. These two gases are both acid and thus their affinity to react with an alkaline solution is high. By reacting with CO_2, less solution will be available for SO_2. Besides, there is an absorber column destined solely to capturing CO_2. Variations listed in Table 3.2 were considered to quantify the pH value's effect of both SO_2 and CO_2.

3.2.1.2 Baseline case MEA

It has been previously mentioned that a system with a 30 wt% MEA solution is often considered as a good reference point to compare CO_2 capture systems. Consequently it was decided to model a capture system that would fit the same operating conditions as the cases with piperazine promoted potassium carbonate.

In the literature there are several scrubbing systems with a 30 wt% MEA solution. The baseline case for this solvent is based on parameters listed by Abu-Zahra, which have been selected and modelled. More information on Abu-Zahra's work can be found in [90], [91].

Abu-Zahra's models relate to a coal-fired power station, which properties differ from RPP NRW as shown in Table 3.3. In order to guarantee for a certain degree of comparability with the developed piperazine promoted potassium carbonate models, operating parameters listed by Abu-Zahra were used to generate two MEA models based on RPP NRW. The first model represents Abu-Zahra's baseline case and the second an optimized one. Since these cases are not the main focus of this work, only the operation conditions that vary from the rest are listed in Table 3.4.

Table 3.3: Reference values for coal-fired power stations in Abu-Zahra's studies and this work

		Baseline power plant [92]	**RPP NRW [11]**
Net power output	MW	575.5	555.6
Thermal efficiency (LHV)	%	45	45.9

Two more details of Cases I and II that differ from the rest of the developed models refer to absorber/stripper packing and absorber height. Abu-Zahra's baseline used Mellapak structured packing Y125, whereas the developed models for RPP NRW use the type 250X of the same vendor instead. The absorber height was not initially fixed, but rather determined with the new packing and by varying the sol-

vent flow rate, so that the rich loading at the bottom of the absorber column would match the one specified in Table 3.4.

Table 3.4: Parameter definition for modelled cases with MEA

	Baseline Abu-Zahra Case I	Optimised case Abu-Zahra Case II
α_{lean}	0.242	0.320
α_{rich}	0.484	0.493
Stripper pressure [bar]	1.5	2.1

3.2.1.3 Study cases with piperazine promoted potassium carbonate

The purpose of this section is to list the set of operating parameters that have only been varied for this blend.

Given that the total amount of solvent within the scrubbing process is defined by the cyclic loading, $\Delta\alpha$, a small change of it is reflected not only in the electric energy demand of the pumps, but also in the energy demand required for solvent regeneration, as well as in the total cooling duty. Therefore three different cyclic capacities were examined. The respective values of the lean and rich loadings are listed in Table 3.5.

Table 3.5: Lean and rich loadings

Solvent blend	Nomenclature	α_{lean}	α_{rich}
K1	K1-1	0.3000	0.4779
	K1-2	0.3548	0.4826
	K1-3	0.4037	0.4960
K2	K2-1	0.4050	0.5574
	K2-2	0.4430	0.5621
	K2-3	0.4830	0.5597
K3	K3-1	0.5030	0.6327
	K3-2	0.5230	0.6256
	K3-3	0.5430	0.6204

Cross heat exchanger

Due to this component it is possible to recover some of the energy that was originally provided to the reboiler by the power plant in form of steam for the purpose of solvent regeneration. This unit thus represents a feasible alternative to reduce the overall energy penalties of the power plant. The temperature difference dictates the amount of energy that remains available within the system. The more heat that can be transferred, the less the reboiler will need to be provided with steam from

the power plant and hence, more steam can be used for the purpose of electricity generation within the power cycle. For the conducted simulations two temperature differences were contemplated: 5 and 10 K.

Desorber/Stripper

To complete the analysis with different solvent blends it was decided to examine their behaviour at stripper pressures that vary from 0.5 to 3.0 bar. The goal is to quantify the impact of the stripper pressure on the specific energy demand for regeneration of the deployed solvent blend.

Summary

The following parameters remain constant throughout all simulations:

- 90 % CO_2 capture
- Flue gas composition and flow rate
- Flue gas and solvent's temperature at absorber's inlet: 40°C
- Aspen Plus default value of 850 W/(m^2K) for heat transfer coefficient
- Mellapak structured packing 250X
- Absorber height

The following parameter variations have been accounted for in the simulations:

- Three different solvent blends
- Three loading differences per blend
- Two temperature differences of the heat exchanger between absorber and stripper column

Considering every single listed variation a total amount of eighteen different cases have been examined, each of which has been analysed within a pressure range between 0.5 and 3.0 bar. Given that the observed trends are similar only relevant results will be offered in the evaluation of the different cases.

3.2.2 General methodology and specifications in Aspen Plus

Modelling a scrubbing system can be a rather challenging task when doing it for the first time, especially when certain parameters and software specifications are unknown to the user. Publications related to CO_2 capture systems often lack this information, which at certain times might be of invaluable assistance. For this reason a short description of the methodology implemented in this work will be presented.

At the beginning of section 3.2 it was explained that converging single components and then putting them together helps converging complex systems. Since the flue gas has to be preconditioned before reaching the CO_2 scrubber, this will be the first system to focus on.

3.2.2.1 Flue gas conditioning system

Compared to the CO_2 scrubbing systems with MEA and piperazine promoted potassium carbonate, modelling an SO_2 absorber represents a rather simple task in Aspen Plus. The Electrolyte-NRTL framework may also be used in this case. Opposite to the systems described in sections 3.1.2 and 3.1.3 no further modifications are necessary for successfully modelling an SO_2 scrubber system. The user may implement the so called *Electrolyte Wizard (Elec Wizard)* once he/she has entered all available components in the system. These include flue gas composition listed in section 3.2.1 plus sodium hydroxide. This tool can be found in the *Components\Specifications* category and consists of the following steps:

1. Define base components and select reaction generation options.
2. Remove any undesired species or reactions from the generated list.
3. Select simulation approach for electrolyte calculations.
4. Review physical properties and modify the generated Henry components list and reactions.

Each step's specifications depend on what the user is interested in analysing. If for example there are different possible reactions with available components, but only one of these is the focus of an analysis, then it might be better to spare Aspen Plus other available reactions. Such reactions only make a system more complex and hence more computing capacity might be required.

The main goal of flue gas preconditioning is to reduce components content that might cause the CO_2 scrubbing solution to chemically degrade and thus all available flue gas components were considered for generating adequate reactions with the *Electrolyte Wizard*. Salt formation was also included along with *true component approach* to represent electrolyte systems composition in the calculation. This approach was preferred over the *apparent* one due to: its calculation efficiency, it can take into account salt formation, and because it is considered to be more convenient for complex electrolyte systems. For more information on the true and apparent component approach, please refer to [93].

The Electrolyte Wizard generated the following reactions, which were included for simulations:

Type	Stoichiometry
Equilibrium	$H_2O + HSO_3^- \leftrightarrow H_3O^+ + SO_3^{2-}$
	$2H_2O + SO_2 \leftrightarrow H_3O^+ + HSO_3^-$
	$H_2O + HCO_3^- \leftrightarrow CO_3^{2-} + H_3O^+$
	$2H_2O + CO_2 \leftrightarrow HCO_3^- + H_3O^+$
	$2H_2O \leftrightarrow OH^- + H_3O^+$
Salt	$NaOH_{aq} \leftrightarrow H_2O + OH^- + Na^+$
	$Na_2CO_3.NaHCO \leftrightarrow CO_3^{2-} + HCO_3^- + 2H_2O + 3Na^+$
	$Na_2CO_3.10H_2O \leftrightarrow CO_3^{2-} + 2Na^+ + 10H_2O$
	$Na_2CO_3.7H_2O \leftrightarrow CO_3^{2-} + 2Na^+ + 7H_2O$
	$Na_2CO_3.H_2O \leftrightarrow H_2O + CO_3^{2-} + 2Na^+$
	$Na_2CO_3 \leftrightarrow CO_3^{2-} + 2Na^+$
Salt	$Na_2CO_3.3NaHC \leftrightarrow CO_3^{2-} + 3HCO_3^- + 5Na^+$
	$Na_2SO_3 \leftrightarrow SO_3^{2-} + 2Na^+$
	$NaHCO_3 \leftrightarrow HCO_3^- + Na^+$
	$NaOH \leftrightarrow OH^- + Na^+$
Dissociation	$NaOH \rightarrow OH^- + Na^+$

In Aspen Plus, devices are called unit operation models (UOM) and the software refers to each of them as *blocks*. Adding too many UOMs at the beginning of a simulation might unnecessarily increase the systems complexity. It is therefore advisable to add only as may accessories to a system as convergence will not be compromised since the beginning.

The first block to specify is the direct contact cooler (DCC), whose purpose consists in saturating and cooling the flue gas to a temperature of approximate 35°C. This UOM may be represented with a flash drum from the *Separators* category. This can be found within the *Process Flowsheet Window*. The specifications include the previously mentioned temperature and a pressure of “0” bar. This does not mean that the drum will operate in vacuum, but that pressure losses will be neglected within this unit.

Aspen Plus calculates all outgoing streams from a unit operation model (UOM), whereas all entering streams have to be specified by the user beforehand. According to Figure 3.4, the DCC features two inlet and two outlet streams. One of the

inlet streams carries water that will be used to cool down the flue gas, and the other one carries the flue gas itself. Both inlet streams are supposed to enter the flash drum at atmospheric pressure. Their chemical composition and flue gas flow rate are known, whereas water's flow rate for the inlet stream remains unknown. Aspen Plus requires a value higher than zero to be able to start calculations. This means, that the flow rate must not necessarily be known. It suffices to enter a value that can later be manipulated by a so called design specification (design-spec) from the *Flowsheeting Options* category within the *Data Browser*. The goal has to be being able to cool down the flue gas only by varying the water flow rate.

Depending on the degree of accuracy the user intends to reach designing a facility, adding a pump might be considered to supply water to the DCC. The results can be included when accounting for the overall power demand that will ultimately dictate just how big efficiency penalties are for the coal-fired power plant.

Once the DCC is ready the SO_2 scrubber may be added. For this a *RadFrac* UOM from the *Columns* category was used. Simulation specifications correspond to the ones listed in section 3.2.1.1. In the *Setup\Configuration* window the following specifications were assumed for the SO_2 scrubber: rate-based calculations, 25 stages[16], no condenser or reboiler, valid phases: *vapor-liquid* and standard convergence.

The packing can be included by creating a section under SO_2 scrubber*Pack Rating.* Once this has been done the packing type in Table 3.2 and a packing height of 2.5 m can be defined in the *Pack Rating\Section's name\Setup* form. To be able to specify Aspen Plus to automatically calculate the column's diameter, it is necessary to go to the *Pack Rating\Section's name\Rate-based\Design* form and activate the *Design mode to calculate column diameter* check box.

The calculations were previously defined as rate-based. This is only partly true. Due to the high affinity of a sodium hydroxide solution to react with SO_2, equilibrium calculations are considered enough for modelling the SO_2 absorber. On the other hand, only by specifying rate-based calculations will it be possible to access the *Pack Rating\Section's name\Rate-based\Design* form. Since no other reactions were specified in the SO_2 scrubber's Reactions\Specifications form, only equilibrium calculations will be considered.

[16] This is not the number of theoretical stages. A more detailed description on this will be given with specifications of the CO_2 absorber in the following section.

So far only general specifications have been listed for the further desulphurisation. A more detailed description of absorber's simulation specifications will be given in the upcoming section.

There are two important conditions that have to be fulfilled in the SO_2 scrubber: L/G ratio as well as its pH value at scrubber's inlet should be kept constant. For this purpose some *Flowsheeting Options* like calculators and design-specs might offer a comfortable way of determining make-up streams. There is certainly more than one solution to approach this task; one for example might use a *Mixer* and a *Splitter*. The first one could determine whether the recycled stream's pH value matches the inlet specification in Table 3.2, in which case the make-up stream should be as little as possible. Unfortunately setting this stream to zero is not an option in Aspen Plus. Instead a value such as 0.00001 kg/s can be entered. If on the other hand, the pH value of the recycled stream is lower than the required specification, then a small amount of sodium hydroxide solution can be added so that the pH value matches the required one. In a second step L/G ratio can be examined to be kept constant.

For conducted simulations water was always used for the first run and the solution's pH value was adjusted once the solution had run at least once through the SO_2 scrubber.

The flue gas fan is the last unit to add to finally complete the preconditioning system. The corresponding UOM is *Compr* from the *Pressure Changers* category was used. The model is *compressor* and the type is *Isentropic*. A pressure increase of approximately 70 mbar was entered as a parameter, although the final pressure increase can only be estimated once all pressures losses (within SO_2 and CO_2 scrubbers as well as head wash) have been accounted for. It is also possible to define a sensitivity analysis from the *Model Analysis Tools* to tabulate different pressure increases along with the required net work and outlet flue gas temperature, which may not exceed 40°C to comply with assumed CO_2 absorber inlet specifications.

3.2.2.2 Absorber

This column practically represents the core of the scrubbing system and hence detailed information will be provided for its modelling in this section.

Stream specifications

This unit features two entering streams: flue gas and lean solvent, and two outgoing streams: stack and rich solvent. Since the lean solvent stream is a recycled

one, and hence a stripper product stream, it would be –in theory– previously calculated by Aspen Plus (see Figure 3.3). In reality, this stream is probably the most difficult to converge from all existing streams of the scrubbing process. In addition, the absorber should first be modelled as a single unit, for which the composition of this stream must be previously specified. In this context it is important not to consider a CO_2 concentration according to meet the values of the assumed lean loadings presented in Table 3.5.

Both flue gas and solvent solution have been assumed to enter the absorber at 40°C. Though seeing that flue gas leaves conventional purification equipment at a temperature of approximate 48°C this stream would in theory first has to be pretreated. However, one of the advantages of splitting the system of Figure 3.3 consists in increasing modelling flexibility. While it is possible to build one part of the scrubbing system after the other, it is also possible to work on different parts at the same time, for example when a team models such systems, or when a user is able to run parallel calculations, etc. This means that as long as both inlet and outlet specifications of CO_2 and SO_2 absorber respectively match each other, it may not be absolutely necessary to previously design additional flue gas conditioning units for a first approximation of the absorber. This can be done once the final absorber design is available. In a first approach flue gas might be cooled down with water in a flash drum that can be used as direct contact cooler (DCC).

Flowsheeting options

As with different calculation tools it is easier for Aspen Plus to converge when initial conditions are close to the solution. However, when designing a new model the solution is often unknown, so that some assumptions have to be met beforehand to limit the range within the solution should be found. Besides from concentrations of inlet streams, their flow rate has to be indicated. The one corresponding to RPP NRW is known and remains constant throughout all simulations. Solvent flow rate on the other hand is one of the parameters that will be continuously varied, depending on solvent's lean loading and the amount of CO_2 captured. It also fluctuates due to column's geometry and internals. The solvent flow rate can be varied by using a design specification tool in Aspen Plus (design-spec). This can be done either within the absorber column directly or in the *Flowsheeting Option*s' subdirectory. The goal of this tool is to reach a 90 % CO_2 capture from the flue gas. This can be specified by measuring CO_2 concentration of the flue gas outlet stream, which cannot exceed 10 %. Given that CO_2 is chemically bounded in the solvent solution, it will not be present as a pure component in the liquid phase, but rather in a compound like carbamate. Therefore it is easier to measure the CO_2 content

from the flue gas outlet stream. Once the goal has been set, the user has to specify which parameter should be changed to reach it. In this case the solvent flow rate should be varied, for which an upper and a lower limit must be specified.

There is not a fixed value for L/G ratio in the literature i.e. [21, 33, 83], etc. This value is said to always depend on the application and it may vary from approximately 3-8. A low L/G ratio can be the result of a low lean loading, a solvent with high absorption capacity and/or a high solvent concentration, whereas a high L/G ratio can be an indicator of a relative high lean loading, a solvent with a low absorption capacity and/or a low solvent concentration. Considering that the flue gas flow rate amounts to roughly 500 kg/s, an L/G ratio higher than 5 would not only result in an absorber column with massive dimensions, but this would also implicate a high energy requirement for transport of the solvent within the scrubbing cycle, as well as for regeneration purposes. The lower and upper limits for the design-spec can be set to 3 and 5. This is a first approximation and it is possible, that the limits differ from the suggested initial values.

Often enough the design-spec solution is not found within the set limits. In a case like this it might be advisable to temporarily deactivate the design-spec and add a calculator block instead to determine a few parameters like actual rich loading and CO_2 capture rate. This will provide an idea as to how far the design-spec solution is to the actual limits. Once the limits have been reset, the design-spec can be reactivated and iterations converge easier and faster.

Block specifications

Setup. The absorber column is modelled with a RadFrac UOM in the Aspen Plus User Interface. The first specification of this block begins with the submenu *Setup*, which also consists of three categories: *configuration, streams* and *pressure*.

In the configuration submenu, the calculation type can be set to *Rate-Based*. The next parameter to be entered by the user is the number of stages. Unfortunately this step's name can be easily mistaken by *number of theoretical stages*. What AspenTech actually intends to represent is the number of *segments* the column will be discretized into for a better prognosis of results [94]. For instance, if 30 stages are used to model a packing column, then this means that the packing has been cut transversally in 30 equal-sized segments. The sum of all segments represents the whole packing. In this way, the predicted results are more accurate.

When modelling an absorber Hockley [95] suggests an initial number of 20 stages, although according to Tremblay, et al. [96]: "As long as segment heights are rea-

sonable, the number of segments does not influence results". Tremblay's statement is based on an example for a packed MEA column, where he considered a height range from 0.1 to 0.3 m and 20 to 60 segments. The corresponding temperature profiles showed a good agreement.

In the *configuration* submenu, both condenser and reboiler can be set to *none*; valid phases to *vapor-liquid,* and finally convergence can be set either to *standard* or *strongly non-ideal liquid*.

Next specification in the setup submenu is *streams*. This step requires the user to specify at which column's location the feed and product streams enter or leave respectively.

Last specification in the setup submenu is *pressure*. The important part of this step is to remember that it is here, where pressure drop within the column has to be considered. The flue gas has to be able to be emitted, for which atmospheric pressure is needed. Though, if the flue gas at absorber top still has to undergo a further cleaning in a wash section, the hereby generated losses also have to be accounted for. As progress is made and Aspen Plus predicts more accurate values, the initial pressure can be adjusted.

Rate-based Distillation Setup. This submenu consists of four different categories: *specifications, convergence, advanced convergence* and *diagnostics*. In all of these submenus default options are available. Aspen Plus represents a powerful simulation tool that has been developed over several years and that constantly undergoes further improvements. This also means that this software is extremely complex with respect to all the models that have been implemented for an accurate or approximate representation of a wide range of chemical processes. In other words, the default values should not be altered by the user before he or she possesses an extensive comprehension of the options he or she intends to alter. Within the *rate-based distillation setup* there are though a few options that may be worth varying: *maximum number of iterations* and *film discretization ratio*.

The maximum number of iterations can be increased by the user, but it is advised not to do this before simulations have started to run. Usually, when running a simulation the control panel lists information on current simulation's progress. While it is certain that some simulations require more than 50 iterations to converge, it is also true that convergence is not always guaranteed. By monitoring progress on the control panel, the user can determine if reported errors are getting smaller. If this is the case, then it is advisable to increase the number of iterations per run, so that a solution is found, otherwise computing time and power resources

are being wasted on a problem that diverges. It should be noted that unless the user restarts a simulation, Aspen Plus will continue calculations from last results. This has the advantage that less computing time is required to complete calculations. It is hence the user's task to continuously check the control panel for errors and/or warnings. Some of these might make it necessary to restart a simulation, but not all of them. Some warnings for example only intend to report about boundaries that should be double-checked or extended; some others refer to new databanks or indicate that simulations did not converge within the set limits, etc. These sorts of messages require user's intervention to aid convergence.

Film discretization ratio can be found in *Rate-based Distillation Set-up/Specifications* form. It is based on the combination of the *two-film model* and the Maxwell-Stefan diffusion description, which are used to describe mass transfer at the gas/vapour-liquid interface. The two-film model assumes that all of the resistance to mass transfer is concentrated in thin films adjacent to the interface. It also considers the transfer to come about within the thin films by steady-state molecular diffusion alone. Outside the films, in the liquid bulk phase, the level of mixing is assumed to be so high that there is no composition gradient at all. The Maxwell-Stefan equations are used to describe multicomponent diffusion. The equations link diffusion fluxes of the components with the gradients of their chemical potential [37].

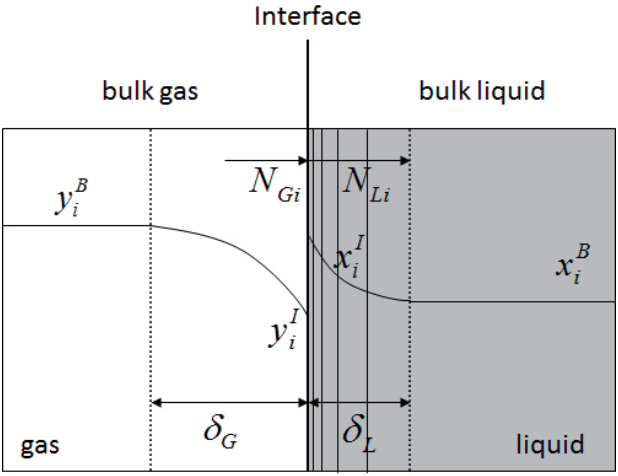

Figure 3.6: Two-film model and film discretization [37, 95]

Nomenclature of Figure 3.6:

N_i	[kmol/(m^{2}s)]	species *i* molar flux
x_i	[kmol/kmol]	species *i* liquid phase mole fraction
y_i	[kmol/kmol]	species *i* gas phase mole fraction
δ	[m]	film thickness
Superscripts		
B	bulk	
I	interface	

In the same way that a packing can be divided into several parts of the same size –the so called column or packing segments– this option allows for an actual discretization of the liquid film running down the packing. Unlike the packing, the discretized films have each a different thickness. The closer the films are to the interface, the thinner they are (see Figure 3.6). As Tremblay, et al. [96] explain, the film discretization ratio controls the size increments of the film. The default value is 2, which means that each film is two times longer than the previous one. Since computation time increases linearly with an increasing film discretization ratio, Tremblay, et al. [96] recommend a maximum ratio of 10.

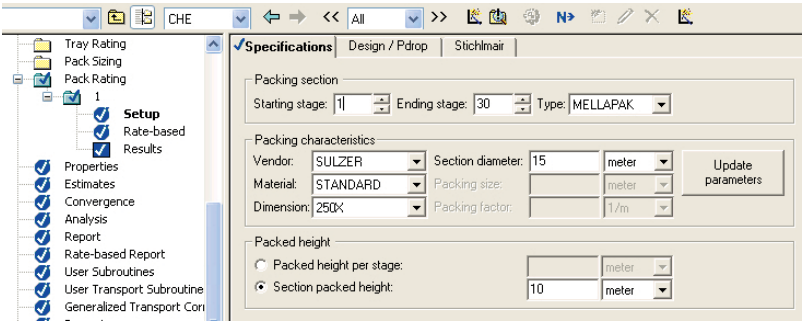

Figure 3.7: Pack Rating/Setup form

Pack Rating. Within Aspen Plus it is possible to design tray or packing columns. The available block options are: *Tray Sizing, Tray Rating, Pack Sizing* and *Pack Rating*. Both absorber and desorber columns were designed using the last option. First of all the user has to specify the number of sections to be designed. In doing so, it is possible to enter only one section, as long as the number of specified stages is reasonable, and as long as the user considers the use of liquid collectors and distributors in the final design. The *Pack Rating/Setup* sheet is depicted in

Figure 3.7. The starting and ending stage in this section refer to the stages previously defined in the *Setup/Configuration* form. Once the user has selected the packing type, he/she will be able to enter packing characteristics such as vendor, material, dimension and section diameter. The user can then choose whether to specify a packed height per stage or a section packed height.

Rate-based calculations can be activated in the *Pack Rating/Rate-based/Specifications* form. In this sheet, the user can choose between four different flow models: *Mixed, Counter-current, Vplug* and *Vplug-Pavg* (see Figure 3.8). They are used to determine the bulk properties needed to evaluate mass and energy fluxes as well as reaction rates [93]. The Mixed flow model is the default. It assumes bulk properties for each phase to be the same as the outlet conditions for that phase leaving that stage. This model is recommended for trays and according to Tremblay, et al. [96] it is also the easiest model to converge. The Counter-current flow model considers bulk properties for each phase to be an average of inlet and outlet properties. In general, this model is supposed to be best suited for packing columns, since it generates more accurate results than the previous one. However, if the packing sections are too large there might be convergence problems. This behaviour has been confirmed by Plaza [78]. He reported difficulties with the Counter-current flow model to match pilot plant conditions, which is the reason why he instead implemented an approximation of the mixed flow model and packing element height. In the VPlug flow model, outlet conditions are used for liquid, whereas average conditions are used for vapour with the exception of pressure, which also assumes the outlet value. This model is recommended for both tray and packing columns. The VPlug-Pavg flow model uses outlet conditions for liquid except for pressure, for which the inlet-outlet average value is used. For vapour, only average conditions are considered.

In order to consider the previously discussed film discretization in simulations, the corresponding option has to be selected by the user. In this case the option can be found in the *Pack Rating/Rate Based/Specifications* form, as shown in Figure 3.9. The option *Filmrxn* is mostly used when very fast reactions are involved. It helps convergence when both equilibrium and kinetic reactions are present [97]. It is also possible to include additional discretization points. These will be specified on the *Pack Rating/Rate-based /Optional* sheet, but in order to activate this input sheet the option *Discrxn* has to be selected instead of *Filmrxn*. The additional points have to be specified in strictly increasing order and, if location is not entered by the user, Aspen Plus will assume an evenly distribution between 0 to 1, which represent the vapour-liquid interface and the edge of bulk liquid (or vapour) re

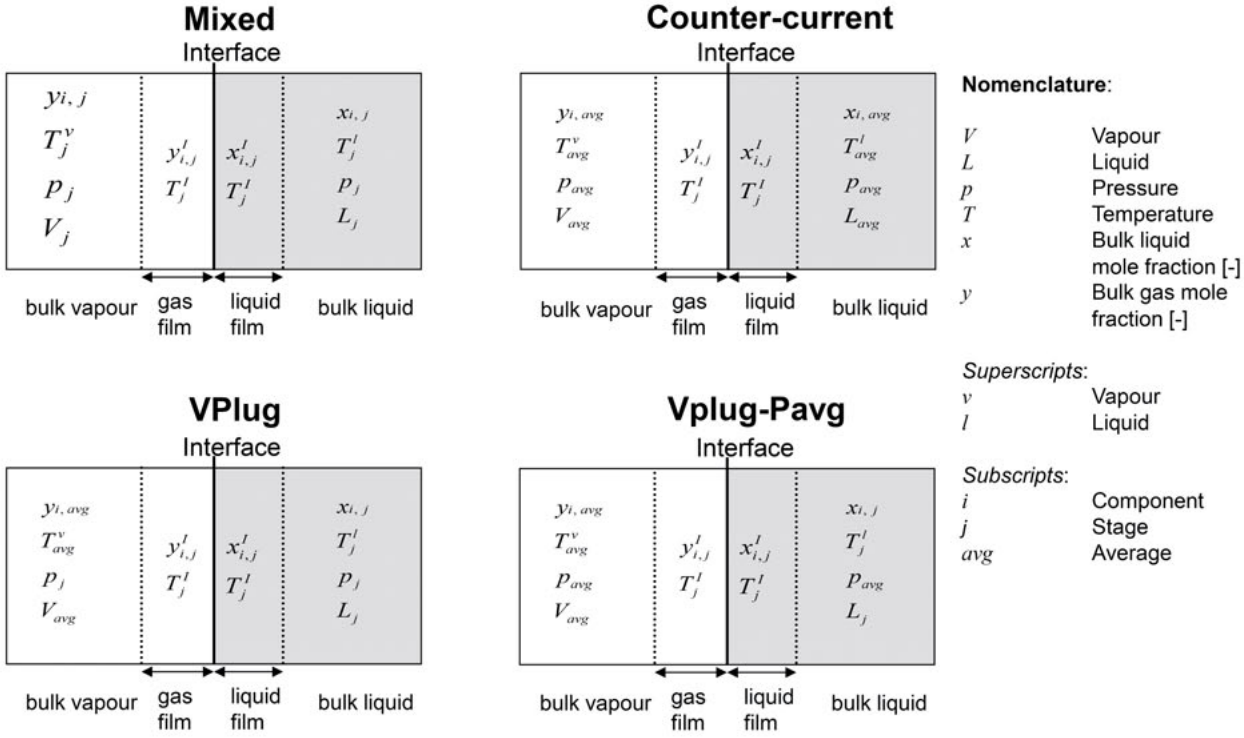

Figure 3.8: Available Flow Model options for rate-based modelling in Aspen Plus

spectively. Additional points can have significant influence on temperature and composition profiles and hence can be used to tune models to plant data [97]. This is exactly the approach used by Hockley [95] to model a CO_2 capture process with aqueous monoethanolamine solution based on a pilot plat of the University of Texas at Austin. Hockley used a film thickness ratio of 5 and added 5 internal discretization points. The results presented by Hockley showed a good agreement of plant data with generated data from the developed Aspen Plus model.

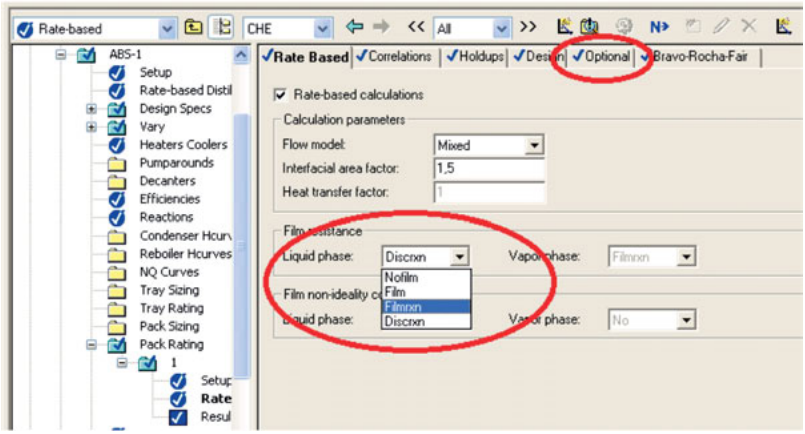

Figure 3.9: Pack Rating/Rate Based/Specifications form for specification of film discretization

Mass-Transfer correlations can be specified in the *Pack Rating/Rate-based/Correlations* form. There are correlations available for trays (bubble-cap, sieve and valve) and packing (random and structured). Recommended correlations are “Onda et al. (1968)” for random packing and “Bravo et al. (1965)” for structured packing. It is important to be consistent and specify the same correlations for *Mass transfer coefficient method* and *Interfacial area method*.

Holdup correlations can be specified in the *Pack Rating/Rate-based/Holdups* form. A helpful tool to calculate column diameter is included in *Pack Rating/Rate-based /Design* sheet. By selecting the checkbox in Figure 3.10 the user can access the *Base parameters* box to modify default values if necessary. This tool allows for adjusting column diameter, even if the user has previously entered a value, to fit the base flood specified in the *Base parameters* box. That is, user’s value entered will be used for a first iteration. If the calculated flood differs from the value set in the *Base parameters* box, Aspen Plus will either increase or decrease the column diameter and run calculations again, until results match the *Base flood* specified

by the user. There are two important aspects to consider when activating this tool: first, the user can specify a maximum flood and second, the user can also specify a stage, at which the entered maximum flood should be considered for the design. It may occur that the specified base flood is exceeded, which depending on the assumed value it may even mean flooding. A glance at the *Pack Rating\Results\Profiles* sheet will help in determining whether the chosen reference stage for design is convenient or not.

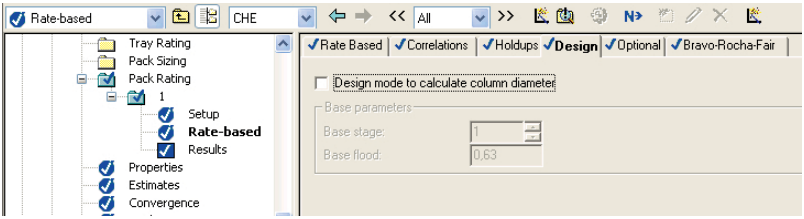

Figure 3.10: Activate design mode to calculate column diameter

Report options. Unless specified, Aspen Plus will only show what we may refer to as *general results*, that is, results regarding overall information of the inlet and outlet streams of the analysed block or UOM. Results' list can be enhanced with additional information that has to be defined in the *Setup/Report Options* sheets: *General, Flowsheet, Block, Stream, Property* and/or *ADA* (see Figure 3.11), depending on user's requirements. These results however, do not include detailed information on Rate-based calculations. Standard properties to be included in column profiles can be selected in the *Report* sheet of the UOM, whereas additional report options for rate based calculation has to be specified in the *Rate-based Report* form (see 2) in Figure 3.12). Generated results for standard properties can be found in *Profiles* and the additional rate based properties in *Interface Profiles, Efficiencies and HETP, Transfer Coefficients* and *Dimensionless Numbers* (see 3) and 4) in Figure 3.12). Rate-based results provide valuable information that can be used in evaluating the column's performance. For instance, within *Interface Profiles* the following parameters can be found: *Temperatures, Compositions, K-Values, Mass Transfer, Heat Transfer, Interfacial Area, Reactions* and *Holdups*. The information is listed for the stages specified by the user, and if applicable for the interface, liquid and vapour.

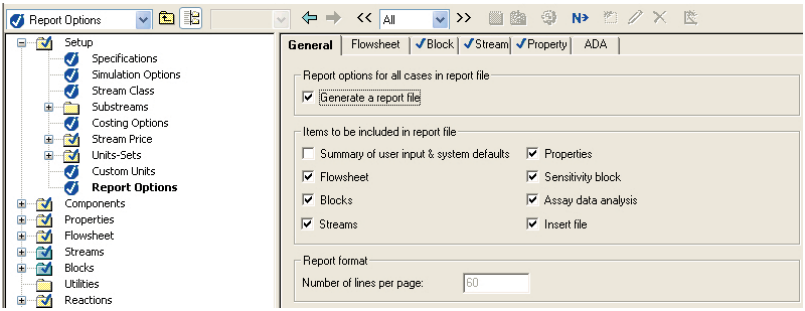

Figure 3.11: General report options specifications

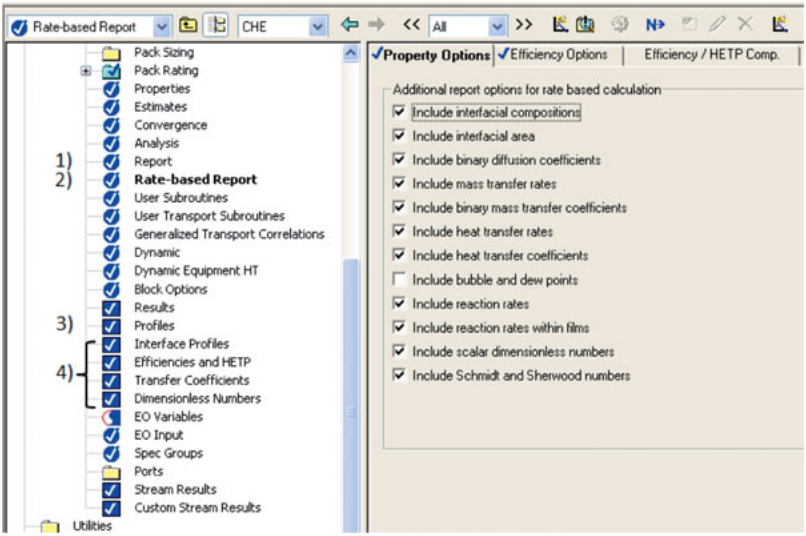

Figure 3.12: Including additional report options. 1) Standard properties, 2) Rate-Based calculation, 3) Results' report on standard properties and 4) Rate-Based calculations specific results

Specifying Reactions. The most important parameters for modelling CO_2-Absorption in Aspen Plus have already been listed, and yet the simulation would still only consider equilibrium in calculations, since the appropriate set of reactions has not been associated with an Aspen Rate-Based Distillation segment. For this, it is necessary to enter the Reactions or Chemistry ID in the *Reactions/Specifications* form of the UOM.

Electrolyte reactions are generated by the *Electrolyte Wizard* and can be found in the *Reactions/Chemistry* form. Non-electrolyte reactions are entered in the *Reactions/Reactions* form as *REAC-DIST* type. These are the reactions that were previously discussed in sections 3.1.2 and 3.1.3.

After this step has been completed, the absorber column model is ready to run in Aspen Plus. This by no means guarantees that the model will converge in the first simulation, but rather provides a basis for an iterative design process that will require the constant input of the user to fulfil the intended task.

3.2.2.3 Heat exchanger and stripper system

Once the absorber model has been completed and simulations with the desired specifications have converged, the next important UOMs to add in the absorption-stripping model are cross heat exchanger and stripper. There are though a few more small UOMs that may also be included such as the rich and lean pumps shown in Figure 3.3.

Block specifications

The first step consists in opening a converged absorber file. Next a *Pump* from the *Pressure Changers* category should be added, which represents the rich pump, since the absorber's bottom outlet stream will be connected to its inlet. For the final design of a pump the discharge pressure should compensate for column's operating pressure, delivery height, as well as some additional losses, but for an initial model it suffices when the discharge pressure is at least as high as the respective column's operating pressure. Once the final design of a column is ready, the previous value can be overwritten. A change of the discharge pressure may have a small influence on simulations, nonetheless an accurate value will aid calculate the required electric power of a pump, which will be used later on to estimate the overall energy demand, as well as the overall efficiency penalties caused by the scrubbing system.

An adequate design of a scrubbing process would also include data related to the main heat exchanger between absorber and stripper. This is possible in Aspen Plus by implementing the UOM *HeatX*, which represents a cross heat exchanger. However, considering that a stripper has to be included in the design, the model might converge more easily by introducing a few intermediate steps, before the model looks as presented in Figure 3.3. A *Heater* from the *Heat Exchangers* category should be added, which represents the cold part of the cross heat exchanger. The outlet stream of the pump is then connected to the heater's inlet. By providing

an outlet temperature close to the expected stripper's temperature the probability of converging is higher. As a further specification the pressure should be set to "0". This does not mean that the heater works in a vacuum. It merely represents pressure losses, which will be neglected.

Next UOM is the stripper, represented with a *RadFrac* block from the *Columns* category. The heater's outlet stream is connected to the stripper's side. Then two more outlet streams have to be added: bottom and top. The procedure for parameter specification is similar to the one described for the absorber, although compared to the absorber the stripper might appear much simpler. In the *Setup/Configuration* form should be set to *Rate-based*. In the previous section it was mentioned that it is recommended to use about 20 stages, but the precise number of stages depends on the height each stage should have and what might appear reasonable, which referred to a height per stage between 0.1 – 0.3 m. The calculations of this work were conducted assuming no condenser, a Kettle reboiler, valid phases: *vapor-liquid* and standard convergence.

In the *Setup/Streams* form, inlet and outlet streams' location can be specified, keeping in mind that the first and last stages represent top and bottom of the column respectively.

As with the absorber, the pressure drop within the column can be specified in the *Setup/Pressure* form. This is an especially sensitive parameter. If the stripper is operating at a pressure higher than atmospheric one, it is imperative to keep pressure losses as small as possible; otherwise the reboiler duty will increase unnecessarily. For regenerating a solvent solution, high temperatures are required, but as a consequence of a pressure drop the temperature within the column decreases proportional to the pressure drop, making it necessary to provide more energy to compensate for this.

In the *Pack Rating/Setup* form, stripper's packing details can be entered analogous to the absorber's packing. Within the *Pack Rating/Rate-based* sheet, the user should only activate *Rate-based calculations* check box so that the *Design* option is available and Aspen Plus can calculate column's diameter. Since chemical reactions are reversed almost instantaneously in the stripper, it is not necessary to account for discretization of stages.

Once the last step is completed, the user may decide whether to activate some additional options with the *Analysis*, *Report* or *Rate-based Report* forms.

The absorber-stripper model still lacks a few UOMs: lean pump, a second heater and a cooler. The lean pump connects the stripper's bottoms stream with the heater, making sure the lean solvent will be able to reach the absorber with the provided discharge pressure. The second heater will be used to reach the desired temperature difference(s) between absorber and stripper bottoms streams, previously defined to be 5 and 10 K in section 3.2.1.

According to Figure 2.1 and Figure 3.3 the last UOM to add to the system is a cooler, which is nothing else than a *Heater* from the *Heat Exchangers* category, but whose discharge temperature is the same as the one specified for the absorber's lean solvent inlet. However there is an important UOM that has not yet been accounted for: a *Mixer* from the *Mixers/Splitters* category that will help calculating a so-called make-up stream. Due to solution's carry-over either at the top of the absorber or stripper, lean solution's flow rate at the stripper's bottom differs from the one at the absorber's inlet. If this difference is not compensated the lean solution's flow rate would in theory steadily decrease, which would arise a series of process instabilities and in worst case yield a standstill of the capture plant. This is in fact one of the main reasons why modelling this sort of processes often enough fails to converge, when the user intends to close the absorber-stripper loop. Thus a *Mixer* should be added to the flowsheet.

For conducted calculations, the mixer was set before the lean cooler, but the position may be defined otherwise by the user as long as the mass balance is right. The mixer should have at least two source streams: a make-up stream and –in this case– the lean solvent's cooler outlet stream, whereas the product stream will be the inlet stream of the lean amine cooler, that is supposed to guarantee an absorber's inlet temperature of 40°C.

A few notes on the mixer. The newly defined make-up stream is an inlet stream and hence it has to be defined in Aspen Plus. However, this is exactly the stream we expect the software to calculate, since it is not known. A helpful tactic is to set the flow rate to an extremely small quantity (0.00001 kmol/hr), that will not affect initial calculations and which value can be subsequently overwritten by using a calculator every time a new iteration begins. An approach that can be used is to define new *property sets* under *Properties\Prop-Sets* to estimate the respective apparent component flow rates (FAPP) of the single components such as water, MEA or piperazine and potassium carbonate. The user can choose any of the units listed by Aspen Plus under *Properties\Prop-Sets\Properties* and then enter phase and actual component under *Properties\Prop-Sets\Qualifiers*. Once this step has been completed a new calculator can be defined to compare the compo-

nents of the mixer's inlet stream (regenerated solvent stream) with the ones of the absorber's lean solvent inlet, which have been previously determined within absorber calculations in section 3.2.2.2. To access single stream components, these may be defined as import/export variables. The difference of the two streams is what should be compensated as a make-up stream. This is by no means the only way to solve the make-up stream issue. The mentioned approach rather points out what the user should pay attention to, namely the mass balance.

Once all UOMs have been respectively connected to each other, there is one last step that will aid convergence: disconnecting the absorber from the rest of the UOMs. This is performed as follows:

- Right-click the absorber bottoms stream connected to the rich pump and selecting "Reconnect Source"
- Left-click anywhere away from any UOM
- Select the disconnected stream, right click and select "Reconcile"
- From the *Type of Variables* category select "Component fractions, total flow"
- Add a new absorber outlet stream

By doing that, results from absorber calculations will also be available for the new UOMs, but having eased the system's complexity.

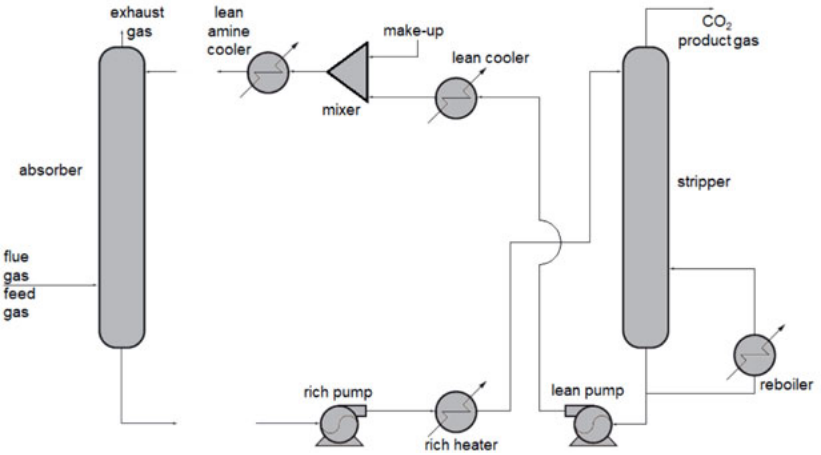

Figure 3.13: Flowsheet of intermediate step for assisting system's convergence

Once these steps are finished, the current flowsheet should look similar to the one presented in Figure 3.13 and first simulations may get started. There are however

a few tools that are not directly required for conducting simulations, but that may prove helpful for troubleshooting or just keeping an overview of the system's performance in general.

Flowsheeting options

In the same way that a design-spec was suggested to vary the absorber's L/G ratio, it can be used to vary the stripper's reboiler duty until a desired lean loading value has been reached. A simple way of doing this consists in first specifying a calculator block that determines the desired stream's loading, in this case the stripper's outlet stream, and then entering this variable as the specification in the design-spec with a respective target value.

When specifying the tolerance of a design-spec it is advisable to be careful setting the right order of magnitude depending on the variable's units that is going to be varied and the entered target. For example, for a target loading of 0.242 it might be useful to start with a tolerance of 0.001 and then tighten it to 0.0001, when the search range can be narrowed. On the other hand, if a duty of 2.5 MW is the target then a tolerance of 1000 might already be enough for calculations. If instead a tolerance of 0.001 would be entered, conducted iterations might never converge. This is of special importance due to the fact that Aspen Plus does not always allows the user to choose the units to work with.

Using calculator blocks enables the user to quickly appreciate the system's performance. Some of the calculators that may be helpful would for example estimate lean and rich loadings, CO_2 concentration of the stack, molality of regenerated solvent solution, specific reboiler duty, etc. There are no written rules to determine the number and kind of calculator blocks to implement in simulations; the user can specify as many calculators as he/she considers necessary.

When design-specs have successfully run it would not go amiss to update block specifications with their results. In this matter calculation time may be reduced. This also helps tightening the range within a solution should be found.

Implementing a cross heat exchanger

Once a design-spec was used to manipulate the reboiler duty until the target lean loading was reached, the next flowsheeting step may be taken. This consists in connecting *lean cooler* and *rich heater* with each other to actually behave like a cross heat exchanger (see Figure 3.3). For this, it is necessary to manually set the heat duty of *rich heater* to be the same as the one from *lean cooler*. The respective heat duty can be found in the *lean cooler* results page. The value for *rich*

heater should be the same, but of opposite sign. The previous temperature specification should then be replaced by “heat duty” instead.

In the *Process Flowsheet Window* a new stream has to be added. From the *Streams* category, a heat stream should be selected with *lean cooler* as source and *rich heater* as destination. Subsequently *rich heater* should be selected and the previous heat duty specification deleted. Since a heat stream has been specified, Aspen Plus requires no further information for simulations to run. The flowsheet should now look like the one depicted in Figure 3.14. Results obtained with this kind of configuration may be used directly for an analysis of the system. However, if further data is necessary from the cross heat exchanger such as required area, then it might be better to substitute this configuration after it has converged by the one originally shown in Figure 3.3. For this purpose *lean cooler*, *rich heater* and the connecting heat stream should be deleted and the UOM *HeatX* from the *Heat Exchangers* category should be added to the flowsheet. In the specifications, the user should make sure to enter “Hot outlet-cold inlet temperature difference”. In addition, unless the user enters a heat transfer coefficient, Aspen Plus assumes a default value of 850 W/(m^2K). Given that several calculations have been previously conducted, Aspen Plus should be capable of finding a solution with the provided information, since the degrees of freedom have been considerably reduced.

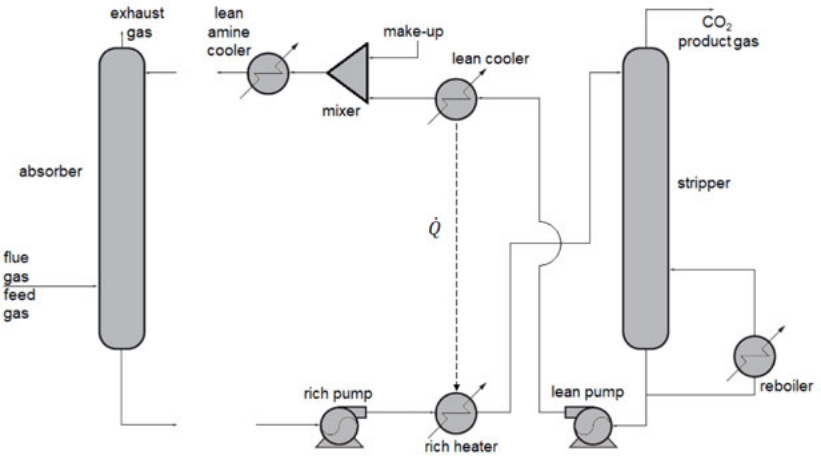

Figure 3.14: Specifying heater and cooler to act as a cross heat exchanger

Completing an absorption-stripping system model

When calculations have been completed and solutions have been found, the system's loop can be finally closed. The first step consists in deleting the rich pump inlet stream and replacing it by the absorber bottoms stream. Running a simulation before finally closing the whole loop will not do any harm. Small intermediate steps help Aspen Plus finding a solution, above all when modelling highly non-ideal systems. As previously mentioned in section 3.2.2.2, if no errors are reported, the run can be saved and adjusted for the next run, which will start calculations with the already available results from the previous run, thereby reducing computing time.

The last step entails connecting the absorber's lean amine inlet stream to the mixer's outlet stream. Before doing this, calculations are needed for estimating the make-up stream and ensuring the molality of the mixer's outlet solvent solution, which corresponds to the one used at the absorber's inlet, otherwise there will be serious convergence issues.

Model Analysis Tools

Having a converged absorber-stripper system is only the first part of the work. Once this has been completed, the actual analysis may be undertaken for which Aspen Plus offers different tools, depending on the user's requirements: *Sensitivity*, *Optimization*, *Constraint*, *Data Fit* and *Case Study*. The first of these tools serves, as the name suggests, the purpose of conducting sensitivity analyses. The advantage of implementing this tool resides in being able of gathering relevant information within a single table without having to navigate single UOMs looking for results, which often enough the user ends up losing track of things. It is also possible to plot results and to export results into a program like Excel for further evaluation.

Depending on a model's difficulty and effect of planned variations on the system, computing time of a sensitivity analysis might take a few seconds, a couple of minutes or even several hours.

4 Technical analysis

The focus of this chapter is to account for all operating parameters that affect the scrubber system's outcome. This includes flue gas preconditioning, scrubbing process, column geometry, as well as integration with the power plant (RPP NRW). For this purpose, generated results from Aspen Plus simulations are graphically presented and discussed. As the analysis is conducted it may be necessary to select some parameters. Not all variations introduced in section 3.2 will be accounted for in the end, only the promising ones that seem to be able to contribute to power plants overall efficiency penalties' reduction. The technical analysis results will be used in the next chapter, since they represent the basis required for a cost analysis.

Previous to start with the technical evaluation some important factors will be introduced, which will allow for a better understanding of results and optimum parameter selection in the following sections.

4.1 Important packed columns facts and considerations

Column geometry can have a great influence on the efficiency of a process. A well dimensioned column is capable of restraining energy penalties to a minimum. Packed columns performance has been established to depend directly from pressure drop of a gas flowing upward countercurrently to liquid flow. This dependency is depicted in Figure 4.1. At low liquid rates ($\dot{L}$), pressure drop is fairly similar to that of dry packing, meaning that pressure drop occurs due to flow through different open spaces in the bed. Consequently, pressure drop is proportional to approximately the square of the gas velocity, as can be seen in the regions AC and A'C'. This also applies at higher liquid rates, where the openings in the bed are smaller [21].

Four zones can be identified in Figure 4.1. In zone I gas and liquid flow countercurrently without affecting each other. It is not until Zone II when liquid and gas phases will start affecting each other. At C'C an accumulation of liquid, better known as liquid holdup, starts taking place. This point marks the beginning of the loading region (Zone III). In this region, pressure drop is not proportional to the square of the gas velocity anymore but to a power higher than two. Zone III represents the area where the highest possible loading is achieved at acceptable pressure losses. According to Sattler [33], column design at 80 % proximity to flood

point ensures column stability. At D'D liquid holdup has increased so much, that the packing voids have completely been covered. At this point column instability occurs with a rising liquid accumulation in the column. Pressure drop rockets upwards usually with only a slight change in gas rate. This behaviour is referred to as flooding [21, 33].

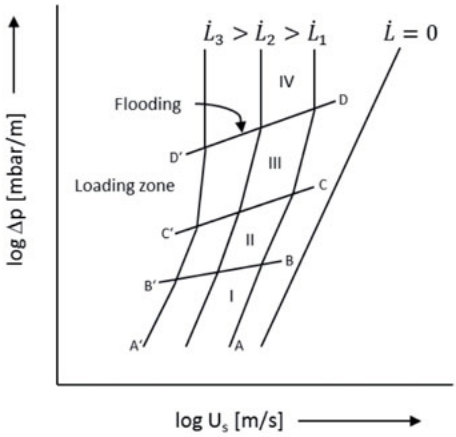

Figure 4.1: Pressure drop characteristics of packed columns.

There are characteristic pressure-drop curves for each packing type –random or structured– with which it is possible to determine important operation parameters, i.e. proximity to flood point. Such curves are usually calculated by using a solution like water as a basis. However, to be able to work with different fluids, like the MEA or carbonates-piperazine solutions of the present work, there are other factors that help selecting or rating packings. An important parameter to consider is the solution's viscosity. Some vendors offer an operation range depending on it. According to Green, et al. [21], the first pressure drop correlation of packed columns flood points was developed back in 1938 by Sherwood, Shipley, and Holloway [98]. This was done based on laboratory measurements conducted basically on the air-water system with random packing. Ever since, this kind of correlations have been further developed for air and liquids other than water, until a correlation –first introduced by Eckert [99]– was modified and simplified by Strigle [100] to become what is now called the generalized pressure drop correlation (GPDC). This correlation is represented in the so-called GPDC chart, which was originally introduced in English units and is now depicted in metric units in Figure 4.2 and Figure 4.3 for random and structured packing respectively. The ordinate is the capacity parameter (CP) defined as:

$$CP = C_s F_p^{0.5} \nu^{0.05} \tag{4.1}$$

Where,

F_p	[m^{-1}]	Packing factor[17]
ν	[m^2/s]	Kinematic viscosity of liquid
C_s	[m/s]	C-factor based on tower superficial cross-sectional area
CP	[units consist with equation (4.1) and its symbols]	Capacity factor

C_s is known as the *C-factor* and denotes a gas load term. The C-factor is considered the best parameter for comparing systems capacities of different physical properties [21]. It represents the superficial gas velocity (u_s) corrected for vapour and liquid densities [101]. According to Green, et al. [21] u_s is usually based on the tower cross sectional area (A_T). However, it may also be based on either the net (A_N) or on the bubbling area (A_B) and hence, it is advised to be careful whenever the basis of area data is not clearly specified.

$$C_s = u_s \sqrt{\frac{\rho_G}{\rho_L - \rho_G}} \tag{4.2}$$

Where,

u_s	[m/s]	Superficial gas velocity
ρ_G	[kg/m^3]	Gas density
ρ_L	[kg/m^3]	Liquid density

The GPDC chart abscissa is the same dimensionless flow parameter or F-factor (F_{LG}) used for trays, which represents the ratio of liquid kinetic to vapour kinetic energy. High F_{LG} values are characteristic of high liquid rates and high pressures, whereas low flow parameters stand for vacuum and low liquid rate operation.

$$F_{LG} = \frac{L}{G}\left(\frac{\rho_G}{\rho_L}\right)^{0.5} \tag{4.3}$$

Where,

L	[$kg/(s \cdot m^2)$]	Liquid mass velocity
G	[$kg/(s \cdot m^2)$]	Gas phase mass velocity

[17] Empirical factor characteristic of packing size and shape. Data for common packings is usually listed in distillation texts.

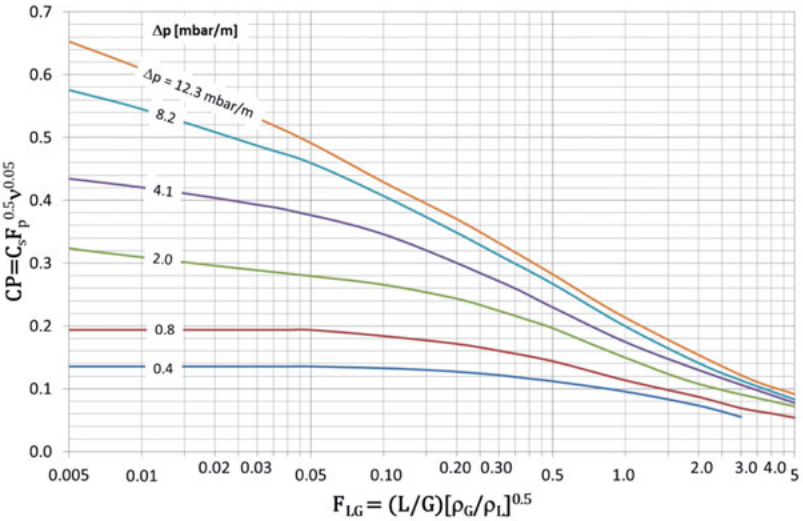

Figure 4.2: Generalized pressure drop correlation for random packing only. Chart in metric units based on Stringel's chart in English units [100].

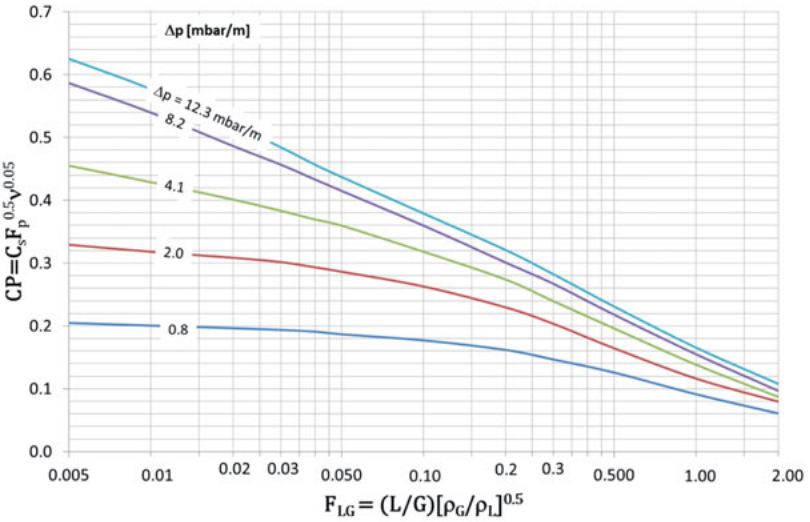

Figure 4.3: Generalized pressure drop correlation for random packing only. Chart in metric units based on Kister and Gill's chart in English units [102].

Both GDPC charts in Figure 4.2 and Figure 4.3 lack the flood curve and hence their ability to predict flood is thereby constrained. To correct this, implementation of the Kister and Gill equation is recommended, which allows finding the pressure drop at the flood point, as follows:

$$\Delta p_{flood} = 0.12 F_p^{0.7} \tag{4.4}$$

Once Δp_{flood} has been calculated, it is up to the column designer to define how close to the flood point the column should operate.

The required data to calculate F_{LG} is usually available. With F_{LG} the corresponding capacity factor (CP) may be determined from either Figure 4.2 or Figure 4.3 – depending on the packing type–. Since CP is now known, equation (4.1) may be used to determine the C-factor (C_s), whose value may then be substituted in equation (4.2) to calculate the towers superficial gas velocity based on the cross sectional area (u_s). With help of the gas rate ($\dot{V}_G$) and u_s, the cross sectional area is determined, with which finally the column's diameter may be calculated.

$$u_s = \frac{\dot{V}_G}{A_T} = \frac{\dot{V}_G}{\left(\frac{\pi \cdot d^2}{4}\right)} \tag{4.5}$$

Where,

A_T	[m^2]	Column cross-sectional area
d	[m]	Column diameter
$\dot{V}_G$	[m^3/s]	Gas rate

When calculating column geometry, Aspen Plus implements an approach to maximum capacity that varies according to the implemented packing type to make sure that design and operation succeed. According to the Aspen Plus Reference [93] for Norton packings (IMTP 40 and 50 used in the SO_2 scrubber): "…approach to maximum capacity refers to the fractional approach to the maximum efficient capacity. Efficient capacity is the operating point at which efficiency of the packing deteriorates due to liquid entrainment. The efficient capacity is approximately 10 to 20 % below the flood point." For Sulzer's Mellapak (Type 250X used in simulations of: desorber as well as SO_2 and CO_2 absorbers) maximum capacity is defined in Aspen Plus as the operating point at which a pressure drop of 12 mbar/m (1.47 in-water/ft) of packing is reached. This is, though, not the optimum operation point but the one at which stable operation is still possible. In order to guarantee that the

previous pressure drop is not reached the gas load that corresponds to the maximum capacity should be 5 to 10 % below the flood point. A design range between 0.5 and 0.8 for approach to flooding is recommended by Sulzer. This agrees with an 80 % proximity to the flood point recommended by Sattler [33].

Once the principles of column geometry calculation and the corresponding assumptions for simulations have been explained, the obtained results with Aspen Plus will be discussed in shortly.

4.2 Flue gas preconditioning

The resulting diameters calculated with Aspen Plus for L/G ratios between 1.5 and 4.0 can be appreciated in Figure 4.4. According to the simulation parameters listed in section 3.2.1.1 six pH values ranging from 6.0 to 7.2 were considered. However a first results appraisal showed only a difference in diameter size depending on L/G ratio or packing used, but not due to the pHs. In fact, the difference in size attributed only to the pH value is practically non-existent. A graphical representation of these results would thus only lead to an overlapping of several points, so instead an average value of results for all pHs is presented in Figure 4.4 for each L/G ratio and packing kind.

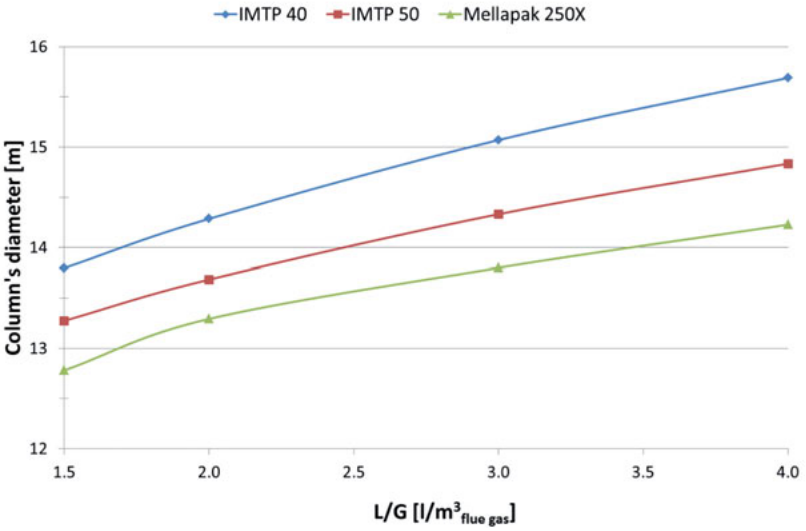

Figure 4.4: SO_2 scrubber's diameter as a function of the L/G ratio for all pHs.

In general, the column diameter increases with an increasing L/G ratio. This behaviour was to be expected and can be explained with Figure 4.1 and Equation (4.5). This figure shows how low superficial gas velocities (u_s) result from increasing liquid mass velocities, which in turn leads to bigger diameters when substituted in Equation (4.5).

Figure 4.4 also illustrates how column diameters for a given L/G ratio increase or decrease depending on the packing used. The smallest diameters result from using a structured packing, such as Mellapak 250X. In case of random packings IMTP 50 and IMTP 40, bigger diameters are required with the last one to reach a target SO_2 concentration below 10 $mg/m^3_{flue\ gas}$. The difference in diameter size between random packings derives from diverse packing characteristics like void fraction or nominal packing size. By having specified the same maximum fractional capacity for all packings in Aspen Plus, the software calculates according to vendor specifications the proximity to the flood point. The void fractions of IMTP 40 and IMTP 50 are 97 and 98 % respectively, which yields to a higher gas strain for type IMTP 40 than for IMTP 50 and hence, in order to still maintain a constant fractional capacity the diameter has to be increased.

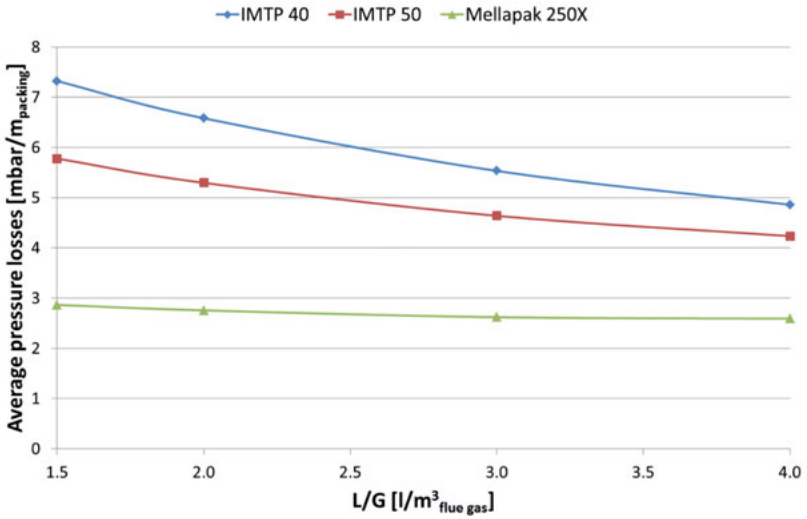

Figure 4.5: Average pressure losses as a function of the L/G ratio for all pHs.

Besides the diameter, it is important to contemplate the associated pressure losses within a column, which will help rate its performance. Figure 4.5 shows the pre-

dicted average pressure losses for all packings and pHs. As with Figure 4.4, the difference of results between a pH of 6.0 and 7.2 is so small that to avoid overlapping of results an average value is given instead. Random packings' behaviour is described with a slope in blue and red for IMTP 40 and IMTP 50 correspondingly, meaning that by increasing the L/G ratio related pressure losses decrease. Albeit the Mellapak 250X's behaviour also declines as the L/G ratio increases, the trend is much more flat than the ones of the random packings, appearing to be almost constant. Structured packings are not only highly efficient, but they also exhibit lower pressure drop per theoretical stage than random packings, which is a major advantage for applications where overall pressure drop within a column should be kept as low as possible.

As the liquid to gas ratio increases, column diameter is adjusted to fulfil an approach of 80% proximity to the flood point. The smaller IMTP 40's void fraction and related higher gas strain implicate higher average pressure losses than the ones expected with IMTP 50, which is exactly the trend illustrated in Figure 4.5.

Figure 4.4 and Figure 4.5 showed the calculated diameters and related average pressure losses per meter for different L/G ratios and all packing types. There is though a parameter that has not yet been discussed: the packing height actually needed to restrict the SO_2 content below 10 $mg/m^3_{flue\ gas}$. This is depicted in Figure 4.6. As with the previous figures, results for all considered pHs are so close to one another, that instead only the lowest and the highest pH are given in Figure 4.6. The diagram shows three main groups that correspond to the analysed packings (Mellapak 250X, IMTP 40 and IMTP 50). In addition, the number next to each point of Figure 4.6 indicates the equivalent L/G ratio.

The scrubber's packing section was divided into 25 segments for simulation purposes. This made it easier to take a look at the column's profiles to determine at what height the targeted SO_2 concentration had already been reached, or whether the packing height would have to be increased in case the targeted SO_2 concentration would be outside the set boundaries. All presented points in Figure 4.6 guarantee a concentration below 10 $mg/m^3_{flue\ gas}$. However, even when two points overlap since they share the same packing height, the respected SO_2 concentration is not identical. Simulations showed a discrepancy in range from 8.41 to 9.99 $mg/m^3_{flue\ gas}$. A table with all important results and parameters is provided in Appendix A.1.

According to results shown in Figure 4.6, an increase of pressure losses as a result of a decreasing L/G ratio was to be expected. For instance, assuming a constant pH of 7.2 and random packing IMTP 50 and an L/G ratio of 1.5, it would be

necessary to have a column diameter of 13.28 m for column operation at 80 % proximity to the flood point. This implicates the use of a packing height of 2.5 m in order to reach the target outlet SO_2 concentration, which would result in pressure losses of 14.43 mbar. If instead, the L/G ratio is 3.0, the diameter's size increases respectively to 14.34 m in order to maintain the same proximity to the flood point. By these means, not only does the SO_2 has a higher probability to get absorbed in the abundant sodium hydroxide solution –compared to a smaller L/G ratio of 1.5–, but the cross sectional area has been expanded. This increases the contact area that is available for mass transfer and concomitantly the packing height needed to reach the same SO_2 outlet concentration decreases to 2.1 m, which in turn reduces pressure losses to 9.73 mbar.

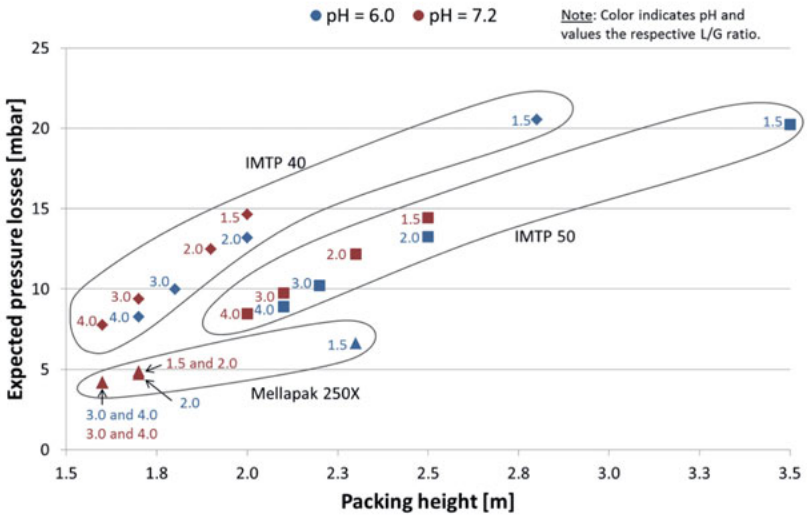

Figure 4.6: Required packing height to guarantee an SO_2 concentration < 10 $mg/m^3_{flue\ gas}$ and corresponding pressure losses for all packing types.

An interesting fact is that although Figure 4.5 indicated that the highest specific pressure losses are reached with random packing IMTP 40, Figure 4.6 illustrates that the highest pressure losses actually result from using IMTP 50. This is due to packing characteristics. While a higher void fraction from type IMTP 50 yield a lower gas strain and thus a smaller diameter, the lower void fraction of type IMTP 40 causes a higher liquid accumulation throughout the packing. This fact and the bigger diameter favour mass transfer, hence enhancing capacity. Therefore the required packing height for IMTP 40 is smaller than for IMTP 50, and though spe-

cific pressure losses are higher for IMTP 40, overall pressure losses within the SO_2 scrubber are indeed smaller than for IMTP 50.

Independently of packing kind, the highest pressure losses are always reached with a liquid to gas ratio of 1.5. The difference of required packing height and related pressure losses is so pronounced at L/G = 1.5 and pH = 6.0, that it makes this parameter combination unfeasible for further consideration. The problem does not seem to be the low L/G ratio, but the pH value instead. SO_2 and CO_2 are acid gases. The idea behind using a sodium hydroxide solution is to be able to catch SO_2 fast and efficiently. By using a solution with a higher acidity[18] -compared to the other considered pHs-, SO_2 cannot be captured as easily as expected. So in order to fulfil the target outlet SO_2 concentration, packing height increases faster than with a pH higher than 6.0, thus pressure losses skyrocket. By increasing L/G ratio, the final SO_2 concentration in the solution is lower, even if the solution's pH remains the same, so the effect of dramatically increasing packing height is lessened.

Sulzer's Mellapak 250X shows –as was the case before– the best results in terms of keeping pressure losses as low as possible. For a pH of 6.0 a packing height of 2.3 m would be required. For all other pH values and L/G ratios, the required packing height ranged from 1.6 to 1.7 m, which is far below the smallest packing height needed by random packings.

A total of 72 cases were needed to cover the SO_2 scrubber's parameter combinations presented in section 3.2.1.1. In order to continue appraising results of the different cases, it is important to take a look at CO_2 losses at the scrubber's outlet due to carry-over in the sodium hydroxide solution. Since CO_2 is also an acid gas, it has a high affinity to react with the solution used to reduce SO_2 concentration in the flue gas. The lower the solution's acidity, the more pronounced this effect occurs. However, this behaviour should be restricted. Opposite to CO_2 capture with amines, where amine regeneration allows for their constant reuse and hence only a small portion of the solvent has to be added in form of a make-up stream, CO_2 or SO_2 capture with a sodium hydroxide solution does not allow for solvent regeneration, but it will rather be treated as waste or process water, if it previously undergoes an appropriate treatment. This is a costly solution and thus was only considered as a retrofit option of an existent FGD plant, where SO_2 concentration has already been limited to a maximum of 200 $mg/m^3_{flue\ gas}$. Therefore, Figure 4.7 illustrates the CO_2 amount that remains in the flue gas after SO_2 concentration has

[18] The pH of an aqueous solution may vary between 1 and 14. A neutral solution has a pH of 7.0. Below that value aqueous solutions are considered acidic. The lower the pH, the higher the acidity is.

been limited. The diagram shows how CO_2 carry-over increases with an increasing pH, which can be explained with CO_2's affinity to react with the solution and its intensification as the pH increases. Figure 4.7 also depicts how a stronger carry-over takes place as the L/G ratio grows. Gas rate remains constant through all calculations, thus as the L/G ratio increases more liquid is available to contact the flue gas. This implies a higher solution's pH at the scrubber's bottom, which again yields to a higher CO_2 reaction rate with the sodium hydroxide solution.

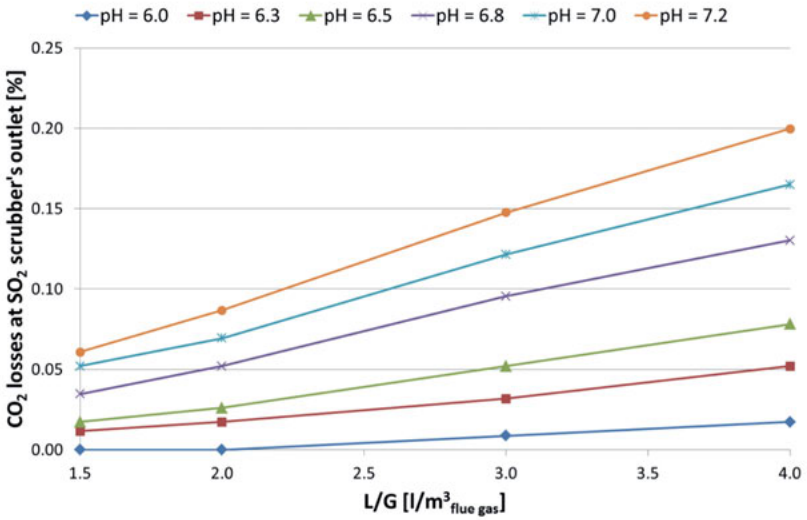

Figure 4.7:CO_2 losses due to carry-over in NaOH solution for different pHs and L/G ratios.

The actual solution's pH at the scrubber's bottom is depicted in Figure 4.8. The diagram shows the dependency of the solution's pH from liquid to gas ratio. The initial solution's pH, indicated in the legend, decreases in all cases due to higher acidity caused mainly by SO_2 but also by CO_2. Nonetheless, solution's acidity decreases as the liquid to gas ratio increases. As with Figure 4.6, a significant difference is observed for a pH of 6.0 that behaves almost logarithmically, whereas the rest of the curves become flatter as pH increases. This results in having to increase the required packing height as the solution's acidity increases, which confirms the trend observed in Figure 4.6. Results illustrated in Figure 4.8 also confirm that solution's pH at the bottom decreases faster for higher initial solution's acidity, which in turn limits its capacity to carry-over SO_2, thereby also confirming results shown in Figure 4.7.

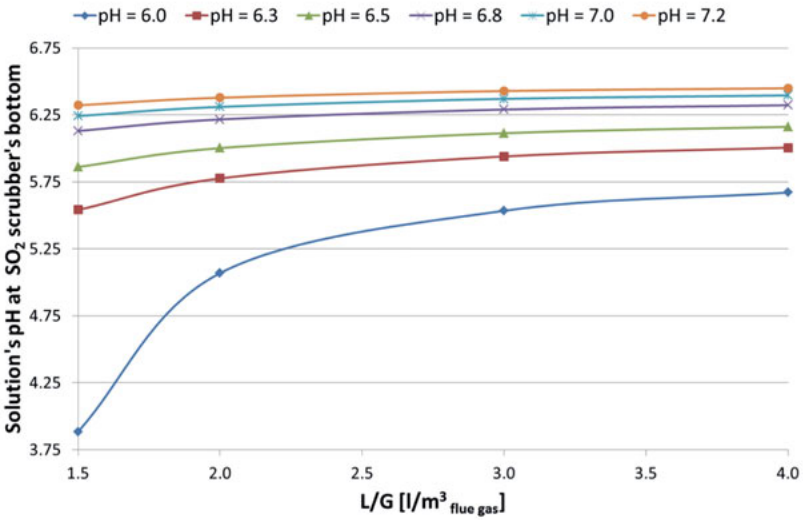

Figure 4.8: Solution's pH at SO_2 scrubber's top and bottom for different L/G ratios. Legend indicates pH at scrubber's top.

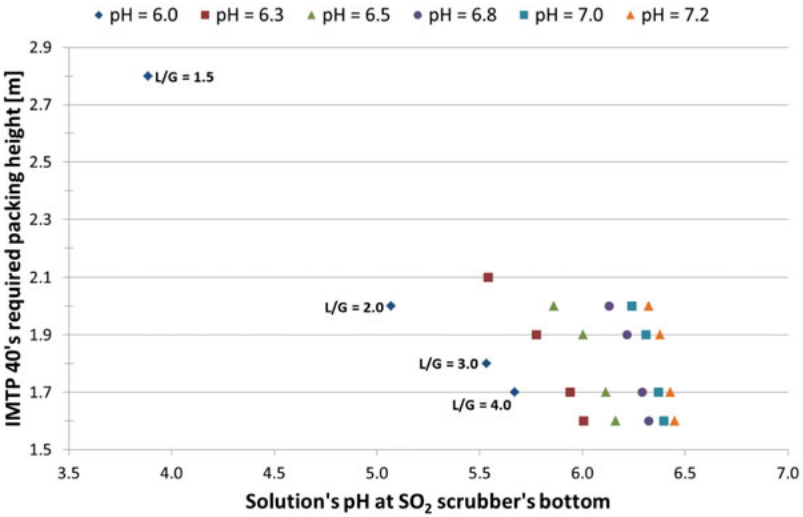

Figure 4.9: Required packing heights for IMTP 40 for different solution pH's and L/G ratios. Legend indicates pH at scrubber's top.

Since IMTP 40's and IMTP 50's results are similar, the influence of the solution's pH on packing geometry is exemplified in Figure 4.9 only for random packing IMTP 40. The Figure's legend indicates solution's initial pH at the top, whereas the x-axis final one at the bottom. Each dot in the diagram represents a fixed pH and L/G ratio. For instance, for a pH of 6.0, the dot representing a liquid to gas ratio of 1.5 requires the highest packing height of 2.8 m and corresponds to the lowest pH of 3.8 at SO_2 scrubber's bottom. By augmenting the liquid to gas ratio, the solution's pH at the scrubber's bottom increases, and the required packing height decreases. This trend is observed until the initial pH reaches a value of 6.5. Starting at this pH, the required packing height does not decrease anymore due to the initial solution's pH, but solely due to the corresponding L/G ratio. As shown in Figure 4.8, at a pH of 6.0 and a liquid to gas ratio of 1.5 the solution's acidity increases so fast that the packing height required to securing a concentration limit of 10 $mg_{SO_2}/m^3_{flue\ gas}$ has to be incremented.

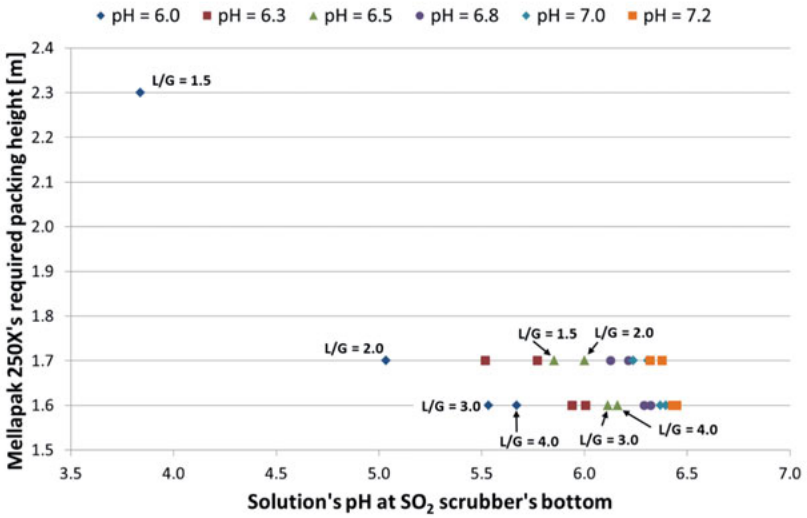

Figure 4.10: Required packing heights for Mellapak 250X for different solution pH's and L/G ratios. Legend indicates pH at scrubber's top.

Results depicted in Figure 4.10 for structured packing Mellapak 250X indicate that there seems to be no influence from the solution's pH over the required packing. With exception of a solution's inlet pH of 6.0 and a liquid to gas ratio of 1.5, the packing height remains constant for all pHs for liquid to gas ratios of 1.5 to 2.0 and 3.0 to 4.0, with packing heights of 1.7 m and 1.6 m respectively. Both packings,

structured and random one (IMTP 40) actually do have the same behaviour, but it cannot be appreciated in Figure 4.10 due to the packing's capacity nature and to the calculation approach used. As has been illustrated in the previous figures, Mellapak 250X's capacity is higher than that of the random packings, which involves smaller diameters and packing heights for capturing the same amount of SO_2.

As was mentioned before while discussing results shown in Figure 4.6, the calculation approach included entering an initial packing height for simulation purposes, which was assumed to be 2.5 m for all packings, random and structured. The packing height was then divided into 25 segments of the same size resulting in a length of 0.1 m each. Due to Mellapak 250X's higher capacity, the targeted SO_2 concentration is reached at a packing height of 1.6 m or 1.7 m depending on the L/G ratio. This can be better appreciated in Figure 4.11, where the dots indicate packing height's location, at which the corresponding SO_2 concentration in flue gas was calculated. Under these conditions, the outlet SO_2 concentration is below the limit of 10 $mg/m^3_{flue\ gas}$, but ranges between 8.42 and 9.99 $mg/m^3_{flue\ gas}$ respectively (see Figure 4.11). To tighten the tolerance used to estimate packing height, so that the same behaviour shown in Figure 4.9 could also be appreciated in Figure 4.10, it would be required to rerun simulations and increase the number of segments required, or reduce the initial assumed height of 2.5 m to a maximum of 1.8 m. However, it is not necessary that calculations' results are more detailed, given that the available ones do allow for a comparison of packing performance. A more rigorous calculation would only be required once parameters such as L/G ratio, solution's pH and packing type have been chosen for column design, which would include one case instead of 72[19].

Figure 4.11 shows –independently of the liquid to gas ratio– a logarithmic increase of packing height as the SO_2 concentration in the flue gas decreases. The red line stands for target SO_2 concentration limit. A comparison of all curves at 10 $mg/m^3_{flue\ gas}$ shows how the required packing height to meet the target is actually slightly different for each L/G ratio: higher for low L/G ratios and vice versa. As a matter of fact, the same trend is observed for all packings, as depicted in Figure 4.12.

All packings are represented in Figure 4.12 with diamonds and squares for random packings IMTP 40 and IMTP 50, and triangles for structured packing Mellapak 250X. Each dot indicates the SO_2 concentration at the equivalent height. The abscissa shows a maximum SO_2 concentration of 200 $mg/m^3_{flue\ gas}$ which

[19] 72 cases were needed to cover the SO_2 scrubber's parameter combinations presented in section 3.2.1.1.

corresponds to the maximum allowed concentration in flue gases according to German regulations (13. BImSchV previously introduced in section 3.2.1.1). This concentration was assumed in the flue gas for simulation purposes, though in Figure 4.12 only a maximum concentration of 188 $mg/m^3_{flue\ gas}$ can be appreciated. This is a result of cooling the flue gas with water from approximately 48°C (flue gas temperature after conventional FGD) to 35°C. Water has a pH of 7.0 and is considered neutral. As was identified earlier in Figure 4.7, solutions with a pH between 6.8 and 7.2 were the ones to show the highest CO_2 carry-over rates. This effect is not limited to CO_2 but includes SO_2 as well, since they both are acid gases and thus an SO_2 carry-over in water takes place previously to entering the SO_2 scrubber.

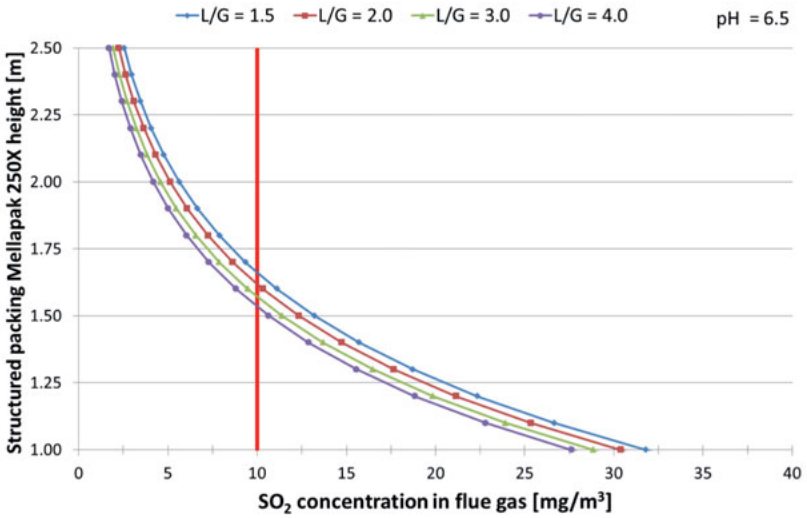

Figure 4.11: SO_2 reduction in flue gas due to L/G ratio and related packing height for Mellapak 250X and solution's pH of 6.5.

In Figure 4.12 it can be observed how the distance between points is bigger at the beginning of absorption and smaller at the target concentration. This behaviour is a sign of how capture process effectiveness slows down as the SO_2 concentration decreases resulting in a higher complexity or rather higher packing height required to capture a relatively small amount of SO_2.

Given that data for concentrations and corresponding heights is available from simulation results, it is possible to obtain a trend line for each packing that allows

predicting the required packing height, in case that the flue gas SO_2 concentration is lower than the one used in this work. The flue gas composition is affected by different factors such as coal type, combustion and flue gas cleaning technologies. The resulting formulas for a pH of 6.5 and a liquid to gas ratio of 3.0 are as follow:

$$h_{IMTP\ 40} = -0.579ln(SO_2) + 3.0253 \quad (4.6)$$

$$h_{IMTP\ 50} = -0.719ln(SO_2) + 3.7625 \quad (4.7)$$

$$h_{Mellapak\ 250X} = -0.542ln(SO_2) + 2.83 \quad (4.8)$$

Where,

$h_{packing\ type}$	[m]	Packing height
SO_2	[mg/m^3]	Target SO_2 concentration

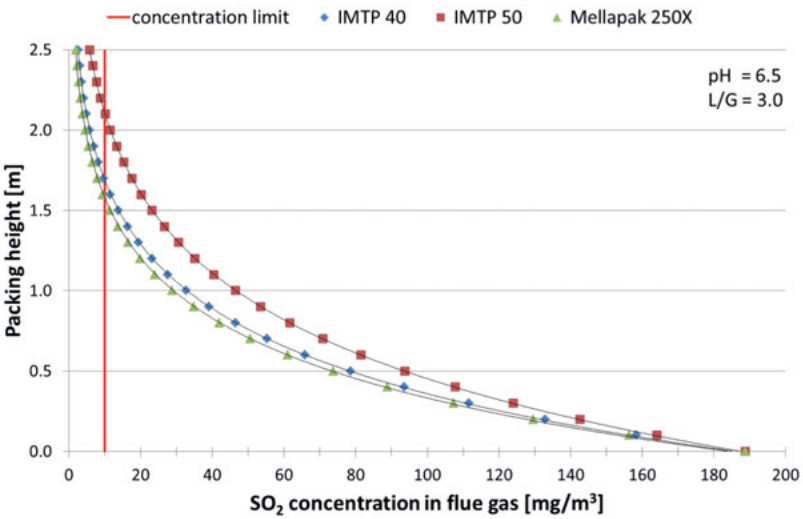

Figure 4.12: SO_2 concentration in flue gas and related packing height for all packings and a liquid to gas ratio of 3.0 and solution's pH of 6.5.

Optimal parameters

After having analysed results from Figure 4.4 to Figure 4.11, it is possible to start setting some design parameters. To begin with, the structured packing Mellapak

250X favours small column geometry at the time that a high packing performance is guaranteed. This packing will hence be set for design.

The liquid to gas ratio will be set to a value of 3.0. Using lower ratios implicates having to increase the required packing height, thereby incrementing the overall pressure losses within the SO_2 scrubber. Using a higher L/G ratio generally reduces the required packing height, but it also increases column diameter. However, since the packing has been set to Mellapak 250X, increasing the liquid to gas ratio from 3.0 to 4.0 would only result in a bigger diameter without any packing height reduction at all (see Figure 4.10). In addition, using a higher L/G ratio also entails higher CO_2 carry-over rates than with a liquid to gas ratio of 3.0.

A solution's pH of 6.5 was selected for column design. Using a higher pH does not result in decreasing the required packing height. Besides, at this pH it is possible to further limit the CO_2 carry-over in the liquid solution to a minimum before compromising packing height due to a too low pH, as was seen in Figure 4.8 for a pH of 6.3 and even more extreme for a pH of 6.0.

4.3 Scrubbing process

4.3.1 Solvent flow rate

K1, K2 and K3 are the three different piperazine-potassium carbonate blends that were contemplated for comparison with a reference solution of 30 wt% MEA. In addition, three initial lean loading values were considered for each blend, resulting in nine different points located in Figure 4.13 that correspond with nomenclature listed in Table 3.5.

Figure 4.13 shows the solvent mass flow rates required to capture 90 % CO_2 depending on the loading difference reached for K1, K2 and K3 in blue, red and green accordingly. In general, the required flow rate decreases as the loading difference increases. A lower initial lean loading enables a higher CO_2 absorption and concomitantly a reduction of the solvent flow rate required for the same amount of CO_2.

The decrease of solvent flow rate is not only related to an increase of loading difference, but also has to do with solvent characteristics. K1 is the solution with highest piperazine and lowest potassium carbonate concentration; K2 is an equimolar solution and K3 shows the opposite piperazine-potassium carbonate relationship than K1, meaning a low piperazine and a high potassium carbonate

concentration. A high piperazine concentration thus allows for a higher absorption capacity, resulting in a higher loading difference and hence decreasing the required solvent flow rate for CO_2 capture. The difference between the lowest and highest solvent flow rate sums up to over 3000 kg/s. Considering that columns diameter depend directly on mass flow rate and that the lower the flow rate the smaller the diameter, using a solvent blend with a high absorption capacity such as K1 with a low lean leading, like K1-1, might be of advantage. This though only applies to column diameter. Another important issue to consider is the related reboiler duty to regenerate the solvent. This aspect will be considered in this chapter later.

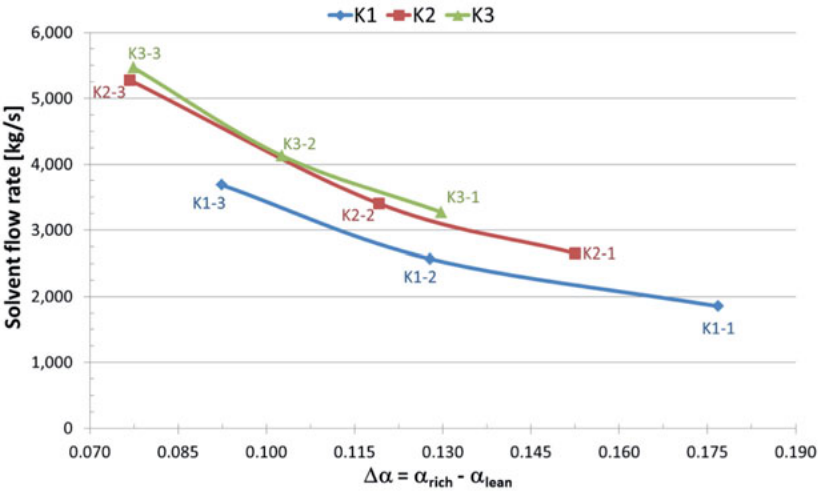

Figure 4.13: Solvent mass flow rates required to capture 90 % CO_2 depending on the loading difference for K1, K2 and K3

4.3.2 Absorber

In the previous section it was pointed out that the approach used to analyse simulation results consisted in dividing packings into several segments. This approach also applies to absorber and desorber columns, since it provides an insight into intrinsic interactions taking place at different locations of the column, allowing for detection of parameters that might have significant influence –positive or negative– towards the absorption-desorption system. Figure 4.14 shows how the segment approach works. In this example the column's packing height is indicated,

which is considered as a section. A column may have different packing sections and –if specified by the user– the segmentation approach may be used for all of them. Figure 4.14 shows 30 segments, which correspond to the number of segments used for absorber analysis indicated in section 3.2.2.2. As the figure shows, in each segment an analysis takes places at molecular level, making model predictions more reliable. In the following figures each point corresponds to one segment and the sum of all of them represents a complete section from top to bottom.

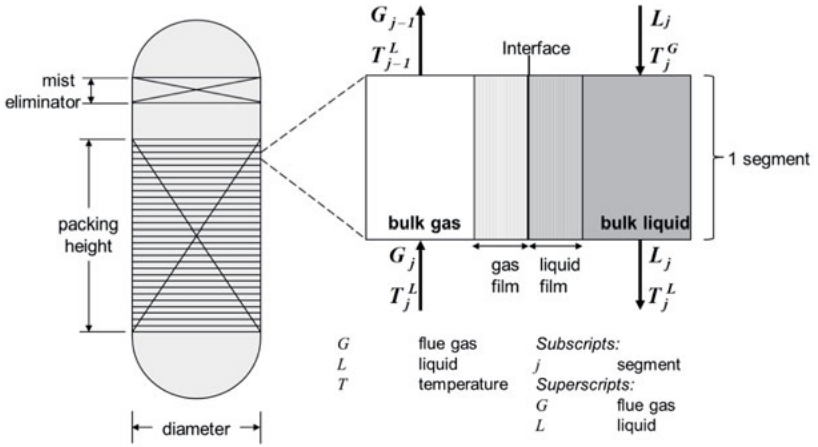

Figure 4.14: Packing segmenting approach in Aspen Plus

30 wt% MEA solutions have been widely studied within the last years and consequently the cases introduced in section 3.2.1.2 will only serve to rate the performance of the three introduced piperazine-potassium carbonate blends. Thus the following diagrams will focus on analysing K1, K2 and K3.

Aqueous solutions of piperazine activated potassium carbonate enter the absorber at the top. Once they get in contact with the flue gas, exothermic reactions start taking place. For this reason it is important to take a look at the column's temperature profile, which is depicted in Figure 4.15. K1, K2 and K3 are represented in blue, red and green curves respectively. For each blend three curves can be identified, which are related to a low, medium or high solvent's lean loading as listed in Table 3.5. As shown in Figure 4.15 the curves for the lowest lean loadings (K1-1, K2-1 and K3-1) are the ones that reach the highest temperatures of each blend within the column. In general, the reached temperature decreases as the initial lean loading increases. This can be explained with the solvent's capability of ab-

sorbing CO_2, which increases as the lean loading decreases, so that as soon as the solvent contacts the flue gas, more solvent is available to start reacting with CO_2, thereby enhancing the effect caused by exothermic reactions.

The reached temperature is also affected by the piperazine-potassium carbonate concentration of each blend. The blue curves are the ones that reach the highest temperatures, followed by the red and green ones accordingly. The blue curves represent K1, the blend with the highest piperazine and lowest potassium carbonate concentration. As the piperazine concentration decreases and the potassium carbonate one grows, each blend's maximum temperature drops. This suggests piperazine being responsible for temperature raise in the column. As a matter of fact, this result should not be surprising, since the term "piperazine promoted potassium carbonate" already points out piperazine's outcome on the blend. According to Maun [47] for a one mol solution, the heat of absorption of potassium carbonate is approximately 27.6 kJ/mol$_{CO_2}$, whereas experimental calculations indicated piperazine's heat of absorption to be approximately 79 kJ/mol$_{CO_2}$. The heat of absorption of piperazine and potassium carbonate varies depending on the concentration of each component in a solution, but the previous values help understanding piperazine's dominance in a solution under the same conditions. While piperazine reacts with CO_2 to products such as piperazine carbamate or protonated piperazine, potassium carbonate reacts to carbonate.

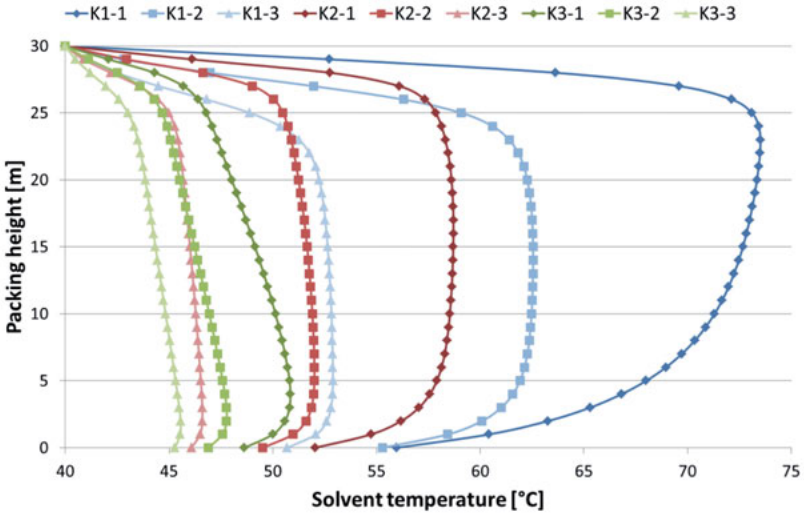

Figure 4.15: Absorber's temperature profiles for piperazine-potassium carbonate blends

The reason why piperazine was added to potassium carbonate solutions was to improve each blend's capability of capturing CO_2 in terms of capacity and kinetics. Potassium carbonate solutions alone are able to capture CO_2, but they react slowly. As was seen in Figure 4.13, the lower the piperazine concentration in a solution, the higher required flow rate to capture the same amount of CO_2. This is due to the lower reaction rate of potassium carbonate with CO_2 compared to the one of piperazine. As piperazine concentration increases, liquid flow rate decreases, thereby also affecting heat transfer. The raise in temperature is hence more pronounced in blends with a high piperazine concentration and vice versa, which is the trend observed in Figure 4.15.

All curves show a temperature drop close to the column's bottom. This is caused by preconditioned flue gas entering the column at the bottom and ascending to the top. The flue gas enters the column at a temperature of 40°C and starts cooling down the blends, as soon as they contact each other. Since blends with low piperazine concentration, or a high lean loading do not experience a blatant raise in temperature, their temperature drop due to the incoming flue gas is not as pronounced as the rest of the blends, above all K1-1.

4.3.3 Reboiler duty

With respect to heat demand for solvent regeneration purposes, Figure 4.16 depicts an overview of simulation results for all cases listed in section 3.2.1.3. These include three different piperazine promoted potassium carbonate blends, six different pressures varying in a range from 0.5 to 3.0 bar, two temperature differences (relating to the main heat exchanger between absorber and stripper columns) and three cyclic capacities for each blend. Each blend is represented by a symbol: diamonds for K1, triangles and circles for K2 and K3 respectively. Depending on the cyclic capacity it is possible to allocate results according to nomenclature introduced in Table 3.5.

The potassium carbonate – piperazine ratio of each blend shows a clear influence on calculated heat duty. Curves are avoided in this diagram due to the amount of presented points. By drawing lines K1 would show a negative parabolic trend, K2 a more pronounced positive parabolic trend –compared with K1– and K3 would show a linear drop with increasing cyclic capacity. A more detailed discussion of results will follow shortly, once Figure 4.16 has helped screening results. The goal is to find a cyclic capacity for each blend that will allow for a low specific reboiler duty at the time that column geometry will affect the overall system the least. In

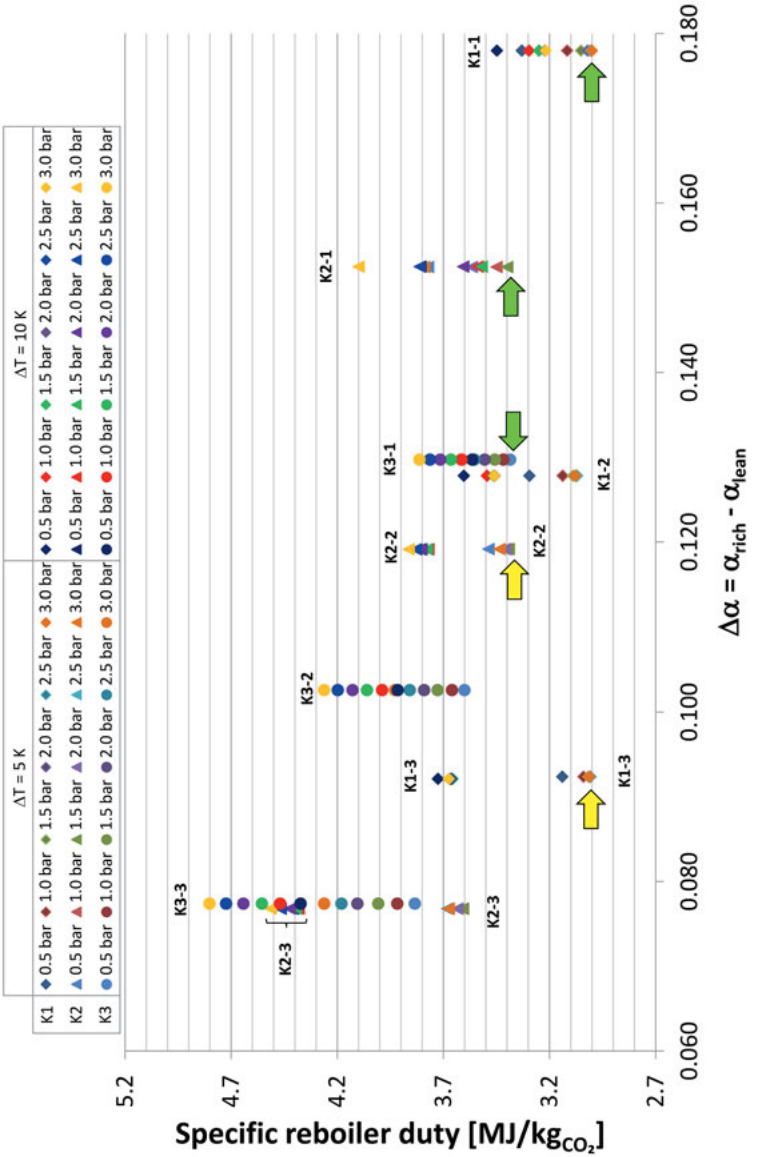

Figure 4.16: Compendium of energy demand for solvent regeneration for the studied potassium carbonate blends K1, K2 and K3. Results reported in Aspen Plus simulations. Nomenclature as presented in Table 3.5

this figure potential blends are marked with arrows. The green ones indicate selected blends; the yellow ones a viable option that was yet not set as an operation parameter.

At the beginning of chapter 2 it was mentioned that reboiler heat duty consists of three purposes: reversing reactions that took place in the absorber column, increasing the solvent's temperature for operation in the stripper column and generating stripping steam, as follows:

$$\dot{Q}_{reboiler} = \dot{Q}_{heat\ of\ absorption} + \dot{Q}_{sensible\ heat} + \dot{Q}_{stripping\ steam} \tag{4.9}$$

Solvent blends with a low cyclic capacity require in general a lower heat of absorption, which is related to reaching a lower temperature within the absorber column than blends with a higher cyclic capacity, like in the case of K1-3 and K1-1. A low cyclic capacity also means that less stripping steam is needed for solvent regeneration. Considering these two aspects, a low cyclic capacity seems to be a better operation parameter than a higher one. However, the sensible heat has not yet been contemplated. As was shown in Figure 4.13, low cyclic capacities yield high solvent circulation rates. This is what has a significant effect on the sensible heat and concomitantly on the reboiler duty. That is why in Figure 4.16 although K1-3 has a lower cyclic capacity than K1-1, the resulting reboiler duty is not much lower than K1-1's. In both cases the reboiler heat duty amounts to 3.0 MJ/kg_{CO_2}.

A higher circulation rate is not only related to a higher sensible heat. It also means that column geometry and ancillaries are affected. In general this implicates bigger equipment and a higher electrical pump demand. For this reason K1-1 was chosen over K1-3.

K1-2 has a cyclic capacity between K1-1 and K1-3's. Its reboiler duty is higher than these two. Though K1-2's cyclic capacity is lower than K1-1's, the circulation rate is so high, that the advantages of having a lower heat of absorption and a lower need for stripping steam do not suffice to compensate for the required sensible heat that result from the higher circulation rate, thereby making K1-2 not a suitable blend.

Something similar happens with K2. In this case the two most viable options are K2-1 and K2-2. Again these two have fairly similar heat duties of approximately 3.4 MJ/kg_{CO_2}, so as with K1 the decisive factor here is also the required circulation rate and related geometry, that make K2-1 the better choice. K3 presents only one option that offers the lowest heat duty for regeneration of around 3.4 MJ/kg_{CO_2}.

Simulations considered stripper operation at different pressures for all blends and cyclic capacities. The results can also be found in Figure 4.16. There is no obvious pressure at which the reboiler duty is the lowest. Instead, the apparent optimal pressure differs for each blend according to its composition. Best results for K1-1, K2-1 and K3-1 seem to be 3.0 bar, 1.5 bar and 0.5 bar respectively. In order to determine whether these deductions are accurate, stripper's performance will be considered for the pressure range of 0.5 bar to 3.0 bar.

So far the main heat exchanger's temperature difference has not yet been discussed. Results in Figure 4.16 show overall a lower reboiler duty by reducing the temperature difference by 5 K. This behaviour was expected. A lower temperature difference is associated with a higher heat recovery and consequently with a reduction of the sensible heat required, which reflects in a lower reboiler duty. A temperature difference of 5 K was hence set as operation parameter.

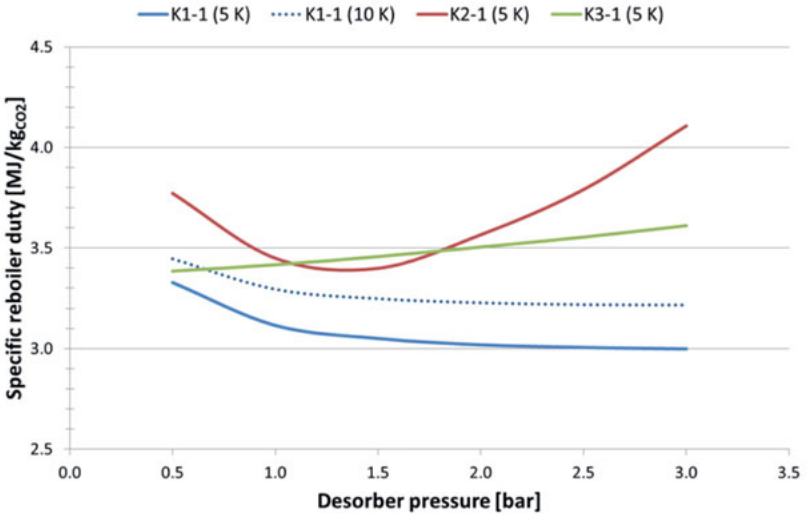

Figure 4.17: Comparison of calculated specific reboiler duties at different stripper pressures for selected blends at a heat exchanger's temperature differences of 5 K and 10 K

The specific heat reboiler duty for the three selected blends K1-1, K2-1 and K3-1 for all stripper operating pressures is shown in Figure 4.17. Continuous lines represent a heat exchanger's temperature difference of 5 K, whereas the dotted line serves as comparison for K1-1 at a temperature difference of 10 K. The blue curves represent K1-1, which is the blend with the highest piperazine and lowest

potassium carbonate concentration. The red curve illustrates K2-1's trend. This is the blend with an equimolar concentration of potassium carbonate and piperazine. The green curve shows K3-1's behaviour. K3-1 is also the blend with the lowest piperazine and highest potassium carbonate concentration.

Apparently, K1-1's higher piperazine concentration favours a low reboiler duty at higher pressures. Starting at a stripper pressure of about 2 bar there is no significant change to be observed. For a temperature difference of 5 K at 2.0 bar, the specific heat reboiler duty is slightly higher than at 3.0 bar, where 3.0 MJ/kg_{CO_2} are required for solvent regeneration. The highest reboiler duty is reached at low pressures, especially at 0.5 bar, where the calculated reboiler duty amounts to 3.33 MJ/kg_{CO_2}.

At a temperature difference of 10 K the blend's behaviour remains constant, except that the reboiler's duty increases proportional to the lower heat recovery that is achieved by using a higher heat exchanger's temperature difference. In this case, the highest and lowest specific reboiler duties are 3.45 MJ/kg_{CO_2} at a stripper pressure of 0.5 bar and 3.22 MJ/kg_{CO_2} at 3.0 bar.

K3-1 shows a reboiler duty linear drop as stripper pressure rises. This behaviour corresponds to that of a solvent with a low heat of absorption, which matches K3-1 characteristics, since the potassium carbonate – piperazine ratio is the highest of all blends. The lowest and highest reboiler duties are 3.39 MJ/kg_{CO_2} at a pressure of 0.5 bar and 3.61 MJ/kg_{CO_2}.

Opposite to K1-1 or K3-1, where a continuous reboiler duty increase or decrease can be detected, K2-1 shows a positive parabolic trend, where a minimum reboiler duty of 3.4 MJ/kg_{CO_2} can be identified at a stripper pressure of 1.5 bar. Since K2-1 is an equimolar solution of potassium carbonate and piperazine, it appears that either potassium carbonate or piperazine reactions dominate the solvent's behaviour depending on the stripper pressure used. At lower pressures from 0.5 bar to 1.5 bar reboiler duty decreases as the stripper pressure increases, thereby indicating a piperazine dominance over the blend. Then at 1.5 bar a minimum is reached and suddenly the trend is reversed meaning that as the stripper pressure increases, reboiler duty rises. This is a sign that the pressure range between 1.5 bar and 3.0 bar is dominated by potassium carbonate reactions, which demand a higher heat for regeneration at upper stripper pressures. Cullinane and Rochelle [65] reported having observed the same behaviour in potassium carbonate – piperazine blends at low lean loadings and high cyclic capacities and explained it with the influence of K^+ ions and their impact on HCO_3^-/CO_3^{2-}. Further simulations revealed

the parabolic progression to be less and less pronounced for initial lean loading values higher than K2-1's.

During appraisal of Figure 4.16 it was mentioned that when the heat exchanger's temperature is reduced by a difference of 5 K, lower reboiler duties are required for solvent regeneration. The following diagrams will help appreciating the implications related to such a measure.

4.3.4 Lean-rich heat exchanger

Figure 4.18 depicts required heat transfer capacities depending on the temperature difference at different stripper pressures for the indicated blends. The continuous curves represent a ΔT of 5 K and the dotted ones 10 K. The blue lines belong to K1-1, the red ones to K2-1, and the green ones to K3-1. Independently of the blend, all curves show a growing trend with increasing stripper pressure. This is normal considering that stripper operating temperatures increase proportionally to a pressure increment, thereby raising the needed heat transfer capacity in order to achieve the given temperature difference.

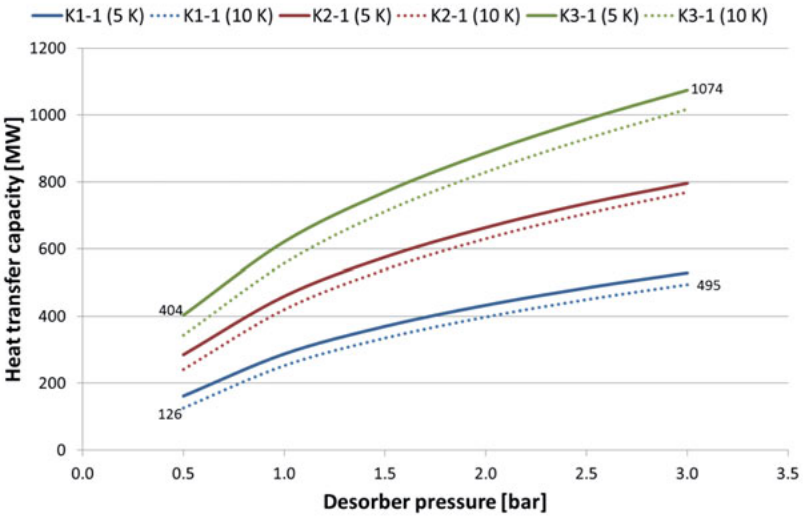

Figure 4.18: Comparison of required heat transfer capacities for two temperature differences at several desorber pressures for selected blends (heat transfer coefficient of 850 W/m²K assumed)

The lowest and highest heat transfer capacities belong to K1-1 and K3-1 respectively. K1-1 requires 126 MW at 0.5 bar stripper pressure and 495 MW at 3.0 bar, both for a temperature difference of 5 K. On the other hand, K3-1 needs 404 MW at 0.5 bar and 1074 MW at 3.0 bar, both for a temperature difference of 10 K. K2-1 requires heat transfer capacities between K1-1 and K3-1. These results are also a consequence of circulation rates. Even if a blend might have a low concentration of piperazine, like K3-1, and thus a lower heat of absorption than for example K1-1, circulation rates are so high that they affect the required heat transfer capacity due to the associated sensible heat, as discussed in Figure 4.16.

A temperature difference reduction from 10 K to 5 K does not seem to affect much the required heat transfer capacity. However, to be able to confirm this, the required area shown in Figure 4.19 still has to be assessed.

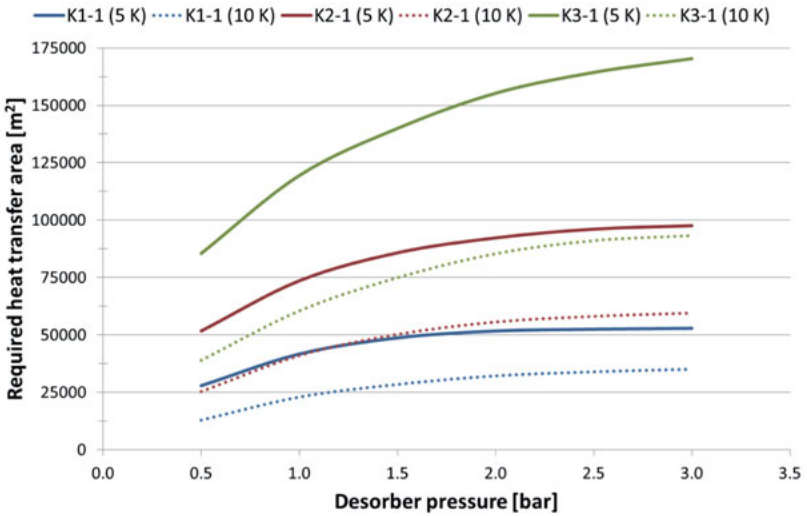

Figure 4.19: Required heat transfer area for two temperature differences at several desorber pressures for selected blends (heat transfer coefficient of 850 W/m²K assumed)

While Figure 4.18 did not suggest a big impact by reducing the heat exchanger's temperature difference, Figure 4.19 leaves no doubt that the expected outcome is indeed huge. As with Figure 4.18, continuous curves represent also a ΔT of 5 K and dotted ones 10 K. The same applies to curves colours: blue for K1-1, red for K2-1 and green for K3-1.

In this case the lowest required areas are reached by using a ΔT of 10 K and vice versa, the highest result from a ΔT of 5 K. So far K1-1 is the blend that has shown the best results with respect to required reboiler duty, circulation rate and heat transfer capacity. The lowest reboiler duties, as showed in Figure 4.17 are reached with ΔT of 5 K and a stripper operation range between 2.0 and 3.0 bar. This means, that at a stripper pressure of 2.0 bar a heat transfer area of almost 52,000 m^2 is required and at a 3.0 bar almost 53,000 m^2.

As previously shown in Figure 4.17, K2-1's lowest reboiler duty is reached at a stripper pressure from 1.5 bar and ΔT of 5 K. The associated area amounts to approximately 86,000 m^2. Results also revealed that K3-1's lowest reboiler duty is linked to a stripper pressure of 0.5 bar and ΔT of 5 K.

The extreme difference between areas required for ΔT of 5 K or 10 K can be explained with the following equation:

$$\dot{Q} = k \cdot A \cdot \Delta\theta \tag{4.10}$$

Where,

A	[m^2]	Heat transfer area
k	[W/m^2K]	Heat transfer coefficient
$\dot{Q}$	[W]	Heat transfer capacity
$\Delta\theta$	[K]	Temperature difference

Calculation of the required area implies not only using different heat transfer capacities, but also a different ΔT. This fact and circulation rates lead to Figure 4.19's results.

The same occurs when taking a look at K1-1, K1-2 and K1-3 depicted in Figure 4.20. K1-1 and K1-3 were the two cases in Figure 4.17 with low reboiler duties and hence considered as a potential option for operation. As illustrated in Figure 4.20, the required area to guarantee for the desired heat transfer increments considerably by setting the heat transfer's temperature difference to 5 K (continuous lines) than for ΔT of 10 K. The trend is exactly the same as shown in Figure 4.19 and applies to all blends. The comparison of K1-1 with K1-3 indicates that by selecting K1-1 the related area is at stripper pressure of 2 bar about 20,000 m^2 and at 3 bar about 18,000 m^2 lower than by choosing K1-3. In the same way that heat transfer design is affected by using K1-1 instead of K1-3, it is expected that higher circulation rates, such as K1-3's, implicate bigger pumps and associated demand. This

corroborates the previous selection of K1-1 at the end of the assessment on Figure 4.17.

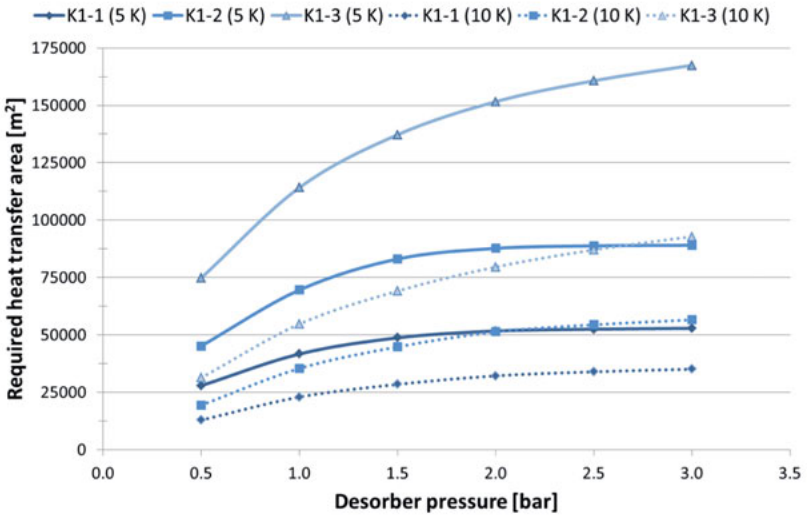

Figure 4.20: Required heat transfer area for two temperature differences at several desorber pressures for K1-1, K1-2 and K1-3 (heat transfer coefficient of 850 W/m²K assumed)

So far results have indicated that K1-1 does not only offer the lowest reboiler duty of all studied blends, but it also promises the lowest circulation rate and thus the smallest geometry. These conditions contribute to reducing both investment and operation costs, which still have to be considered for an accurate appraisal of the overall scrubbing system and which will be done at a later point. The solvent blend K1-1 along with its potassium carbonate – piperazine ratio and initial lean loading will hence be set as operation parameters and further analysed.

4.3.5 Cooling duty

The specific cooling duties for the three selected blends K1-1, K2-1 and K3-1 for all stripper operating pressures are shown in Figure 4.21. Continues curves denote a heat exchanger temperature difference of 5 K, whereas the dotted line represents a ΔT of 10 K. The blue lines depict K1-1, the red line K2-1, and the green one K3-1. Results in Figure 4.21 show an extreme resemblance to the ones displayed in Figure 4.17. This can be explained with the blends concentration: K1-1 has the highest concentration of piperazine and the lowest concentration of potas-

sium carbonate; K2-1 is the blend with an equimolar concentration of both components and K3-1 has the lowest and highest contents of piperazine and potassium carbonate respectively. As it has previously been discussed, the blend's concentration plays an important role in determining the required solvent flow rate: the higher the piperazine concentration, the lower the solvent rate. This made a difference in Figure 4.15 and Figure 4.17 with respect to the maximum reached temperature within the absorber column, as well as with the specific reboiler duty for regeneration. Despite the solvent's high heat of absorption it was possible to still get a lower reboiler duty than the one required for K2-1 or K3-1. This was mainly due to the fact that heat of absorption alone does not match the required reboiler duty, but is merely a part of it (see equation (4.9)), and hence, the lower sensible heat needed for K1-1's reduced flow rate contributed to lowering the reboiler duty. The same effect is observed in Figure 4.21. Cooling and reboiler duties are proportional to each other: the higher the reboiler duty, the higher the cooling duty and vice versa.

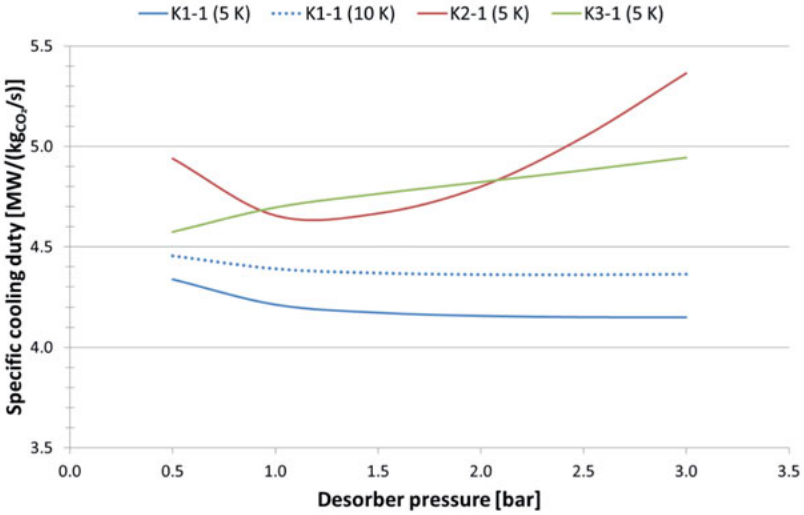

Figure 4.21: Comparison of calculated specific cooling duties at different stripper pressures for selected blends at heat exchanger's temperature differences of 5 K and 10 K

The lowest cooling duties correspond to K1-1 at a temperature difference of 5 K. Results are analogue to the ones presented in Figure 4.17, where duties decreased as the desorber operating pressure increased. There is also a difference

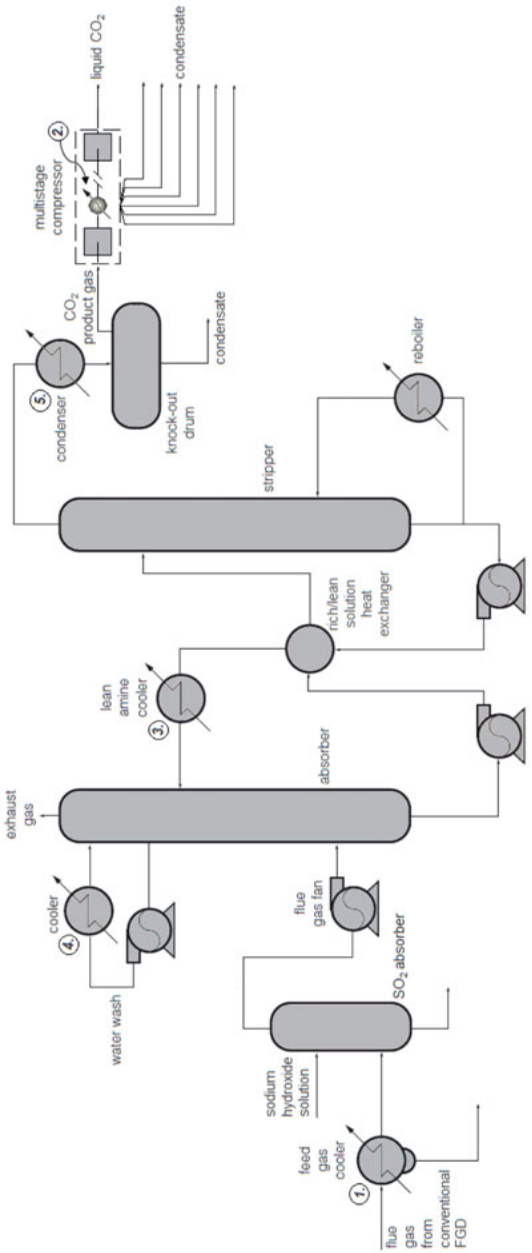

Figure 4.22: Process flow diagram for CO_2 capture from flue gas by chemical absorption as contemplated so far in this work

between K1-1's results depending on the lean-rich heat exchanger temperature used. Cooling duties at 5 K are lower than at 10 K, which was indeed expected. By choosing a lower heat exchanger temperature difference it is not only possible to spare steam destined for solvent regeneration, but it also allows for cooling duty reduction, since more heat may be transferred from lean to rich solvent, thereby sinking the lean solvent outlet temperature.

Cooling duties shown in Figure 4.21 are total duties and result from adding up cooling duties within the scrubbing cycle (see Figure 4.22), which are:

1. *Flue gas preconditioning* represents the cooler previous to the SO_2 scrubber from Figure 4.22,
2. *CO_2 cooler* refers to the cooling duty required by a multistage compressor for conditioning CO_2 prior to be transported to its final storage location,
3. *Lean cooler* applies to the lean amine cooler previous to reaching the absorber column,
4. *Absorber top* represents the cooling duty required by a head wash to reduce the stack's temperature to 40°C and
5. *Desorber top* describes the cooling duty demand for separating water from CO_2 previous to reaching the compressor.

By displaying total duties single components it is possible to identify locations within the scrubbing cycle that are susceptible to being affected by a blend's composition, operation parameters or both. This is exactly the purpose of Figure 4.23, which depicts single specific cooling duties for K1-1, K2-1 and K3-1 at a lean-rich heat exchanger temperature difference of 5 K. In Figure 4.23 *preconditioning* and *CO_2 cooler* specific duties are identical for all blends and remain constant independently of the desorber's operating pressure. This has a simple explanation: flue gas flow rate is the same for all simulated cases since they all assume RPP NRW's flue gas is to be treated. *Preconditioning* results are hence identical no matter which blend was used. In addition, since flue gas flow rate is constant, so is CO_2 flow rate. One of the main simulation parameters is a CO_2 capture rate of 90 %. At desorber's top the steam-CO_2 ratio may differ according to which blend was used and at what pressure (see purple bars), but after CO_2 has been separated from water its flow rate does not vary anymore, since it corresponds to the target capture rate.

The green bars in Figure 4.23 represent *lean cooler* results, which are only affected by a blend's composition and remain constant independently of the desorber pressure. This is due to a lean-rich heat exchanger's design parameter: on one hand the exchanger should only allow for as much heat transfer that the exchanger's outlet temperature exceeds the absorber's rich solvent temperature by 5 K; on

the other hand, blends temperature at absorber's bottom varies only when a different blend is used (see also Figure 4.15), i.e. K1-1, K2-1 or K3-1. However, for the same blend no temperature rise occurs. So in conclusion, albeit the temperature at desorber's bottom rises as pressure increases, the temperature at lean-rich heat exchanger's outlet does not vary, thus allowing for a constant cooling duty for each blend. The operating pressure does have an effect on the blend's temperature, but it is absorbed by the lean-rich heat exchanger, so that the blend's temperature at the cooler's inlet stays constant.

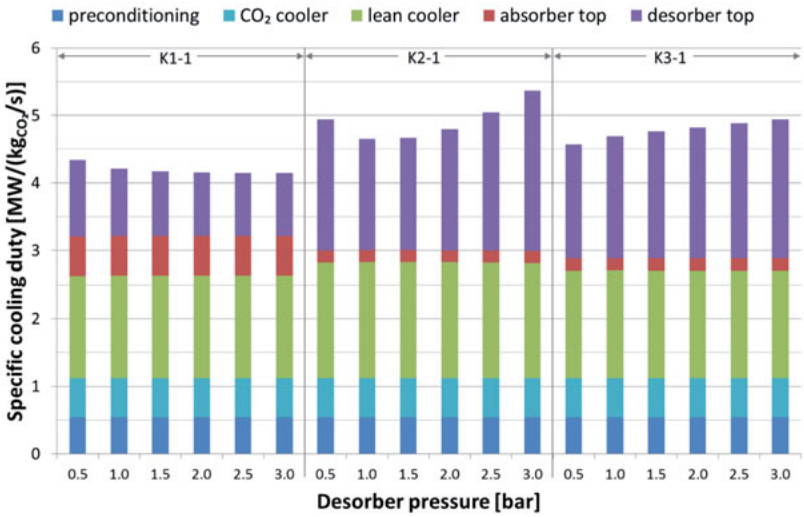

Figure 4.23: Specific cooling duties for selected blends for a lean-rich heat exchanger temperature difference of 5 K

Figure 4.15 showed different absorber temperatures, which also included K1-1, K2-1 and K3-1. The bottom temperatures decreased proportional to a blend's heat of absorption. K1-1 showed the highest bottom temperature followed by K2-1 and K3-1. As was mentioned just a few lines above, the absorber's bottom temperature is used as a reference for the lean-reach heat exchanger. The exchanger's specification is a temperature difference of 5 K between the "cold" rich amine solution (at the absorber's bottom) and the lean amine solution leaving the lean-rich heat exchanger. So, since the temperatures are lower for K3-1 and K2-1 the cooling duties should in theory be lower. The reason why this is not the case lies within each solution's mass flow rate and the related sensible heat. Even though K3-1's and K2-1's temperatures are lower than K1-1's, their mass flow rates are so much

higher that a higher cooling duty is required to reach the targeted inlet temperature of 40°C.

The cooling duty *absorber top* is represented with red bars in Figure 4.23. A wash section is supposed to reduce solution's carry-over as much as possible. The cooling duty required for this task is equivalent to the stack's temperature previous to reaching the wash section. As has been explained in Figure 4.15 the blend's composition has a strong influence on the solvent's flow rate and the temperature increase the solvent suffers. This is a consequence of exothermic reactions that take place during the chemical absorption of CO_2. Since gas and liquid phases are permanently in contact with one another in the absorber column, a raise of the gas temperature is inevitable. Although the gas temperature decreases as it approaches the lean solvent's inlet close to absorber's top, it does not suffice to fully compensate the effect of exothermic reactions. That is why the stack's temperature varies between 55°C, 47°C and 43°C for K1-1, K2-1 and K3-1 respectively, thus giving place to the different values presented in Figure 4.23. The related cooling duties are 66.6 MW_{th} for K1-1, 18.4 MW_{th} for K2-1 and 13.6 MW_{th} for K3-1.

The purple bars represent the cooling duty demand at desorber's top needed to separating water and reagent's rests from the stripped CO_2. This is probably the most complex duty to explain, since it is directly related to the reboiler duty. As it was mentioned in Figure 4.16's results discussion, the reboiler duty results from adding up heat of absorption, sensible heat and the heat required for stripping steam, as displayed in equation (4.9). Each of these factors contributes to altering *desorber top* cooling duty. In addition, a blend composition and the assumed lean loading contribute to influence the overall reboiler duty. Furthermore, the reboiler duty is directly affected by the stripper's operating pressure, as was previously discussed in Figure 4.17's results. A closer look at Figure 4.23's results reveals analogue results to those of Figure 4.17's, which is due to the direct relationship to the overall reboiler duty, as was the case in Figure 4.17.

K1-1's *desorber top* cooling duty in Figure 4.23 drops as consequence of increasing stripper pressure. K1-1's low cooling duty results –compared to ones of K2-1 and K3-1– are probably an indicator and result of K1-1's high heat of absorption. That is, K1-1's piperazine concentration is the highest of the three contemplated blends in Figure 4.23 thus implicating that K1-1's heat of absorption is the highest. This was also confirmed in Figure 4.15's absorber temperature profiles. However, this turned out to be of advantage considering the resulting required mass flow rate and its related sensible heat, as was shown from Figure 4.18 to Figure 4.20. The high heat of absorption also turns to be of advantage when calculating the

heat required for stripping steam, which represents the third term in equation (4.9). This can be explained using the same analogy Freguia used in [70]. According to him CO_2 has a heat of absorption in MEA that is more than twice that of H_2O. Piperazine's heat of absorption is higher than MEA, thus CO_2 has a heat of absorption in piperazine that is more than twice that of H_2O. Considering the Clausius-Clapeyron thermodynamic relationship represented in equation (4.11), this means that as the pressure and consequently the temperature increase, CO_2's vapour pressure rises faster than the vapour pressure of water does. In other words, the higher the pressure, the higher the CO_2 to H_2O ratio in the gas phase at the column's top. This ends up in a lower amount of steam required to strip CO_2, which agrees with K1-1's *desorber top* cooling duty results in Figure 4.23. Simulation results revealed that the targeted capture rate of 90 % CO_2, which corresponds to a mass flow rate of 105 kg/s, was reached with a tolerance below ± 0.1 %. For that matter, the highest vapour rate at desorber's top belongs to a pressure of 0.5 bar and amounts to almost 160 kg/s, whereas the lowest one was reached at 3.0 bar and amounts to approximately 140 kg/s. The related CO_2 concentrations are 66 wt.-% and 74 wt.-% at 0.5 bar and 3.0 bar respectively.

$$\frac{d \ln p^*}{dT} = \frac{\Delta H_{l-v}}{dRT^2} \tag{4.11}$$

Where,

$\Delta H_{l\text{-}v}$	[J/mol]	Water's heat of vaporisation or CO_2's heat of desorption
p^*	[Pa]	Vapour pressure of a component
R	[J/mol K]	Universal gas constant
T	[K]	Temperature

K1-1's high heat of absorption turned out to be an advantage rather than a disadvantage once all factors for calculating the overall reboiler duty were considered. K3-1's case is the opposite of K1-1's. Of all blends, K3-1 is the one with the highest potassium carbonate – piperazine ratio. Unlike K1-1 this blend shows a linear growing *desorber top* cooling duty as the pressure increases. As discussed in Figure 4.17 this behaviour is characteristic of blends with low heat of absorption, which matches K3-1's composition due to the higher potassium carbonate concentration. Even though CO_2 has a heat of absorption that is more than twice that of H_2O, piperazine's effect is overweighed by the higher potassium carbonate concentration of K3-1. As a result, more vapour is needed to strip the same amount of CO_2 (105 kg/s), thereby increasing the overall reboiler duty. A further increase occurs due to K3-1's high flow rate and its related high sensible heat.

K2-1's *desorber top* cooling duty represents a combination of the behaviours observed with K1-1 and K3-1. Again, this is due to the fact that this cooling duty is directly proportional to the overall reboiler duty. Just as was the case in Figure 4.17 K2-1 shows a parabolic trend, where a minimum cooling duty is identified at 1.0 bar. This suggests that at lower pressures piperazine reactions dominate, whereas at higher pressures potassium carbonate reactions take the lead. This phenomenon has already been explained in Figure 4.17's discussion of results.

With respect to the overall cooling duty, K1-1 is the blend with the lowest duty. This occurs despite K1-1's high heat of absorption, as previously discussed.

4.3.6 Absorber intercooling

The calculated temperature profiles for all blends were previously introduced and discussed in Figure 4.15, and K1-1's profile showed the most pronounced temperature increase that looks like a bulge towards the upper part of the packing. This coincides with results presented by Reddy, et al. [103], which correspond to CO_2 capture of flue gas with a CO_2 concentration of 13 Vol.-%, characteristic of coal-fired power plants (hard coal), like in the case of RPP NRW.

Since equilibrium and reaction kinetics are temperature dependant, absorber temperature profiles can be a good indicator of capture rates. In general, higher operating temperatures are associated to faster kinetics, but too high temperatures might turn contra productive by limiting the solvent's cyclic capacity. A solution to this is offered by Reddy, et al. [103], who propose to reduce the solvent's temperature by removing a portion of the reaction heat towards the absorber's bottom. This can be accomplished with what is known as *absorber intercooling*, illustrated in Figure 4.24. The idea is to extract the solvent, which is not yet fully loaded and therefore known as semi-rich solvent, cool it and then reintroduce it in the column to keep reacting with CO_2 until it reaches the column's bottom.

Even though the principle of absorber intercooling seems simple, not every absorber is apt for this kind of system. Reddy, et al. [103] compared the temperature profiles of two different sorts of flue gases, both of which used a 30 wt.-% MEA aqueous solution for CO_2 capture. The first and second flue gas CO_2 compositions were 13 Vol.-% and 3 Vol.-%. They represent typical flue gas compositions of combustion with hard coal and natural gas respectively. Results showed that a higher CO_2 concentration calls for a more evident increase in temperature. By adding an intercooling system it was possible to slightly reduce the temperature bulge at the upper part of the column, while the lower part of the column operated

significantly cooler. This proved to be an advantage, since reaction kinetics was only slightly hindered at the top of the column, at the time that solvent carrying capacity was improved. The second flue gas with a CO_2 concentration of 3 Vol.-% showed without intercooling an overall lower temperature profile with more moderated temperature bulge. Reducing the liquid temperature is not advisable in this case, since an overall lower operation temperature would only hinder reaction kinetics thereby preventing the benefits of intercooling.

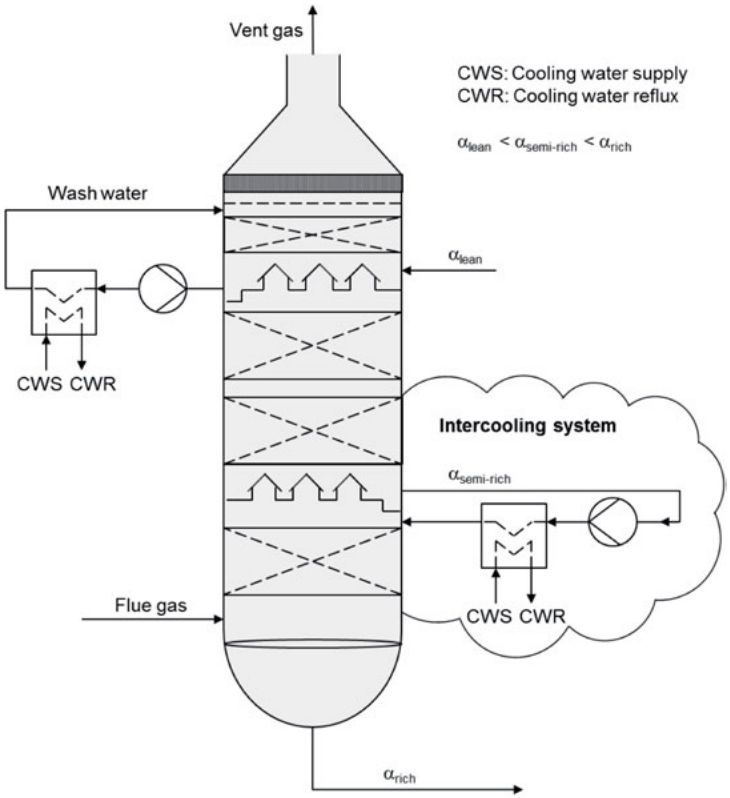

Figure 4.24: Fluor's intercooling system as presented by Reddy, et al. [103]

Given the advantages of absorber intercooling and seeing that the requisite of a CO_2 flue gas composition of approximately 13 Vol.-% is fulfilled, it was decided to implement an intercooling system with K1-1 as a solvent for the purpose of absorber optimisation.

In section 3.2.1 the boundary conditions for absorber simulation were listed. These included an initial packing height of 30 m. However, besides from packing other column's internals such as support grids, collectors and distributors still have to be considered, which increment the column's final height. This makes a packing height of 30 m hardly feasible. This is the part where absorber intercooling becomes an important optimisation tool, then by implementing it correctly it may be possible to design both a shorter and smaller column, than the one required for 30 m packing. However, results obtained with 30 m packing are still valuable. The solvent's final cyclic capacity with this packing height is high, so that it serves as a target during optimisation.

The first step in this process consisted in reducing the packing height from 30 m to 10 m. The reduction effects are illustrated in Figure 4.25. In order to be able to compare profiles and capture rates of different heights, they were normalised. Results for a packing height of 30 m are represented in blue and for 10 m in red. Lines show the respective temperature profile, whereas bars depict the related CO_2 removal per packing segment. Both temperature curves show a distinctive bulge. Considering the normalised height, the blue bulge's development appears to be faster than the red one. The effect is comparable to the one shown in Figure 4.15, except that in this case lean loadings are the same and packing height was varied. By reducing the packing height, the carrying capacity is immediately affected. As a result of a packing height reduction from 30 m to 10 m the solvent's cyclic capacity declines from 0.178 $mol_{CO_2}/mol_{alkalinity}$ to 0.162 $mol_{CO_2}/mol_{alkalinity}$. A packing height of 30 m allows for an extended contact time between liquid and gas. This ends in a high cyclic capacity, thus enabling for a low circulation rate. By reducing the packing height to 10 m, the solvent circulation rate has to be increased to guarantee for a capture 90 % CO_2. This explains why the liquid temperature raises faster with a packing height of 30 m than with 10 m. A packing height of 30 m requires a liquid to gas ratio of 3.61 l/m^3 and a packing height of 10 m a ratio of almost 4 l/m^3. In order to maintain a proximity to the flood point of 80 % in the column for both cases, the diameter of the shorter column has to be enhanced.

The maximum temperature is in both cases around 73°C. The liquid temperature at the column's bottom is for a packing height of 30 m about 2°C lower than for 10 m. Having a constant gas flow rate in both cases means that a lower liquid circulation rate cools down faster than a higher one, which is the effect observed in Figure 4.25.

The blue and red bar diagrams reveal CO_2 capture rates per segment. According to specifications in section 3.2.2.2 CO_2 scrubbers were simulated assuming 30

segments and each bar represents one of them. Figure 4.25 illustrates how CO_2 is absorbed as soon as the solvent enters the column at the top. The blue bars though seem to capture more than double as much CO_2 as the red ones in the first segments. In reality this is only a deception. Albeit both columns have the same number of segments, the segment size of each packing is different. The red bars' segment size is about a third of the blue ones. Having the same segment size for both columns would mean raising the number of segments of the red one to a total of 90 segments, but that would dramatically increase the system's complexity. Instead it was decided to tighten the segment size by reducing the packing height to 10 m, which is in any case desirable for more detailed overall absorber analysis during optimisation.

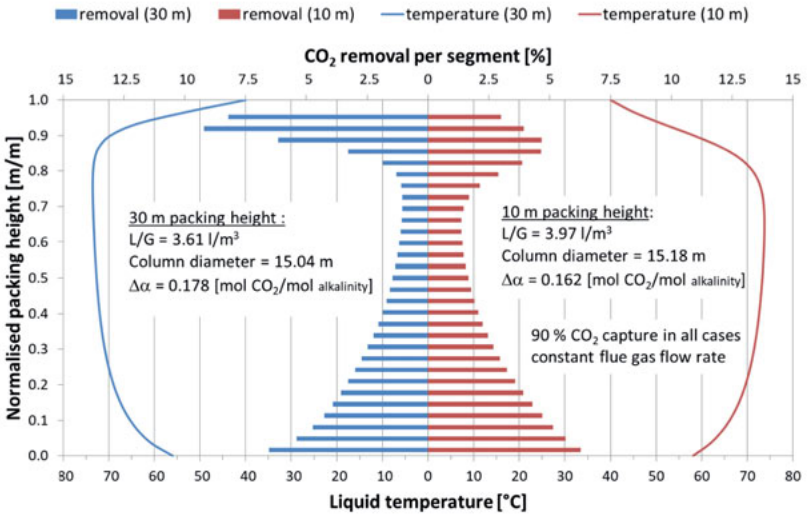

Figure 4.25: Comparison of temperature profiles and CO_2 removal per segment using K1-1 as solvent for an absorber column with packing heights of 30 m and 10 m and a constant capture rate of 90 % CO_2

Something that can be observed in Figure 4.25 (from top to bottom) is how CO_2 capture raises fast, which coincides with the relatively low liquid temperatures at the top. As soon as the temperature has reached a maximum, CO_2 capture declines rapidly. In other words, exothermic reactions result in a increase in liquid temperature, which in turn favours kinetics, until the liquid temperature rises so much that the solvent carrying capacity is compromised. A slight temperature decrease then contributes to enhance the carrying capacity again. In Figure 4.25 this

occurs due to the ascending flue gas, which enters the column at a temperature of approximately 40°C. For this reason the CO_2 capture rate grows constantly in the lower part of the column until the solvent finally reaches the bottom. Though lower temperatures also tend to limit kinetics, the liquid temperature is still higher than when it is introduced in the column. Apparently this temperature is still high enough, so that kinetics is not hindered.

Having reduced the packing height from 30 m to 10 m leads to a shorter column, but not to a smaller one. From now on the column with 10 m packing height will be considered as the basis for optimisation. The task consists in implementing an intercooling system that allows for an enhancement of the solvent carrying capacity to at least 0.178 mol CO_2 per mol alkalinity, that represents so far the best K1-1's cyclic capacity.

There are different approaches to implement an intercooling system that depend on the goal that wants to be achieved. One way consists in setting a temperature target to be reached and calculate the required duty for that to happen. The approach implemented for this work consisted in gradually incrementing the cooling to duty in 10 MW steps, until the new cyclic capacity was at least 0.178 mol CO_2 per mol alkalinity or higher, which matches the original carrying capacity with 30 m packing height.

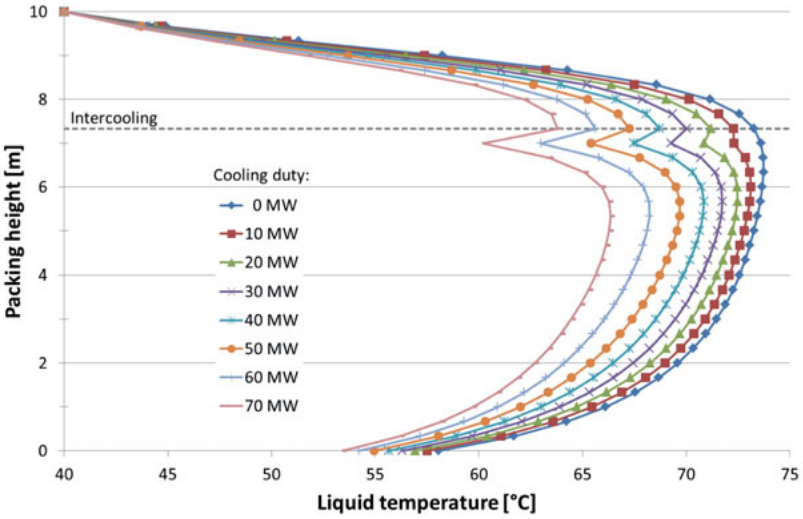

Figure 4.26: Temperature profiles for different cooling duties and a constant packing height of 10 m

The advantage of taking small steps for an intercooling system implementation is that results allow a more detailed analysis of what happens within the column. This approach however is not necessary to build-in this sort of system. Figure 4.26 displays different temperature profiles that correspond each to a different cooling duty that varies between 0 MW and 70 MW. The blue line indicates the temperature profile of an absorber column with 10 m packing height and no intercooling. The points in each line specify the location of each segment. The diagram also shows a single dashed line at a constant packing height of 7.3 m, which represents the location of the intercooling system. At this point the liquid temperature is 73.3°C.

The diagram illustrates how the liquid temperature within the column gradually decreases as the cooling duty increases. In addition, Figure 4.26 shows the evolution from one to two bulges. This is a direct consequence of the solvent's cooling. The higher the cooling duty, the more pronounced the bulges are. Once the solvent has been cooled down, it is again capable of reacting with CO_2 which provokes a raise in temperature, though not so extreme as the one without intercooling. Hence, the absorber should operate at an overall lower temperature, but without hindering reaction kinetics. When the solvent has reached about the column's middle the liquid temperature does not increase again due to the cooling effect of the flue gas. Although the flue gas' temperature rises after having entered the absorber, its temperature is still low enough to prevent the solvent's temperature from rising again. Furthermore, the solvent has by this time absorbed a good portion of CO_2, so that its loading capacity has been limited. The more CO_2 absorbed in the upper part of the column, the higher solvent loading and the less CO_2 will be captured in the lower part of the column. This is indeed the trend that can be observed in Figure 4.27, which depicts the CO_2 removal per stage depending on the cooling duty.

Each line's course in Figure 4.27 indicates a rapid CO_2 capture at the beginning of absorption at the column's top. To facilitate results analysis and comparison, the same colours used in Figure 4.26 have been used in Figure 4.27 for the corresponding cooling duty. The blue diamond's curve represents the temperature profile for the column without intercooling. In this case the highest removal of 4.62 % CO_2 is reached at a packing height of 9 m and starts declining immediately afterwards, as soon as the solvent's temperature exceeds 70°C, until the solvent reaches a minimum at a packing height of 6.3 m. This is the point at which the solvent starts to cool down due to the ascending flue gas and its lower temperature. As a result of that CO_2 absorption experiences a boost, which holds until the solvent reaches the column's bottom.

A boost is also experienced by the intercooled solvent and is proportional to the cooling duty, however its location defers from that of the reference case (10 m packing height, no intercooling). At 10 MW cooling duty, the declining trend stops shortly and then the red line's course resumes the same trend explained before. Starting at a cooling duty of 20 MW the declining trend right below the intercooling line does not only stop, but instead a growing trend is observed. This trend is also perceived above the intercooling's location. This relies on the cooling effect of the solvent. On the one hand, the solvent is extracted, cooled down and then reinserted right below its extraction point. The location, at which the solvent is reinserted, coincides with the highest CO_2 removal observed. Not only has the solvent carrying capacity been enhanced, but the ascending flue gas is also cooled down, so even though the solvent –above the extraction point– has not yet been cooled down by the intercooling system, its temperature is lower than without the intercooling due to the cooling effect of the flue gas. That is the reason why CO_2 removal is higher towards the column's top.

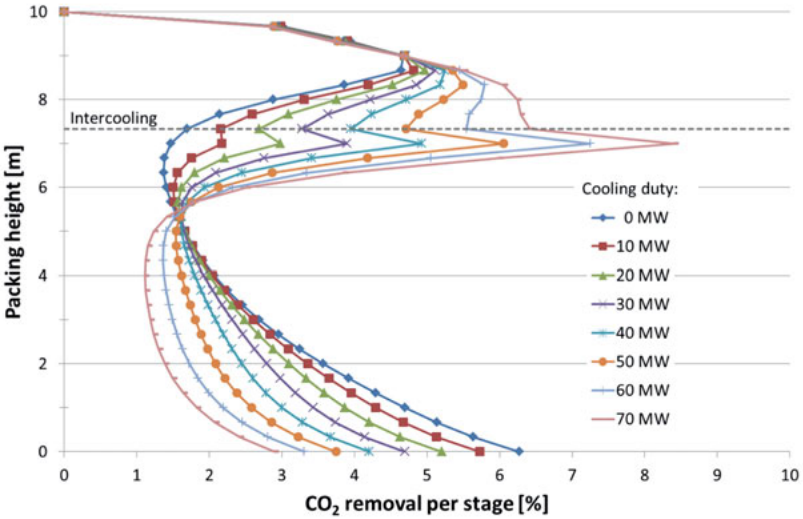

Figure 4.27: Comparison of CO_2 removal per stage for different cooling duties. Total capture of 90 % CO_2 for all cases

Plaza, et al. [80] explain, that the intercooling effects are maximised when the temperature bulge coincides with a mass transfer pinch. This is related to the capacity of both gas and liquid to draw heat off the column. Apparently at this state a critical L/G ratio is reached, at which the heat caused by CO_2 absorption is evenly

carried out of the column, resulting in a temperature bulge towards the column's middle. This is also what can be observed in Figure 4.26 and Figure 4.27. In the beginning the temperature bulge is located at the upper half of the column, but as the cooling duty increases the bulge defers towards the middle of the column. The CO_2 removal per stage reveals on the other side, that mass transfer is enhanced gradually, proportional to the growing cooling duty. The lower capture rate in the lower part of the column is merely a sign that the solvent carrying capacity has almost nearly been exhausted.

The intercooling's location was set by taking a look at the temperature profile of the column with 10 m packing height and determining the point at which the temperature reached a maximum. There are about three segments with a temperature above 73°C. Given that the difference between their temperatures was less than 1°C, the point at a packing height of 7.3 m was fixed for intercooling implementation. Since results showed that the temperature bulge moved towards the middle of the column –as predicted by Plaza, et al. [80] for maximizing intercooling effects–, no further modifications were undertaken.

To exemplify the difference in column performance by setting a different intercooling location, Figure 4.28 presents results with the same cooling duty of 60 MW at two different packing heights: 9.3 m and 7.3 m in in blue and red respectively. In Figure 4.26 and Figure 4.27 temperature profiles and CO_2 removal per stage revealed how a decline in CO_2 capture is related to an extreme increase in temperature. By installing an intercooling system before a temperature maximum is reached, it might be possible to reverse this effect. That is exactly the idea behind intercooling at 9.3 m packing height. However, results presented in Figure 4.28 indicate that although the overall column temperature is indeed lower than in Figure 4.26, a new maximum is reached above 70°C. This is still a very high temperature that –if only partly– still affects the solvent carrying capacity. Moreover, the expected temperature bulge does not appear at the middle of the column, but is instead located at the upper part of the column.

A comparison of CO_2 removal per stage shows that the capture is approximately the same in the first three stages of the column (from top to bottom). It is not until the fourth stage that the blue and red capture rates clearly differ from each other. This is due to the intercooling at 9.3 m packing height. In this case, the positive intercooling effects are observed. However, since the system was not implemented as suggested by Plaza, et al. [80], the benefits of intercooling fade almost as soon as they appear. Compared to that, results in red show a more even distribu-

tion. The difference between results in blue or red is due to the column's capability to carry heat out of the column, which is more limited at a packing height of 9.3 m.

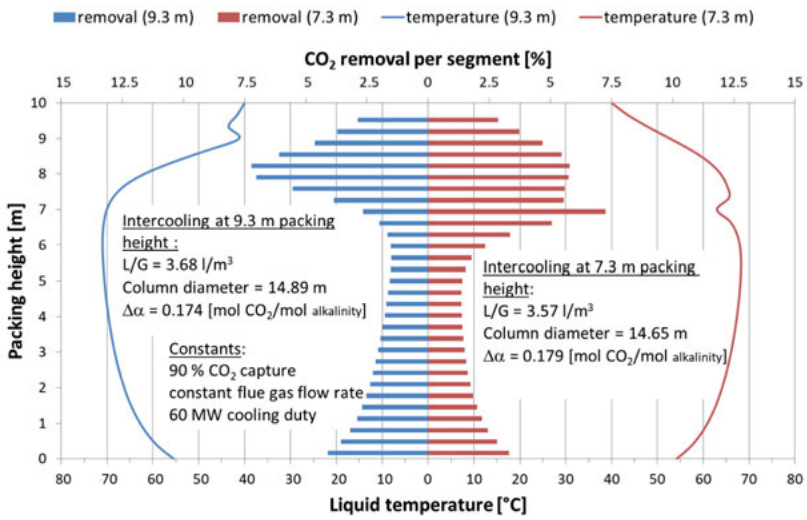

Figure 4.28: Temperature profiles and CO_2 removal per stage with a cooling duty of 60 MW at a height of 9.3 m and 7.3 m

The column's performance is nonetheless better than without intercooling, for example, the diameter can be reduced from approximately 15.0 m to 14.9 m. This might not seem relevant, but considering the packing height of 10 m, it still represents a reduction of 67 m^3 packing. At a more suitable location, such as 7.3 m packing height, the final diameter is approximately 14.65 m and the total packing volume reduction 122 m^3. In both cases, the same cooling duty was used and merely the location was different. This stresses the importance of an adequate intercooling.

The reason for deploying an absorber intercooling system was to conduct an optimisation of the previous modelled absorber column with 30 m packing height. Results regarding L/G, diameter and new cyclic capacity are presented in Figure 4.29; all of them as a function of the cooling duty. A single red square represents the original reference (30 m packing height, no intercooling) parameters. The blue diamond's line displays the expected changes due to intercooling influence. All diameters were calculated using an 80 % approach to flooding, as stated in section 3.2.1. The blue curve indicates a growing linear trend as cooling duty increas-

es, but this applies only to the cyclic capacity. As a consequence cyclic capacity increment, it is possible to reduce the required L/G, thereby allowing for a smaller column diameter. Results also suggest the cyclic capacity reached with a cooling duty of approximately 54 MW is equivalent to that of the 30 m packing height reference. Hence, results with a higher cooling duty already represent an improvement. Not only can the required packing height significantly be reduced, but solvent carrying capacity is enhanced, and with it L/G and related diameter can be reduced. These aspects contribute to having a much smaller and more efficient absorber column.

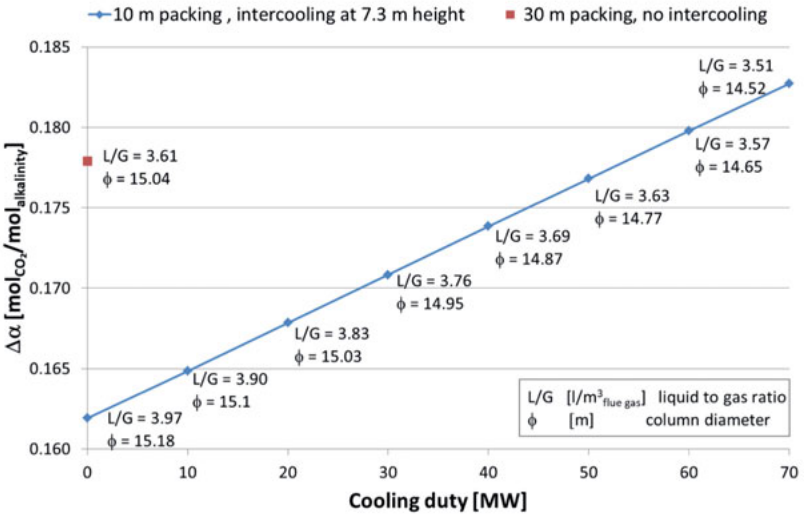

Figure 4.29: Resulting L/G ratios and related column diameters for different cooling duties

When comparing the 30 m packing height reference's results with those of the blue diamond's curve in Figure 4.29 there is one thing that catches the observer's eye: although cyclic capacity and L/G are in good agreement with the blue diamond's curve results, the presented diameter for 30 m packing height is bigger than expected. The explanation to this can be traced back to an intercooling's side-effect that has not yet been mentioned: liquid retention. Without intercooling the temperatures within the absorber column reach up to 73°C. At temperatures like this it is possible that instead of absorption, desorption takes place. That combined with carry-over result in an increased gas flow rate. In other words, even though the flue gas flow rate at absorber's inlet was assumed constant for all cases, it does not remain that way throughout the column. By reducing the solvent

temperature with an intercooling system, desorption and related carry-over slow-down proportional to the cooling duty. The higher the cooling duty, the lower the gas flow rate at the column's top. Since the column with 30 m packing height does not have an intercooling system, its gas flow rate is higher than that of 10 m packing height and 54 MW cooling duty, meaning that the original column has a higher gas load. In order to satisfy an 80 % approach to flood in all cases the column diameter has to be increased, which is the reason why this column's diameter is bigger than first anticipated.

A decline in gas flow rate as a side-effect of absorber intercooling is directly associated to emission reduction at the column's top. Potassium carbonate is considered an environment-friendly substance and related emissions do not represent a problem. That and because of their low heat of absorption is why potassium carbonate was considered as a solvent for CO_2 capture in the first place. Compared to potassium carbonate, amines are significantly harmful, thus their emissions have to be carefully controlled. In the *Technical Instructions on Air Quality Control* (TA-Luft from the name in German) there are restrictions listed for several substances [104]. Since amines deployment restrictions from TA-Luft do not correspond directly with the ones used in this work, a proper correlation between both had to be found first. The closest one was found in chapter 5, "Requirements to Provide Precautions against Harmful Effects on the Environment", and within that chapter amines properties are located in subsection 5.2.7.1.1[20] class II.

Figure 4.30 illustrates the remaining concentration of piperazine in the flue gas at the column's top. Blue diamonds represent the temperature, while red squares show the concentration on piperazine left in the flue gas at the column's top. The less piperazine is found in the flue gas, the better. Besides emission restrictions, by remaining within the liquid, piperazine is capable of reacting with CO_2 and will not have to be compensated with a make-up stream. Figure 4.30 shows a clear positive intercooling effect. Without cooling (10 m packing height) piperazine's flue gas concentration amounts to 960 mg/m^3, whereas with a cooling duty of 70 MW the concentration is reduced to approximately 580 mg/m^3.

In Figure 4.31 different piperazine concentrations in flue gas are displayed. According to TA-Luft a maximum piperazine concentration of 0.5 mg/m^3 is allowed. However, even when the flue gas is further cooled with water to a temperature of 40°C, the remaining concentration still is almost 16 mg/m^3 thus making a further wash section essential.

[20] Assumptions and conclusions regarding amine classification in TA-Luft were made within a research project mentioned in section 3.2.1. For more information, please refer to Behr, et al. [38].

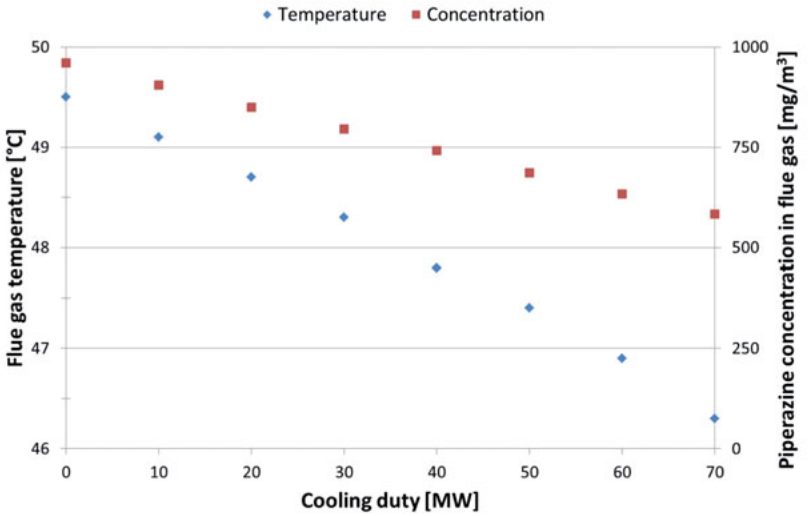

Figure 4.30: Intercooling influence on flue gas temperature and piperazine concentration at absorber's packing top

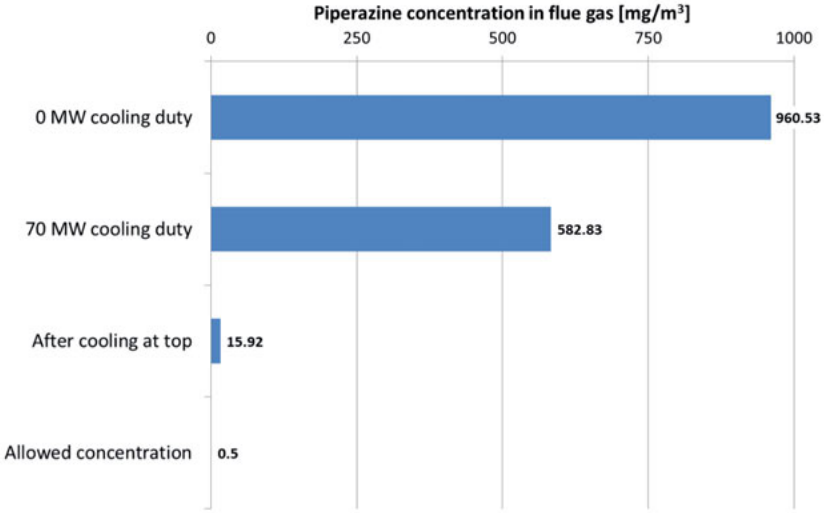

Figure 4.31: Comparison of piperazine concentrations in flue gas

In spite of having already reached the target cyclic capacity with a cooling duty of 54 MW, temperature profiles shown in Figure 4.26 and CO_2 removal rates in Figure 4.27 reveal that it is possible to increase the cooling duty up to 70 MW without dramatically hindering kinetics. In addition, results in Figure 4.29 confirm the possibility of reaching an ever higher cyclic capacity than the one achieved with 30 m packing height. Therefore, it was decided to implement intercooling with a duty of 70 MW_{th} for design of the scrubbing system.

A comparison of the initial and final column performance with 10 m packing height is depicted in Figure 4.32. Blue and red results indicate a cooling duty of 0 MW and 70 MW correspondingly. Without intercooling the highest CO_2 removal per segment takes place at the lower column's part, whereas with intercooling the highest CO_2 removal is found at the upper half of the column. Thanks to a suitable intercooling location it is possible to improve column's efficiency noticeably. The cyclic capacity is increased from 0.162 $mol_{CO_2}/mol_{alkalinity}$ to 0.183 $mol_{CO_2}/mol_{alkalinity}$. This also yields to a diameter reduction from 15.18 m to 14.52 m and hence, to packing volume savings of 152 m^3. A cooling duty of 70 MW will be henceforth one of the final design parameters.

Presented intercooling results might give the impression that the cooling duty may be increased at will. This would be though a wrong assumption. In the first place, absorber analysis with an intercooling system was only conducted for a maximum cooling duty of 70 MW, since at that duty the targeted cyclic capacity of 0.178 $mol_{CO_2}/mol_{alkalinity}$ had already been exceeded. Moreover, by increasing the cooling duty alone it is not guaranteed that the solvent carrying capacity will be enhanced, since this depends on operation parameters that cause the temperature bulge to correspond with a mass transfer pinch, as previously explained. Besides, temperature profiles (see Figure 4.26) showed that the column already operates at an overall lower temperature. By raising the cooling duty the column's overall temperature might fall so much, that kinetics might be hindered, thereby counteracting the benefits of intercooling.

Intercooling results have proved useful in improving absorber's performance and geometry. There is yet another important factor that still needs to be considered: *solvent regeneration*. Figure 4.33 depicts required specific reboiler duties for the previously selected blends K1-1, K2-1 and K3-1 and compares them with intercooling results represented by "K1-IC" and a blue dashed line. The number in parenthesis indicates the lean-rich heat exchanger's temperature difference. All blends are presented in the same colour as Figure 4.17, where they were first introduced and discussed.

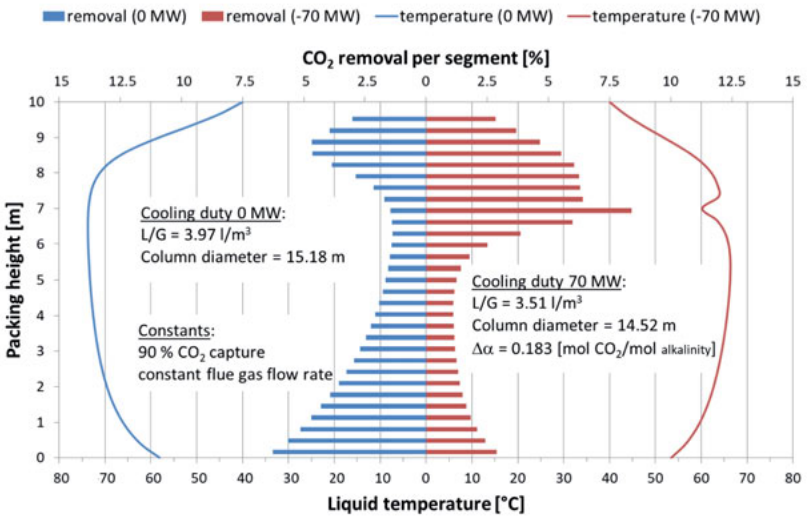

Figure 4.32: Temperature profiles and CO_2 removal per segment for an absorber column with 10 m packing height with and without intercooling

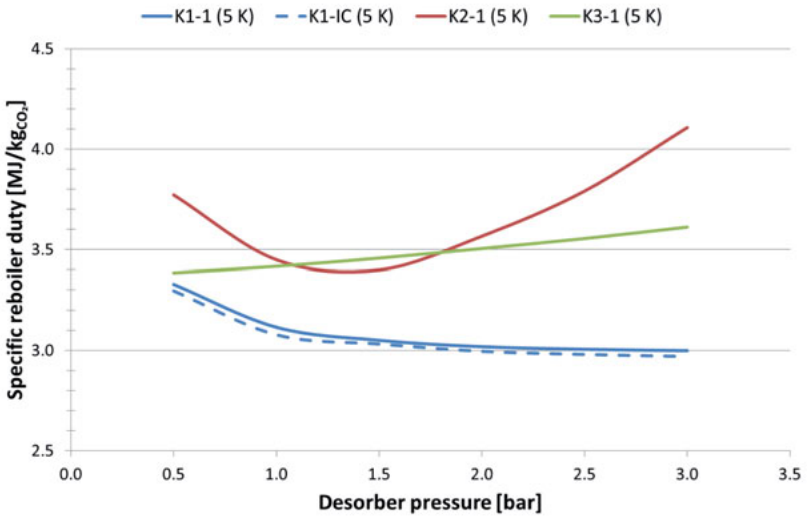

Figure 4.33: Comparison of calculated specific reboiler duties at different stripper pressures for previously selected blends with intercooling results at a heat exchanger's temperature difference of 5 K

According to Figure 4.33, K1-IC's reboiler duty is lower than K1-1's even though K1-IC's cyclic capacity is higher than K1-1's (see Table 4.1). This behaviour can be explained by considering the influence of three factors on the scrubbing system: K1-IC's temperature at absorber's bottom, K1-IC's lower flow rate, and its related lean-rich heat exchanger area.

Since both liquid solutions (K1-1 and K1-IC) consist of approximately the same chemical composition, it is possible to assume that the lower flow rate is easier to heat up or cool down in comparison with the bigger one for K1-1. In other words, it should be possible to reduce the lean-rich heat exchanger's size when implementing absorber intercooling. However, results in Table 4.1 indicate that this is not the case. This table lists the lower and higher limits with respect to required heat exchanger specific area, depending on the desorber's operating pressure. Independently of the used desorber pressure, results indicate a higher required heat exchanger's area for K1-IC than for K1-1. Unlike expected, K1-IC's required heat transfer capacity is not lower than K1-1's. It actually is higher, which ends up in a larger lean-rich heat exchanger area. A glance at this heat exchanger's inlet and outlet streams in Figure 4.34 helps understanding what at first may seem improbable.

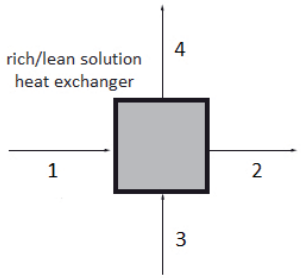

Nomenclature:

1	*Cold rich solvent from absorber's bottom*
2	*Hot rich solvent to desorber's top*
3	*Hot lean solvent from desorber's bottom*
4	*Cold lean solvent to amine cooler (previous to absorber)*

Figure 4.34: Rich-lean heat exchanger's inlet and outlet solvent flow rates

Table 4.1: Selected blends' compilation of cyclic capacities and related specific heat exchanger area

Solvent blend	Nomenclature	$\Delta\alpha$	Required lean-rich heat exchanger area [m^2/kg_{CO_2}]	
			Desorber pressure: 0.5 bar	Desorber pressure: 3.0 bar
K1	K1-1	0.178	265.96	503.85
	K1-IC	0.183	284.92	574.45
K2	K2-1	0.152	492.83	929.46
K3	K3-1	0.130	814.32	1,622.38

According to simulation parameters introduced in section 3.2.2 a temperature difference of 5 K was set between streams 4 and 1 in Figure 4.34. This restriction applies to all simulated cases. This, however, does not restrict stream 1's temperature which varies depending on whether an absorber intercooling system is implemented or not. The mentioned restriction merely sees to it, that temperature difference between streams 1 and 4 is been kept constant at 5 K. When using intercooling, stream 1's temperature is about three degrees lower than without it. Hence, stream 4's temperature is also lower when using intercooling.

On the other hand, stream 3's temperature corresponds to the lean solvent at desorber's outlet. This temperature is not influenced by the heat exchanger, but is instead a product of process conditions and solvent's chemical properties. This temperature remains nearby constant for K1-1 and K1-IC. This means that, the lean solvent at desorber's bottom has to be further cooled down for K1-IC due to intercooling effects and design specifications (5 K difference between streams 1 and 4). In order to fulfil this, heat exchanger's area has to be enhanced. In addition, K1-IC's flow rate is lower than K1-1's, so that the larger exchanger's area also results in a higher rich solvent temperature at desorber's inlet (stream 2), thus actively contributing to reduce the reboiler duty required for solvent regeneration.

In summary, although K1-IC's cyclic capacity is higher than K1-1's, the benefits of having a lower solvent flow rate seem to outweigh the higher regeneration energy that is related to a higher carrying capacity. It is though debatable to assume that in general by incrementing a solvent's cyclic capacity, the resulting specific reboiler duty required for regeneration will decrease. Presented results arose from implementing absorber intercooling, which led to a lower rich solvent flow rate and temperature but also to an enhancement of the lean-rich heat exchanger's area. There have also been cases, like the one presented by Abu-Zahra, et al. [90], where a lower specific reboiler duty was reached with a cyclic capacity of 0.32 mol_{CO_2}/mol_{MEA} than with 0.25 mol_{CO_2}/mol_{MEA}. Abu-Zahra worked with MEA instead of piperazine promoted potassium carbonate solutions. Nonetheless, presented results should not be generalized. It is not the cyclic capacity's increase alone, but rather the sum of all implemented measures –from absorber intercooling to using a bigger lean-rich heat exchanger– that lead to a specific reboiler duty's reduction.

Absorber intercooling does not only affect a column's geometry but also has an impact in the scrubbing process overall cooling duty. Figure 4.35 shows a comparison of the results before and after absorber intercooling implementation. The legends correspond to the ones introduced for Figure 4.23 with an addition: *abs. intercooling* represented with orange bars. The overall specific cooling duties remain

practically constant and no difference can be detected by just looking at the diagram. Since cooling duty results have already been discussed, only results related to absorber intercooling will be contemplated in this section.

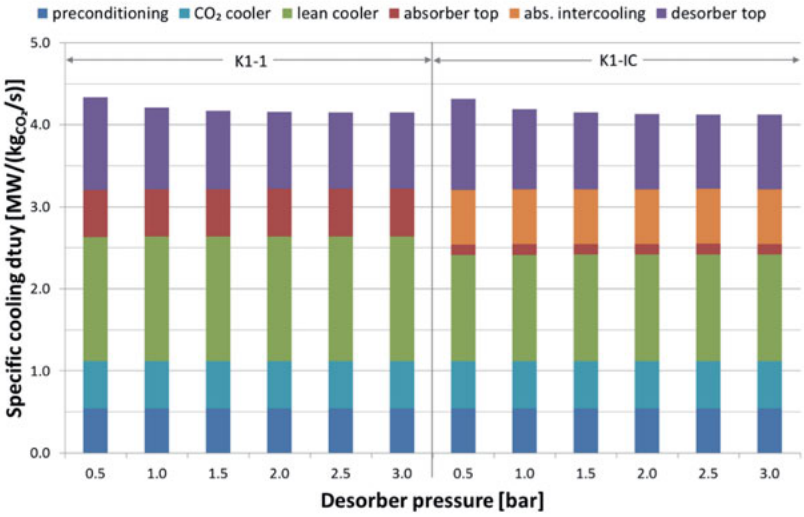

Figure 4.35: Comparison of specific cooling duties before and after adding absorber intercooling

Preconditioning and *CO_2 cooler* duties are the same for all studied cases, as noted in Figure 4.23 with blends K1-1, K2-1 and K3-1. This trend also applies to *desorber top* -represented in purple bars- when comparing results before and after absorber intercooling. Results vary for this category only due to the implemented stripper pressure, but not due to absorber intercooling.

The most notable effect on cooling duties due to absorber intercooling is detected for *lean cooler* as well as *absorber top* represented in green and red bars respectively. The reason for lean cooler's cooling duty decrease is the same as the one mentioned for Figure 4.23: rich amine solution's temperature (at absorber's bottom) and mass flow rate. Without absorber intercooling the reference temperature for the lean-rich heat exchanger is higher than with intercooling, so that the exchanger's outlet temperature and consequently the lean cooler's inlet temperature is also higher resulting in a greater cooling duty demand. In addition, the mass flow rate is higher than when implementing absorber intercooling, so that here also a slight effect is observed with intercooling that contributes to decreasing the *lean cooler*'s duty.

Figure 4.30 showed that the gas temperature at absorber's top is affected by absorber intercooling in the same way that the amine solution's temperature is affected, as displayed in Figure 4.26. Without intercooling, the stack's temperature at absorber's top is around 49.5°C and with intercooling is approximately 46.3°C. The flue gas flow rate is about 435 m^3/s and thus cooling this flow rate down to 40°C represents a tough task. In consequence, even though the temperature difference with and without absorber intercooling may only make about 3 C, the difference in specific cooling duty amounts to almost 0.5 MW/kg CO_2 in Figure 4.35.

The last category in Figure 4.35 is destined for *abs. intercooling* in orange bars. The specific cooling duty is 67 MW/kg CO_2 and corresponds to the one given in Figure 4.32. The sum of *lean cooler*, *absorber top* and *abs. intercooling* specific duties for K1-IC match the sum of *lean cooler* and *absorber top* for K1-1 for the reasons mentioned previously.

All in all it can be said that although there certainly are differences regarding total duties' single components, the difference in overall cooling duties for the blend K1-1 with and without intercooling can hardly be appreciated. This does not mean that absorber intercooling does not have any advantages. On the contrary, it has so far been demonstrated that by implementing absorber intercooling positive effects result in terms of column geometry, solvent mass flow rate, but also in terms of a reduced reboiler duty.

4.4 Column geometry

After having analysed different components' operating conditions and their effect on the scrubbing process, it is possible to continue with equipment design. As was explained in section 3.2.2, Aspen Plus is capable of calculating column geometry. It was also mentioned that simulations were conducted assuming a variable diameter. By having detected favourable conditions at which the scrubbing process should operate, it is possible to use results for final column design.

So far, the simulation tool has delivered parameters such as loadings, packing height, pressure drop, column diameter, etc. However, a packing column consists of several so-called *internals*, which are also necessary for column operation. These are for instance support grids, liquid collectors, feed pipes, liquid distributors, locating grids, steam inlet pipes, circulation pipes, column sump, skirts and/or anchorages. Calculating a column's height implicates accounting for internals, which is this section's purpose.

Column design was conducted for:

1) SO_2 absorber
2) CO_2 absorber
   a) MEA Case I
   b) MEA Case II
   c) K1-IC
   d) K1-1
3) Desorber
   a) MEA Case I at p = 1.5 bar
   b) MEA Case II at p = 2.1 bar
   c) K1-IC at p = 0.5 bar
   d) K1-IC at p = 1.0 bar
   e) K1-IC at p = 1.5 bar
   f) K1-IC at p = 2.0 bar
   g) K1-IC at p = 2.5 bar
   h) K1-IC at p = 3.0 bar
   i) K1-1 at p = 2.0 bar

Yagi, et al. [105] suggest a flue gas velocity of approximately 10 m/s at absorber's inlet. Following design parameters used in [82] the previous velocity ends in a flue gas feed size[21] of 6.5 x 6.5 m. In addition, a distance of 1 m was assumed for the sump, as well as for the distance between flue gas inlet and the lowest packing. Weiß [83] recommends using collectors and distributors every 3-5 m.

Resulting columns' dimensions are presented in Table 4.2 for SO_2 and CO_2 scrubbers. The first one is based on parameters presented at the end of section 4.2. The calculated packing height was 1.54 m, which with a column diameter of 13.86 m results in a packing volume of 232.3 m^3. Due to the short packing height, it suffices to calculate overall column height with only one liquid distributor.

The previous list shows all cases considered for column dimensioning. MEA cases (2a and 2b) correspond to the ones introduced in section 3.2.1.2. K1-IC represents the CO_2 absorber with intercooling and K1-1 denotes the original absorber without intercooling. The lowest height is reached with K1-IC due to positive intercooling effects discussed in section (4.3.6). The second lowest column uses MEA as a solvent and corresponds to Case I (see Table 3.4). This column (2a from the list) is almost 6 meters taller than K1-IC's.

The third and fourth highest columns use MEA and K1-1 respectively and are 27 and 28 meters taller than the shortest column. These last two cases (2b and 2d)

[21] Reference power plant used in [82] is identical with the one used in this work, so that the same flue gas feed size may be assumed.

only have the immense height in common. Case 2b uses a 30 wt.-% MEA solution and a relatively high lean loading (α_{lean} = 0.32 mol_{CO_2}/mol_{MEA}), whereas case 2d uses a piperazine promoted potassium carbonate solution (K1-1) and for this kind of solution a low lean loading (α_{lean} = 0.30 mol_{CO_2}/mol_{K1-1})[22]. MEA Case II (or 2b) was selected as a reference because it promised a low reboiler duty and thus a more efficient process. However, it is not until dimensioning of the required column is undertaken that the magnitude of such parameters can actually be quantified. By setting the initial lean loading to a relatively high value lower energy is required for regeneration purposes, but instead the solution's amount has to be increased in order to guarantee for a certain capture, i.e. 90 % CO_2. As was explained in section 4.1 a flow rate increase has a lower gas velocity as a consequence and the outcome is a bigger column diameter (see equation (4.5)). In addition, due to the – for MEA– relatively high lean loading of MEA Case II, the related packing height is higher than for MEA Case I since a higher specific area is needed for solvent loading.

In contrast to MEA Case II, K1-1 uses a lean loading and yet the overall height amounts 53.5 m, from which 30 m alone correspond to the required packing height. Given that every 3-5 m collectors and distributors have to be placed to guarantee for an effective solution distribution along the whole packing, further 10 m have to be added to column height. The rest of the parameters are the same for all cases. The lean loading is also in this case responsible for the extreme packing height. K1-1 has a low loading and hence CO_2 is rapidly absorbed. However, due to exothermic reactions that take place and due to the low liquid flow rate, the solution's temperature increases rapidly, which at first favours kinetics, until the solvent's carrying capacity is compromised. This has already been extensively discussed in section (4.3.6).

In a way, MEA Case I and K1-1 (cases 2a and 2d from the list) are comparable with one another. Dugas, et al. [106] report from a temperature bulge present for MEA solutions with lean loadings at similar conditions to the ones presented in this work. The highest temperatures reported by Dugas, et al. [106] varied between 70-75°C, which fit the same range as K1-1. This suggests that MEA could also benefit from absorber intercooling in the same way as K1-1 did. This was though not considered in this work and may be subject of future studies.

All CO_2 scrubbers are capable of capturing the same amount of CO_2. Nevertheless there are clear dimension differences. It is questionable if a column with a height

[22] Please note that lean loadings of different solvents are not directly comparable since each solvent has different characteristics and hence its own absorption capacity. The final cyclic capacity depends on several factors as has been mentioned along this work.

higher than 50 m will be built, above all considering column diameters of approximately 15 m. Even if this might be the case, it might be more efficient to use several smaller columns that have all together the same capture capacity. This was not either considered in this work and may as well be subject of future studies.

Table 4.2: Calculated absorber geometry

	Diameter	mfc[23]	Flue gas feed size	Distance between flue gas inlet and lowest packing	Number of collectors and distributors	Sump	Packing height	Head wash	Total height	Packing volume
	[m]	[-]	[m]	[m]	[-]	[m]	[m]	[m]	[m]	[m^3]
NaOH (SO_2 absorber)	13.86	0.8000	6.5	1	1	1	1.54	5	16.0	232.3
MEA Case I	16.20	0.8000	6.5	1	3	1	14.70	5	31.2	3029.0
MEA Case II	17.07	0.8000	6.5	1	7	1	34.0	5	54.5	7785.2
K1-IC	14.45	0.8032	6.5	1	3	1	10.0	5	26.5	1640.4
K1-1	15.11	0.8032	6.5	1	10	1	30.0	5	53.5	5380.7

Desorber design parameters such as maximum fractional capacity and sump were calculated using the same assumptions as with absorber columns. The rich solution feed size results from using an inlet liquid velocity of 10 m/s. Collectors and distributors were included considering packing sections of 4 m each.

In general, all desorber columns are smaller than their respective absorber. This is partly due to the operating pressure but also due to the fact that the flue gas flow rate does not cross this column. Instead, the solution is in contact with steam generated by the reboiler.

Desorber geometry comparison is in this case rather complicated. Common (simulation) design parameters for all desorber columns are CO_2 recovery rate and maximum fractional capacity, which was kept nearly constant at 0.8 and corresponds to a column design at 80 % proximity to flood point. All desorber columns are different except for K1-IC and K1-1, both at $p_{desorber}$ = 2.0 bar. Although reboiler duty was calculated to be slightly lower (see previous section), column geometry does not seem to be affected. It might be possible to reduce the size of K1-IC column by decreasing the packing height, until the target lean loading with absorber intercooling matches the one without intercooling. This in turn would increase the required mass flow rate within the scrubbing cycle and in the end the reboiler duty would match K1-1's.

[23] Maximum fractional capacity; please refer to the beginning of section 3.2.1.

An important factor for diameter estimation is the expected desorber operating pressure. Since simulations were undertaken allowing for a variable diameter, the packing height stays constant for K1-IC and K1-1, whereas column diameter decreases as the related operating pressure grows. This is the reason why the required packing volume drops with increasing pressure, which also confirms the fact that higher pressures have a positive effect in terms of enhancing the solvent regeneration efficiency, both in term of lowering the needed reboiler duty and reducing packing volume.

Results reported by Abu-Zahra in [90] also suggest a better regeneration at higher pressures. This is partly seen for MEA Case I and II in Table 4.3. If these two cases would have the same lean and rich loadings, then their packing height would be the same independently of the desorber pressure and only the resulting column diameter would vary. However, since the used loadings are different, the required packing height is not constant. Case I's lean loading is 0.242 mol_{CO_2}/mol_{MEA} and Case II's 0.32 mol_{CO_2}/mol_{MEA}. Case I needs a higher packing height in order to reach the target loading and vice versa.

Table 4.3: Calculated desorber geometry

Solvent	Desorber pressure	Diameter	mfc	Rich solution feed size	Number of collectors and distributors	Sump	Packing height	Total height	Packing volume
	[bar]	[m]	[-]	[m]	[-]	[m]	[m]	[m]	[m^3]
MEA Case I	1.5	10.30	0.8096	0.5	3	1.0	12.0	16.5	999.9
MEA Case II	2.1	9.40	0.8096	0.6	3	1.0	10.0	14.6	694.0
K1-IC	0.5	11.10	0.8010	0.4	2	1.0	8.0	11.4	774.2
K1-IC	1.0	9.87	0.8000	0.4	2	1.0	8.0	11.4	612.6
K1-IC	1.5	9.30	0.8038	0.4	2	1.0	8.0	11.4	543.4
K1-IC	2.0	9.00	0.8034	0.4	2	1.0	8.0	11.4	508.9
K1-IC	2.5	8.75	0.8072	0.4	2	1.0	8.0	11.4	481.1
K1-IC	3.0	8.60	0.8051	0.4	2	1.0	8.0	11.4	464.7
K1-1	2.0	9.00	0.8034	0.4	2	1.0	8.0	11.4	508.9

4.5 Integration into the power plant

Up to now, the scrubbing system has been the focus of all calculations. This has helped detecting adequate operating parameters in terms of low energy requirement or geometry. To be able to account for these parameters' effects on a coal-fired power plant in terms of efficiency penalties, it is necessary to determine the

interface(s) between scrubbing system and power cycle. These include both thermal requirement and auxiliary power, which will be the focus of this section.

4.5.1 Thermal requirement

When referring to this topic it is common to think of the steam that has to be delivered from RPP NRW to the scrubbing process. However, there is also the cooling duty, that has to be accounted for and which is also provided by the power plant. Hence, *steam tapping* and *cooling duty* will be discussed in this section.

4.5.1.1 Steam tapping

The reference power plant North Rhine-Westphalia (RPP NRW) introduced in section 1.3.1 represents the basis for all efficiency penalties appraisal related calculations. Efficiency losses result from supplying the scrubbing system with heat –in form of steam and cooling water– and electricity. This section will focus on accounting for the amount of steam that will be extracted from the power cycle and will translate this in terms of efficiency penalties. Losses due to cooling water and electricity will be considered subsequently. Given that power plant related data was indispensable for completing this section, RPP NRW was modelled with the commercial software EBSILON®Professional V 9.00 from Evonik Industries. Implemented simulation parameters correspond to the ones presented in Table 1.1 in section 1.3.1.

Results presented in the previous section indicate that K1's required reboiler duty decreases as the stripper operating pressure increases. This suggests that by setting a high stripper pressure, the expected power plant's efficiency losses will also be low. Nonetheless, steam parameters are a direct function of the stripper's operating pressure, meaning that depending on required steam quality and flow rate the effect on RPP NRW varies. In other words, the apparent optimal operation parameters for the CO_2 scrubbing process may not necessarily correspond to the ones at which the lowest efficiency penalties are expected. Hence, by contemplating the strippers operating pressure in a range between 0.5 and 3.0 bar, it should be possible to identify a pressure, at which efficiency losses are the least.

At first sight, it may seem as if the power cycle would have several possible locations to tap steam, for example: before or after HP, IP or LP turbines, or directly from a steam pipe usually intended for preheating purposes. However, the main problem with steam extraction consists in tapping only as much steam from a pipe that an imbalance of the boiler's thermal load may be avoided. This excludes most of the mentioned options, since a considerable amount of steam is needed to meet

the calculated reboiler heat demand. According to simulations' results, required steam parameters for all contemplated desorber pressures are met by extracting steam between IP and LP turbines. Given that the steam has already flown through HP and IP turbines, extracting steam at this location is not a bad choice at all. Independently of steam parameters, amount and/or tapping location efficiency penalties occur from altering the power cycle simply by tapping steam, thus the real task consists in keeping power cycle's alterations as simple as possible. For this reason, the interface between scrubbing process and power cycle was set between IP and LP turbines and a full load operation was considered at all times.

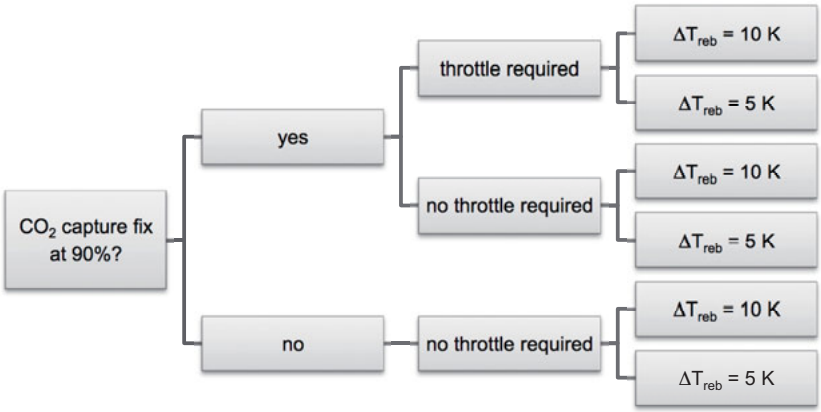

Figure 4.36: Possible steam tapping scenarios

In order to better understand and account for the consequences of steam tapping on the power cycle, different scenarios have been contemplated as shown in Figure 4.36. The first step consists in defining whether CO_2 capture should be fixed at 90 % or if only so much steam should be tapped, so that no further measures have to be taken to keep the steam cycle stable. For example, depending on the required steam amount, as well as its parameters, it might be necessary to build in a throttle to guarantee for a certain pressure within the tapped steam's pipeline. By building-in such a throttle though, irreversibilities arouse that lead to unavoidable efficiency penalties.

By not fixing CO_2 capture to 90 % a throttle does not have to be build-in and related irreversibilities are avoided, whereas by fixing CO_2 capture to 90 % a throttle may or may not have to be build-in. Whether or not a throttle would have to be im-

plemented depends on both required steam parameters and related amount. This will be presented as part of the results in shortly.

The reboiler temperature difference is the last parameter that was considered for determining efficiency penalties due to steam tapping. Since the reboiler is the device that is provided with tapped steam, it made sense to analyse its effect on the power plant by contemplating two temperature differences: 10 K and 5 K for each of the presented scenarios, as displayed in Figure 4.36.

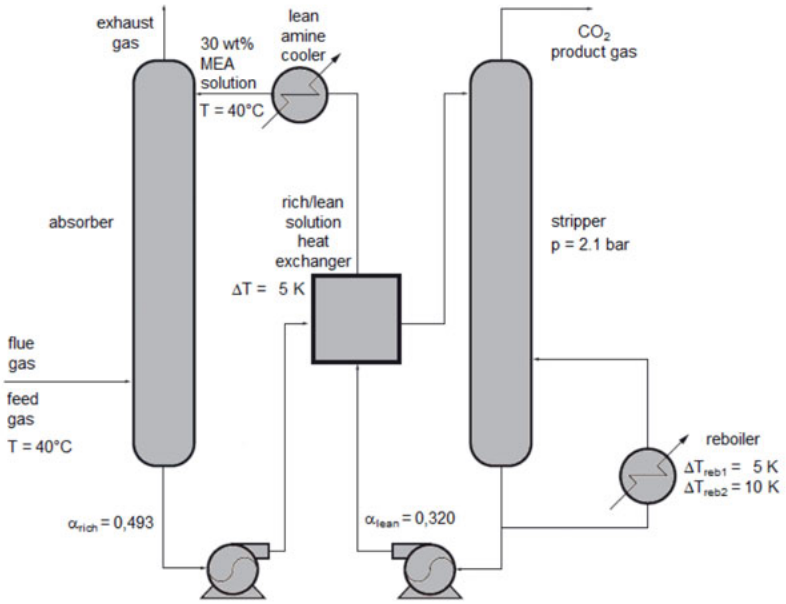

Figure 4.37: Main parameters overview of Abu-Zahra's adapted case to match RPP NRW's flue gas conditions

It has previously been mentioned that a system with a 30 wt% aqueous MEA solution is commonly used in the literature as a base to compare CO_2 capture systems. Since most parameter variations have been carried out by now, it is time to introduce results that will allow for an appraisal of the developed system with K1-IC compared to an MEA system. As stated in section 3.2.1.2 the implemented MEA system is based on Abu-Zahra's work[24], however the developed system is not identical. Abu-Zahra's reference power plant is different than RPP NRW. For this reason it was decided to use Abu-Zahra's operation parameters that lead to an optimised case. These were then used to design a new scrubbing system that

[24] Please refer to [90].

would match RPP NRW's flue gas composition and flue gas flow rate. In addition, the parameters that had proved most suitable to reducing the reboiler duty in piperazine promoted potassium carbonate systems were also implemented in the new MEA system, with the exception of absorber intercooling, which is not commonly considered for comparison purposes in the literature. A summary of the used simulation parameters is presented in Figure 4.37.

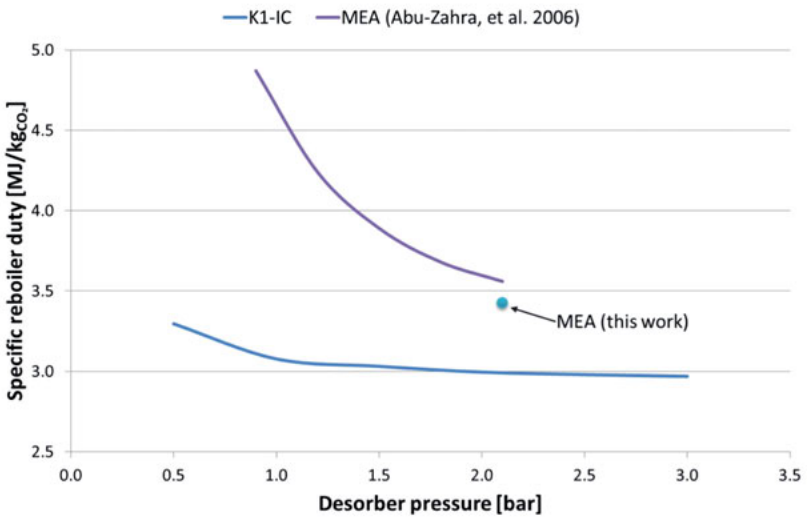

Figure 4.38: Comparison of specific reboiler duties for K1-IC with MEA (literature values [90]) and modified Abu-Zahra's optimised case to match RPP NRW's operation parameters (see section 3.2.1.2 and Table 3.4)

Two curves and a dot are displayed in Figure 4.38. The blue curve corresponds to K1-IC, the purple one to Abu-Zahra's results from the literature, and the blue dot represents Abu-Zahra's adapted case to match the same operation conditions as K1-IC and RPP NRW's flue gas composition. This is exactly the case that will be used for comparison when appraising integration results due to steam tapping. The blue dot shows an even lower specific reboiler duty than the one presented by Abu-Zahra. There are different reasons for this. To begin with, it has already been mentioned that the corresponding flue gas compositions were not identical, since purple curve's results derive from using a different power plant and coal. Moreover, not even the equipment used was the same, i.e. column packings used by Abu-Zahra were Mellapak Y125, whereas all conducted simulations assumed the use of Mellapak 250X. Since it was important to guarantee for a certain degree of

comparability with the piperazine promoted potassium carbonate systems, it was indispensable to use the same conditions for all systems, including MEA. Nevertheless, the calculated specific reboiler duty shows a good approximation to Abu-Zahra's results from the literature.

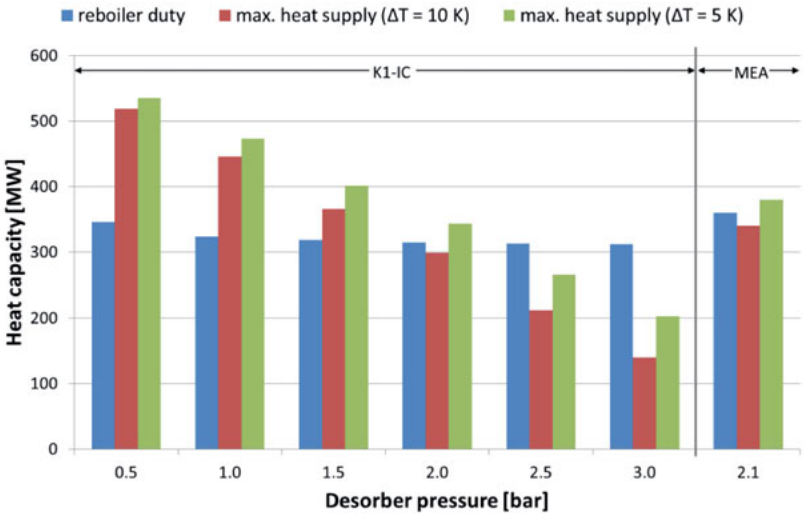

Figure 4.39: Comparison of required reboiler heat demand for solvent regeneration, assuming a CO_2 capture rate of 90 % with actual maximum available power plant's heat capacity to avoid building in a throttle for two temperature differences (ΔT_{reb} 10 and 5 K)

The first results regarding steam tapping are displayed in Figure 4.39, which shows the required heat capacity for K1-IC at a stripper operation pressure range that varies from 0.5 to 3.0 bar and for MEA at a pressure of 2.1 bar. The blue bar indicates the calculated reboiler duty for a 90 % CO_2 capture. The red and green bars stand for RPP NRW's maximum available heat capacity to supply the scrubbing process with a reboiler temperature difference of 10 K and 5 K respectively without having to build in a throttle. These two bars represent results delivered by the simulation programm Ebsilon®Professional. By comparing a red and green bar with a blue one is possible to visualize whether a throttle will be needed or not. If a blue bar is lower than the red or the green one, then no throttle will be required, and vice versa, if any of the red and green bars is lower than the blue one, then a throttle will be indispensable. Getting back to Figure 4.39 this means that for K1-IC there is no need to use a throttle for a pressure range between 0.5 and 1.5 bar independently of the used reboiler temperature difference, whereas starting at a

pressure of 2.5 bar a throttle becomes unavoidable. There are though, two stripper operation pressures at which the reboiler temperature difference does make a difference: 2.0 and 2.1 bar for K1-IC and MEA respectively. At these pressures it is only possible to avoid building in a throttle by using a reboiler temperature difference of 5 K.

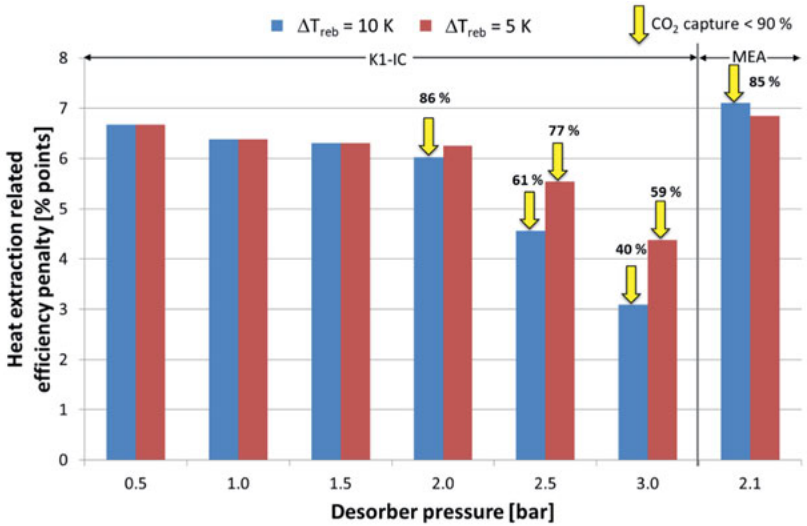

Figure 4.40: Efficiency penalties due to steam extraction for regeneration purposes under the assumption that no throttle is built in. Aimed CO_2 capture rate is 90 % unless indicated otherwise

Even though a throttle was not built in in any case displayed in Figure 4.40, there are still efficiency penalties that result from extracting steam from the power plant's water-steam cycle. These are depicted in Figure 4.40. The aimed CO_2 capture was set to 90 %, however, as has already been explained with Figure 4.39, not all scenarios can guarantee for it without having to build in a throttle. Hence, some cases are marked with a yellow arrow to indicate the maximum CO_2 capture rate that can be reached with the available amount of steam. Within a pressure range that varies from 0.5 to 1.5 bar the target CO_2 capture rate is fulfilled even without a throttle. This changes starting at a pressure of 2.0 bar. Under these conditions the aimed CO_2 capture can only be reached when a reboiler temperature difference of 5 K is used for K1-IC, otherwise it remains below 90 % and decreases as the desorber pressure increases. MEA results at a pressure of 2.1 bar are comparable to K1-IC's at 2.0 bar: the targeted CO_2 capture can only be reached by implementing a reboiler temperature difference of 5 K. With respect to efficiency penalties, the

lowest ones can be found at higher pressure rates. This though is merely due to the extracted amount of steam, which is only as high that building in a throttle is prevented. As a result, only a low amount of steam leaves the power cycle so that efficiency losses are correspondingly low. Nonetheless, the extracted steam does not suffice to guarantee for solvent regeneration that would secure a CO_2 capture rate of 90 %.

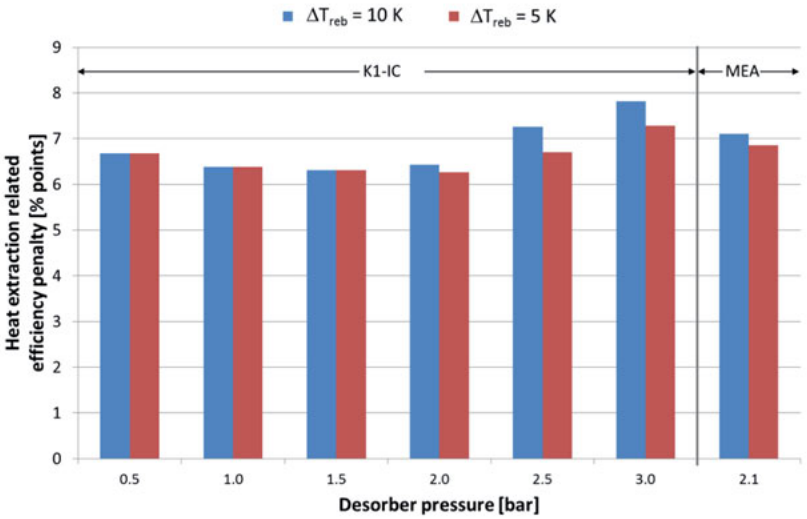

Figure 4.41: Efficiency penalties due to steam extraction for regeneration purposes assuming a CO_2 capture rate of 90 % is guaranteed at all times

Building in a throttle causes a further decrease of the overall power plant efficiency, but it also secures the target CO_2 capture rate. This can be seen in Figure 4.41. As could be observed in Figure 4.40, efficiency losses due to steam extraction for K1-IC decrease as the pressure increases, but only within a range between 0.5 and 1.5 bar independently of the reboiler temperature difference. Starting at a pressure of 2.0 bar the efficiency penalties continue to decrease, however this occurs only when using a reboiler temperature difference of 5 K. It is at this pressure that calculated efficiency losses are the lowest, amounting to 6.26 percentage points. Later on, the efficiency losses keep on growing proportional to the increasing desorber pressure, the required throttle, and its related losses due to irreversibilities. With MEA the lowest calculated efficiency penalties are expected when using a reboiler temperature difference of 5 K at a pressure of 2.1 bar. In this case the losses amount to 6.85 % (percentage points) compared to

7.10 % when using a reboiler temperature difference of 10 K at the same pressure. By setting a lower reboiler temperature difference it is possible to avoid building in a throttle, since the available heat capacity is higher than the one actually required for solvent regeneration.

After having accounted for efficiency penalties that result from tapping a part of the power cycle's steam it is possible to quantify what is left from the original power plant efficiency. Figure 4.42 shows the expected power plant net efficiencies for a CO_2 capture of 90 % at all times, after the previous losses have been accounted for. The efficiencies are represented with a blue and a red curve depending on the used reboiler temperature difference of either 10 K or 5 K. Calculated net efficiencies are in general higher for a reboiler temperature difference of 5 K, which has to do with the capability of being able to avoid building in a throttle. The highest efficiency for ΔT = 5 K amounts to 39.64 % at a desorber pressure of 2.0 bar for K1-IC. At the same temperature difference a decline in net efficiency is observed at a pressure higher than 2.0 bar and at a pressure higher than 1.5 bar for ΔT = 10 K.

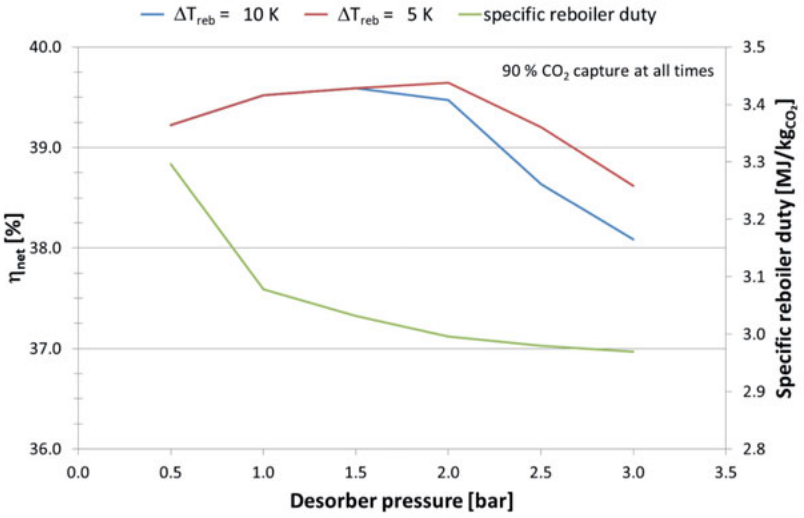

Figure 4.42: Desorber pressure effect on K1-IC's specific reboiler duty and resulting power plant net efficiency for two reboiler temperature differences

The green line in Figure 4.42 represents KI-IC's required reboiler duty for solvent regeneration. This curve has previously been shown in Figure 4.33 and is presented here to help comparing desorber pressure's effect on required reboiler du-

ties and related power plant efficiency losses. In general, it is common to assume that by choosing operation parameters that lead to a low reboiler duty the expected efficiency penalties will also be kept as low as possible. However, as Figure 4.42 depicts the former statement is a misconception. While it is true that the reboiler duty makes out for the highest efficiency losses in a power plant, it cannot be denied that the lowest reboiler duty itself results in the lowest power plant net efficiency. This depends directly on the required steam parameters that result from the implemented desorber pressure. The required regeneration temperature at the reboiler is directly proportional to the operating pressure. The higher the pressure, the higher the required regeneration temperature will be. This affects both steam rate, as well as steam parameters (temperature and pressure): at higher desorber pressures the tapped steam rates are lower due to the higher energetic value of the steam, but at the same time, in order to maintain the steam's high temperature it is necessary to build in a throttle, otherwise the pressure within the steam pipeline would fall so fast, that the extracted steam would not suffice anymore for solvent regeneration. However, a throttle causes further losses due to irreversibilities and hence, the overall net efficiency at higher desorber pressures is lower, although the related specific reboiler duties suggest otherwise. The only way to avoid high efficiency penalties at higher pressures is to set a new CO_2 capture rate below 90 %. Nonetheless, that differs from one of the main goals of this work and hence, results suggest that for K1-IC the most suitable parameters are a desorber pressure of 2.0 bar and a reboiler temperature difference of 5 K. This also applies to MEA at a desorber pressure of 2.1 bar.

4.5.1.2 Cooling demand

Within the scrubbing cycle there are different components that require heat dissipation. This is achieved by using water and the precise amount used depends on the required heat output, as well as on the cooling water (CW) initial temperature T_{CW1}. The heat output is equivalent to the calculated cooling duty that has already been presented in sections 4.3.5 and 4.3.6. T_{CW1} value, on the other hand, depends from the location at which cooling water will be extracted.

There are different possibilities of supplying cooling water from the power plant. A first option consists in installing a second cooling tower for the scrubbing process. A second option is to reduce the steam flow rate to a half of its original value. This would allow reaching a lower temperature and consequently a higher enthalpy difference. A third option consists in extracting a part of the cooling water for the scrubbing process once it has run through the power plant's condenser, but before reaching the cooling tower as depicted in Figure 4.43. The cooling water is ex-

tracted at a temperature T_{out} (equivalent to T_{CW1}) and fed back at a T_{out}*. According to Korkmaz [107], it is also possible to extract the cooling water from the supply line, before it reaches the power plant's condenser. Korkmaz indicates that by extracting and feeding back the water from the return line, condenser operation remains practically constant. Hence, this is the option that was implemented in this work. The overall cooling duty has already been calculated and discussed in sections 4.3.5 and 4.3.6.

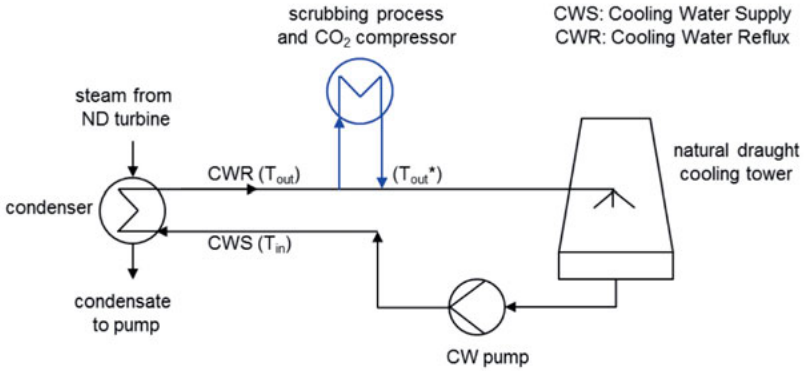

Figure 4.43: Implemented cooling water supply approach based on [107]

4.5.2 Auxiliary power

The electric power required by the scrubbing process can be determined by adding all ancillary components needed for operation. These are flue gas fan, pumps and CO_2 compressor.

Flue gas fan

In order to account for the electric demand of this component, it is indispensable to consider all pressure losses that have to be compensated by the flue gas fan. This is a necessary step to guarantee that flue gas pressure is equivalent to the atmospheric one, otherwise the flue gas will not be able to leave the absorber column.

Pressure losses arise due to flue gas flowing through columns internals. The main obstacles for flue gas are packings, as well as collectors and distributors. Aspen Plus is capable of estimating specific pressure losses depending on operating conditions and the packing kind. Once the packing height is known, it is possible to calculate packing related pressure losses for all columns. Pressure losses due to

collectors and distributors were assumed to be 3 mbar/m. Final packing heights and number of collectors and distributors were presented in Table 4.2 and Table 4.3, so that once it has been determined which components need to be considered all relevant pressure losses can be estimated. This can be done by taking a look at the flue gas fan's main task mentioned above. In other words, all components that stay in the flue gas' way have to be considered. These are: SO_2 absorber and CO_2 absorber, not only including packings, collectors and distributors, but also the wash section at absorber's head. Other possible additional losses were considered by adding 10 mbar to each case. Resulting single and overall pressure losses, as well as the required electric power, are summarised in Table 4.4.

The electric power is a direct function of the pressure difference that has to be provided by the flue gas fan. This is however only one important design parameter. The flue gas temperature at the fan's inlet is also a decisive factor that directly affects the required electric power. In general, the colder the flue gas, the lower the electric demand. The flue gas temperature is though limited by combustion and conventional flue gas cleaning, and by the scrubbing process itself. Since the temperature assumed for absorber operation is 40°C, it made sense to target this value as the fan's outlet temperature. To achieve this, the inlet temperature was set to 35°C, as was explained in section 3.2.1.1.

A comparison of results presented in Table 4.4 shows that both MEA Case I and K1-IC have equivalent total losses, albeit Case I's packing height is 4.7 m larger than K1-IC's. The reason for this lies in the specific pressure losses, which are lower for Case I than for K1-IC. It is also due to specific pressure losses that Case II shows a lower total loss than K1-1, even though Case II's packing height is 4 m bigger than K1-1's.

Table 4.4: Pressure losses to be compensated by flue gas fan and related power demand

	SO_2 absorber	Collectors and distributors	Packing	Head wash	Additional losses	Total losses	Electric power
	[mbar]	[mbar]	[mbar]	[mbar]	[mbar]	[mbar]	[MW_{el}]
MEA Case I	4.2	9	26.8	9.1	10	60	3.16
MEA Case II	4.2	21	62.0	9.1	10	107	5.55
K1-IC	4.2	9	24.1	12.1	10	60	3.16
K1-1	4.2	30	72.4	12.1	10	130	6.69

Given that apparently small pressure losses (in mbar) already cause electric demand to sky rocket, it is imperative to keep pressure losses that are to be compensated by a flue gas fan as low as possible. Korkmaz [107] pointed out the pos-

sibility of substituting flue gas fan by an exhaust fan or suction blower at absorber's top. This has the advantage that the flow rate at absorber's top is lower than at the inlet, which in theory should reduce the electric demand. In this work the flue gas fan was implemented previous to absorber's inlet for two reasons: To profit from the slightly higher CO_2 partial pressure and because the flue gas temperature at the absorber's inlet is 5°C lower than at absorber's top, which results in an even lower electric power requirement than the one reported by Korkmaz [107][25], although the same isentropic efficiency (85%) and almost same mechanical efficiency (99.5%) were assumed, including flue gas composition and mass flow, then his work is also based on RPP NRW. There is though a difference towards Kormaz's work: his definition of flue gas conditioning is not the same. He assumed SO_2 reduction had already taken place and that the temperature would still be approximately 47°C when the flue gas reached a cooler previous to the fan. At that point the flue gas temperature was reduced to 37°C and was set as the fan's inlet temperature.

Given that this work also includes SO_2 reduction, a direct contact cooler was placed before the SO_2 scrubber to prevent carry over losses of NaOH solution, in order to keep NaOH make up as low as possible. This measure allowed for a flue gas temperature of 35°C at the fan's inlet. However, Korkmaz's option of placing an exhaust blower at absorber's top was not analysed. This may be subject of future studies.

Pumps

There are two main pumps within the scrubbing cycle, whose required electric power also needs to be considered for calculation of the power plant's overall efficiency losses. The pumps are named after the solution's concentration they transport: *lean* and *rich*. The first one transports lean solution from desorber's bottom to the inlet location at absorber's top. The second one pumps rich solution from absorber's bottom to desorber's top. These two pumps are responsible for the highest electric demand due to pumps. A third pump that needs to be accounted for is used as part of flue gas conditioning equipment. Its demand is constant and according to calculations amounts to 0.28 MW_{el}. Pressure needed by each pump was determined by considering static head, column's operation pressure as well as assumed additional pressure losses of 1 bar.

[25] Electric power reported by Korkmaz [107] amounted to approximately 3.6 MW_{el} for the option with a flue gas fan previous to absorber inlet.

Parameters needed for pressure losses and hence for electric power calculation are displayed in Table 4.5 and Table 4.6 for lean and rich pump respectively. In addition, an essential consideration for pressure difference calculation is column height or rather solution's inlet height of each column. This can be determined with help of the tables introduced in section 4.4.

Table 4.5: Lean pump parameters for pressure losses calculation and related electric power

	Desorber Pressure	ρ_{lean}	$\dot{V}_{lean}$	Additional pressure losses	Total required Δp lean pump	Electric power
	[bar]	[kg/m^3]	[m^3/s]	[bar]	[bar]	[MW$_{el}$]
MEA Case I	1.5	1,052.51	2.06	1	3.7	0.54
MEA Case II	2.1	1,067.51	3.07	1	6.2	1.37
K1-IC	0.5	1,125.01	1.52	1	3.4	0.55
K1-IC	1.0	1,125.01	1.52	1	3.4	0.47
K1-IC	1.5	1,125.01	1.52	1	3.4	0.38
K1-IC	2.0	1,125.01	1.52	1	3.4	0.28
K1-IC	2.5	1,125.01	1.52	1	3.4	0.18
K1-IC	3.0	1,125.01	1.52	1	3.4	0.08
K1-1	2.0	1,125.01	1.57	1	6.4	0.68

Table 4.6: Rich pump parameters for pressure losses calculation and related electric power

	Desorber pressure	ρ_{rich}	$\dot{V}_{rich}$	Additional pressure losses	Total required Δp rich pump	Electric power
	[bar]	[kg/m^3]	[m^3/s]	[bar]	[bar]	[MW$_{el}$]
MEA Case I	1.5	1,093.64	2.08	1	4.3	0.76
MEA Case II	2.1	1,095.14	3.10	1	4.7	1.17
K1-IC	0.5	1,183.20	1.54	1	2.82	0.35
K1-IC	1.0	1,183.20	1.54	1	3.32	0.44
K1-IC	1.5	1,183.20	1.54	1	3.82	0.54
K1-IC	2.0	1,183.20	1.54	1	4.32	0.64
K1-IC	2.5	1,183.20	1.54	1	4.82	0.73
K1-IC	3.0	1,183.20	1.54	1	5.32	0.83
K1-1	2.0	1,183.20	1.57	1	4.32	0.64

With respect to *lean pump* the highest electric power corresponds to MEA Case II. This is due to the solution volume rate, which results from using a relatively high lean loading of 0.32 mol_{CO_2}/mol_{MEA}, but also due to the resulting height that needs to be overcome by the lean pump. K1-IC cases have almost constant parameters with exception of the desorber pressure. Electric power calculations in Aspen Plus consider the existing solution's pressure previous to entering a pump and estimate the difference pressure needed for transporting the solution all the way to absorber's top. That is the reason why electric power differs depending on the imple-

mented desorber pressure. The lowest electric demand is thus found for the highest desorber pressure used, which corresponds to 3 bar.

Rich pump results in Table 4.6 show the same trend as lean pumps'. The highest demand corresponds to MEA Case II. Abu-Zahra [90] suggested parameters used for MEA Case II due to the related low reboiler duty that results from using a solution with a relative high lean loading. However, such a loading also implicates a high volume rate within the scrubbing cycle. Results in Table 4.6 point out the expected consequence in form of a higher electric demand for pumps compared to the other cases. K1-IC's pump related electric demand varies gradually. This is only due to desorber's operating pressure, since all other parameters stay constant. K1-1's relative low electric demand –compared to MEA Case I– is the result of static head and operating pressure, which are both lower than MEA Case I.

Multistage compressor

This is the only UOM that was not simulated. Instead, results regarding this component were calculated with parameters listed in Table 4.7. Considering that desorber pressure varies depending on the analysed case, it was necessary to set a reference pressure for comparison purposes. The reference pressure was set to a value of 2 bar. This implicates an additional electric demand for cases with a desorber pressure below 2 bar, which results into higher power plant's efficiency losses. For cases with a higher pressure an additional work may be gained won from expanding CO_2 back to 2 bar, which contributes to reducing efficiency losses. These two cases were calculated with equations (4.12) and (4.13) respectively. An average ambient temperature of 11°C corresponds to German conditions and thus this is the value assumed for calculations.

Table 4.7: Assumed parameters for calculation of compressor's net work based on [107]

Parameter	Unit	Assumed value
Specific net work	kW_{el}/kg CO_2	297.0
Specific cooling duty	kW_{th}/kg CO_2	559.0
Initial temperature	°C	40
Initial pressure	bar	2
Final pressure	bar	200
Isentropic efficiency	%	85
Number of stages	-	8

$$P_{compression} = \dot{m}_{CO_2}\left[w_{comp} + \frac{1}{\eta_{is}} \cdot T_{amb}\left(-R_{CO_2} \cdot ln\frac{p_{des}}{p_{ref}}\right)\right] \quad (4.12)$$

$$P_{expansion} = \dot{m}_{CO_2}\left[w_{comp} + \eta_{is} \cdot T_{amb}\left(-R_{CO_2} \cdot ln\frac{p_{des}}{p_{ref}}\right)\right] \quad (4.13)$$

Where,

$P_{compression}$	[kW]	Electric demand by compression
$P_{expansion}$	[kW]	Electric demand by expansion
$\dot{m}_{CO_2}$	[kg/s]	CO_2 mass flow rate
p_{des}	[bar]	Desorber pressure
p_{ref}	[bar]	Reference pressure
R_{CO_2}	[kJ/kg·K]	CO_2 gas constant
T_{amb}	[bar]	Ambient temperature
w_{comp}	[kJ/kg]	Specific compressor work
η_{is}	[-]	Isentropic efficiency

Multistage compressor results are displayed in Table 4.8. The column “Compressor work” results from calculations with parameters listed in Table 4.7. The electric demand of this column is the same for all cases, since only the constant CO_2 mass flow rate and not the corresponding desorber pressure is considered for all cases. The next column displays additional or reduced work as a result of the correction undertaken for comparison purposes. The last column shows the expected total electric demand. According to results in Table 4.8 K1-IC and K1-1 at a desorber reference pressure of 2 bar require an electric power of approximately 31 MW_{el}.

In general, the electric demand decreases as desorber pressure increases due to the growing pressure ratio. The highest electric power is required by K1-IC at a desorber pressure of 0.5 bar. This result was expected, since this is also the lowest desorber pressure and hence the case with the lowest pressure ratio. According to conducted calculations an additional work of about 9 MW_{el} is required to increase CO_2's pressure from 0.5 to 2.0 bar.

Table 4.8: Multistage compressor results

	Desorber pressure	Compressor work	Additional work due to compression or expansion	Total electric power
	[bar]	[MW_{el}]	[MW_{el}]	[MW_{el}]
MEA Case I	1.5	31.18	1.91	33.09
MEA Case II	2.1	31.18	-0.23	30.95
K1-IC	0.5	31.18	9.19	40.38
K1-IC	1.0	31.18	4.60	35.78
K1-IC	1.5	31.18	1.91	33.09
K1-IC	2.0	31.18	0.00	31.18
K1-IC	2.5	31.18	-1.07	30.12
K1-IC	3.0	31.18	-1.94	29.24
K1-1	2.0	31.18	0.00	31.18

A CO_2 expansion does contribute to reducing power plant's overall efficiency penalties, but not in the same relation as compression increases them. The lowest demand is still reached with K1-IC at a desorber pressure of 3 bar and amounts to approximately 29 MW_{el}.

5 Analysis of economic feasibility

The previous chapter focused on interpreting simulation results and identifying optimal operation parameters for both scrubber system and power plant, until design could take place. This chapter focuses now on putting all components to work by conducting an economic analysis that will allow for feasibility estimation of the different technologies presented in this work. Results such as CO_2 avoidance cost or levelised cost of electricity (LCOE) will also facilitate comparison with other capture technologies used for a power plant such as RPP NRW.

Before the actual economic analysis is conducted there are a few definitions that first have to be introduced for a better understanding of presented results.

5.1 Basis of calculations and boundary conditions

Calculation methodology is based on two main sources: Abu-Zahra's parametric study of the economic performance based on monoethanolamine [92] that has already been mentioned on several occasions; and a zero emissions platform (ZEP) capture report [108]. Abu-Zahra's publication served as a guide for economic calculation and delivered data regarding the capture process, whereas the ZEP publication was used for economic appraisal of RPP NRW with and without post combustion capture of CO_2.

Financial and other boundary conditions considered for economic analysis are displayed in Table 5.2. Just as with the technical analysis RPP NRW was kept as reference coal-fired power plant. Generic technical parameters are presented in Table 5.1 together with those of the ZEP's study reference power plant. Both power plants are ultra-supercritical with fairly similar operation parameters. In addition, ZEP's power plant was retrofitted with a post-combustion capture plant employing advanced amines with CO_2 compression, which guarantees a good basis for comparison. The study does not mention though details about the post combustion capture plant. Another important consideration that both power plants –ZEP and RPP NRW– have in common is the fact that steam turbine design has not been modified in order to supply a considerable steam amount to the scrubbing system for the purpose of solvent regeneration. Instead, steam extraction is assumed to be taken from an overflow line and a throttle is used to hold pressure during part load operation [108].

Table 5.1: Generic technical parameters of each reference power plant case

Parameters		ZEP Power Plant [108]	RPP NRW
Fuel type		Pulverised hard coal	Pulverised hard coal
Net electricity output	MW_{el}	736	555.6
HP turbine steam inlet pressure	bar	280	285
IP turbine inlet steam reheat	°C	620	620
Net full load plant efficiency	% LHV	46	45.9
Plant load factor	h/year	7500	7500
Plant life	years	40	40
CO_2 emissions calculated from fuel carbon content	t/MWh	0.759	0.750

Table 5.2: Financial and other boundary conditions used in this work based on [108]

Parameters		
Economic life time	Years	40
Depreciation	Years	40
Fuel price	€/GJ (LHV)	2.4
Fuel price escalation	% per year	1.5
Operating hours per year	hours per year	7500
Standard emission factor	t_{CO_2}/MWh_{th}	0.344
Interest rate	%	8
Operation and maintenance (O&M) cost escalation	%	2

The following equations are based on the procedure used on a research project by Behr, et al. [38]. They were all implemented in the economic analysis.

As indicated in equation (5.1), CO_2 avoidance cost results from the difference of levelised fuel costs before and after CO_2 capture divided by CO_2 emissions also before and after carbon capture. This term is an important indicator of a technology's feasibility. By comparing the CO_2 avoidance cost to the price of an European Emission Allowance (EUA) –also known as CO_2 certificate– it can be determined whether a plant should be retrofitted with a scrubber system or not, since one of both options is cheaper.

$$C_{av,\,CO_2} = \frac{LCOE_{ref} - LCOE_{CC}}{e_{CO_2,\,ref} - e_{CO_2,\,CC}} \tag{5.1}$$

Equations (5.2) and (5.3) indicate how specific CO_2 emissions with and without CO_2 capture were calculated. The specific CO_2 emission factor for hard coal is listed in Table 5.2.

$$e_{CO_2,\,ref} = e_b \cdot \frac{1}{\eta_{ref}} \tag{5.2}$$

$$e_{CO_2,\,CC} = e_b \cdot \left(\frac{100 - R_{CC}}{100}\right) \cdot \left(\frac{1}{\eta_{ref} - \Delta\eta}\right) \tag{5.3}$$

Where,

C_{av,CO_2}	[€/t_{CO_2}]	CO_2 avoidance cost
e_b	[t_{CO_2}/MWh]	Specific CO_2 emission factor for hard coal
$e_{CO_2,ref}$	[t_{CO_2}/MWh]	Specific CO_2 emissions of RPP NRW
$e_{CO_2,CC}$	[t_{CO_2}/MWh]	Specific CO_2 emissions of RPP NRW with carbon capture
$LCOE_{ref}$	[€/MWh]	RPP NRW's levelised cost of electricity
$LCOE_{CC}$	[€/MWh]	Cost of electricity with carbon capture
η_{ref}	[%]	RPP NRW's net efficiency
$\Delta\eta$	[% points]	Efficiency losses due to CCS
R_{CC}	[%]	CO_2 capture rate (0% < R < 100%)

The levelised cost of electricity (LCOE) of RPP NRW with and without CO_2 capture were calculated with equation (5.4). LCOE results as a sum of capital and operational expenditures, as well as the fuel cost. Strictly speaking this last term also belongs to operational expenditures. However, the chosen representation allows for a graphic interpretation of fuel cost effect on the overall cost of electricity.

$$LCOE_i = \frac{1}{h} \cdot \left(CAPEX_i \cdot a + \frac{OPEX_i}{P_i}\right) + \frac{C_{fuel}}{\eta_i} \tag{5.4}$$

$$a = \frac{(1+r)^T \cdot r}{(1+r)^T + r} \tag{5.5}$$

Where,

a	[-]	Annuity factor	
$CAPEX$	[€/MW]	Capital expenditure	
C_{fuel}	[€/MWh]	Levelised fuel cost	$\frac{€}{MWh} = \frac{€}{GJ} \cdot \frac{3.6s}{1h}$

$LCOE_i$	[€/MWh]	Levelised cost of electricity	
h	[h]	Operating hours	
i	[-]	RPP NRW or carbon capture (CC)	
$OPEX$	[€]	Operational expenditure	$€ = \frac{M€}{year \cdot 10^6}$
P_i	[MW]	Power plant net output	
r	[-]	Interest rate	
T	[-]	Plant life	
η_i	[-]	Power plant net efficiency	

5.2 Discussion of results

Table 5.3 lists results for scrubbing systems CAPEX. MEA cases I and II correspond to MEA, whereas K1-IC and K1-1 correspond to piperazine activated potassium carbonate with and without intercooling respectively. For the cost estimation it was assumed that Abu-Zahra's data in [92] match the adapted case for this study (MEA Case I), except for total cost. The sum of equipment cost in the publication does not match the amount listed by Abu-Zahra. The actual resulting cost is listed in the Table 5.3's last row.

Equipment cost estimation was conducted based on the procedure described in a research report [39]. This calculation considers the liquid to gas ratios of MEA Case I (as the reference) and the respective analysed case (MEA Case II, K1-IC at p_{des} = 0.5 bar, etc). Intercooling cost estimation used Case I's lean cooler as reference, but instead of liquid to gas ratios, related temperature differences were considered. Absorber and stripper columns were calculated with a different approach. The original approach mentioned before was used for spray columns and not for packing ones, so that a one to one implementation was excluded. Instead a new approach was developed, which consisted in considering liquid to gas ratios but only to 75 % and including a packing volume factor to 25 %, as shown in equation (5.6).

$$Column\ price = Column_i \cdot \left\{0.75 \cdot \left[\frac{(L/G)_{new}}{(L/G)_{ref}}\right] + 0.25 \cdot \left[\frac{V_{new}}{V_{ref}}\right]\right\} \tag{5.6}$$

Where,

$Column_i$	[M€]	Price of selected reference column
L/G_{new}	[l/m^3]	New column's liquid to gas ratio
L/G_{ref}	[l/m^3]	Reference column's liquid to gas ratio (MEA Case I)
V_{new}	[m^3]	New column's packing volume
V_{ref}	[m^3]	Reference column's packing volume (MEA Case I)

Table 5.3: Overview of equipment cost [92]

Equipment	MEA Case I	MEA Case II	K1-IC						K1-1
Desorber pressure [bar]	1.5	2.1	0.5	1.0	1.5	2.0	2.5	3.0	2.0
	Cost [M€]								
Reboiler	0.81	1.01	0.58	0.58	0.58	0.58	0.58	0.58	0.58
Stripper	3.43	3.80	2.51	2.37	2.31	2.29	2.26	2.25	2.29
Lean/rich heat exchanger	0.42	0.52	0.30	0.30	0.30	0.30	0.30	0.30	0.30
Lean cooler	0.21	0.26	0.15	0.15	0.15	0.15	0.15	0.15	0.15
Reflux condenser	0.14	0.17	0.10	0.10	0.10	0.10	0.10	0.10	0.10
DCC water cooler	0.12	0.12	0.12	0.12	0.12	0.12	0.12	0.12	0.12
DCC (feed direct cooler)	0.54	0.54	0.54	0.54	0.54	0.54	0.54	0.54	0.54
Intercooling	0.00	0.00	0.05	0.05	0.05	0.05	0.05	0.05	0.00
Storage tank	0.73	0.91	0.52	0.52	0.52	0.52	0.52	0.52	0.52
Gas scrubber	0.26	0.26	0.26	0.26	0.26	0.26	0.26	0.26	0.26
Gas blower	3.10	6.36	3.12	3.12	3.12	3.12	3.12	3.12	3.12
Absorber fluid pump	0.59	0.74	0.42	0.42	0.42	0.42	0.42	0.42	0.42
Condenser fluid pump	0.01	0.01	0.01	0.01	0.01	0.01	0.01	0.01	0.01
Stripper fluid pump	0.60	0.75	0.43	0.43	0.43	0.43	0.43	0.43	0.43
Cold water pump	2.04	2.54	1.47	1.47	1.47	1.47	1.47	1.47	1.47
Absorber	10.94	17.25	7.38	7.38	7.38	7.38	7.38	7.38	10.75
Total	23.94	35.24	17.97	17.83	17.77	17.74	17.72	17.70	21.07

Results in Table 5.3 show that an absorber column is a scrubber system's most expensive component followed by gas blower and stripper column. Depending on the selected case the cost for an absorber varies between 40-45 % of the total

equipment cost. MEA Case II represents the most expensive case in Table 5.3, which does not only have to do with absorber geometry, but with the geometry of the whole system in general. This is also the reason why K1-IC at p_{des} = 3 bar is the cheapest case. In reality the costs of K1-IC cases most probably increase proportional to the desorber's operating pressure. However, conducted column design was kept at a basic level for comparison purposes. A scrubber system's implementation requires detail engineering, which is usually conducted once a case has been selected. K1-IC cases show an overall lower equipment cost than MEA cases I and II or K1-1. Absorber columns, for example, are on average 3 million euros cheaper than MEA or K1-1. Without intercooling absorber prices are almost the same for Case I and K1-1 at p_{des} = 2 bar. The most expensive equipment belongs to Case II due to the L/G ratio used and the resulting equipment dimensions, which also contribute to increase the scrubbing system's overall cost.

The scrubbing process does not only consist of equipment in real life. Table 5.4 lists a series of parameters that have to be considered in order to determine a scrubbing system total capital investment. As with Table 5.3, Table 5.4 consists of information provided by Abu-Zahra in [92]. However, the correction undertaken in Table 5.3 was also accounted for in Table 5.4, so that inside battery limits (ISBL) and purchased equipment do not match Abu-Zahra's data. Since these results are needed for calculation of total direct cost, fixed and total capital investment, these values also differs from Abu-Zahra's in Table 5.4. Table 5.5 summarizes cost estimation results for all studied cases based on data presented in Table 5.4.

Investment costs vary between 150 and 167 million euros in Table 5.5. The cheapest option is MEA Case I with 150.53 million euros. K1-IC at p_{des} = 2 bar represents the case that has shown the best overall results so far. This option's cost exceed Case I's by almost 7.5 million euros, although the equipment costs are lower. This can be explained with K1-IC's start-up and solvent costs. Assumed solvent costs are as follow: 40.3 €/kg K_2CO_3, 63.3 €/kg PZ and 26.3 €/kg MEA. In addition, a price reduction of 45 % was contemplated for the tonne price. Even if L/G ratios are lower when using piperazine promoted potassium carbonate solutions, the price is higher than MEA, which results in greater start-up and solvent costs for these systems.

$$DC_{total} = ISBL + OSBL \tag{5.7}$$

$$Cal_{fixed} = DC_{total} + IC_{total} + Compressor \tag{5.8}$$

$$CaI_{total}\ (CAPEX) = CaI_{fixed} + WoI + Startup + Solvent \tag{5.9}$$

Where,

CaI_{fixed}	[M€]	Fixed capital investment
$Compressor$	[M€]	CO_2 compressor investment
DC_{total}	[M€]	Total direct cost
IC_{total}	[M€]	Total indirect cost
$ISBL$	[M€]	Inside the battery limits
$OSBL$	[M€]	Outside the battery limits
$Solvent$	[M€]	Solvent cost
$Startup$	[M€]	Start-up cost
WoI	[M€]	Working investment

Table 5.6 lists general operational expenditure (OPEX) results for all scrubbing systems. Solvent makeup was not considered in the analysis. OPEX calculation was conducted using the procedure implemented in a previously mentioned research project by the University of Stuttgart [39]. The data used for this purpose can be found in [92] and has been summarised in Table 5.6 as follows:

- Maintenance [109]
- Taxes, insurances
  - Local taxes [110]
  - Insurance [110]
- Cooling water, working hours, operating resources
  - Cooling water [92]
  - Activated carbon [61]
  - Operating labor (OL) [111, 112]
  - Supervision and support labor
  - Operating supplies
  - Laboratory charges
- Miscellaneous
  - Plant overhead cost [92]
  - General expenses [110]
    - Administrative cost
    - Distribution and marketing
  - R&D cost

Table 5.4: MEA Case I total capital investment [92]

	Percentage of purchased cost	Used	Cost MEA Case I [M€]
Direct cost			
ISBL (Inside Battery Limits)			48.65
Purchased equipment [113, 110]	100	100	23.94
Purchased equipment installation [110]	25-55	-	10.54
Instrumentation and control [110]	8-50	20	3.99
Piping [110]	20-80	40	7.98
Electrical [110]	15-30	11	2.20
OSBL (Outside Battery Limits)			8.98
Building and building services [110]	10-80	10	2.00
Yard improvements [110]	10-20	10	2.00
Services facilities [110]	30-80	20	3.99
Land [110]	4-8	5	1.00
Total direct cost			57.63
Indirect cost			
Engineering [112]	10	10	5.37
Construction expenses [112]	10	10	5.37
Contractor's fee [112]	0.5	0.5	0.27
Contingency [112]	17	17	9.12
Total indirect cost			20.13
CO_2 compressor investment cost [114]			31.73
Fixed capital investment			109.49
	Percentage of FCI	Used	Cost [M€]
Fixed capital investment	100	100	109.49
Working investment [110]	12-28	25	26.38
Start-up cost and MEA cost [110]	8-10	10	14.66
Total capital investment (CAPEX)			150.53

Table 5.5: Total capital investment for studied cases. Results based on input data by Abu-Zahra [90, 92]

	MEA Case I	MEA Case II	K1-IC						K1-1
Desorber pressure [bar]	1.5	2.1	0.5	1.0	1.5	2.0	2.5	3.0	2.0
	Cost [M€]								
Total direct cost	57.63	68.93	51.66	51.52	51.46	51.43	51.41	51.39	54.76
Total indirect cost	20.13	20.13	20.13	20.13	20.13	20.13	20.13	20.13	20.13
CO_2 Compressor investment	31.73	31.73	31.73	31.73	31.73	31.73	31.73	31.73	31.73
Fixed capital investment	109.49	120.79	103.52	103.38	103.32	103.29	103.27	103.25	106.62
Working investment	26.38	26.38	26.38	26.38	26.38	26.38	26.38	26.38	26.38
Start-up cost and solvent cost	14.66	19.39	28.31	28.31	28.31	28.31	28.31	28.31	28.31
Total capital investment (CAPEX)	150.53	166.57	158.21	158.07	158.01	157.98	157.96	157.94	161.30

Table 5.6: Expected scrubbing systems operation costs. Results based on input data by Abu-Zahra [90, 92]

	MEA case I	MEA case II	K1-IC						K1-1
Desorber pressure [bar]	1.5	2.1	0.5	1.0	1.5	2.0	2.5	3.0	2.0
	Cost [M€]								
Maintenance (4% of CAPEX)	4.38	4.83	4.14	4.14	4.13	4.13	4.13	4.13	4.26
Taxes, insurance(s) (3% of CAPEX)	3.28	3.62	3.11	3.10	3.10	3.10	3.10	3.10	3.20
Cooling water, working hours, operating resources	5.06	5.06	5.06	5.06	5.06	5.06	5.06	5.06	5.06
Miscellaneous	4.40	4.40	4.40	4.40	4.40	4.40	4.40	4.40	4.40
OPEX	17.12	17.92	16.71	16.70	16.69	16.69	16.69	16.69	16.92

According to results in Table 5.6 systems with piperazine promoted potassium carbonate solutions are the ones with the lowest operational expenditures. This is exactly the opposite result to capital expenditures. Even the system with K1-1 (without intercooling or any sort of optimisation) has lower operational expenditures than any of the MEA systems (cases I and II). This is an indicator of the overall better performance of PZ/K_2CO_3 systems, which require a higher investment, but also yield fruit by lowering operation costs.

Table 5.7: Comparison of economics from literature with analysed scrubbing systems results

Economics		Reference PF[26] hard coal without capture [108]		Reference PF hard coal with post-combustion capture [108]	RPP NRW without capture
Performance Data					
Power plant capacity (net)	MW_{el}	736		616	555.6
Engineering, procurement, and construction costs (EPC)	M€	1,141-1,152		1,416-1,601	861
EPC cost, net	€/kW	1,550-1,565		2,300-2,600	1,550
Owner's cost (including contingencies)	% EPC	10		10	10
Total investment cost	M€	1,255-1,267		1,558-1,762	946
Fuel costs	€/GJ (LHV)	Low Middle High	2.0 2.4 2.9	2.0 2.4 2.9	2.0 2.4 2.9
Low fuel cost (€2.0/GJ)					
Levelised CAPEX	€/MWh	19 19.0-19.1		30 28.1-31.8	19.0
Levelised O&M	€/MWh	7.1		13.7 13.1-14.5	7.1
Levelised fuel cost	€/MWh	18.3		22.2 21.6-22.2	18.3
Levelised electricity cost (LCOE)	€/MWh	44.5 44.4-44.6		65.9 62.9-68.5	44.5
CO_2 avoidance cost	€/t CO_2	-		32.1 27.5-36.0	-
Middle fuel cost (€2.4/GJ)					
Levelised CAPEX	€/MWh	19 19.0-19.1		30 28.1-31.8	19.0
Levelised O&M	€/MWh	7.1		13.7 13.1-14.5	7.1
Levelised fuel cost	€/MWh	22.0		26.6 25.9-26.6	22.0
Levelised electricity cost (LCOE)	€/MWh	48.1 48.1-48.3		70.3 67.2-72.9	48.1
CO_2 avoidance cost	€/t CO_2	-		33.3 28.5-37.2	-
High fuel cost (€2.9/GJ)					
Levelised CAPEX	€/MWh	19 19.0-19.1		30 28.1-31.8	19.0
Levelised O&M	€/MWh	7.1		13.7 13.1-14.5	7.1
Levelised fuel cost	€/MWh	26.6		32.2 31.3-32.2	26.6
Levelised electricity cost (LCOE)	€/MWh	52.7 52.7-52.8		75.9 72.6-78.5	52.7
CO_2 avoidance cost	€/t CO_2	-		34.7 29.7-38.6	-

[26] Pulverised fuel

RPP NRW with post combustion capture								
MEA Case I	**MEA Case II**	**K1-IC p_{des} = 0.5 bar**	**K1-IC p_{des} = 1.0 bar**	**K1-IC p_{des} = 1.5 bar**	**K1-IC p_{des} = 2.0 bar**	**K1-IC p_{des} = 2.5 bar**	**K1-IC p_{des} = 3.0 bar**	**K1 p_{des} = 2.0 bar**
430.45	433.91	425.98	435.24	439.95	442.99	440.27	433.82	439.06
1,012	1,028	1,038	1,019	1,019	1,019	1,019	1,019	1,022
2,350	2,369	2,393	2,342	2,317	2,301	2,315	2,349	2,329
10	10	10	10	10	10	10	10	10
1,113	1,131	1,142	1,121	1,121	1,121	1,121	1,121	1,125
2.0 2.4 2.9	2.0 2.4 2.9	2.0 2.4 2.9	2.0 2.4 2.9	2.0 2.4 2.9	2.0 2.4 2.9	2.0 2.4 2.9	2.0 2.4 2.9	2.0 2.4 2.9
29.0	28.7	29.3	28.7	28.4	28.2	28.3	28.8	28.4
14.5	14.6	14.5	14.2	14.0	13.9	14.0	14.2	14.1
23.7	23.5	23.9	23.4	23.2	23.0	23.1	23.5	23.2
67.1	66.8	67.7	66.3	65.5	65.1	65.5	66.5	65.7
34.7	34.2	35.6	33.3	32.1	31.4	32.1	33.6	32.5
29.0	28.7	29.3	28.7	28.4	28.2	28.3	28.8	28.4
14.5	14.6	14.5	14.2	14.0	13.9	14.0	14.2	14.1
28.4	28.2	28.7	28.1	27.8	27.6	27.8	28.2	27.9
71.9	71.5	72.5	70.9	70.2	69.7	70.1	71.2	70.4
36.3	35.8	37.3	34.8	33.6	32.8	33.5	35.2	33.9
29.0	28.7	29.3	28.7	28.4	28.2	28.3	28.8	28.4
14.5	14.6	14.5	14.2	14.0	13.9	14.0	14.2	14.1
34.3	34.1	34.7	33.9	33.6	33.4	33.6	34.1	33.7
77.8	77.4	78.5	76.8	76.0	75.4	75.9	77.0	76.2
38.3	37.7	39.5	36.8	35.5	34.6	35.4	37.2	35.8

Table 5.7 lists RPP NRW's economics before and after post-combustion capture has been implemented. Table 5.7 also compares RPP NRW's results with those of the power plant that was used as a reference in the previously mentioned ZEP study and which will be referred to as ZEP PP. This comparison will help validate results. ZEP study's calculations were conducted for three different fuel costs: low, middle and high. These vary from 2.0 €/GJ to 2.9 €/GJ. At the beginning of this section a fuel cost of 2.4 €/GJ was listed as one of the assumed parameters for economics calculation (see Table 5.2). That price was kept as reference through economic analysis. The use of a low and a high fuel cost in Table 5.7 is solely due to validation purposes. Later diagrams will all assume a fuel price of 2.4 €/GJ unless it is otherwise mentioned.

ZEP PP's reference data in Table 5.7 is listed in ranges and not precise values. This is due to the fact that in the related study two cases were considered: a so-called *BASE* option that represents a power plant employing today's technologies (higher cost range) and a so-called *OPTI* option, which stands for a commercial power plant, assuming foreseen improvements and improved integration (lower cost range).

Engineering, procurement, and construction costs (EPC) are listed in million euros. The difference between ZEP PP and RPP NRW is due to different power plant sizes. This price was calculated based on *EPC cost, net* in Table 5.7, which lists €/kW. RPP NRW has a lower net power plant capacity and thus a lower EPC. The ZEP study indicates a specific EPC cost in a range of 2,300-2,600 €/kW once the power plant has been retrofitted with post combustion capture. Studied cases with RPP NRW show a range of approximate 2,300-2,400 €/kW and hence a good agreement with the previous value.

In the same way that the power plants' different capacities influence EPC they influence the total investment cost. ZEP PP requires a total investment between 1,255-1,267 million euros, whereas RPP NRW needs 946 million euros. After a retrofit with post-combustion capture the total investment cost increases to 1,558-1,762 million euros and 1,110-1,145 million euros for ZEP PP and RPP NRW respectively.

Presented results show in general a good agreement with data from the ZEP study. For example, considering the middle fuel cost of 2.4 €/GJ, LCOE varies for studied cases in the range of 69.7-72.5 €/MWh, whereas ZEP listed data is in the range of 67.2-72.9 €/MWh. For the same fuel cost, CO_2 avoidance costs for studied cases are calculated to be in the range of 32.8-37.3 €/t CO_2. These results match ZEP PP's, which lie in a range of 28.5-37.2 €/t CO_2. The following diagrams

will illustrate the comparison between the different results based on a middle fuel cost of 2.4 €/GJ.

In general, diagrams display different sections: *MEA, K1-IC, K1-1* and occasionally *RPP NRW*. Each section is separated by a red line. The x-axis indicates the used desorber pressure for each case. MEA represents Cases I and II. K1-IC depicts the selected K1 solution with intercooling, whereas K1-1 represents also a K1 solution but without any sort of optimisation.

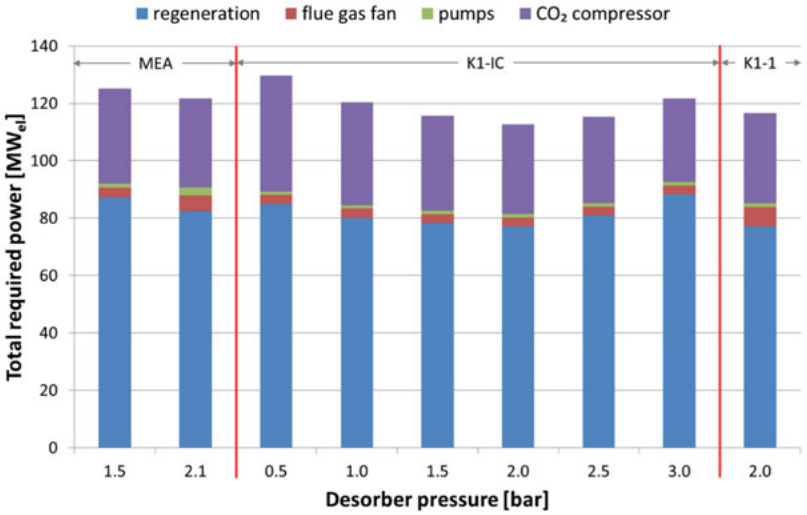

Figure 5.1: Total required power due to post-combustion capture of CO_2

Figure 5.1 shows the total required power that has to be provided by RPP NRW once it has been retrofitted with post-combustion capture. According to Figure 5.1 most of the electric energy is required for regeneration purposes, which was an expected result. K1-IC at p_{des} = 2 bar is the case with the lowest energy requirement for regeneration (77 MW_{el}). The lowest energy demand required with MEA can be reached at a desorber pressure of 2.1 bar (82 MW_{el}). K1-1 has an energy requirement practically identical to K1-IC's, since the difference between K1-1's and K1-IC's required reboiler duty was small. The advantage of K1-IC compared to K1-1 lied more in the reduced column geometry than in reboiler duty reduction (see section 4.3.6).

The second cause for efficiency penalties is the CO_2 compressor. Although this unit operates with a constant CO_2 flow rate, the initial pressure is not the same for each case, whereas the final pressure corresponds to 200 bar in all cases. To guarantee for comparibility between the different cases, a reference pressure of 2 bar at compressor's inlet was assumed. This results in an additional energy input for desorber pressures below the reference and an energy gain for desorber pressures above 2 bar, as shown in Figure 5.1. According to it, the lowest demand is expected with K1-IC at p_{des} = 3 bar (29 MW_{el}) and the highest with K1-IC at p_{des} = 0.5 bar (40 MW_{el}). This is understandable since these two values represent opposite extremes from all represented cases. The case with the highest initial desorber pressure is the one that in the end demands the lowest energy and vice versa. The third cause for efficiency penalties is the flue gas fan. This unit compensates pressure losses that take place mostly in the absorber column. It is in this piece of equipment that good column geometry plays an important role in decreasing efficiency penalties. Calculations showed that the lowest demand is reached with MEA at p_{des} = 1.5 bar, as well as for all K1-IC cases. For MEA and K1-IC the demand accounted for approximate 3 MW_{el}. Since absorber columns operate at atmospheric pressure there is only one absorber column design for all studied K1-IC cases and hence the flue gas fan's electric demand is constant. The fact that electric demand is the same for MEA at p_{des} = 1.5 bar is a coincidence. This was not expected but has to do with the specific pressure losses that reached within this absorber column, which were in fact lower than those with K1-IC. This has to do with the solution's properties and column geometry. It would be possible to reduce these losses by increasing the absorber's diameter. However, since it was decided to keep a constant maximum fractional capacity of 80 %, the column's diameter was kept as Aspen Plus had calculated. The highest demands can be detected in Figure 5.1 for Case II (MEA at p_{des} = 2.1 bar) and K1-1 at p_{des} = 2 bar. These are the cases that have the biggest absorbers, so that they require an electric demand of almost 6 and 7 MW_{el} respectively.

The last cause for efficiency penalties is due to pumps within the scrubbing cycle. Albeit pump's contribution to decreasing RPP NRW's efficiency might seem small, it still accounts for more than 1 MW_{el} in all cases. The lowest demand is reached with K1-IC cases (1.19 MW_{el}). This is due to intercooling's effect on column geometry. Given that Case I (MEA at p_{des} = 1.5 bar) requires an absorber that is almost 5 m higher than K1-IC's this results in an increased energy demand of 1.58 MW_{el}, which is also the equivalent of K1-1's energy demand for pump operation (1,6 MW_{el}). The reason why these two demands are so similar might seem surprising, considering the calculated heights of both columns: 31.2 m and 53.5 m, for Case I and K1-1 respectively. There are yet two factors that contribute to relativize this

fact. For one, Case I's flow rate is about 0.5 m^3/s higher than K1-1's. Moreover, K1-1's desorber pressure is 0.5 bar higher than Case I's, which represents an advantage for K1-1. This is due to the reduced energy that has to be implemented in increasing the solution's pressure for transport purposes. The result is hence a fairly similar energy demand for the pumps of two different columns.

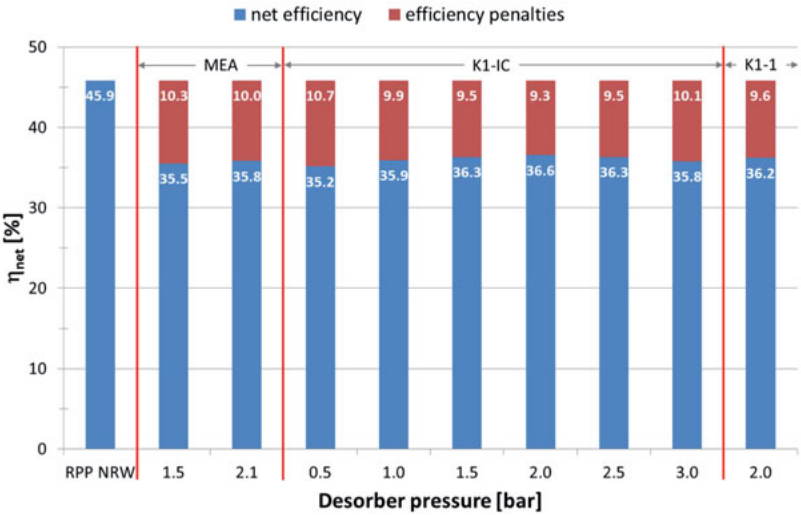

Figure 5.2: Overall efficiency penalties due to post-combustion capture of CO_2

Figure 5.2 shows RPP NRW's final net efficiency after having considered all efficiency penalties. Again, this diagram has four different sections that correspond to RPP NRW, MEA (Cases I and II), K1-IC at different desorber pressures and K1-1 at p_{des} = 2.0 bar. Blue and red bars indicate RPP NRW's net efficiency and efficiency penalties respectively. The lowest efficiency penalties account for 9.3 efficiency points and are reached with K1-IC at p_{des} = 2.0 bar. There is a big difference in results for K1-IC cases depending on the used desorber pressure. The lowest power plant efficiency corresponds to a desorber pressure of 0.5 bar.

MEA cases loose at least 10 efficiency points. RPP NRW's efficiency amounts to 35.5 % for Case I and 35.8 % for Case II. This last case is the one that was calculated by considering Abu-Zahra's optimised parameters. There is indeed a slight efficiency boost by using these parameters; however, the resulting increased solution's flow rate limits a higher impact. Even K1-1 is able to achieve a higher overall plant efficiency (36.2 %).

Figure 5.3 depicts calculated levelised cost of electricity for all RPP NRW and compares them with studied cases. LCOE consist of the sum of levelised fuel, O&M and CAPEX represented in blue, red and green bars respectively. Levelised fuel costs increase in a range between 5.6 €/MWh and 6.4 €/MWh. The lowest value is reached with K1-IC at p_{des} = 2.0 bar, while the highest increase corresponds to Case I (MEA at p_{des} = 1.5 bar). In general, cases with piperazine promoted potassium carbonate show lower fuel costs than MEA. The lowest fuel cost with MEA can be reached with Case II at p_{des} = 2.1 bar.

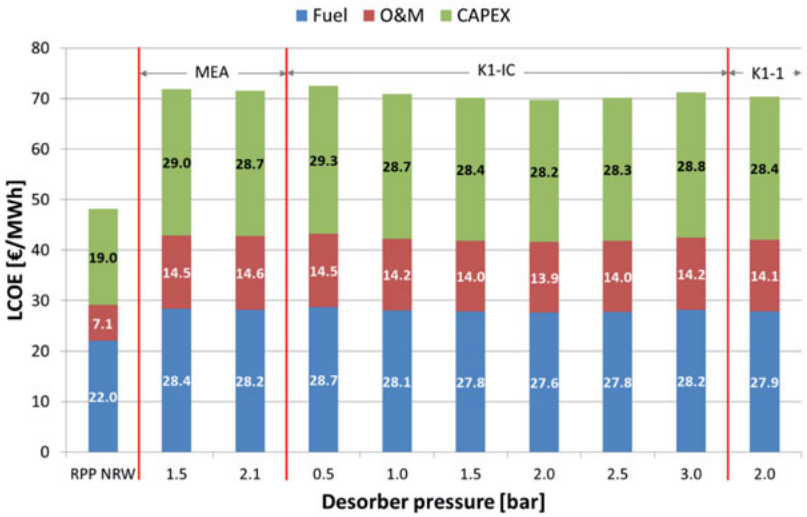

Figure 5.3: Calculated LCOE

Levelised O&M costs practically duplicate once RPP NRW is retrofitted with a CO_2 scrubbing system. The costs increase from originally 7.1 €/MWh to at least 13.9 €/MWh (K1-IC at p_{des} = 2.0 bar). The highest rise corresponds to Case II (MEA at p_{des} = 2.1 bar). This case represents an optimised version in Abu-Zahra's study [90]. That was the reason why this case was considered as a good reference for comparison. Even though this case is related to a low reboiler duty, results indicate that operating conditions might not actually be as favourable as first thought. The same applies to K1-IC cases at desorber pressures higher than 2.0 bar, which are also related to low reboiler duties, even lower than at p_{des} = 2.0 bar. K1-1 on the other hand has a levelised O&M cost of 14.1 €/MWh. The reasons for the relative high costs have all a different nature depending on the selected case. Case II for example has a relative low reboiler duty, but this case operates with a high so-

lution flow rate that circulates within the scrubbing cycle. K1-IC cases on the other hand have both low solution flow rates, but operate at higher desorber pressures, which require the use of a throttle when tapping steam out of the power plant. The consequences of the previous facts have already been extensively discussed in sections 4.3 and 4.5.

Levelised CAPEX are the last costs represented in Figure 5.3. RPP NRW requires 19.0 €/MWh without CO_2 capture. These costs increase to a range between 28.2 €/MWh and 29.0 €/MWh. The lowest and highest levelised CAPEX correspond to K1-IC at p_{des} = 2.0 bar and Case I (MEA at p_{des} = 1.5 bar) respectively. Although equipment cost estimation showed that some of the studied cases required a higher investment than others, results in Figure 5.3 consider the power plant's electric energy output. Thus some cases that might have seem low-priced in the beginning –like Case I– actually belong to the expensive ones in Figure 5.3. Given that K1-IC at p_{des} = 0.5 bar does not only involve high investment costs, but also is the case with the lowest power plant efficiency, this is the option with the highest calculated levelised CAPEX of 29.3 €/MWh.

As previously mentioned LCOE consists of the sum of levelised fuel, O&M and CAPEX. RPP NRW's LCOE without CO_2 capture amounts to 48.1 €/MWh. By retrofitting the power plant with a CO_2 scrubbing system LCOE rises to at least 69.7 €/MWh. This result corresponds to K1-IC at p_{des} = 2.0 bar. The highest LCOE for K1-IC systems amounts to 72.5 €/MWh at p_{des}= 0.5 bar. LCOE estimation for MEA cases add up to 71.9 €/MWh and 71.5 €/MWh at a desorber pressure of 1.5 bar and 2.1 bar respectively. Abu-Zahra's optimised case adapted for RPP NRW reaches indeed a lower LCOE, which corroborates Abu-Zahra's results. K1-1's LCOE mounts up to 70.4 €/MWh. This is an even lower LCOE than Abu-Zahra's Case II (MEA at p_{des} = 2.1 bar) and slightly higher than the best result of all the studied cases. Despite K1-1's enormous absorber column, the performance of this system is so good, that its LCOE is the third lowest from all studied cases. The implementation of such a system is though still questionable, above all considering K1-IC's performance at the same desorber pressure.

At the beginning of chapter 5 the term *CO_2 avoidance cost* was introduced. This term basically describes how much a EUA at least has to cost to make a scrubbing system technology feasibly available. Estimated CO_2 avoidance costs for all studied scrubbing systems are depicted in Figure 5.4. Assuming that RPP NRW would not be equipped with a CO_2 capture system, its CO_2 avoidance cost would be the equivalent of a EUA. The lowest calculated CO_2 avoidance cost mounts up to 32.8 €/t CO_2 and is indicated with a red horizontal line in Figure 5.4. This represents the

fair value and corresponds to K1-IC at p_{des} = 2.0 bar. This means that retrofitting RPP NRW with a CO_2 scrubbing system becomes a feasible option starting at a EUA value of 32.8 €/t CO_2.

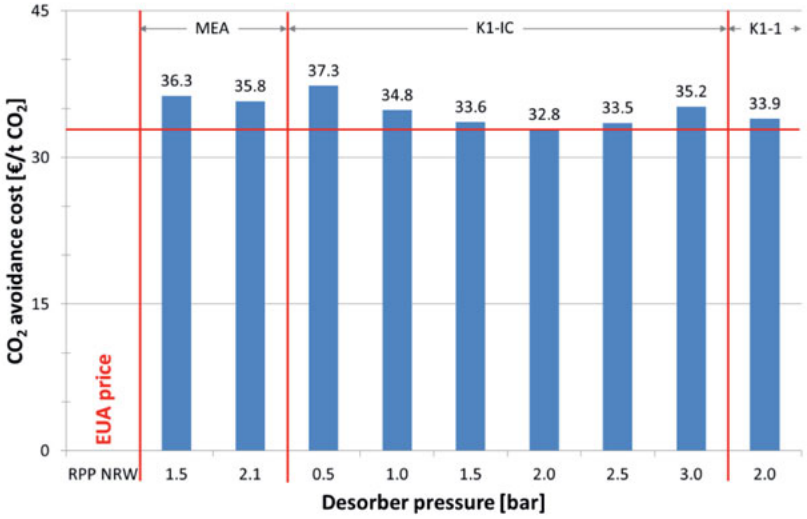

Figure 5.4: CO_2 avoidance cost

The advantage of a CO_2 scrubbing system can be seen once the fair value has been exceeded. Figure 5.5 shows an example for a EUA price of 40 €/t CO_2. In addition to levelised fuel, O&M and CAPEX, the price for the needed EUAs has to be considered to account for the correct LCOE. In general, all scrubbing systems have a cost due to EUA of approximately 4.0 €/MWh, whereas RPP NRW without CO_2 capture has a levelised EUA cost of 30.0 €/MWh. RPP NRW and K1-IC at p_{des} = 2 bar have LCOE of 78.1 €/MWh and 73.5 €/MWh. LCOE suffers an increase that varies between 25.4 €/MWh and 28.3 €/MWh.

Assuming the EUA price would increase to up to 80 €/t CO_2 scrubbing systems effect on the LCOE becomes even clearer, as presented in Figure 5.6. The levelised EUA price for scrubbing systems varies in a range of 7.5 €/MWh to 7.8 €/MWh. The levelised EUA price for RPP NRW on the other hand amounts to 60 €/MWh. The levelised cost of electricity for RPP NRW without CO_2 capture comes to 108.1 €/MWh. By retrofitting the power plant with a scrubbing system LCOE amounts to a range between 77.2 €/MWh and 80.3 €/MWh.

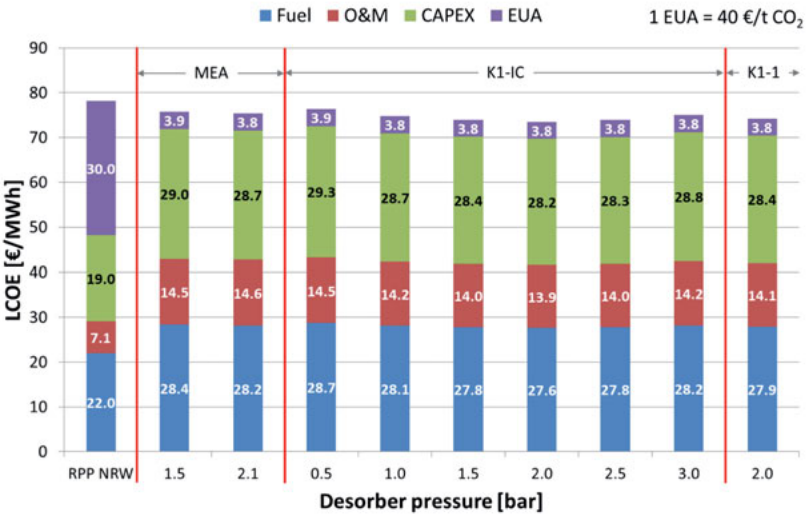

Figure 5.5: LCOE at EUA = 40 €/t CO_2

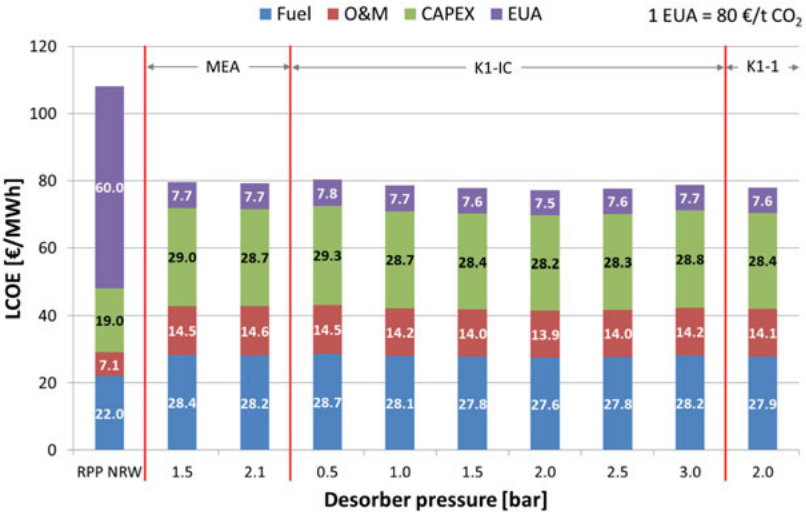

Figure 5.6: LCOE at EUA = 80 €/t CO_2

Equipping RPP NRW with a CO_2 scrubbing system certainly increases LCOE drastically. An investment in this sort of technology can hence only be justified if the CO_2 avoidance cost is lower than the value of a EUA, which has been determined to be at least 32.8 €/MWh for K1-IC at a desorber pressure of 2.0 bar.

6 Summary

Anthropogenic emissions of CO_2 have contributed to intensify the greenhouse effect and thus influence the weather in a global scale provoking climate change. One of the main sources of anthropogenic CO_2 is related to energy generation with fossil fuels.

This work focuses on reducing CO_2 emissions from advanced coal-fired power plants and the main objective is to keep related efficiency losses as low as possible. For this purpose the *Reference Power Plant North Rhine Westphalia* (RPP NRW) serves as a basis. This power plant is retrofitted with a post combustion capture plant based on chemical absorption of CO_2. The simulation tool Aspen Plus is used to model scrubbing systems for the capture of 90 % CO_2 from the power plant's flue gases. In order to fulfil this objective, there were several steps to follow. Below is a description of each one of them and their corresponding results.

I. Identifying suitable parameters for minimizing scrubbing systems energy demand.

This is achieved by comparing single components performance at different operating conditions and analysing their effect on the overall scrubbing system. To this end, the system boundary includes preconditioning, CO_2 scrubbing process and compression. Due to solvent's affinity of chemically reacting with CO_2, which causes solvent degradation, it is imperative to count with flue gas preconditioning. This takes place after flue gases have been treated in conventional gas purification plants such as DENOX or FGD. Preconditioning is analysed at different operation conditions which include liquid to gas ratios, different pH values and three different packing types. Results suggest the use of a liquid to gas ratio of at least 3.0 l/m^3 flue gas, a scrubber solution's pH of 6.5 and a structured packing are selected as design parameters, since they guarantee for low pressure losses, moderate packing height and limited solution's make up.

II. Analyse piperazine promoted potassium carbonate solutions to see if they are suitable for implementation in a CO_2 capture process.

Scrubbing systems modelling is conducted with three piperazine promoted potassium carbonate solutions: *K1, K2, and K3*. These differ from each other in their concentration of either piperazine or potassium carbonate in the respective solution. In addition, different lean loadings are considered for each solution. Results indicate that solutions with a high concentration of piperazine and a low concentra-

tion of potassium carbonate –such as K1– show an overall better performance than the other two cases with K2 and K3. Not only are the required solvent flow rates lower, but a series of positive effects is triggered by using K1 as a solvent. For example, lower solvent flow rates do not only allow for smaller equipment, but K1 related flow rates also require an overall lower reboiler duty than K2 or K3 solutions. Further evaluation is therefore conducted with the lowest studied lean loadings for K1, K2, and K3. In order to relate each solvent with its lowest lean solution, the following nomenclature is introduced: K1-1, K2-1, and K3-1. Solvent analysis is directly related to absorber performance. In this case, results indicate a significant difference in temperature profiles depending on the used solvent solution. The higher the piperazine concentration the bigger the temperature difference reached within the absorber. This is explained with piperazine's heat of absorption, which is higher than that of potassium carbonate, but also due to the enhanced capacity of absorption that comes along with low lean loadings and their resulting low flow rates.

III. Evaluating operating conditions variation related to the scrubbing cycle.

This includes temperature difference of the lean-rich heat exchanger and desorber pressure (p_{des}). The analysis focuses on the effects on absorber performance, reboiler and cooling duties, as well as on the equipment's geometry. Lean-rich heat exchanger analysis reveals a definite reboiler duty reduction by decreasing the temperature difference between hot inlet and cold outlet to 5 K. However, the required heat exchanger area experiences a substantial increase. This is also one of the cases where the effect of solvent flow rate on equipment geometry can be observed: the higher the solvent flow rate the more area is required for heat transfer. Regarding desorber pressure analysis, K1-1, K2-1, and K3-1 all show a different behaviour. This is attributed to the different compositions of each solution. A high piperazine concentration causes the reboiler duty to decrease with increasing desorber pressure, whereas the opposite effect is observed for solutions with a low content on piperazine. The solution with an equimolar piperazine-potassium carbonate concentration (K2-1) represents a special case, which seems to be influenced by piperazine at pressures below 1.5 bar and by potassium carbonate at higher pressures. Desorber pressure analysis also affects other scrubbing cycle parameters such as cooling duty, which is estimated for K1-1, K2-1 and K3-1 keeping in mind that there are different locations within the scrubbing cycle that have to be accounted for. These are preconditioning (flue gas cooler), CO_2 cooler, lean cooler, absorber top, and desorber top. In general, results are analogue to those of the reboiler duty.

IV. Conduct a deeper absorber analysis.

This can be done after having detected a suitable solvent, lean loading, adequate temperature difference of the lean-rich heat exchanger and knowing the effects of the desorber pressure on cooling and reboiler duties. High absorber temperature profiles suggest a fast absorption of CO_2. However, results reveal a weakening of CO_2 absorption at high temperatures. To counteract this effect absorber intercooling is implemented. Since K1-1 reaches overall better results than K2-1 and K3-1, only K1-1 is further considered. The resulting process operates with K1-1 and absorber intercooling and is thus referred to as “K1-IC”. Absorber intercooling proves to be a useful measure to enhance absorption. Thanks to it, it is possible to reduce column and packing height, solvent flow rate and even the reboiler duty required for solvent regeneration. Absorber intercooling is though not always appropriate. The performance of solvents such as K2-1 or K3-1 that do not reach temperatures as high as K1-1 might decline instead of improving. Solvents with high lean loadings might benefit from heating rather than cooling, as suggested in [38].

V. Integration of CO_2 scrubbing system into RPP NRW.

To be able to achieve the main objective of keeping power plant’s efficiency losses as low as possible it is necessary to integrate the scrubbing system into the power plant. Given that required steam parameters are directly affected by the used desorber pressure, an optimum pressure is not selected at this point. As it turns out, desorber pressure has a significant effect on the power plant’s efficiency. In order to maintain the required steam parameters it is sometimes necessary to build in a throttle, which causes irreversibilities that end up decreasing the power plant’s efficiency. This occurs at desorber pressures higher than 2.0 bar. At this last pressure it might be necessary to build in a throttle, but only if the reboiler temperature difference (ΔT_{reb}) is 10 K. For a ΔT_{reb} of 5 K it is possible to avoid a throttle, which allows for higher power plant efficiency. Given that a first optimised scrubbing system with a piperazine promoted potassium carbonate solution (K1-IC) is available, it can be compared with a reference from the literature: 30 % MEA solution at a desorber pressure of 2.1 bar based on results presented by Abu-Zahra in [90]. This represents an optimised case from the previous author and is hence a proper example for comparison with K1-IC. The integration of the scrubbing system with MEA into the power plant is analogue to K1-IC at p_{des} = 2.0 bar, the only difference is that the system with MEA requires a slightly higher reboiler duty. The most important realisation regarding to thermal requirement consists in the fact that an apparent low reboiler duty is not necessarily related to low power plant efficiency.

Steam tapping is the main efficiency penalties cause, but not the only one. Further integration analysis considers auxiliary power. There are other components required in a scrubbing process that have not yet been accounted for, but that are also responsible for reducing a power plant's electric energy output. The most important are multistage compressor, flue gas fan (from preconditioning), and pumps.

In order to fulfill the main objective of keeping efficiency losses as low as possible it is necessary to compare all studied cases. For this purpose another MEA case is introduced, which has also been reported by Abu-Zahra in [90, 92], and which he referred to as *baseline case* also with a 30 % MEA solution but a desorber pressure of 1.5 bar. In general, results show good agreement with data from the literature. RPP NRW's efficiency decreases from 45.9 % (LHV) to a range between 35.2 % and 36.6 %. The best results correspond to K1-IC at a desorber pressure of 2.0 bar. Abu-Zahra's optimised MEA case at p_{des} of 2.1 bar reaches a maximum efficiency of 35.8 %. Conducted calculations prove to reduce the required energy demand, thereby contributing to keeping efficiency losses as low as possible, which satisfies the main objective.

VI. A*nalysis of economic feasibility.*

After calculating overall efficiency penalties it is possible to conduct an economic analysis, which is the last step of this work. This helps estimating scrubbing systems feasibility. Results show that the levelised cost of electricity (for a middle fuel cost of 2.4 €/GJ) increases significantly from 48.1 €/MWh to at least 69.7 €/MWh after RPP NRW is retrofitted with a CO_2 scrubbing system. The lowest CO_2 avoidance cost adds up to at least 32.8 €/t CO_2. This is the price that EUAs have to have in order to make CO_2 capture technologies a feasible option. Once that price is exceeded a CO_2 scrubbing system makes it possible to have lower LCOEs than without it.

In *conclusion*, the most promising case for capturing CO_2 from flue gases and keeping RPP NRW's as low as possible are reached with the solvent solution K1-IC a lean-rich heat exchanger temperature difference of 5 K, a desorber pressure of 2.0 bar. In addition, integration with RPP NRW requires a reboiler temperature difference of 5 K. Feasibility of implementation depends on the EUA price and the aforementioned lowest value.

Future work

Studied scrubbing systems with piperazine promoted potassium carbonate solutions do not experience any sort of optimisation rather than identifying suitable operation parameters and absorber intercooling. It might be possible to reduce the estimated efficiency penalties for example by improving heat integration within the scrubbing cycle. Other authors have reported about the advantages of using lean and semi-lean solutions, which tend to reduce reboiler duty.

MEA cases for comparison purposes do not count with absorber intercooling. The case with the lower lean loading at p_{des} = 1.5 bar might benefit from it, whereas the case with the higher lean loading at p_{des} = 2.1 bar might show a better performance by applying heat to the absorber. This might improve reaction kinetics and hence a lower solvent flow rate might be needed. It is suspected that a desorber pressure of 2.1 bar might be slightly high. A study with a low and a high lean loading at a desorber pressure of 2.0 bar would be preferable, in order to stay below the range of thermal solvent degradation.

Economic analysis does not include solvent degradation. This is an important part that can be accounted for in the future. Potassium carbonate solutions are said to have a lower degradation rate than MEA. The same applies to piperazine; however the related degradation rate of K1-1 is missing.

Regarding EUAs it was previously said, that CO_2 scrubbing systems would only be able to compete with a power plant without CO_2 capture once the value of EUAs is higher than the CO_2 avoidance cost. So far the price is far below 32.8 €/t CO_2. It seems that without political intervention this price might never be reached and hence there is a lack of interest in CO_2 capture technologies in the energy sector. Some events though have proved in the past that it is possible to change a nation's technological direction overnight. The best example is Germany after the nuclear disaster in Fukushima in 2011, which caused the nation to rethink its technological development and which gave way to the so called *Energiewende* (German for *energy transition*). Climate change is real and so are feasible CO_2 capture technologies.

A Appendixes

A.1 Detailed compilation of flue gas conditioning simulation results

The following table displays simulation results for studied SO_2 scrubber cases for different packings. Although results vary depending on the studied case, variations are small so that a good part of them overlap, as was shown in section 4.2 (Figure 4.6).

Table A.1.1: Simulation results for studied SO_2 scrubber cases

Packing type	pH	L/G [$l/m^3_{flue\ gas}$]	Diameter [m]	Δp [mbar/m]	Packing height [m]	Concentration [mg SO_2 / $m^3_{flue\ gas}$]	Δp [mbar]
IMTP 40	6.0	1.5	13.80	7.33	2.80	9.65	20.53
		2.0	14.29	6.59	2.00	9.77	13.18
		3.0	15.07	5.54	1.80	8.76	9.97
		4.0	15.69	4.87	1.70	8.41	8.27
IMTP 50	6.0	1.5	13.28	5.78	3.50	9.50	20.24
		2.0	13.68	5.30	2.50	9.26	13.25
		3.0	14.33	4.64	2.20	9.33	10.22
		4.0	14.83	4.24	2.10	8.86	8.90
Mellapak 250X	6.0	1.5	12.78	2.87	2.30	9.87	6.60
		2.0	13.29	2.75	1.70	9.98	4.67
		3.0	13.80	2.62	1.60	9.99	4.19
		4.0	14.23	2.59	1.60	9.17	4.15
IMTP 40	6.3	1.5	13.80	7.33	2.10	9.00	15.39
		2.0	14.29	6.59	1.90	9.50	12.51
		3.0	15.07	5.54	1.70	9.87	9.41
		4.0	15.69	4.86	1.60	9.75	7.78
IMTP 50	6.3	1.5	13.28	5.78	2.50	9.93	14.45
		2.0	13.69	5.30	2.40	9.02	12.72
		3.0	14.33	4.64	2.20	8.93	10.21
		4.0	14.84	4.24	2.00	9.93	8.47
Mellapak 250X	6.3	1.5	12.78	2.87	1.70	9.70	4.88
		2.0	13.30	2.75	1.70	8.83	4.68
		3.0	13.80	2.62	1.60	9.59	4.19
		4.0	14.23	2.59	1.60	8.90	4.15

Packing type	pH	L/G [l/m³ flue gas]	Diameter [m]	Δp [mbar/m]	Packing height [m]	Concentration [mg SO_2 / m^3 flue gas]	Δp [mbar]
IMTP 40	6.5	1.5	13.80	7.31	2.00	9.89	14.63
		2.0	14.29	6.58	1.90	9.29	12.51
		3.0	15.08	5.53	1.70	9.74	9.41
		4.0	15.70	4.86	1.60	9.65	7.78
IMTP 50	6.5	1.5	13.28	5.78	2.50	9.55	14.45
		2.0	13.69	5.30	2.30	10.00	12.18
		3.0	14.34	4.64	2.20	8.81	10.21
		4.0	14.84	4.24	2.00	9.84	8.47
Mellapak 250X	6.5	1.5	12.79	2.87	1.70	9.35	4.87
		2.0	13.30	2.75	1.70	8.64	4.68
		3.0	13.80	2.62	1.60	9.64	4.19
		4.0	14.23	2.59	1.60	8.82	4.15
IMTP 40	6.8	1.5	13.80	7.32	2.00	9.65	14.64
		2.0	14.29	6.58	1.90	9.13	12.50
		3.0	15.08	5.53	1.70	9.63	9.40
		4.0	15.70	4.86	1.60	9.57	7.77
IMTP 50	6.8	1.5	13.28	5.78	2.50	9.33	14.44
		2.0	13.69	5.29	2.30	9.85	12.17
		3.0	14.34	4.64	2.20	8.71	10.20
		4.0	14.84	4.23	2.00	9.77	8.47
Mellapak 250X	6.8	1.5	12.79	2.86	1.70	9.14	4.87
		2.0	13.30	2.76	1.70	8.50	4.69
		3.0	13.81	2.62	1.60	9.37	4.19
		4.0	14.23	2.59	1.60	8.75	4.14
IMTP 40	7.0	1.5	13.81	7.32	2.00	9.56	14.63
		2.0	14.30	6.58	1.90	9.07	12.49
		3.0	15.08	5.53	1.70	9.59	9.39
		4.0	15.70	4.85	1.60	9.54	7.77
IMTP 50	7.0	1.5	13.28	5.77	2.50	9.26	14.43
		2.0	13.69	5.29	2.30	9.79	12.17
		3.0	14.34	4.63	2.10	9.96	9.73
		4.0	14.85	4.23	2.00	9.74	8.46
Mellapak 250X	7.0	1.5	12.79	2.86	1.70	9.07	4.86
		2.0	13.30	2.76	1.70	8.45	4.69
		3.0	13.81	2.62	1.60	9.34	4.19
		4.0	14.24	2.59	1.60	8.72	4.14

Packing type	pH	L/G [l/m^3 flue gas]	Diameter [m]	Δp [mbar/m]	Packing height [m]	Concentration [mg SO_2 / m^3 flue gas]	Δp [mbar]
IMTP 40	7.2	1.5	13.81	7.31	2.00	9.51	14.63
		2.0	14.30	6.57	1.90	9.03	12.49
		3.0	15.08	5.52	1.70	9.56	9.39
		4.0	15.70	4.85	1.60	9.52	7.76
IMTP 50	7.2	1.5	13.28	5.77	2.50	9.21	14.43
		2.0	13.69	5.29	2.30	9.75	12.17
		3.0	14.34	4.63	2.10	9.94	9.73
		4.0	14.85	4.23	2.00	9.71	8.46
Mellapak 250X	7.2	1.5	12.80	2.86	1.70	9.02	4.86
		2.0	13.30	2.76	1.70	8.42	4.69
		3.0	13.81	2.62	1.60	9.32	4.19
		4.0	14.24	2.59	1.60	8.70	4.14

List of references

[1] E. Rubin, L. Meyer and H. de Coninck, “Carbon Dioxide Capture and Storage - IPCC Special Report,” Cambridge University Press, New York, USA, 2005.

[2] IPCC, “Second Assesment Report (TAR), Climate Change,” 1996.

[3] D. Lübbert, “CO_2 -Bilanzen verschiedener Energieträger im Vergleich,” Wissenschaftliche Dienste des Deutschen Bundestages, 2007.

[4] AGEB, “Arbeitsgemeinschaft Energiebilanzen,” 2015. [Online]. Available: http://www.ag-energiebilanzen.de/. [Accessed 03 11 2015].

[5] IEA, “World Energy Outlook 2012,” France, 2012.

[6] IEA GHG, “Improvement in Power Generation with Post Combustion Capture of CO_2,” 2004.

[7] L. Kucka, “Modellierung und Simulation der reaktiven Absorption von Sauergasen mit Alkanolaminlösungen,” Shaker Verlag, Dortmund, Germany, 2003.

[8] IEA GHG, “CO_2 capture ready plants,” 2007.

[9] G. Versteeg, “CO_2 Post Combustion Capture Solvent Development "The Quest for the Holy Grail" Panacee or Fata Morgana,” Neuss, Germany, 2009.

[10] K. Görner, CO_2: Abtrennung, Speicherung, Nutzung, M. Fischedick, K. Görner and M. Thomeczek, Eds., Springer Verlag, 2015.

[11] VGB PowerTech Service GmbH, “Konzeptstudie Referenzkraftwerk Nordrhein-Westfalen (RKW NRW),” VGB PowerTech e.V., Essen, Germany, 2004.

[12] “energiespektrum: Effiziente Kohleverstromung,” [Online]. Available: http://www.energiespektrum.de/index.cfm?pid=1442&pk=73486.

[Accessed 07 11 2015].

[13] P. Reddy, Clean Coal Technologies for Power Generation, 1st. ed. ed., CRC Press, 2013.

[14] Ö. Korkmaz, G. Oeljeklaus and K. Görner, “Analysis of retrofitting coal-fired power plants with carbon dioxide capture,” *Energy Procedia,* no. 1, pp. 1289-1295, 2009.

[15] E. Rubin, A. Rao and M. Berkenpas, “A Multi-Pollutant Framework for Evaluating CO_2 Control Options for Fossil Fuel Power Plants,” Proceedings from the First National Conference on Carbon Sequestration, Washington, DC, USA, 2001.

[16] H. Herzog and D. Golomb, “Carbon Capture and Storage from Fossil Fuel Use,” Encyclopedia of Energy, 2004.

[17] D. Helm and C. Hepburn, Eds., The Economics and Politics of Climate Change, USA: Oxford University Press, 2009.

[18] M. Gupta, I. Coyle and K. Thambimuthu, “CO_2 Capture Technologies and Opportunities in Canada: "Strawman Document for CO_2 capture and Storage (CC&S) Technology Roadmap",” 1st Canadian CC&S Technology Roadmap Workshop, Canada, 2003.

[19] S. Schroeter, “Stefan Schroeter, Energiejournalist - Berichte über die Energiewirtschaft in Ostdeutschland, Mittel- und Osteuropa,” 28 04 2014. [Online]. Available: http://stefanschroeter.com/824-vattenfall-schliesst-seine-oxyfuel-pilotanlage.html#.Vj8ryb9CiSY. [Accessed 08 11 2015].

[20] J. Adánez, A. Abad, F. García-Labiano, P. Gayán and L. de Diego, “Review - Progress in Chemical-Looping Combustion and Reforming technologies,” *Progress in Energy and Combustion Science,* vol. 38, 2012.

[21] D. Green and R. Perry, Perry's Chemical Engineers' Handbook, 8th Edition ed., USA: McGraw-Hill, 2007.

[22] M. Tuinier, M. van Sint Annaland, G. Kramer and J. Kuipers, “Cryogenic CO_2 capture using dynamically operated packed beds,” *Chemical Engineering Science,* vol. 65, 2010.

[23] T. Melin, A. Brügger, L. Eilers, S. Geißler, R. Gruber, B. Klinkhammer, M. Medved, S. Sommer and K. Voßenkaul, *Membranverfahren I : Skript zur Vorlesung,* Germany: RWTH Aachen, 1999/2000.

[24] K. Simons, Membrane Technologies for CO_2 Capture, University of Twente, the Netherlands, 2010.

[25] T. Norby and R. Haugsrud, Nonporous Inorganic Membranes, 1st. ed., A. Sammells and M. Mundschau, Eds., Weinheim, Germany: KGaA, Wiley-VCH Verlag GmbH & Co., 2006.

[26] L. Robeson, “Correlation of separation factor versus permeability for polymeric membranes,” *Journal of Membrane Science,* vol. 62, no. 2, pp. 165-185, 1991.

[27] S. Stern, “Polymers for gas separations: the next decade,” *Journal of Membrane Science,* vol. 94, no. 1, pp. 1-65, 1994.

[28] B. Freeman, “Basis of Permeability/Selectivity Tradeoff Relations in Polymeric Gas,” *Macromolecules,* vol. 32, pp. 375-380, 1999.

[29] E. Chen, Carbon Dioxide Absorption into Piperazine Promoted Potassium Carbonate using Strucktured Packing, University of Texas at Austin, 2007.

[30] “Climate Change Connection,” Manitoba Eco-Network, 19 09 2014. [Online]. Available: climatechangeconnection.org/emissions/CO2_equivalents.htm. [Accessed 13 11 2015].

[31] H. Dieter, C. Hawthorne, M. Zieba and G. Scheffknecht, “Progress in Calcium Looping Post Combustion CO_2 Capture: Successful Pilot Scale Demonstration,” *Energy Procedia,* vol. 37, pp. 48-56, 2013.

[32] C. Hawthorne, M. Trossmann, P. Galindo Cifre, A. Schuster and G. Scheffknecht, “Simulation of the carbonate looping power cycle,” *Energy Procedia,* vol. 1, pp. 1387-1394, 2009.

[33] K. Sattler, Thermische Trennverfahren: Grundlagen, Auslegung, Apparate., 3. überarbeitete Aufl. ed., Weinheim: WILEY-VCH Verlag GmbH, 2001.

[34] J. Canadell, C. Le Quéré, M. Raupach, C. Field, E. Buitenhuis, P. Ciais, T. Conway, N. Gillett, R. Houghton and G. Marland, “Contributions to accelerating atmospheric CO_2 growth from economic activity, carbon intensity, and efficiency of natural sinks,” *PNAS,* vol. 104, no. 47, pp. 18866-18870, 2007.

[35] K. Trumper, M. Bertzky, B. Dickson, G. van der Heijden, M. Jenkins and P. Manning, “Jenkins, M., Manning, P. June 2009. The Natural Fix? The role of ecosystems in climate mitigation. A UNEP rapid response assessment,” Printed by Birkeland Trykkeri AS, Norway, Cambridge, UK, 2009.

[36] IEA - Clean Coal Centre, “Post-Combustion Carbon Capture from Coal Fired Plants - Solvent Scrubbing,” IEA Clean Coal Centre and IEA Greenhouse Gas R&D Programme, London, UK, 2007.

[37] E. Kenig, L. Kucka and A. Górak, “Rigorous Modeling of Reactive Absorption Processes,” *Chem. Eng. Technol.,* vol. 26, no. 6, pp. 631-646, 2003.

[38] P. Behr, A. Maun, E. Heischkamp, A. Tunnat, R. Goldschmidt, E. Erich, G. Oeljeklaus and K. Görner, “Chemische Absorptions-Verfahren zur CO_2-Abtrennung aus Rauchgasen - Teilprojekt B,” Essen, 2012.

[39] IFK - Universität Stuttgart, “Verfahrenstechnische Untersuchung und Weiterentwicklung von Aminwaschverfahren zur CO_2-Abtrennung aus Kraftwerksrauchgasen - Teilprojekt A,” Stuttgart, 2011.

[40] P. Feron, “The potential for improvement of the energy performance of pulverized coal fired power stations with post-combustion capture of carbon dioxide,” *Energy Procedia,* vol. 1, pp. 1067-1074, 2009.

[41] K. Maneeintr, R. Idem, P. Tontiwachwuthikul and A. Wee, “Synthesis, Solubilities, and Cyclic Capacities of Amino Alcohols for CO_2 Capture from Flue Gas Streams,” *Energy Procedia,* no. 1, pp. 1327-1334, 2009.

[42] E. da Silva and H. Svendsen, “Study of the Carbamate Stability of Amines Using ab Initio Methods and Free-Energy Perturbations,” *Ind. Eng. Chem. Res.,* vol. 45, no. 8, pp. 2497-2504, 2006.

[43] E. da Silva and H. Svendsen, “Computational chemistry study of reactions, equilibrium and kinetics of chemical CO_2 absorption,” *International Journal*

of Greenhouse Gas Control, vol. 1, no. 2, pp. 151-157, 2007.

[44] J. Brouwer, P. Feron and N. ten Asbroek, “Amino-acid salts for CO_2 capture from flue gases,” 2005.

[45] P. Singh, J. Niederer and G. Versteeg, “Structure and activity relationships for amine-based CO_2 absorbents-II,” *Chemical Engineering Research and Design,* no. 87, pp. 135-144, 2009.

[46] A. Rayer, K. Sumon, A. Henni and P. Tontiwachwuthikul, “Kinetics of the Reaction of Carbon Dioxide (CO_2) with Cyclic Amines Using the Stopped-Flow Technique,” *Energy Procedia,* no. 4, pp. 140-147, 2011.

[47] A. Maun, Optimierung von Verfahren zur Kohlenstoffdioxid-Absorption aus Kraftwerksrauchgasen mithilfe alkalischer Carbonatlösungen, University of Duisburg-Essen, Germany, 2013.

[48] H. Thee, Y. Suryaputradinata, K. Mumford, K. Smith, G. da Silva, E. Kentish and G. Stevens, “A kinetic and process modeling study of CO_2 capture with MEA-promoted potassium carbonate solutions,” *Chemical Engineering Journal,* no. 210, pp. 271-279, 2012.

[49] J. Cullinane and G. Rochelle, “Kinetics of Carbon Dioxide Absorption into Aqueous Potassium Carbonate and Piperazine,” *Industrial & Engineering Chemistry Research,* vol. 45, no. 8, p. 2531–2545, 2006.

[50] S. Bishnoi and G. Rochelle, “Absorption of carbon dioxide into aqueous piperazine: reaction kinetics, mass transfer and solubility,” *Chemical Engineering Science,* vol. 55, no. 22, pp. 5531-5543, 2000.

[51] A. García-Abuín, D. Gómez-Díaz, J. Navaza and I. Vidal-Tato, “Kinetics of Carbon Dioxide Chemical Absorption into Cyclic Amine Solutions,” *AIChE Journal,* vol. 57, no. 8, 2011.

[52] P. Singh, Amine Based Solvent for CO_2 Absorption "From Molecular Structure to Process", University of Twente, The Netherlands, 2011.

[53] R. Rowland, Q. Yang, P. Jackson and M. Atalla, “Amine mixtures and the effect of additives on the CO_2 capture rate,” *Energy Procedia,* vol. 4, pp. 195-200, 2011.

[54] Q. Zhuang, R. Pomalis, L. Zheng and B. Clements, “Ammonia-based carbon dioxide capture technology: issues and solutions,” *Energy Procedia,* vol. 4, pp. 1459-1470, 2011.

[55] V. Darde, CO_2 capture using aqueous ammonia, Center for Energy Resources Engineering - Technical University of Denmark, 2011.

[56] V. Darde, W. van Well, E. Stenby and K. Thomsen, “CO_2 capture using aqueous ammonia: kinetic study and process simulation,” *Energy Procedia,* vol. 4, pp. 1443-1450, 2011.

[57] H. Jilvero, F. Norman, K. Andersson and F. Johnsson, “Thermal Integration and Modelling of the Chilled Ammonia Process,” *Energy Procedia,* vol. 4, pp. 1713-1720, 2011.

[58] P. Versteeg and E. Rubin, “Technical and economic assessment of ammonia-based post-combustion CO_2 capture,” *Energy Procedia,* vol. 4, pp. 1957-1964, 2011.

[59] C. Ahn, H. Lee, Y. Chang, K. Han, C. Rhee, J. Kim, H. Chun and J. Park, “Determination of Ammonium Salt/Ion Speciation in the CO_2 Absorption Process Using Ammonia Solution: Modeling and Experimental Approaches,” *Energy Procedia,* vol. 4, pp. 541-547, 2011.

[60] H. Knuutila, M. Anttila, E. Borresen, O. Juliussen and H. Svendsen, *CO_2 capture with sodium carbonate,* Trondheim, Norway, 2006.

[61] D. G. Chapel, C. L. Mariz and J. Ernest, “Recovery of CO_2 from Flue Gases: Commercial Trends,” Saskatchewan, Canada, 1999.

[62] W. Echt, “Technologies for Efficient Purification of Natural and Synthesis Gases,” UOP, 2015. [Online]. Available: http://www.uop.com/technologies-for-efficient-purification-of-natural-and-synthesis-gases/. [Accessed 2015 11 2015].

[63] CATACARB, CATACARB Eickmeyer & Associates, Inc., 2015. [Online]. Available: http://catacarb.com/our-company/. [Accessed 13 11 2015].

[64] B. Grover and E. Bergen, “CO_2 Recovery from Flue Gas by the Benfield Process,” in *Petroenergy 1983*, Houston, Texas, 1983.

[65] J. Cullinane and G. Rochelle, *Properties of Concentrated Aqueous Potassium Carbonate/Piperazine for CO_2 Capture,* 2nd Annual Conference on Carbon Sequestration, Alexandria, Virginia, May 5-8, 2003, 2003.

[66] J. Cullinane and G. Rochelle, “Carbon dioxide absorption with aqueous potassium carbonate promoted by piperazine,” *Chemical Engineering Science,* vol. 59, no. 17, pp. 3619-3630, 2004.

[67] H. Knuutila, H. Svendsen and O. Juliussen, “Kinetics of carbonate based CO_2 capture systems,” *Energy Procedia,* vol. 1, pp. 1011-1018, 2009.

[68] E. Kenig, L. Kucka and A. Górak, “Rigorose Modellierung von Reaktivabsorptionsprozessen,” *Chemie Ingenieur Technik,* vol. (74), pp. 745-764, 2002.

[69] S. Freeman, R. Dugas, D. van Wagener, T. Nguyen and G. Rochelle, “Carbon dioxide capture with concentrated, aqueous piperazine,” *International Journal on Greenhouse Gas Control,* pp. 119-124, 4 2010.

[70] S. Freguia and G. T. Rochelle, “Modeling of CO_2 Capture by Aqueous Monoethanolamine,” *AIChE,* vol. 49, no. 7, pp. 1676-1686, 2003.

[71] D. Austgen, G. Rochelle, X. Peng and C. C. Chen, “Model of vapor-liquid equilibria for aqueous acid gas-alkanolamine systems using the Electrolyte NRTL equation,” *Ind. Eng. Chem. Res.,* vol. 28, pp. 1060-1073, 1989.

[72] F. Jou, A. Mather and F. Otto, “The Solubility of CO_2 in a 30 Mass Percent Monoethanolamine Solution,” *Can. J. Chem. Eng.,* vol. 73, no. 1, pp. 140-147, 1995.

[73] R. Dugas, Pilot Plant Study of Carbon Dioxide Capture by Aqueous Monoethanolamine, The University of Texas at Austin, USA, 2006.

[74] R. Dugas, P. Alix and E. Lemaire, “Creation of an Aspen RateSep Absorber Model for the Evaluation of CASTOR Pilot Plant Data.,” *American Chemical Society, Division of Petroleum Chemistry,* vol. 53, pp. 89-92, 2008.

[75] R. Dugas, Carbon Dioxide Absorption, Description, and Difussion in Aqueous Piperazine and Monoethanolamine, University of Texas at

Austin, 2009.

[76] M. Hilliard, A Predictive Thermodynamic Model for an Aqueous Blend of Potassium Carbonate, Piperazine, and Monoethanolamine for Carbon Dioxide Capture from Flue Gas, University of Texas at Austin, USA, 2008.

[77] G. Rochelle, A. Sexton, S. Freeman, R. Dugas, X. Chen, R. Tsai, D. van Wagener, J. Plaza, J. Davis and Q. Xu, "CO_2 Capture by Aqueous Absorption - 4th Quaterly Progress Reports 2008," The University of Texas at Austin, 2009.

[78] J. Plaza, Modeling of Carbon Dioxide Absorption with Aqueous Monoethanolamine, Piperazine and Promoted Potassium Carbonate, University of Texas at Austin, USA, 2012.

[79] J. Cullinane, Thermodynamics and Kinetics of Aqueous Piperazine with Potassium Carbonate for Carbon Dioxide Absorption, University of Texas at Austin, 2005.

[80] J. Plaza, E. Chen and G. Rochelle, Absorber Intercooling in CO_2 Absorption by Piperazine Promoted Potassium Carbonate, vol. 56, AIChE Jounal, 2010, pp. 905-914.

[81] M. Hillliard, Thermodynamics of Aqueous Piperazine/Potassium Carbonate/Carbon Dioxide Characterized by the Electrolyte NRTL Model within Aspen Plus, University of Texas at Austin, USA, 2005.

[82] ef-Ruhr-Forschungsprojekt, "Analyse zur Nachrüstung von Kohlekraftwerken mit einer CO_2-Rückhaltung," Germany, 2009.

[83] S. Weiß, Thermisches Trennen - Ausrüstungen und ihre Berechnungen, Stuttgart: Deutscher Verlag für Grundstoffindustrie, 1999.

[84] F. Kammermaier, Neuartige Einbauten zur Unterdrückung der Maldistribution in Packungskolonnen, Lehrstuhl für Fluidverfahrenstechnik der Technischen Universität München, 2008.

[85] M. Sander and C. Mariz, "The Fluor Econamine Process: Past Experience and Present Day Focus," *Energy Conversion and Management,* vol. 33, no. 5-8, pp. 341-348, 1992.

[86] P. Moser, S. Schmidt, G. Sieder, H. García and T. Stoffregen, “Versuchsergebnisse aus der Post Combustion Capture Pilotanlage in Niederaußem,” Dresden, 2010.

[87] Sulzer Chemtech, “Internals for packed columns,” [Online]. Available: http://www.sulzer.com/mr/-/media/Documents/ProductsAndServices/Separation_Technology/Distillation_Absorption/Brochures/Internals_for_packed_columns.pdf. [Accessed 02 2012].

[88] Koch-Glitsch, *Intalox Packed Tower Systems - Packed Tower Internals,* USA, 2010.

[89] M. Schultes and J. Halbirt, “Column Internals - Product Bulletin 1101,” Raschig GmbH Jaeger Products, Inc., Germany, USA.

[90] M. Abu-Zahra, L. Schneiders, J. Niederer, P. Feron and G. Versteeg, “CO_2 capture from power plants Part I. A parametric study on the technical performance based on monoethanolamine,” *International Journal of Greenhouse Gas Control,* 2006.

[91] M. Abu-Zahra, Carbon Dioxide Capture from Flue Gas - Development and Evaluation of Existing and Novel Process Concepts, Technische Universiteit Delft, 2009.

[92] M. Abu-Zahra, J. Niederer, P. Feron and G. Versteeg, “CO_2 capture from power plants Part II. A parametric study on the economical performance based on mono-ethanolamine,” *International Journal of Greenhouse Gas Control,* 2007.

[93] AspenTech, “Aspen Plus Help - Aspen Plus Reference,” USA, 2010.

[94] D. Tremblay, *Personal information provided by Aspen Plus product manager,* Berlin, 2008.

[95] R. Hockley, *A Rate-Based Process Modeling Study of CO_2 Capture with Aqueous Monoethanolamine Solution,* Berlin, Germany: AspenTech, 2008.

[96] D. Tremblay, R. Hockley, T. Suzuki, C. C. Chen, S. Watanasari and B. Hanley, *Process Modeling for Chemicals Modeling Amine Solutions with*

Aspen RateSep, Berlin, Germany: AspenTech, 2008.

[97] AspenTech, “EAP2513 CO_2 Removal Processes: Absorption Using Rate Base Distillation,” 2010.

[98] T. Sherwood, G. Shipley and F. Holloway, “Flooding velocities in packed columns,” *Industrial Engineering Chemistry,* vol. 30, no. 7, pp. 765-769, 1938.

[99] J. Eckert, “Selecting the Proper Distillation Column Packing,” *Chem. Eng. Prog.,* vol. 66, no. 3, pp. 39-44, 1970.

[100] R. F. Strigle, Packed Tower Design and Applications, 2nd. ed., Houston, Texas.: Gulf Publishing Company, 1994.

[101] E. Abkar, H. Kister, J. Scherffius and K. Afshar, “Realistically Predict Capacity and Pressure Drop for Packed Columns,” *CEP Magazine,* July 2007.

[102] H. Kister and D. Gill, *IChemE Symp. Ser. 128,* 1992, p. A109.

[103] S. Reddy, D. Johnson and J. Gilmartin, “Power Plant Air Pollutant Control “Mega” Symposium,” in *Fluor’s Econamine FG Plus Technology For CO_2 Capture at Coal-fired Power Plants*, Baltimore, USA, 2008.

[104] Bundesministerium für Umwelt, Naturschutz und Reaktorsicherheit, 2002.

[105] Y. Yagi, T. Mimura, M. Iijima, K. Ishida, R. Yoshiyama, T. Kamijo and T. Yonekawa, in *Improvements of carbon dioxide capture technology from flue gas*, Canada, 2005.

[106] R. Dugas, P. Alix, E. Lemaire, P. Broutin and G. Rochelle, “Absorber model for CO_2 capture by monoethanolamine – application to CASTOR pilot results,” *Energy Procedia,* pp. 103-107, 2009.

[107] Ö. Korkmaz, Bewertung von Maßnahmen zur Nachrüstung von Steinkohlekraftwerken mit einer CO_2-Rückhaltung, Essen, Germany, 2011.

[108] ZEP, 15 July 2011. [Online]. Available: www.zeroemissionsplatform.eu/library/publication/166-zep-cost-report-

capture.html.

[109] D. Singh, E. Croiset, P. Douglas and M. Douglas, “Techno-economic study of CO_2 capture from an existing coal-fired power plant: MEA vs. O_2/CO_2 recycle combustion,” *Energy Conversion Management,* vol. 44, no. 19, pp. 3073-3091, 2003.

[110] M. Peters, K. Timmerhaus and W. Roland, Plant Design and Economics for Chemical Engineers, 5th ed. ed., McGraw-Hill, 2003.

[111] A. Rao and E. Rubin, “A technical, economic and environmental assessment of amine-based CO_2 capture technology for power plant greenhouse gas control,” *Environ. Sci. Technol.,* vol. 36, no. 20, pp. 4467-4475, 2002.

[112] A. Rao and E. Rubin, A technical, economic and environmental assessment of amine-based CO_2 capture technology for power plant greenhouse gas technology, Carnegie Mellon University, 2002.

[113] R. Perry, D. Green and J. Maloney, Perry's Chemical Engineers' Handbook, 7th ed. ed., New York: McGraw-Hill, 1997.

[114] C. Hendriks, T. Wildenborg, P. Feron, W. Graus and R. Brandsma, “EC-case carbon dioxide sequestration,” 2003.

[115] G. F. Versteeg, P. S. Kumar, J. A. Hogendoorn and P. H. Feron, “Method for absorption of acid gases”. Patent WO 03/095071 A1, 2003.

[116] Vattenfall, “The Schwarze Pumpe pilot plant,” 11 12 2012. [Online]. Available: http://www.vattenfall.com/en/ccs/schwarze-pumpe.htm. [Accessed 26 08 2013].

[117] OJ EC, “Directive 2001/80/EC of the European Parliament and of the Council of 23 October 2001 on the limitation of emissions of certain pollutants into the air from large combustion plants,” *Official Journal of the European Communities,* vol. 44, no. 1, p. 1, 2001.

Die Reihen der Fortschritt-Berichte VDI:

1 Konstruktionstechnik/Maschinenelemente
2 Fertigungstechnik
3 Verfahrenstechnik
4 Bauingenieurwesen
5 Grund- und Werkstoffe/Kunststoffe
6 Energietechnik
7 Strömungstechnik
8 Mess-, Steuerungs- und Regelungstechnik
9 Elektronik/Mikro- und Nanotechnik
10 Informatik/Kommunikation
11 Schwingungstechnik
12 Verkehrstechnik/Fahrzeugtechnik
13 Fördertechnik/Logistik
14 Landtechnik/Lebensmitteltechnik
15 Umwelttechnik
16 Technik und Wirtschaft
17 Biotechnik/Medizintechnik
18 Mechanik/Bruchmechanik
19 Wärmetechnik/Kältetechnik
20 Rechnerunterstützte Verfahren (CAD, CAM, CAE CAQ, CIM ...)
21 Elektrotechnik
22 Mensch-Maschine-Systeme
23 Technische Gebäudeausrüstung

ISBN 978-3-18-395303-5